University of Bath

PHD

Organometallic compounds of the early transition elements.

Griffin, G. F.

Award date:
1978

Awarding institution:
University of Bath

Link to publication

Alternative formats
If you require this document in an alternative format, please contact:
openaccess@bath.ac.uk

Copyright of this thesis rests with the author. Access is subject to the above licence, if given. If no licence is specified above, original content in this thesis is licensed under the terms of the Creative Commons Attribution-NonCommercial 4.0 International (CC BY-NC-ND 4.0) Licence (https://creativecommons.org/licenses/by-nc-nd/4.0/). Any third-party copyright material present remains the property of its respective owner(s) and is licensed under its existing terms.

Take down policy
If you consider content within Bath's Research Portal to be in breach of UK law, please contact: openaccess@bath.ac.uk with the details. Your claim will be investigated and, where appropriate, the item will be removed from public view as soon as possible.

Download date: 05. May. 2023

ORGANOMETALLIC COMPOUNDS OF THE EARLY TRANSITION ELEMENTS

Submitted by G.F. Griffin

for the degree of Ph.D.

of the University of Bath

1978

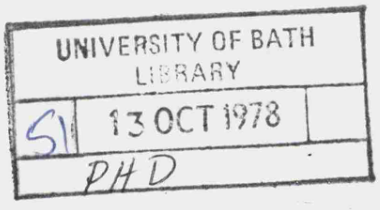

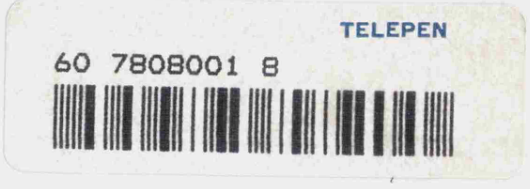

COPYRIGHT

Attention is drawn to the fact that copyright of this thesis rests with its author. This copy of the thesis has been supplied on condition that anyone who consults it is understood to recognise that its copyright rests with its author and that no quotation from the thesis and no information derived from it may be published without the prior written consent of the author .

This thesis may be made available for consultation within the University Library and may be photocopied or lent to other libraries for the purposes of consultation.

G. F. Griffin.

ProQuest Number: U441276

All rights reserved

INFORMATION TO ALL USERS
The quality of this reproduction is dependent upon the quality of the copy submitted.

In the unlikely event that the author did not send a complete manuscript
and there are missing pages, these will be noted. Also, if material had to be removed,
a note will indicate the deletion.

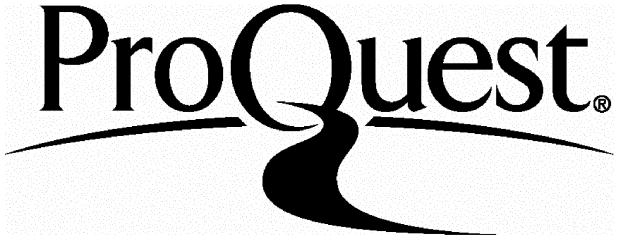

ProQuest U441276

Published by ProQuest LLC(2015). Copyright of the Dissertation is held by the Author.

All rights reserved.
This work is protected against unauthorized copying under Title 17, United States Code.
Microform Edition © ProQuest LLC.

ProQuest LLC
789 East Eisenhower Parkway
P.O. Box 1346
Ann Arbor, MI 48106-1346

Dedication

This thesis is dedicated to

my Mother for her patience

and encouragement throughout

my education.

Acknowledgement

I would like to thank the staff of the School of Chemistry especially Dr. B.J. Brisdon, my supervisor, for their help and encouragement throughout the course of this work. I gratefully acknowledge the award of a Science Research Council grant.

My thanks are also due to Mrs. V. Edwards for typing this thesis, and to Dr. M. Cartwright and Dr. R.J. Hobson for assistance in proof reading the typescript.

Abstract

The di-(2-pyridyl)amine (dpa) complexes $M(CO)_4dpa$ (M = Cr, Mo or W) and their anionic derivatives $[MX(CO)_3dpa]^-$ (X = halide) have been prepared and compared chemically and spectroscopically with the corresponding 2,2'-bipyridyl (bipy) complexes. During these investigations a new procedure has been developed for determining the CO force constants for cis-$L_2M(CO)_4$ complexes. This procedure was tested by successfully predicting the spectra of $C^{18}O$ labelled cis-$I_2Fe(CO)_4$ species and then applied to a wide range of complexes and the results compared with Cotton-Kraihanzel and Jernigan force constant calculations.

The tetracarbonyl and anionic tricarbonyl derivatives, $M(CO)_4L_2$ and $[MX(CO)_3L_2]^-$ (L_2 = bipy or dpa), have been used to extend the range of known molybdenum and tungsten complexes containing the $M(\eta^3\text{-allyl})(CO)_2$ unit, and by employing a new low temperature synthesis the previously unknown chromium(II) complexes $[CrX(\eta^3\text{-allyl})(CO)_2bipy]$ (X = Cl, Br, I or NCS) have also been isolated as maroon solids. These complexes are essentially diamagnetic and appear to be analogous to the molybdenum and tungsten compounds but due to their lack of stability in solution a complete spectral characterisation was not possible.

It was found that some potentially three-electron donor ligands (LL_a) react in the presence of pyridine (py) to displace both the acido-group (X = Cl or Br) and the bidentate ligand dpa or bipy from the complexes $[MX(\eta^3\text{-allyl})(CO)_2L_2]$ to give the complex $[M(LL_a)(\eta^3\text{-allyl})(CO)_2py]$. Variable temperature

n.m.r. spectroscopy showed these complexes to be fluxional in solution, and the data was consistent with a pseudo-molecular rotation mechanism. While this thesis was in preparation, the crystal structure of [Mo(acac)(η^3-allyl)$(CO)_2$py] was determined independently and shown to be of lower symmetry than other [M(η^3-allyl)$(CO)_2$(bidentate)(monodentate)] complexes.

Contents

Abbreviations

acac	acetylacetonate anion (pentane-2,4-dionate anion)
adpa	N-acetyldi-(2-pyridyl)amine
assym (or ass)	assymmetric
bdpa	N-benzoyldi-(2-pyridyl)amine
bipy	2,2'-bipyridine
b.pt	boiling point
Bu	butyl (n-normal, t-tertiary)
c	velocity of light (3.00×10^8 ms^{-1})
cht	cycloheptatriene
cisA,cisB	valence interaction force constants
C-K	Cotton-Kraihanzel
COC	capped octahedron
Cp	η^5-cyclopentadienyl
Cpca	cyclopentadienylcarboxaldehyde (C_5H_4CHO)
CTP	capped trigonal prism
dedc	diethyldithiocarbamate anion
diars	1,2-bis-(dimethylarsino)benzene
dmdc	dimethyldithiocarbamate anion
dme	1,2-dimethoxyethane
DMF	N,N-dimethylformamide
dmpe	1,2-bis-(dimethylphosphino)ethane
dpa	di-(2-pyridyl)amine
dpam	bis-(diphenylarsino)methane
dppe	1,2-bis-(diphenylphosphino)ethane
dppm	bis-(diphenylphosphino)methane
dpsp	1,3-bis-(diphenylstibino)propane
dth	2,5-dithiahexane
E	unit matrix
en	1,2-diaminoethane
Et	ethyl

Abbreviations (contd)

F	potential energy matrix
F^{γ}_{ij}	symmetry force constant
f_{ij}	valence force constant
G	kinetic energy matrix
GLC	gas chromatography
H_a, H_s, H_c	η^3-allyl protons (a-anti, s-syn, c-central carbon atom)
hfacac	hexafluoroacetylacetonate anion ($CF_3COCHCOCF_3$)
HMPA	hexamethylphosphoramide $[(Me_2N)_3P]$
I	infra-red band intensity
K_1, K_2	valence carbonyl stretching force constants
L	Lewis base
LL_a	three-electron donor ligand
M	reciprocal of the apparent reduced mass of $C^{18}O$
Me	methyl
m/e	mass per unit charge
m.pt.	melting point
mtb	1,2-bis-(methylthio)benzene
mtn	1,8-bis-(methylthio)naphthalene
N	Avogadro constant (6.022×10^{23} mol^{-1})
nbn	norbornadiene (bicyclo[2.2.1]hepta-2,5-diene)
n.m.r.	nuclear magnetic resonance
OAc	acetate anion
Ph	phenyl
phen	1,10-phenanthroline
Pr	propyl (i-iso)
pse	1,2-bis-(i-propylseleno)ethane
py	pyridine
pz	pyrazolyl (Hpz=pyrazine; $\overline{CH : CHCH : NNH}$)

R	alkyl or aryl
R_{in}, R_{Out}	resultant change in dipole moment
R^{γ}	symmetry operation
r_i	internal coordinate
S^{γ}	symmetry coordinate
salal	salicylaldehate anion (OC_6H_4CHO)
sal:NPh	N-phenylsalicylaldiminate anion (OC_6H_4CHNPh)
sym (or s)	symmetric
THF	tetrahydrofuran
tmen	N,N,N',N'-tetramethyl-1,2-diaminoethane
$tolSO_2$	p-toluenesulphinate anion
tpa	tri-(2-pyridyl)amine
trans	valence interaction force constant
X	ratio cisB/cisA
Y	ratio trans/cisA
γ	symmetry mode
Δ	change in dipole moment
δ	n.m.r. band position in ppm relative to TMS ($\delta_{TMS} = 0$)
λ	Eigen value obtained from a secular determinant
μ	reciprocal of the reduced massof CO
μ (BM)	magnetic moment in Bohr magnetons
ν	vibrational band position in cm^{-1}
π	normalising factor
σ	mirror plane
χ	a character from a character table
χ_M	molar magnetic susceptibility

CHAPTER 1

INTRODUCTION

CHAPTER 1

INTRODUCTION

1.1 Historic background

This work is concerned mainly with compounds of the type $[M^{II}X(\eta^3\text{-allyl})(CO)_2L]$ (where M is a group VIA metal, X is a uni-negative ligand and either L or X, but not both, is a bidentate chelating ligand), and as such is dependent on the following historic roots.

(a) Coordination compounds: The first recorded coordination compound was probably Prussian blue which was prepared in 1704 by the German artist Diesbach[1-3], who heated animal refuse together with soda ash in an iron pot. Subsequent work[1] led to the isolation of potassium hexacyanoferrate(II). However, interest in this area was not really stimulated until 1798 when Tassaert isolated the complex $[Co(NH_3)_6]Cl_3$-hexammine-cobalt(III) chloride[4].

Even though this was an accidental discovery, Tassaert realised its importance. A stable compound was formed by the combination of two stable molecules, namely $CoCl_3$ and NH_3, and resulted in cobalt having a valency in excess of three.

These observations could not be explained and therefore led to much interest and speculation in this area, consequently many more such compounds were isolated, until in 1893 Werner[4,5] proposed a theory to account for the bonding and stereochemistry of this class of compounds.

Werner proceeded to substantiate his theory by much careful experimentation including the separation of stereoisomers and optical isomers in order to prove the octahedral nature of six-coordinate complexes. His work laid the foundation for the whole of modern coordination chemistry.

(b) Metal carbonyl complexes: This very important area of inorganic chemistry was instigated in 1888 when Mond isolated and correctly formulated the compound $Ni(CO)_4$ [6] which he called "Nickel-Carbon-Oxide". Discoveries of carbonyl derivatives of iron and other transition metals quickly followed and the group VIA carbonyls $M(CO)_6$ were subsequently synthesised in 1926 by the reductive carbonylation of their chlorides[7-11].

$$MCl_x + 6CO \xrightarrow{PhMgBr} M(CO)_6$$

(x = 3 for Cr; 5 for Mo and 6 for W).

Recently chromium has been added to the list of metals which will combine directly with carbon monoxide[12].

$$CrCl_3.3THF \xrightarrow{K/C_6H_6} Cr \xrightarrow[280\ atm.,\ 220^\circ C]{CO/THF} Cr(CO)_6 \quad (>50\%\ yield)$$

In recent years metal carbonyls have proved of enormous synthetic value in organometallic chemistry, organic syntheses and in catalysis.

(c) Organometallic Chemistry: Despite the discovery of Zeise's salt {$K[PtCl_3(C_2H_4)]$ - potassium trichloro-η^2-ethylene-platinate(II)[13]} in 1827, the structure of this π-olefin complex remained an enigma for many years and was not finally confirmed until 1953[13], more than a century after its isolation. σ-Alkyl compounds[14-17] followed shortly after Zeise's discovery, but only in the last 25 years or so have extensive studies been carried out on compounds with organic ligands containing delocalised electron systems such as Cp_2Fe[18] and $Co(\eta^3\text{-}C_4H_7)(CO)_3$[19,20]. This latter compound was the first transition metal - allyl complex to be isolated and as such is significant to the work in this thesis. The complex was prepared by the high pressure reaction between $HCo(CO)_4$ and 1,3-butadiene in glacial acetic acid and forms as a red-brown distillable liquid (b.pt. 35°C at 1mm Hg).

$$HCo(CO)_4 + C_4H_6 = Co(C_4H_7)(CO)_3 + CO$$

Subsequently[20] this compound and the parent allyl complex $Co(C_3H_5)(CO)_3$ were prepared from the reaction between $Na[Co(CO)_4]$ and the allylic bromides C_3H_5Br and C_4H_7Br. (This latter halide was a mixture of 1-bromobut-2-ene and 3-bromobut-1-ene).

^{1}H-nmr spectroscopy revealed the allyl complex to have three types of hydrogen atoms in the ratio 1 : 2 : 2 thus supporting a symmetric structure such as that tentatively proposed in 1960 (Figure 1-1).

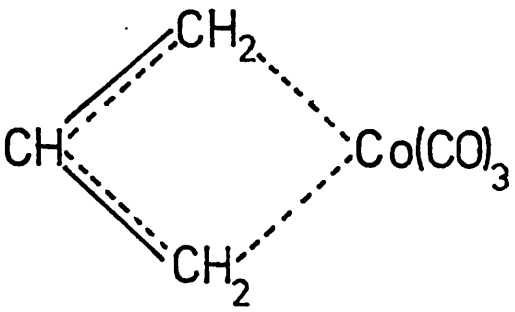

Figure 1-1. The structure initially proposed for $Co(C_3H_5)(CO)_3$

Since these beginnings and especially in the last few years there has been a tremendous growth and diversification in all three of these areas of inorganic chemistry. Both organometallic and coordination compounds have extensive applications, for example in medicine (e.g. platinum - ammine complexes in the treatment of cancer[21]), as fuel additives [e.g. Et_4Pb and $Mn(\eta^5\text{-}MeC_5H_4)(CO)_3$], in electroplating {e.g. $[Ni(CN)_5]^{3-}$ } and as catalysts for a variety of organic reactions [e.g. $WCl_2(CO)_4$ in olefin disproportionation[22], hydroformulation of olefins using $HCo(CO)_4$,[23] and olefin isomerisation using a $Pt(Ph_3P)_2Cl_2\text{-}SnCl_2$ mixture[21]]. But most important of all is the catalytic role played by metal ions in the life processes of animals and plants [e.g. magnesium in chlorophyl[24], iron in haemoglobin[24], cobalt in vitamin B_{12} (cyanocobalamine)[24,25] and molybdenum in enzymes such as nitrogenase and xanthene oxidase[26].]

1.2 Metal carbonyl chemistry

Carbon monoxide is an extremely weak Lewis base and it is initially surprising to find it forming such stable transition metal complexes. However, consideration of the bonding in CO reveals the presence of low energy anti-bonding orbitals[16] (Figure 1-2), which are capable of accepting electron density

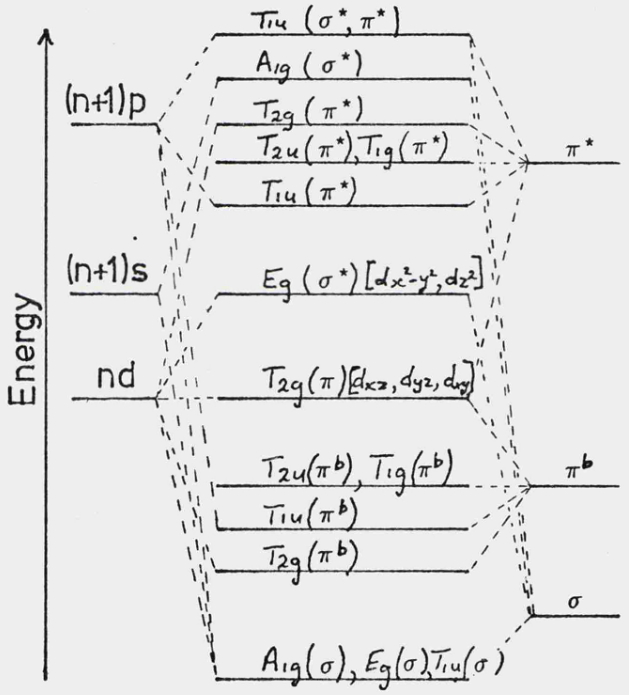

Figure 1-2. Bonding scheme for $M(CO)_6$ complexes.

from the metal. This leads to the synergic effect in which the metal to ligand π-bond strengthens the ligand to metal σ-bond and vice versa. Hence the greater the electron density on the metal the greater will be the synergic effect.

As the metal to carbon back-bonding increases the effective C - O bond order should decrease, and consequently the C - O bond order is frequently used as a sensitive indicator of the extent of back-bonding, and of the electron density on the carbon and, by inference, the metal atoms.

1.2.1 Infra-red spectroscopy of carbonyl complexes.

It is fortuitous that the energy required to stretch a metal carbonyl C - O bond falls in the range 2100 - 1700cm^{-1} and that this region of the infrared spectrum is virtually free of other molecular vibrations; hence infra-red spectroscopy has been used extensively in studying these complexes[27]. In addition the fact that the C - O stretching energy (2100 - 1700cm^{-1}) is so much greater than the other molecular stretching energies (M - C 560 - 360cm^{-1}; M - N 600 - 200cm^{-1} [28]), means that there will be very little interaction between the C - O stretching and other molecular vibrations. Consequently, and to a first approximation, the C - O stretching vibrations can be assumed to be pure, thus allowing them to be considered in isolation from the rest of the molecule. This is the so called high energy factored model and greatly simplifies the vibrational analysis of these complexes, thus leading to the calculation of approximate carbonyl force constants.

For molecules of high symmetry, such as $M(CO)_6[O_h]$ and <u>trans</u>-$L_2M(CO)_4$ $[D_{4h}]$ (i.e.complexes in which all the carbonyl groups are chemically equivalent), the observed band position

can be taken as being directly proportional to the C - O stretching force constant. Whereas for lower symmetries it is useful to quantify the observed band positions in terms of C - O stretching force constants (K_1, K_2, etc) which differentiate between chemically or symmetrically differing carbonyl groups in the same molecule. The actual calculation of force constants will be discussed further in chapter 7.

The majority of complexes discussed in this work are of the type $L_2M(CO)_4$ or $L'_4M(CO)_2$ (where the L' groups need not all be the same) and only compounds of this type will be considered further.

1.2.1.1 Infra-red spectroscopy and isomerism

Infra-red spectroscopy is also useful in differentiating between possible isomeric forms of substituted carbonyl complexes. Consideration of the complex $L_2M(CO)_4$ shows there to be two possible isomeric forms, namely cis and trans (Figure 1-3), and application of group theory leads to the assignment of the point groups indicated.

Application of the procedures outlined in sections 1 to 3 of the appendix produces the vibrational modes shown in figure 1-3.

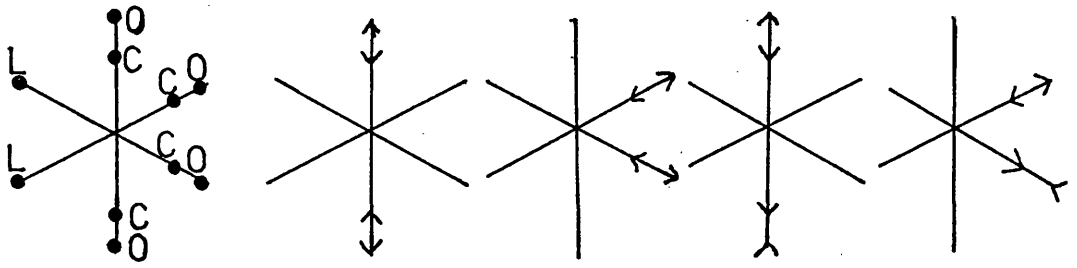

cis-$L_2M(CO)_4$	A_1	A_1	B_1	B_2
C_{2v}	ir + R	ir + R	ir + R	ir + R

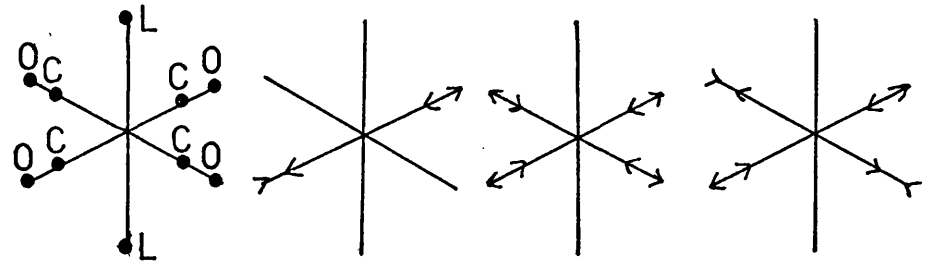

trans-$L_2M(CO)_4$	E_u	A_{1g}	B_{1g}
D_{4h}	ir	R	R

Figure 1-3 Isomeric forms and C – O stretching vibrations for $L_2M(CO)_4$

In order for a molecular vibration to be infra-red active the vibration has to cause a dipole change. Such a change occurs whenever the vibrational mode commutes as one of the cartesian coordinates. (e.g. inspection of character tables[29,30] reveal that for C_{2v} symmetry the B_1 mode commutes as the x-axis and is therefore infra-red active). Similarly any vibrational mode which commutes as the product of two axis (e.g. x^2, xy, etc) will give rise to a change in the polarisability of the molecule and will be Raman active. (e.g. Inspection of symmetry tables reveal that the B_1 mode commutes as the product xz and is therefore Raman active as well as infra-red active as referred to above).

Hence, the vibrational modes given in figure 1-3 will have the activities shown. As a Raman spectrophotometer was not available for experimentation this form of spectroscopy will not be considered further.

It can be seen that infra-red spectroscopy readily differentiates between the cis- and trans-isomers of $L_2M(CO)_4$; the cis-isomer giving rise to a maximum of four bands and the trans-isomer giving rise to only one band in the C - O stretching region of their spectra.

Similar considerations for the system $MAB(CO)_2L_2$, where L_2 is a chelating bidentate ligand { e.g. $[MoCl(\eta^3\text{-allyl})(CO)_2bipy]$ } shows the possibility of four isomers (Figure 1-4).

Application of sections 1 to 3 of the appendix reveals that each isomer may give rise to two infra-red active vibrational modes (Figure 1-4). Thus in order to differentiate between

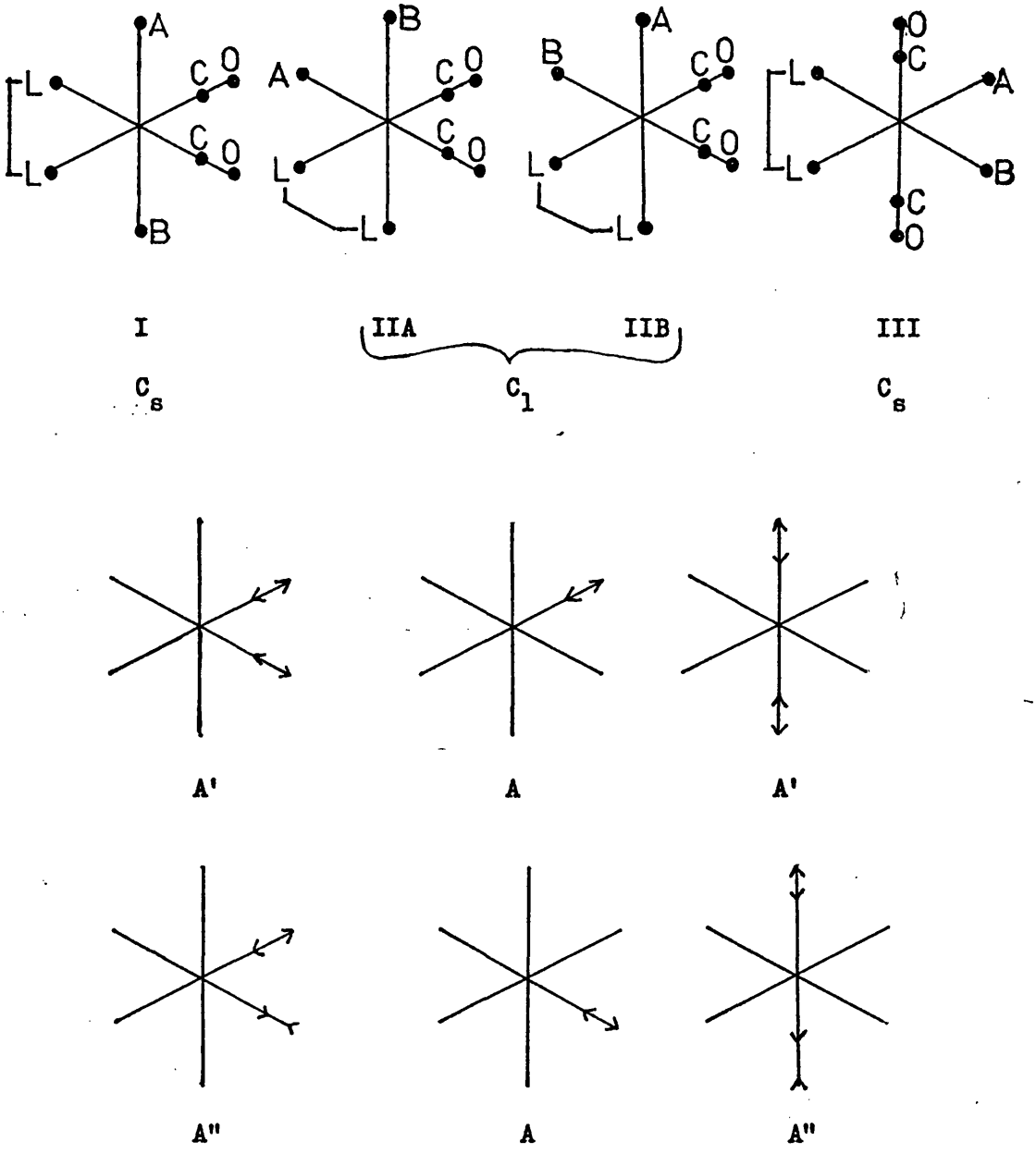

Figure 1-4 Isomers and infra-red active vibrational modes for $[MAB(CO)_2L_2]$ species

these isomers (IIA and B must be taken as being equivalent for this discussion) it is necessary to consider band intensities and isotopically enriched spectra.

The application of quantum mechanics shows that the band intensity of an infra-red active vibration is a function of the square of the overall dipole change caused by that vibration.[27] Consideration of an isolated pair of carbonyl groups (Figure 1-5) reveals that the overall dipole change, obtained by the vector

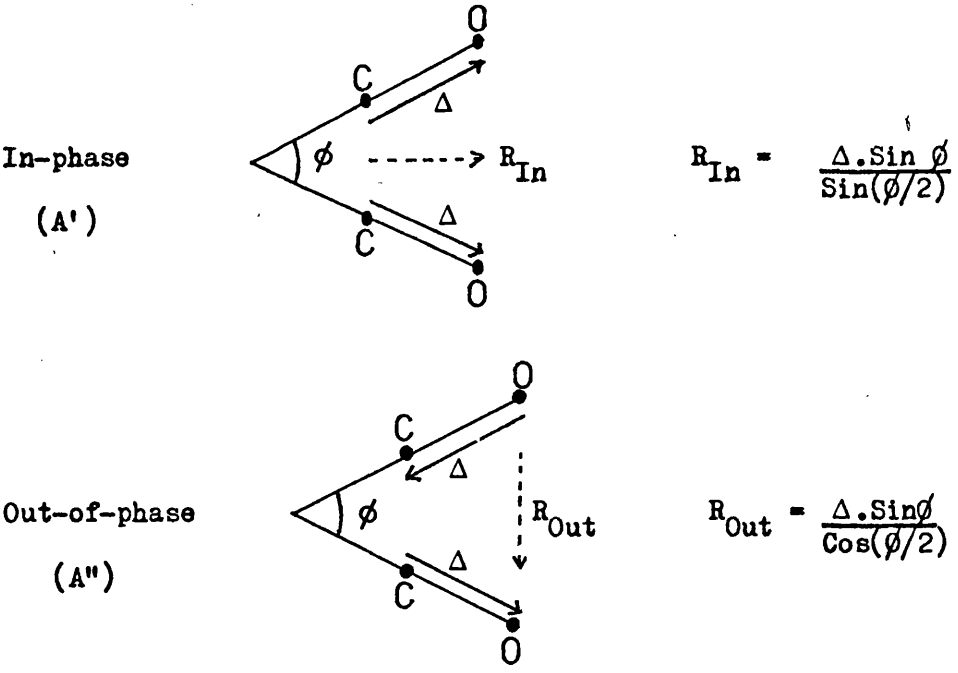

$$R_O/R_I = \tan(\phi/2) = \sqrt{I_{Out}/I_{In}}$$

Figure 1-5 Dipole changes (Δ) and infra-red band intensity (I) ratios for the dicarbonyl grouping.

addition of the individual dipole changes, is related to the angle between the two carbonyl groups ϕ (Figure 1-5). These relationships are $Sin^{-1}(\phi/2)$ and $Cos^{-1}(\phi/2)$ for the in-phase and out-of-phase vibrations respectively. Hence the infra-red spectrum of the cis-dicarbonyl isomers, I and II (figure 1-4), should exhibit two bands of approximately equal intensity (ϕ = 90, Tan 45 = 1), whereas for the trans-dicarbonyl isomer, III(figure 1-4), the in-phase vibration should have zero intensity[27,31] (ϕ = 180, Tan 90 = ∞ and R_{In} = Sin 180 = 0). Thus from these intensity considerations it is possible to decide whether the two carbonyl groups are mutually cis or trans to each other.

On substituting one carbonyl group by labelled carbon monoxide ($C^{18}O$ or ^{13}CO), the C_s structures (I and III) will each give rise to only one species (Figure 1-6) whereas the C_1 structure (II) will give rise to two species.[32]

Optical isomers have not been included in this discussion or figure 1-6 as they have no bearing on the number of observed bnads in the infra-red spectrum. Thus by means of infra-red spectroscopy and isotope exchange studies it is possible to differentiate between structures I, II and III (Figures 1-4 and 1-6).

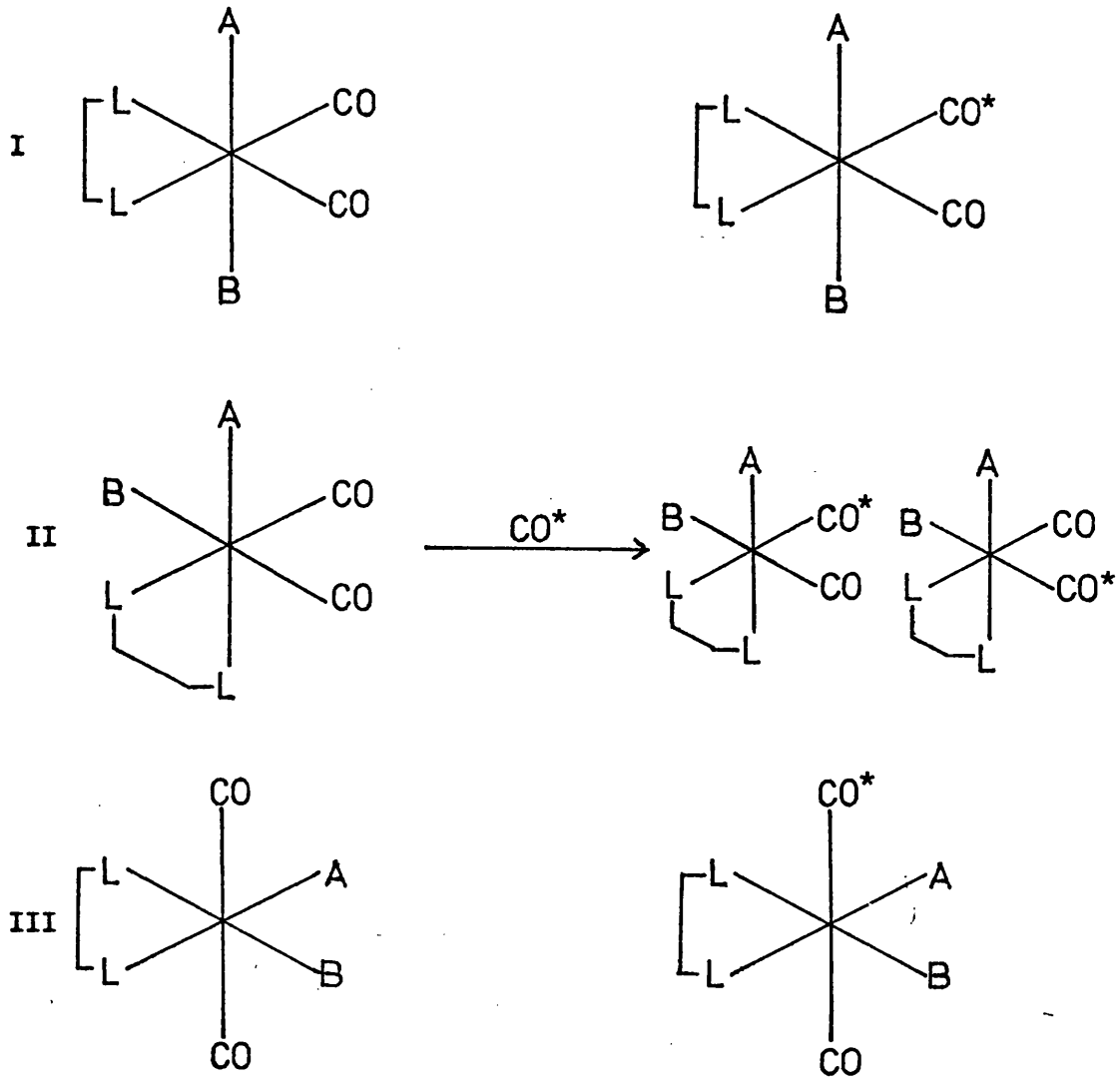

Figure 1-6 Isotope exchange studies on $MAB(CO)_2L_2$

During this work isotope exchange studies have not been attempted, and as such infra-red spectroscopy has only been used to indicate the mutually cis-nature of the carbonyl groups for the dicarbonyl complexes discussed in chapters 3 and 4. Other spectroscopic techniques (e.g. ^{1}H- or ^{13}C-n.m.r) are capable of yielding further information on the arrangement of the non-carbonyl ligands.

1.2.2 Reactions of metal carbonyl complexes

Metal carbonyl complexes undergo many and varied reactions leading to an extensive number of substituted, carbene and organometallic complexes. Thus it is necessary to restrict the coverage given here, and as the reactions studied in this thesis mainly involve substitution and redox reactions of the early transition-metal carbonyls only these types of reaction will be considered further.

1.2.2.1 Substitution reactions

One or more carbonyl groups may be successively replaced in metal carbonyls by a wide variety of anionic, neutral and occasionally cationic ligands. Substitution reactions are usually brought about by thermal or photochemical means and proceed by either an associative or dissociative mechanism depending upon the reaction conditions, the metal atom and the substituting ligand. Activation energies of several substitution reactions of the hexacarbonyls have been measured and shown to increase in the order Mo < Cr < W,[33] which parallels the increase in force constants for the M - C stretching vibrations (1.81, 2.03 and 2.15 mdyneÅ^{-1} for Mo, Cr and W respectively). Thus kinetic measurements confirm the experimentally observed high reactivity of $Mo(CO)_6$ compared with $Cr(CO)_6$ and $W(CO)_6$.

Photochemical reactions normally occur via an S_n1 mechanism in which the rate determining step is loss of CO. This scheme

$$M(CO)_6 \xrightarrow{h\nu} M(CO)_5 + CO$$

$$M(CO)_5 + CO \longrightarrow M(CO)_6$$

$$M(CO)_5 + L \longrightarrow M(CO)_5L$$

was proposed as early as 1934[34,35] and subsequent work in low temperature matrices revealed $M(CO)_5$ species with C_{4v} symmetry. In many instances interaction occurred between the $M(CO)_5$ moiety and the matrix material yielding species such as $Mo(CO)_5N_2$ [36] and $Cr(CO)_5CH_4$ [37]. Such interactions probably have a significant effect on the rates of reaction of hexacarbonyls even in such "non-coordinating" solvents as saturated hydrocarbons.

Thermal reactions are often too mild for this mechanism to be applicable, and second-order pathways have been found in some instances[38]. Thus thermal substitution of halide ion for CO in $M(CO)_6$, where M = Cr, Mo or W, has been shown to occur by either of two associative mechanisms.

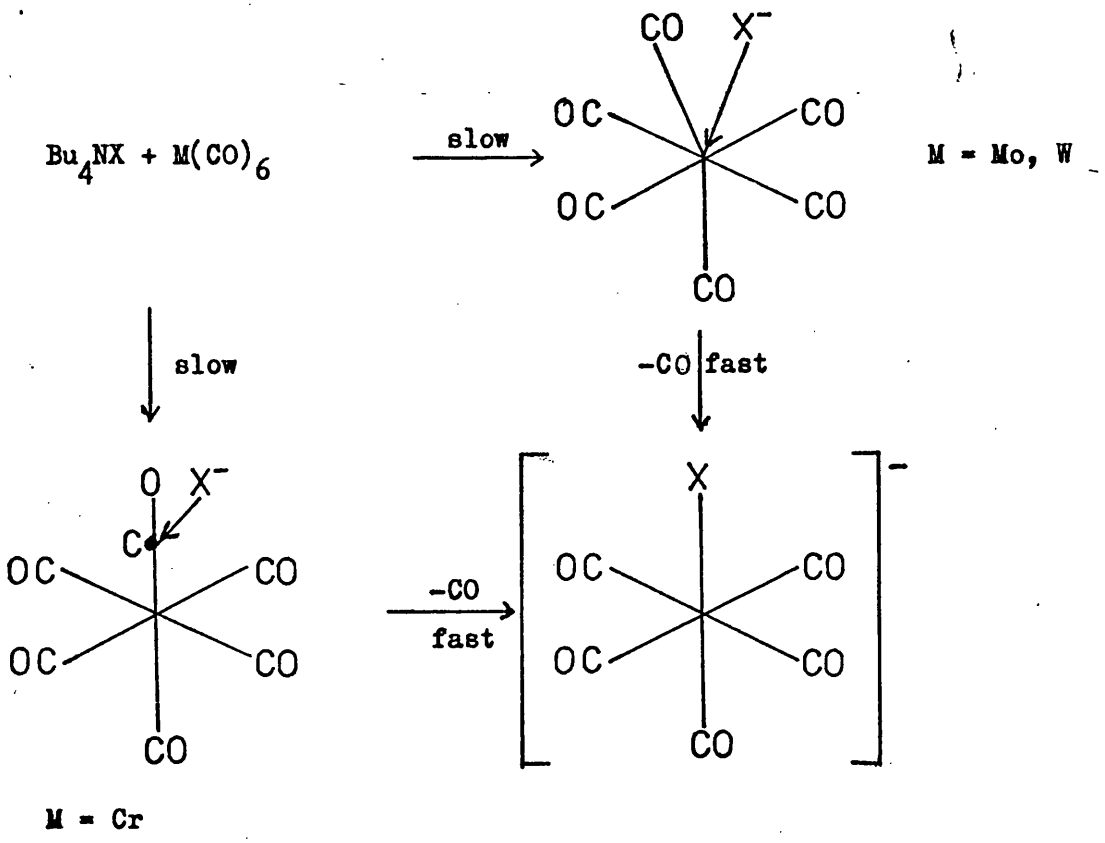

From a preparative point of view, both photochemical and thermal methods are used extensively for obtaining substituted metal carbonyls. Both methods suffer from a lack of specificity in many instances, particularly for mono-substitution reactions, and one of the two specialised procedures outlined below are often used to overcome this problem.

$$M(CO)_6 \xrightarrow{h\nu\ /THF} M(CO)_5.THF + CO \qquad (1)$$

$$M(CO)_5.THF \xrightarrow{L} M(CO)_5.L + THF$$

$$R_4NX + M(CO)_6 \longrightarrow R_4N[M(CO)_5X] + CO \qquad (2)$$

$$R_4N[M(CO)_5X] + L \xrightarrow{CH_2Cl_2} M(CO)_5L + R_4NX$$

The second route[39] has been used successfully for the preparation of many monosubstituted products containing potentially bidentate ligands of the type $R_2ECH_2CH_2ER_2$, where E = N or P and R = alkyl or aryl.[40] This in turn has allowed detailed investigation of the rate of chelation of bidentate ligands in these complexes.[41]

$$M(CO)_5L - L \longrightarrow M(CO)_4L_2 + CO$$

The final degree of substitution achieved in a carbonyl complex will be strongly dependent upon the electronic and steric properties of the substituents.

Ligands can be divided into two broad classes; (i) those with only σ-donating properties (generally those with N and O-donor atoms, such as R_3N and RCO_2^-) and (ii) ligands which enter into metal to ligand back-bonding using π-molecular orbitals (generally those with the heavier donor atoms and unsaturated ligands such as ethylene or benzene).

Naturally the extent of back-bonding from the metal to the carbonyl groups in such complexes will be a function of the electron density on the metal atom, which in turn will be a function of the electron donating and accepting properties of the ligand. To a first approximation the extent of electron donation by a simple σ-donating ligand will be related to the basicity of the ligand. The situation is more complicated for back-bonded ligands as the carbonyl groups and the ligand will compete for the available electron density.

Graham[42] used simple molecular orbital theory to obtain the following relationships for complexes of the type $LM(CO)_5$:

$$\Delta k_1 = \Delta\sigma + 2\Delta\pi \quad \text{and} \quad \Delta k_2 = \Delta\sigma + \Delta\pi$$

In these relationships k_1 and k_2 are the C - O stretching force constants for the carbonyl groups *trans* and *cis*, respectively, to the ligand; and all the values are relative to arbitrary standards [e.g. $MeMn(CO)_5$ and $C_6H_{11}NH_2Mo(CO)_5$].

These relationships assume that the σ- and π-bonding orbitals are completely separable (based on symmetry arguments) and that the σ-bonding framework will not be affected by changes in the degree of back bonding. As stated earlier metal carbonyls owe their stability to the synergic effect. Thus, it seems reasonable to assume that any change in the extent of back-bonding will effect the extent of σ-donation by the carbonyl ligands. This would lead to far more complex relationships between k_1 and k_2 than those derived by Graham[42].

A consequence of the M - CO back-bonding is that for ligands with a lower π-acidity than carbon monoxide, it becomes increasingly difficult to replace successive carbonyl groups. Hence, for example, the reaction between pyridine and $Mo(CO)_6$ will stop at the trisubstituted complex $Mo(CO)_3(py)_3$. Where ligands have appreciable π-acidity further substitutions become possible (e.g. phosphines, arsines and isonitriles).[43] The ligand PF_3 appears to have very similar π-acidity to carbon monoxide[43] and may completely displace carbon monoxide from carbonyl complexes. Thus $Mo(CO)_6$ will react with PF_3 to form the complete series of complexes $Mo(CO)_{6-x}(PF_3)_x$ where x = 1 to 6.

1.2.2.1.1 The ligands bipy and dpa

The ligands bipy and dpa have been used extensively throughout this work, with their complexes being compared chemically (Chapters 3 to 5) and physically by means of C - O stretching force constants (Chapter 7), hence further discussion in this section will be largely restricted to complexes containing these ligands.

Bipy has an extensive and well reviewed[44-46] coordination chemistry which extends beyond carbonyl compounds to halo-complexes,[44,46] isoleptic compounds such as $Cr(bipy)_3$[47] and to non-metals {e.g. $(bipy)_3B$ and $[bipyCH]^+$}[44]. This ligand is frequently encountered as a substituent in carbonyl complexes, which tend to be less air and moisture sensitive than similar complexes with other N-donor ligands. Table 1-1 summarises the important zero-valent group VI metal carbonyl derivatives containing this ligand.

Table 1-1

2,2'-Bipyridine complexes of the zero-valent group VI elements

Complex	Metal	Ligand (L)	Reference
cis-$M(CO)_4bipy$	Cr,Mo,W		48
fac-$M(CO)_3bipyL$	Cr,Mo,W	py,Ph_3P,$(EtO)_3P$	49
	Mo,W	NH_3,SO_2	50,51
	Mo	Ph_2S, RNH_2	52,53
		R=Et, i-Pr, n-Bu, allyl	
fac-$[M(CO)_3bipyL]^-$	Mo,W	Cl,Br,I,NCS,N_3,CN	54
	Cr	CN,NCS	54
cis-$M(CO)_2(bipy)_2$	Mo,W		55
cis-$M(CO)_2bipyL_2$	Mo	Ph_3P, SO_2	51
	Cr,Mo	$(EtO)_3P$	49
$M(bipy)_3$	Cr,Mo,W		44
$[M(CO)_3bipy]_2$	Cr,Mo,W		56

The ligand dpa has not been studied in as much depth as bipy, but its general chemistry seems similar to that of bipy. Many metal complexes of dpa are known (Table 1-2), and its coordination chemistry has been reviewed.[57] However, the metal carbonyl chemistry seems to have been completely ignored, with the exception of the complex $Mo(CO)_4dpa$.[59]

Table 1-2

Selected metal-di-(2-pyridyl)amine complexes

Complex	M	L[a]	Geometry	Ref.
$M(CO)_4dpa$	Cr,Mo,W		cis-oct	58,59
$M(CO)_3Ldpa$	Mo	Py,MeCN, Ph_3PO	fac-oct	58
ML_4dpa	Mo	Br	cis-oct	58
$ML_2(dpa)_2$	Fe,Ni	Cl,Br,NCS	trans-oct	60,61,62
	Co	NCS	oct	63
$[ML_2(dpa)_2]L.H_2O$	Co	Br	cis-oct	64
$[M(dpa)_3]L_2$	Fe,Co,Ni	I,ClO_4	oct	60-63,65
$[ML(dpa)_2]L$	Cu	Cl,I*	T.B.P.[b]	66,67
ML_2dpa	Ni	Cl	oct,tet?	60,62
	Ni	Br,I	tet	60,62
	Fe,Co	Cl,Br,I		61,63
$[M(dpa)_2]L_2$	Cu	ClO_4*,PF_6	tet	66,68

(a) For entries marked with an asterisk the structure has been confirmed by X-ray analysis

(b) T.B.P. stands for trigonalbipyramidal.

The work in this thesis demonstrates that, at least for the group VIA metals, the ligands dpa and bipy have similar metal (0) carbonyl chemistries, but differences are more pronounced in the allyldicarbonyl series [MX(η^3-allyl)$(CO)_2L_2$]. Differences between bipy and dpa occur because of the following factors.

(i) Due to the acyclic amine group, coordinated dpa is far more flexible than coordinated bipy. This allows dpa to more readily temper its geometry to the steric and electronic requirements of the metal atom.

(ii) The ligand dpa is a stronger base than bipy (pK_a values of 6.99[57] and 4.44[69] respectively).

(iii) It is possible for the acyclic amine group of dpa to enter into chemical reactions as discussed in section 1.2.2.2.

(iv) In sterically crowded molecules the acyclic amine group may have a significant effect on the structure adopted.

(v) The ligand dpa in a strain free configuration will form a dihedral angle between each of its pyridine rings and the $N_2M(CO)_2$ plane,[57] and as such the pyridine rings will not be available for back-bonding with the metal. Whereas it has been suggested[70] that bipy acts as a weak π-acid in its metal carbonyl complexes.

(vi) The chelate rings formed by bipy and dpa are five- and six-membered respectively. Thus on comparison with the ligands 1,2-diaminoethane (en) and 1,3-diaminopropane (pn),[71] which also form five- and six-membered rings respectively, one might expect bipy to exhibit the greater chelate effect.

However, inspection of molecular models and crystal structures[72,73] reveal that bipy causes a compression of the NMoN bond angle of approximately 18° for octahedral molybdenum(0) complexes. Whereas Mossbauer spectroscopy shows that both $[Fe(dpa)_3]^{2+}$ and $[Fe(tpa)_2]^{2+}$ have accurate O_h symmetries[57,61,65]. Similarly molecular models indicate that dpa should cause very little compression of the NMN bond angle in molybdenum and tungsten(0) species. Thus dpa may possibly exhibit a greater chelate effect than bipy.

1.2.2.2 Attack on coordinated ligands.

So far only substitution reactions occurring at the metal atom have been considered. It is also possible for reactions to occur at the coordinated ligands, thereby modifying the ligand. The coordinated ligand may undergo intramolecular attack by a species coordinated to the same metal atom, which effectively leads to an insertion reaction, or react with non-coordinated ligands. In this latter case the metal is supporting and activating one of the reactants, generally towards nucleophilic attack (e.g. carbene formation.[74])

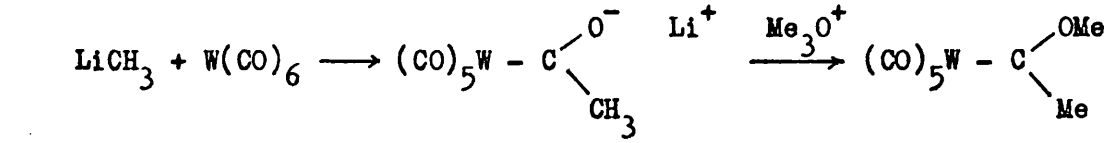

In this type of reaction the metal ion often acts as a template holding the ligand in the correct geometry for addition or substitution reactions to occur. Examples of two of the many known ligand substitution reactions are given below.[17,75,76]

Friedel-Craft acylation:

$$Cp_2Fe + MeCOCl \xrightarrow{AlCl_3} (\eta^5\text{-}MeCOC_5H_4)_2Fe + 2HCl$$

Halogenation:

$$(acac)_3Cr + 3Br_2 \longrightarrow (2\text{-bromoacac})_3Cr + 3HBr$$

These reactions are thought to involve the attack of an electrophile at the reaction site followed by the liberation of a proton to give the observed products.

With some ligands, such as dpa, one could additionally propose a dissociative mechanism (e.g. Scheme 1-1)

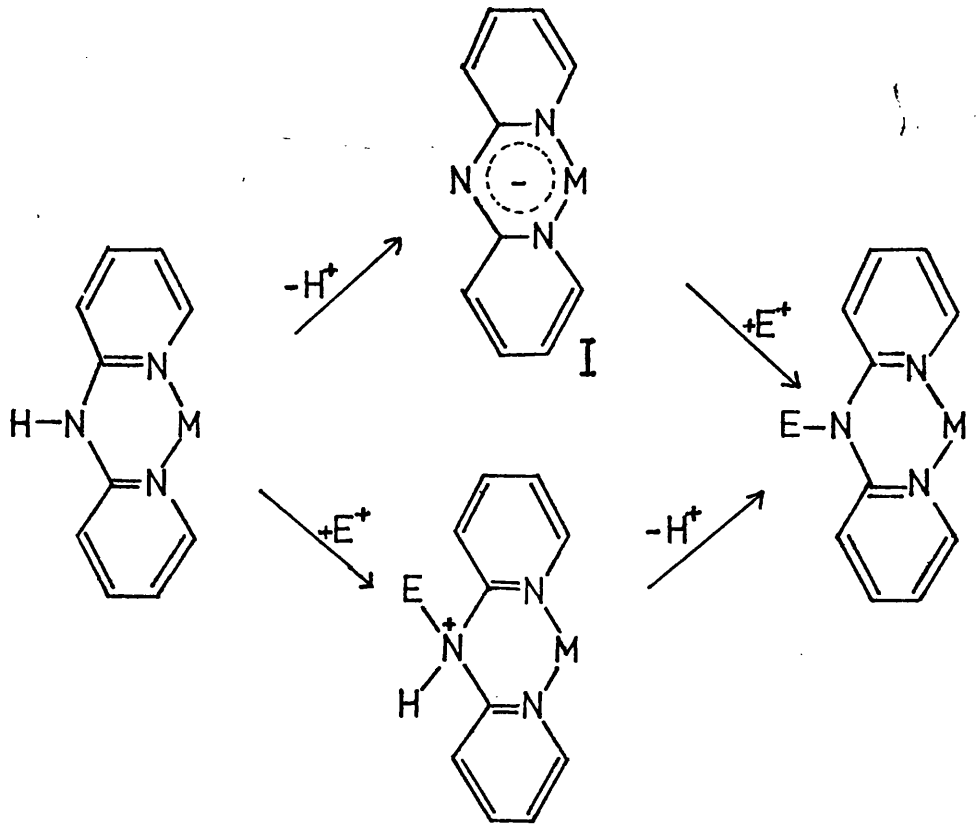

Scheme 1-1 Possible substitution mechanisms for dpa complexes.

The deprotonated ligand (dpa-H) has been isolated in the complex $Pd(dpa-H)_2$ [75] but an X-ray study revealed that the pyridine rings are far from coplanar and therefore the chelate ring cannot exhibit much delocalisation (e.g. I in scheme 1-1). Thus the negative charge created by deprotonation will be largely localised on the acyclic amine atom.

The protonated ligand (dpa) is geometrically more favourable for complex formation than the deprotonated species, as the pyridine rings are aromatic and the pyridine - pyridine dihedral angle will relieve any NMN bond angle compression. Consequently deprotonation is not a general property of dpa complexes and has only been observed with the metals palladium, nickel and copper, and even then electrophilic addition was only possible with the palladium complex.[75]

1.2.2.3 Redox reactions of metal carbonyl complexes.

Redox reactions may be divided into two broad classes (i) electrochemical and (ii) chemical redox systems. This latter category may be further divided for convenience into (ii, a) chemical reductions and (ii, b) chemical oxidations.

1.2.2.3.1 Electrochemical redox reactions

Electrochemistry has an important role to play in the oxidation and reduction of carbonyls. For synthesis, the electrode has the advantages over chemical reagents that (A) by controlling the electrode potential it is possible to introduce energy selectively and hence to control or vary the number of electrons transferred,

and (B) the electrode is often able to simply add or remove an electron from the molecule without causing change in coordination number and stereochemistry as generally occurs with redox reagents. In addition it is possible to determine whether the reaction is reversible and to gain information about the ease of electron transfer.

Both binary metal carbonyls and substituted metal carbonyls have been studied by this technique,[77-81] but few successful anodic oxidations of simple metal carbonyls have been reported.[77] Table 1-3 contains a selection of group VI carbonyl species prepared by this technique.

Table 1-3

Group VI carbonyl species prepared by electrochemical redox reactions

Complex	Reactant	Solvent	Electrode	Ref.
$[Cr(CO)_6]^+$	$Cr(CO)_6$	THF	Pt	77
$[Cr_2(CO)_{10}]^{2-}$	$Cr(CO)_6$	MeCN	Pt	82
$[M_2(CO)_{10}]^{2-}$	$M(CO)_6$ M=Cr,Mo,W	THF	Pt	77
$[CrX(CO)_5]^{n+}$ n=0,1	$[CrX(CO)_5]^-$ X=halide	CH_2Cl_2	Pt	80
$[M(CO)_2(dppe)_2]^{n+}$ n=0,1,2	$M(CO)_2(dppe)_2$ M=Cr,Mo,W,Mn	Me_2CO, CH_2Cl_2, $MeNO_2$	Pt	79
$[MoF(CO)_2(dppe)_2]^+$	$Mo(CO)_2(dppe)_2$	Me_2CO	Pt	79
$[M(CO)_4bipy]^-$	$M(CO)_4bipy$ M=Cr,Mo,W	$(MeOCH_2)_2$	Hg	78
$[M(CO)_4bipy]^+$	$M(CO)_4bipy$ M=Cr,Mo,W	CH_2Cl_2	Pt	81

These studies sometimes yield interesting results when compared with chemical reactions. Thus mild chemical oxidation of the group VI metal carbonyls with for example, iodine yields the relatively stable chromium(I) complex $CrI(CO)_5$ but no stable chromium(II) species, whereas molybdenum and tungsten will form stable metal(II) species [eg. $MX_2(CO)_4$, where X = Cl, Br or NCS] but no isolable metal(I) complexes analogous to chromium. An electrochemical investigation of the complexes $[MX(CO)_5]^-$ (M = Cr, Mo or W and X = Cl, Br or I)[80] substantiates these chemical observations. Molybdenum and tungsten(I) halocarbonyls readily disproportionated to give metal(II) species, whereas chromium(II) halocarbonyls were only stable at -75^oC.

Investigation of the phosphine complexes $[M(CO)_2(dppe)_2]^{n+}$ (M = Cr, Mo, W or Mn and n = 0, 1 or 2)[79] proved particularly interesting from a stereochemical view point. Thus for the molybdenum(0 and II) complexes the cis-isomer is the normally more stable species, whereas for the molybdenum(I) complex the trans-isomer is more stable. During these electrochemical redox reactions the electron transfer process is far more rapid than the stereochemical changes thus it proved possible to study, and differentiate between, all the cis/trans- isomers of these complexes. In addition it was found that the group VI metal(II) species could accept a nucleophile thus forming a more stable seven-coordinate species.

e.g. $[Mo(CO)_2(dppe)_2]^{2+} + F^- \longrightarrow [MoF(CO)_2(dppe)_2]^+$

The resulting complex $[MoF(CO)_2(dppe)_2]^+$ is unusual as metal fluorocarbonyls are rare[83]. This is partly a consequence of the high oxidising power of fluorine preventing it being employed in a similar manner to the other halogens, and it seems quite feasible that under the mild conditions of anion exchange used in chapter 3 that fluoro-analogues may be isolable.

The electrochemical behaviour of the complexes $M(CO)_4$bipy (M = Cr, Mo or W) has also been studied[78,81], and it was observed that on reduction[78] the additional electron occupied a molecular orbital on the bipyridyl ligand. This was confirmed by the esr spectrum of the reduced species which exhibited no hyperfine splitting due to interaction of the unpaired electron with the central metal atom.

1.2.2.3.2 Chemical reductions

Since the metals are already zero-valent in the group VI hexacarbonyls, oxidation reactions are far more common than reductions. However, reaction with strong reducing agents such as the alkali metals or sodium borohydride results in anion and hydride formation.

$$M(CO)_6 + M' \xrightarrow{HMPA} M_2(CO)_{10}^{2-} \longrightarrow M(CO)_5^{2-} \quad 84$$

M' = alkali metal M = Cr, Mo or W

$$M(CO)_6 + NaBH_4 \xrightarrow{THF} HM(CO)_5^- \longrightarrow H_2M_2(CO)_{10}^{2-} \quad 85,86$$

M = W

It has been suggested that the carbonyl monoanions resemble pseudohalide ions in some of their reactions,[87] and the dianions may be classified as transition-metal pseudochalcogenides. A crystal structure determination on the $[Cr_2(CO)_{10}]^{2-}$ ion shows it to be isostructural with the isoelectronic group VII carbonyls $M_2(CO)_{10}$.[88] However, it is substantially more reactive than the group VII decacarbonyls and both $[M_2(CO)_{10}]^{2-}$ and $[M(CO)_5]^{2-}$ ions have a useful synthetic future.

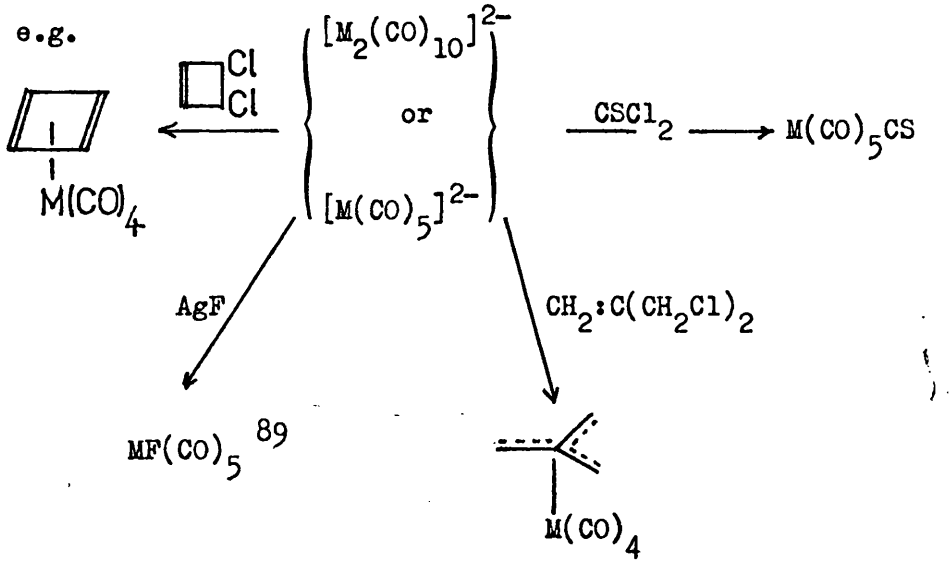

Borohydride reduction of these hexacarbonyls leads to anionic hydride derivatives, rather than simple carbonyl anions. Both $[(CO)_5W(H)W(CO)_5]^-$ and $[H_2W_2(CO)_8]^{2-}$ have been shown to contain hydrogen bridges. In the former anion, the bridge is linear and the carbonyl groups are in an eclipsed configuration for the tetraethylammonium salt, whereas the $[(Ph_3P)_2N]^+$ salt shows a bent bridge with the carbonyl groups staggered.[91]

1.2.2.3.3. Chemical oxidations

As the oxidation state of the metal increases so the M - CO bond weakens. Thus in the absence of controlled conditions halogen oxidations of carbonyls or their derivatives will normally lead to the complete expulsion of carbon monoxide and the formation of metal (IV,V or VI) halides or halocomplexes[45,46,92]. under carefully controlled conditions it is possible to obtain metalhalocarbonyl complexes from binary metal carbonyls or their substitution products.

e.g. $Mo(CO)_6 + Cl_2 \longrightarrow MoCl_2(CO)_4 + 2CO$

$MoCl_2(CO)_4 + bipy \longrightarrow MoCl_2(CO)_3bipy + CO$

$Mo(CO)_4bipy + Cl_2 \longrightarrow MoCl_2(CO)_3bipy + CO$

Table 1-4 lists some of the seven coordinate metal(II) complexes of known structure[93] which have been obtained by such halogen oxidations.

In general metal carbonyl complexes liberate all their carbon monoxide if the oxidation number of the metal is raised above two. The complexes $CpMX_3(CO)_2$[101], where M = Mo or W and X = Cl, Br or I, are exceptional and probably owe their existence to the cyclopentadienyl ring system which is capable of considerably reducing the charge on the metal atom. This is supported by the observation that the cyclopentadienyl ligand in these complexes is far more positive than in normal metallocenes.[27] In addition photoelectron and infra-red spectroscopy both indicate the presence of high electron density on the carbonyl carbon atoms.[27]

Table 1-4

Selected halogen oxidation products.

Complex	Structure[a]	Reference
$Et_4N[WBr_3(CO)_4]$	COC	94
$[WI(CO)_4diars]I$	CTP	95
$MoCl_2(CO)_3(Et_3P)_2$	COC	93
$MoBr_2(CO)_3(dppe)$	COC	96
$WBr_2(CO)_3(dpam)_2$	COC[b]	97
$WI_2(CO)_3(dpam)$	COC	93
$WI_2(CO)_3(dmpe)$	COC	98
$MoCl_2(CO)_2(Me_2PhP)_3$	COC/CTP	99
$MoCl_2(CO)_2(dppm)_2$	COC/CTP[c]	93
$MoCl_2(CO)_2(dpam)_2$	COC[c]	93
$MoBr_2(CO)_2(Me_2PhP)_3$	COC	93
$MoBr_2(CO)_2(dpam)_2$	COC[c]	100
$[WI(CO)_2(dmpe)_2]I$	CTP	93

a) COC = capped octahedral

CTP = capped trigonalprismatic (see section 1.2.3.)

b) monodentate dpam

c) one monodentate and one bidentate dpam or dppm

Such oxidation reactionsare not restricted to the halogens and pseudohalogens and many neutral molecules (for example, metal halides and their derivatives) are capable of oxidative addition reactions with metal carbonyl complexes. Table 1-5 contains some such reaction products for which the crystal structures have been determined.

Table 1-5

Metal(II) complexes from oxidative addition reactions

Oxidant	Reductant	Product	Geometry	Ref.
$M'X_4$	$M(CO)_4L_2$	$MX(M'X_3)(CO)_3L_2$[a]		102
M'=Sn,Ge	M=Mo,W			
X=Cl,Br,I	L_2=bipy,phen,dppe			
$GeCl_4$	$Mo(CO)_4$bipy	$MoBr(GeBr_3)(CO)_3$bipy[b]	COC/CTP	103
$SnMeCl_3$	$M(CO)_4L_2$	$M(\mu\text{-}Cl)(SnMeCl_2)(CO)_3L_2$	COC	104, 105
	M=Mo; L_2=bipy			
	M=W; L_2=dth			
$SnCl_4$	$Mo(CO)_4$dppe	$[Mo(SnCl_3)(CO)_4dppe]^+$ $[SnCl_5(OH_2)]^-C_6H_6$	COC	106, 107
$HgCl_2$	$Mo(CO)_4$bipy	$MoCl(HgCl)(CO)_3$bipy	COC/CTP	108

a) All possible combinations were not isolated.

b) The initial product, $[MoCl(GeCl_3)(CO)_3bipy]$, was treated with sodium bromide.

Of particular interest are the reactions of metal carbonyl derivatives with organic halides, which provide a very valuable route for the synthesis of organometallic complexes.[109-112]

e.g.

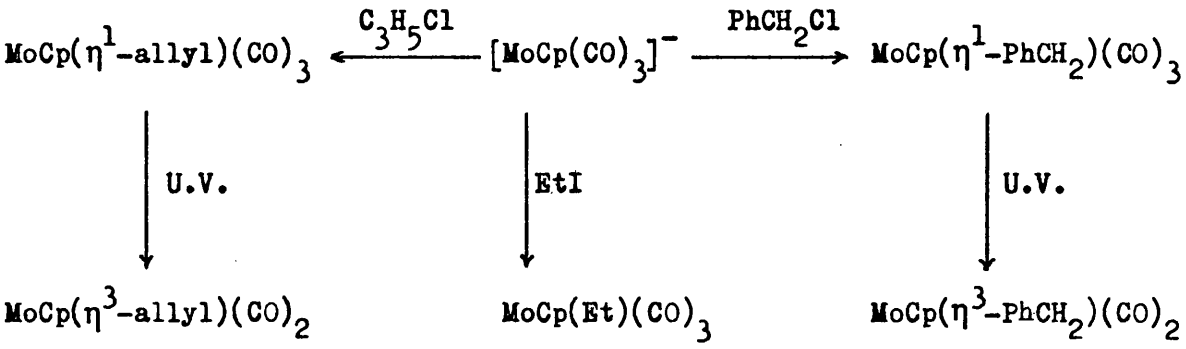

In oxidations employing allylic halides (e.g. C_3H_5Cl and $PhCH_2Cl$) η^1-allyl complexes are not always isolable.[113,114]

e.g. $Mo(CO)_4bipy + C_3H_5Cl \longrightarrow MoCl(\eta^3\text{-allyl})(CO)_2bipy$

1.2.2.3.3.1 Mechanism of oxidative addition

Kinetic studies have been made on several oxidative addition and elimination systems [e.g. $M(CO)_4bipy/HgX_2$(M = Mo or W and X = Cl or Br);[115] $Pd(Ph_3P)_4$/benzyl chloride[116] and McRh/n-butyl bromide/LiCl(Mc = a tetradentate macrocycle)[117]] and the evidence, in these cases, points quite strongly to an ionic Sn2 mechanism as shown in scheme 1-2.

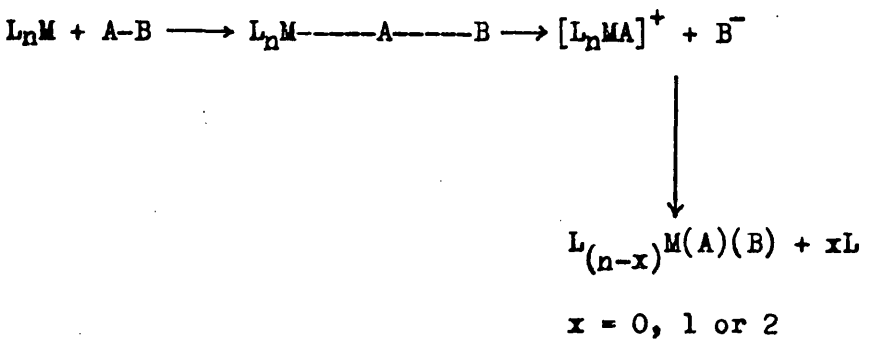

Scheme 1-2. A general S_n2 mechanism for the oxidative addition reaction between L_nM and AB.

The main evidence for such a mechanism is summarised below:

(i) The reaction between optically pure PhCHDCl (α-deuterobenzyl chloride) and $Pd(Ph_3P)_4$ leads to an optically active product $PdCl(PhCHD)(Ph_3P)_2$ [116], in which inversion has occurred at the chiral carbon atom. The optical activity falls to only 50% of that required for the optically pure product (i.e. 25% racemisation has occurred). Inversion at the chiral centre and the retention of optical activity is consistent with an S_n2 mechanism, whereas a radical mechanism should lead to complete racemisation of the product. Hence the 25% racemisation that was observed could be indicative of a competing radical mechanism, but Stille and co-workers consider that racemisation is probably the result of a $\sigma - \pi - \sigma$ benzyl isomerisation.

This reaction has also been studied in the presence of t-nitrosobutane, which acts as a spin trap (i.e. it indicates the presence of radicals), and the resulting esr spectrum was used to support a free radical mechanism; but Stille et. al. found that the same esr signals were formed on adding the spin trap to the isolated product, and consequently such evidence must be regarded as rather inconclusive.

(ii) The complex McRh (Mc = a tetradentate macrocycle) reacts with n-butyl bromide to give the oxidation product trans-[Br(n-Bu)RhMc][117], but when the reaction was carried out in the presence of lithium chloride the analogous chloro-complex was obtained. It was also found that the bromo-product would not undergo anion exchange with lithium chloride under the conditions employed. In addition the ionic complex $[McRh(Me)(MeCN)]BPh_4$ was isolated from the methyl bromide. oxidation which was carried out in the presence of MeCN and $NaBPh_4$.

A mechanism involving an ionic intermediate has also been suggested for the mercuric halide oxidation of the substituted group VI carbonyls,[115] although the proposed reaction scheme was not proved conclusively.

Hence it would appear that an ionic mechanism probably does predominate in these systems but, at this stage, it is not possible to completely discount radical mechanisms as competing or alternative reaction routes.

1.2.3. Seven-coordinate carbonyl complexes.

The majority of complexes discussed in this thesis can be formally considered as seven-coordinate metal(II) species [e.g. $WBr(\eta^3\text{-allyl})(CO)_2bipy$ and $Mo(\eta^3\text{-allyl})(acac)(CO)_2py$] in which the allyl group acts as a bidentate ligand. Alternatively such species may be regarded as six-coordinate complexes with the allyl group occupying only one coordination site. The diamagnetism of these d^4-complexes is in agreement with the seven-coordinate formalism which would lead to the four d-electrons occupying the degenerate $d_{x^2-y^2}$ and d_{yz} metal orbitals.[93]

Recently Drew[93] has extensively reviewed seven-coordinate structures and fortunately of the 34 possible geometries only 3 are normally encountered, namely pentagonal bipyramidal (PB), capped octahedral (COC) and capped trigonal prismatic (CTP) (Figure 1-7). These are idealised geometries and will normally be distorted, especially for the COC and CTP structures, which by means of a small angle change can adopt a low energy intermediate structure COC/CTP which is frequently encountered. This last structure is normally discussed in terms of either one or both of the idealised geometries COC and CTP.

The PB structure is the most commonly observed polyhedron for seven-coordinate species {e.g. $[Mo(CN)_7]^{5-}$}[93] and is encountered with mono- and polydentate ligands.

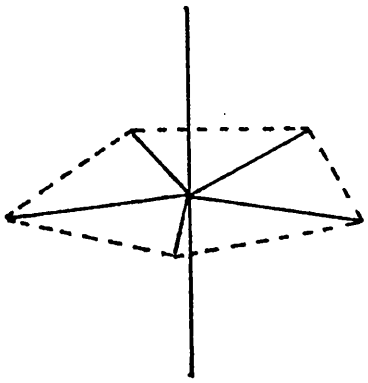

Pentagonal bipyramid

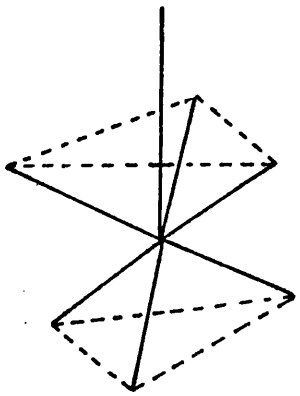

Capped octahedron

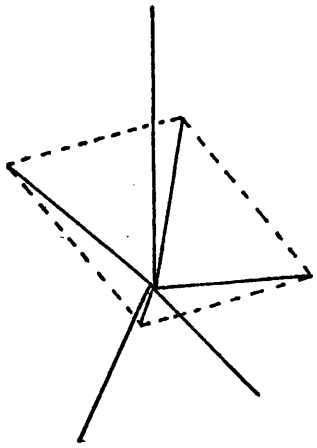

Capped trigonal prism

Figure 1-7. Common seven coordinate geometries.

The COC structure is frequently found for molybdenum and tungsten(II) carbonyl halides {e.g.$[WBr_3(CO)_4]^-$}[93] and complexes containing phosphorus or arsenic donor ligands [e.g. $MoCl_2(CO)_3(Et_3P)_2$].[93]

This may be a consequence of the fact that this geometry allows up to four carbonyl groups to be mutually cis to each other, thereby avoiding any competition between CO groups for the available metal-d_{π} electron density. In addition it is found that this ligand arrangement is often encountered for $ML_5(L-L)$ species [e.g. $MoBr_2(CO)_3dppe$].[93]

The third geometry CTP is not frequently found for monomeric complexes but known examples usually involve molybdenum or tungsten(II) species {e.g. $[MI(CO)_4diars]^+$}[93]. This may be a consequence of the d^4 electron arrangement in these species.

Even though the CTP geometry is rare many examples of the COC/CTP distorted geometries are known [e.g. $MoCl(HgCl)(CO)_3bipy$].[93] Of all the transition metals molybdenum and tungsten exhibit the most extensive seven-coordinate chemistry which is especially prevalent for the metal(II) species.

Unfortunately Drew has in general omitted organometallics from his review[93], hence allyl complexes were not discussed. Complexes of the type $[MX(\eta^3\text{-allyl})(CO)_2L_2]$ adopt the CTP geometry with the allyl group occupying the two coordination sites on the unique edge of the polyhedron[93] (i.e. trans to the capping position). Hence whilst the CTP structure is relatively rare for inorganic complexes it appears to be the predominant geometry for the above metal-allyldicarbonyl complexes[72,73,111,118-128]. Such compounds will be discussed further in section 1.3.1.3.

1.3. Organometallic chemistry

Formally any compound which contains a carbon-metal bond may be placed in this category. Thus metal carbonyl complexes may be classified as organometallic species, but as their chemical behaviour is considerably different from "normal" organometallic compounds, such complexes are invariably considered separately.

σ-Bonded organometallic compounds of the transition metals generally tend to be thermally unstable, even though they may contain quite strong M - C bonds. For example the M - C stretching force constants (K_{mc}) for Me_4Ti is 2.28 mdyneÅ^{-1} compared with a value of 2.25 mdyneÅ^{-1} for Me_4Sn. However, Me_4Ti decomposes at ca. -40°C whereas Me_4Sn is stable at room temperature.[129] Hence this observed instability must be a consequence of kinetic rather than thermodynamic factors, and four low energy decomposition pathways[129,130] have been suggested as follows:

α-hydrogen elimination: $M - CH_3 \longrightarrow MH + \frac{1}{2}C_2H_4$

β-hydrogen elimination: $M - CH_2CH_2R \longrightarrow MH + CH_2{:}CHR$

reductive elimination: $YM - CH_2CH_2R \rightarrow M + YCH_2CH_2R$

dinuclear elimination: $2\,M - CH_2R \longrightarrow 2M + RCH_2CH_2R$

The inability of methyl, trimethylsilylmethyl and similar complexes to undergo β-hydrogen elimination is often given as a reason for their greater stabilities.

π-Bonded organo-transition-metal compounds tend to be thermally more stable than the σ-bonded complexes. This is supposedly due to the metal-ligand back bonding increasing the d-orbital splitting energy (Δ), which in turn makes the above decomposition pathways less energetically favourable[131].

1.3.1. Metal allyl complexes.

The allyl ligand (C_3H_5) has two principle modes of coordination to transition metals; a) η^1-bonded and b) η^3-bonded. In addition to the normal symmetric η^3-bonded ligand, examples are known in which the ligand is unsummetrically η^3-bonded.

[e.g. $PtCl(\eta^3\text{-methylallyl})(Ph_3P)$][17], bridging {eg.$[Pt(\mu\text{-allyl})(acac)]_2$}[132] or ionically bonded [e.g. Li(allyl)][133]. Complexes of this last type do not give rise to ions in solution, and therefore must exist in solution as strongly bound ion-pairs.

These various bonding modes may be detected by means of infra-red and nmr spectroscopy, especially the latter, as will be discussed later.

1.3.1.1. η^1-Allyl complexes.

Isolable η^1-allyl complexes of the transition metals are much less common than their η^3-analogues, and are confined largely to the group VIII metals. Nevertheless η^1-bonded species are often postulated as intermediates, of varying degrees of stability, in the preparation of η^3-allyl complexes[134], and in order to account for the dynamic nature of some η^3-allyl complexes.[133]

The η^1-allyl ligand may be thought of as a simple alkyl ligand and as such its bonding will involve the σ-overlap of an sp^3 orbital of the bonding carbon atom with a suitable metal orbital. Consequently in the known solid state structures[132,135,136] the C - C bond lengths of the allyl ligand are significantly different. A typical skeletal structure of a η^1-bonded allyl complex [trans-$PtCl(\eta^1\text{-allyl})(Ph_3P)_2$] is illustrated in figure 1-8.

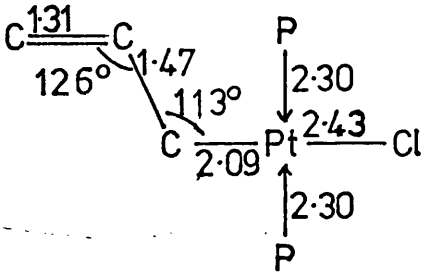

Figure 1-8 The skeletal structure of [$PtCl(\eta^1$-allyl$)(Ph_3P)_2$]

1.3.1.1.1. Infra-red spectroscopy

Several workers have studied the infra-red and Raman spectra of η^1-allyl complexes[137,138] and a tentative assignment has been made for the complex [$Mn(\eta^1$-allyl$)(CO)_5$][137] as listed in table 1-6. This assignment is largely based on comparisons with propene.

Table 1-6.

The vibrational spectrum (4000-700cm^{-1}) of [Mn(η^1-allyl)(CO)$_5$]

Raman[a]	ir[b]	Assignment	
	3085 w	ν_1	ν_{C-H}
	3000 w	ν_2	
	2975 w	ν_3	
	2934 w	ν_5	
	2865 w	ν_4	
1614	1617 s	ν_6	$\nu_{C=C}$
	1465 w		
	1448 w		$\delta_{(H-C=C)}$
1400	1405 w	ν_9- ν_{13}	$\delta_{(C=C-H)}$
	1382 w		$\delta_{(H-C-C)}$
1295	1297 w		
1221	1204 ms		
1082	1080 m		
	1032 w		
	1017 w	ν_{14}-ν_{18}	$\rho_{(C-H)}$
993	989 m		
934	920 w		
	883 s		

a) measured as a benzene solution

b) measured as a CCl_4 solution. The intensities are taken from the thin film spectrum.

For diagnostic purposes the strong band just above 1600 cm^{-1} ($\nu_{C=C}$) is probably the most useful, as it is absent in the spectra of η^3-allyl species.

1.3.1.1.2. ^{1}H-n.m.r. spectroscopy

This form of spectroscopy is far more informative than vibrational spectroscopy. Inspection of figure 1-9 reveals that an $ABCX_2$ pattern is expected for a η^1-allyl species, and

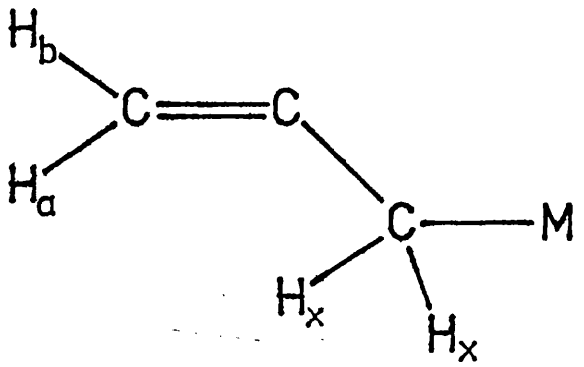

Figure 1-9. An isolated η^1-allyl-metal group.

such a pattern is observed for static systems such as $[Mn(\eta^1\text{-allyl})(CO)_5]$:[139] $\delta(H_a)$=4.92(d, 17 Hz); $\delta(H_b)$=4.68(d, 10 hz); $\delta(H_c)$=6.15(m) and $\delta(H_x)$=1.85(d, 9 Hz) ppm relative to TMS (δ =0). However, it is possible for these systems to be fluxional in which case an AX_4 pattern may be observed, as in the room temperature spectrum of $[Ti(\eta^1\text{-allyl})(Et_2N)_3]$:[133,140] $\delta(H_a, H_b$ and $H_x)$ = 6.45(d, 11 Hz) and $\delta(H_c)$=3.31(m) ppm relative to TMS.

Equivalence of the terminal protons probably occurs by means of a $\sigma-\pi-\sigma$ exchange process. The intermediate π-complex may, in certain cases, be an ionic species as proposed for the dynamic η^1-allyl complexes $(allyl)_2Mg$ and $(allyl)_3B$[133]. On reducing the temperature the rate of interchange of proton environments should slow down and ultimately lead to a static $ABCX_2$ pattern.

1.3.1.1.3 Preparation of η^1-allyl complexes.

These complexes are formed in much the same way as alkyl-metal complexes, although unless carefully controlled the reaction may proceed to a η^3-complex. The principle methods of formation are exemplified below.[17,140,141]

(i) $Na[Mn(CO)_5] + allylX \longrightarrow Mn(\eta^1\text{-allyl})(CO)_5 + NaX$

(ii) $2[Co(CN)_5]^{3-} + allylX \longrightarrow [Co(\eta^1\text{-allyl})(CN)_5]^{3-} + [CoX(CN)_5]^{3-}$

(iii) $TiClR_3 + allylMgX \longrightarrow Ti(\eta^1\text{-allyl})R_3 + MgXCl$

(iv) $Fe(H)Cp(CO)_2 + CH_2{:}CHCH{:}CH_2 \longrightarrow Fe(\eta^1\text{-crotyl})Cp(CO)_2$

(v) $[Co(\eta^3\text{-allyl})(CN)_4]^{2-} + CN^- \longrightarrow [Co(\eta^1\text{-allyl})(CN)_5]^{3-}$

Routes (i) to (iv) are techniques generally used to obtain alkyl complexes, thus only route (v) is specific for this type of compound.

1.3.1.2. η^3-Allyl complexes

This mode of bonding is far more common with transition metals than η^1-bonding.

Structure determinations of a wide variety of these complexes indicate that the allyl group is normally symmetrically bonded (Figure 1-10), with the central carbon atom slightly nearer the metal atom than the two terminal carbon atoms in the molybdenum complexes (Table 1-7). Although in at least

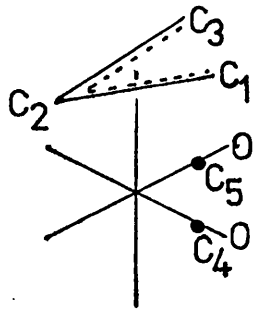

Figure 1-10 Structure of the (η^3-allyl)dicarbonyl metal group.

one example, $[PtCl(\eta^3\text{-methylallyl})(Ph_3P)]$[17], the ligand may be regarded as simultaneously η^1- and η^2-bonded to the metal atom Figure 1-11).

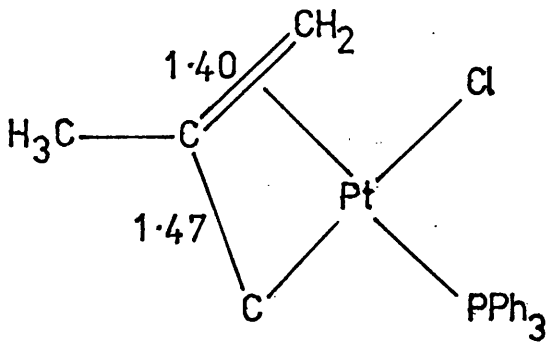

Figure 1-11 An asymmetric η^3-allyl group.

Table 1-7

Geometry of the Mo(η^3-allyl)$(CO)_2$ unit[a]

Ligands	Bond angles(°)[a]	Interatomic distances (Å)							Ref.
	C_1-C_2-C_3	C_1-C_2	C_2-C_3	Mo-C_1	Mo-C_2	Mo-C_3	Mo-C_4	MoOC_5	
bipy, NCS	116	1.42	1.46	2.29	2.20	2.35	1.90	1.96	72
bipy, py	111	1.37	1.47	2.29	2.28	2.31	2.06	1.91	73
dme, CF_3CO_2[b]	114	1.45		2.34	2.16		1.90		119
$PhBpz_3$	116	1.42	1.42	2.34	2.22	2.37			121
Et_2Bpz_2, pzH	117	1.39	1.41	2.34	2.21	2.35	1.95	1.96	120
$H_2B(Me_2pz)_2$	118	1.35	1.42	2.33	2.21	2.36	1.95	1.95	125
L_2[c], Cl	112	1.42	1.42	2.33	2.27	2.33	1.98	1.98	123

a) The atom numbering is given in figure 1-10

b) The pairs of atoms C_1, C_3 and C_4, C_5 were not differentiated in this structure.

c) $L_2 = C_6H_{11}N : CHCH : NC_6H_{11}$

The η^3-allyl ligand has three delocalised π-molecular orbitals[141,142], namely ψ_1 to ψ_3 in figure 1-12. The electron population of these orbitals depends on how one

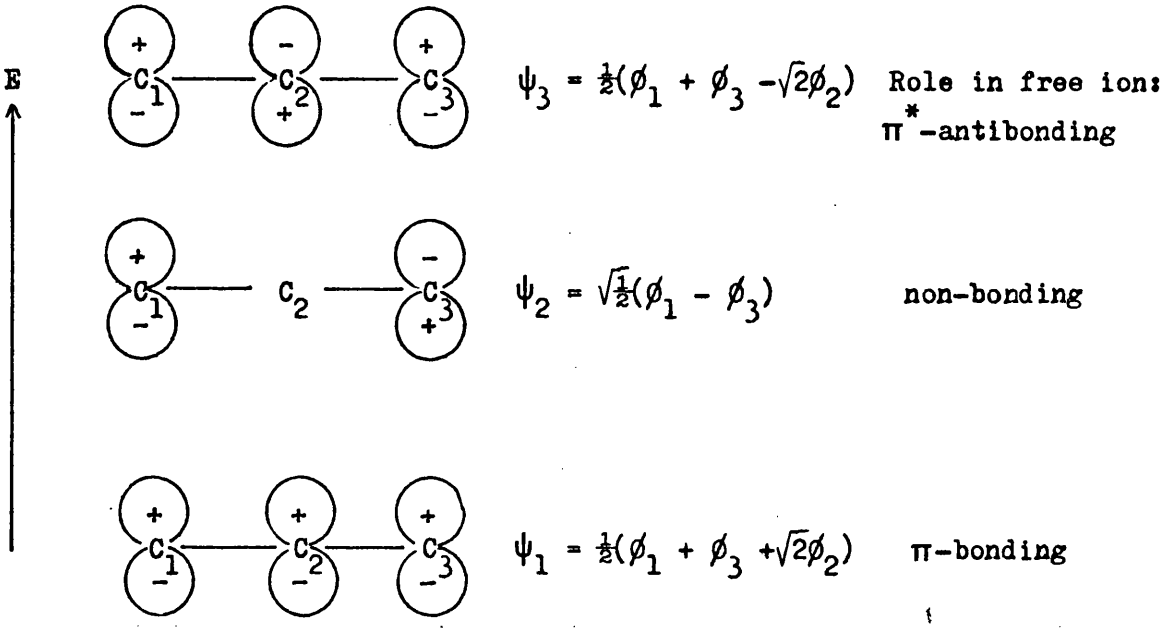

Figure 1-12. Molecular orbitals of the η^3-allyl ligand

chooses to consider the allyl ligand (i.e. as a cation, radical, or anion). In each case ψ_1 will contain two electrons and ψ_3 will be vacant, whilst ψ_2 will be occupied by nought, one or two electrons respectively for the cationic, radical or anionic forms of the ligand.

It is conventional to consider the allyl group as contributing one unit to the oxidation state of the metal. Hence the coordinated allyl group should be considered to be a four electron donor ligand. Thus ψ_1 and ψ_2 are each capable of donating two electrons to the metal atom whereas ψ_3 is

available to accept two electrons from the metal and thereby forming a δ-back bond.

Consideration of the valence orbitals of a metal atom reveals the possible orbital overlaps given in figure 1-13.[131,143]

I $\psi_1 - d_{x^2}$

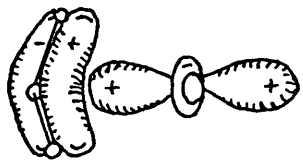

II $\psi_2 - d_{xz}$

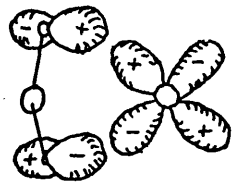

III $\psi_1 - d_{yz}$

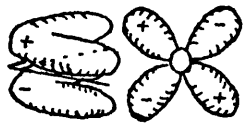

IV $\psi_2 - d_{xy}$

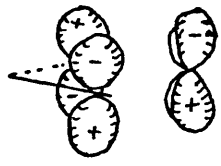

(For clarity the orbital overlap is not shown in IV)

Figure 1-13. Molecular orbital overlaps in η^3-allyl complexes.

The bonding overlaps given in modes I and II (Figure 1-13) are maximised if the allyl group is perpendicular to the z-axis (i.e. as the allyl group is normally pictured), whereas modes III and IV would favour the allyl group lying on the xz plane (i.e. as in a metallocyclobutane). Thus the allyl group will adopt a configuration somewhere between these two extremes so as to maximise the bonding energy. Calculation of the overlap integrals for the various bonding modes shown in figure 1-13 have been made[131,143,144] and the dihedral angle for $[PdCl(\eta^3\text{-allyl})]_2$ is calculated to be about 110^o, which is in good agreement with the observed angle of 111.5^o [131]. Hence bonding modes I and II must be of prime importance in these complexes. In addition it is calculated that very little overlap occurs between ψ_3 and the filled metal - d - orbitals, indicating very little back-bonding in these complexes, although the relative importance and extent of this back-bonding is by no means clear. Some workers feel it is significant whilst others suggest it is negligible[134]. This probable lack of back-bonding is in direct contrast to olefin complexes which owe their stability to this type of bonding.

1.3.1.2.1 Infra-red spectroscopy

Several η^3-allyl complexes[145-150] have been studied by infra-red and Raman spectroscopy, with isotope shifts[146,147] (^1H-^2H and ^{104}Pd - ^{110}Pd) and polarised Raman effects being used to tentatively assign the spectra. Unfortunately the

various workers do not completely agree over the assignment of the pairs of vibrational modes $\nu(C - C - C)_{ass.}$ and $\delta(CH_2)_{ass.}$ or $\nu(C - C - C)_s$ and $\rho_t(CH_2)_s$. This controversy is not critical as both of these pairs of modes will probably be strongly coupled, and therefore each band will be a mixture of the two modes.[146]

Inspection of tables 1-6 (section 1.3.1.1.1) and 1-8 reveal that, even though some assignments may be in doubt, the observation of three moderately intense absorptions in the region 1500 - 1300 cm^{-1} and the absence of an absorption between 1600 and 1700 cm^{-1} in the infra-red spectrum of an allyl complex is strongly indicative of a η^3-allyl group.

Table 1-8

The vibrational spectrum of the η^3-allyl group

allyl $Fe(NO)(CO)_2$ [a]	allyl$Mn(CO)_4$ [b]	allyl$Co(CO)_3$ [c]	$[allylPdCl]_2$ [d]	Assignment
3082 ms	3073 m	3086 w		$\nu(CH_2)$ A"
3048 w	3018 m	3022 w		$\nu(CH)$ A'
3016 m	2972 w	2970 sh		$\nu(CH_2)$ A'
2968 ms	2946 w	2940 w		$\nu(CH_2)$ A'
2932 w	2962 m			$\nu(CH_2)$ A"
1492 s	1394 m	1388 m	1491 w	$\nu(CCC)$ A"
1466 s	1464 s	1476 m	1383 s	$\delta(CH_2)$ A'
1387 s	1499 s	1485 m	1461 s	$\delta(CH_2)$ A"
1229 s	1215 s	1225 m	913 w	$\pi(CH)$ A'
1202 s	1150 w	1186 m	1193 w	$\delta(CH)$ A"
1018 s	1009 m	1071 m	998 m	$\rho_t(CH_2)$ A'
966 ms	1020 m		1024 s	$\nu(CCC)$ A'
926 s	922 m	950 m	968 s	$\rho_w(CH_2)$ A'
916 s	886 m	934 m	943 vs	$\rho_w(CH_2)$ A"
778 ms	773 w	775 m	1230 w	$\rho_r(CH_2)$ A'
752 ms	980 w		767 m	$\rho_r(CH_2)$ A"
722 w	785 m	805 w	767 m	$\rho_r(CH_2)$ A"

a) liquid film, see ref. 146

b) CS_2 solution (CCl_4 used in cut-off regions) see ref. 149

c) liquid film. see ref. 148

d) KBr disc. see ref. 147

1.3.1.2.2. <u>^{1}H-n.m.r. Spectroscopy.</u>

As with η^1-allyl species this form of spectroscopy is also far more informative for η^3-allyl complexes than infra-red spectroscopy. Figure 1-14. shows that an AM_2X_2 [i.e. $H_c(H_s)_2(H_a)_2$]

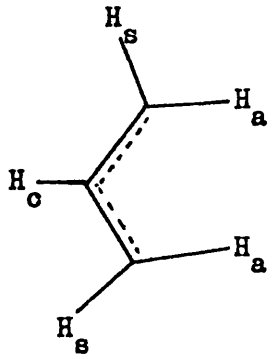

<u>Figure 1-14.</u> An isolated η^3-allyl group

pattern is expected for the η^3-allyl group, provided that $H_s - H_a$ coupling is too small to be observed, and such a pattern is found for static systems such as $[(C_6H_6)Mo(OAc)(\eta^3\text{-allyl})]$ [151]: $\delta(H_c = 3.60(m)$; $\delta(H_s) = 2.92(d,6Hz)$ and $\delta(H_a) = 2.19$ (d,8Hz) ppm relative to TMS.

Assignments of <u>syn</u>- and <u>anti</u>-protons are usually based on the size of the coupling with the H_c proton. By analogy with organic alkene systems (Figure 1-15), <u>trans</u>-coupling constants

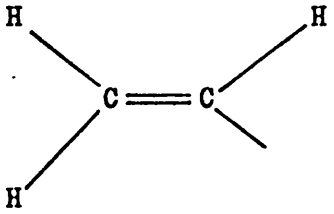

J_{trans} = 12 to 15 Hz

J_{cis} = 6 to 8 Hz

J_{vic} = 0 to 2 Hz

<u>Figure 1-15.</u> Proton coupling constants in alkenes

are expected to be greater than cis- coupling constants, and are typically 9 to 12 and 5 to 8 Hz respectively for η^3-allyl complexes. In a few complexes[152,153] coupling between syn- and anti-protons has been resolved and the H_a and H_s resonances observed as doublets of triplets rather than doublets, and the central proton resonance as fifteen "lines" rather than the normal triplet of triplets predicted by an AM_2X_2 pattern.

However, in some η^3-systems the anti- and syn-protons undergo rapid exchange in which case an AX_4 pattern may be observed [e.g. $Zr(\eta^3\text{-allyl})_4$].

1.3.1.2.3. Fluxional η^3-allyl groups

The η^3-allyl group gives rise to three types of isomerism which are observable by ^{1}H-n.m.r. spectroscopy under the right circumstances. Namely (i) syn-syn, anti-anti exchange, (ii) syn-anti exchange and (iii) conformational changes (rotational isomerism).

(i) Syn-syn, anti-anti exchange

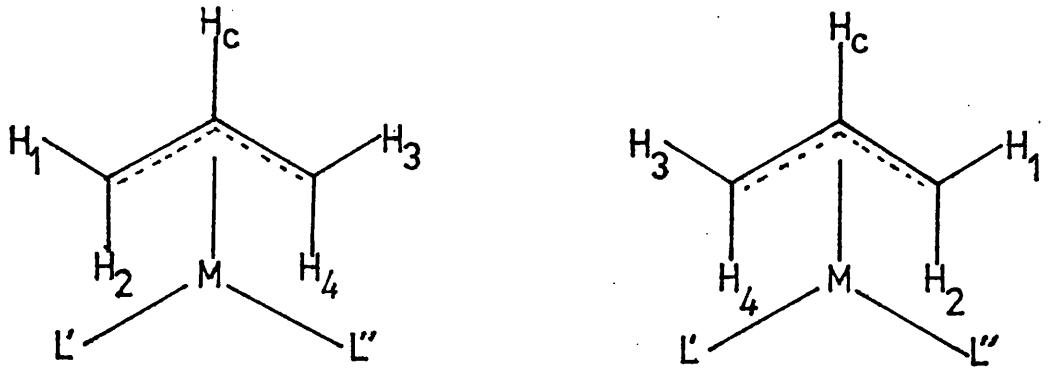

Figure 1-16. Syn-syn, anti-anti proton exchange.

This type of isomerism (Figure 1-16) can only be detected for complexes of low symmetry, such that the terminal allyl carbon atoms are not equivalent (i.e. L' ≠ L"). Thus at low temperatures, or in the absence of excess ligand L' or L", an AMM 'XX' pattern will be observed in the n.m.r. spectrum. Raising the temperature or adding excess ligand will cause the M/M' and X/X' signals to coalesce giving rise to an AM_2X_2 pattern.

Alternatively this process may be thought of as the interchange of the ligands L' and L" (Figure 1-16) which will result in exactly the same experimental observations. Such a process could occur by an associative or dissociative mechanism or by a pseudo-rotation of the molecule. The rate of an associative mechanism should be a function of the concentration of the excess ligand whereas the rate of a dissociative process should be independent of the added ligand. The complex $[PdCl(\eta^3\text{-}2\text{-methylallyl})(Ph_3P)]$[133] shows an associative syn-syn, anti-anti exchange process.

Additionally this form of isomerisation may occur by a rotation about the metal - allyl axis which may be preceded by a ligand association or dissociation reaction. Such rotations are energetically most favourable for five-coordinate species[133], and therefore ligand addition or dissociation may occur to give rise to a pentacoordinate intermediate.

(ii) Syn-anti exchange

This type of isomerism may occur solely at one end, or at both ends of the allyl group. Only in complexes with inequivalent terminal allyl carbon atoms would it be possible to detect the difference between these two processes. The ^{1}H-n.m.r. spectrum of a compound which exhibits syn-anti exchange will typically change from an AM_2X_2 pattern at low temperatures to an AX_4 pattern at higher temperatures.

Exchange at one carbon atom only has been observed for the complex $[(\eta^3$-2-methallyl)$PdCl(PPh_3)]$ [133] and whilst this process primarily involves a π- σ -π mechanism (Figure 1-17) it has been found that the rate is dependent on the concentration

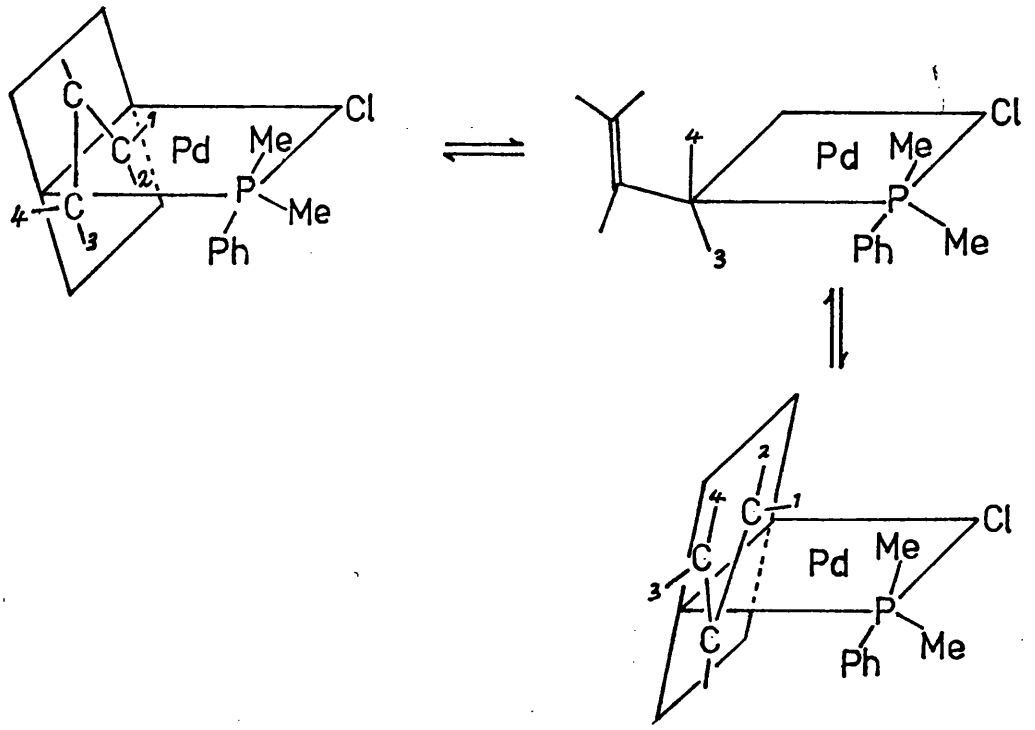

Figure 1-17. Syn-anti exchange of protons 3 and 4.

of the dimer $[PdCl(\eta^3\text{-allyl})]_2$. Thus a mechanism has been suggested[133] which involves complex formation between the monomer and the dimer thereby leading to a η^1-allyl group. This trimeric intermediate probably involves chlorine bridges.[133]

1.3.1.2.4. Preparation of η^3-allyl complexes.

Several general methods of synthesis are available for these complexes, as detailed below, and in addition there are many specific reactions leading to particular complexes as listed later.

(i) General syntheses

(i,a) Allyl-halogen exchange reactions.

These reactions are essentially analogous to the preparation of metal alkyl complexes, and with the exception of $(allyl)SnMe_3$[154,155], probably proceed via a η^1-allyl intermediate.[156]

$$\tfrac{1}{2}[(C_6H_6)MoCl(\eta^3\text{-allyl})]_2 + allylMgCl = (C_6H_6)Mo(\eta^3\text{-allyl})_2 + MgCl_2$$

$$CpMo(CO)_3Cl + allylSnMe_3 = CpMo(\eta^3\text{-allyl})(CO)_2 + SnClMe_3 + CO$$

The synthesis employing $(allyl)SnMe_3$ would not appear to pass through a η^1-allyl intermediate as no such species were observed during the synthesis of $[(\eta^3\text{-allyl})M(CO)_4]$ (M = Mn and Re). In both of these cases the η^1-allyl complex $[(\eta^1\text{-allyl})M(CO)_5]$ is a stable species which does not readily lose carbon monoxide to form the η^3-allyl compound. Thus if these η^1-allyl complexes were intermediates they should be readily detectable.

Abel[154] has suggested an alternative mechanism whereby the uncoordinated olefin double bond of (η^1-allyl)$SnMe_3$ species coordinates to the reacting halide thereby replacing a carbonyl group (Scheme 1-3). This is then followed by the elimination of Me_3SnX and the formation of a η^3-allyl group.

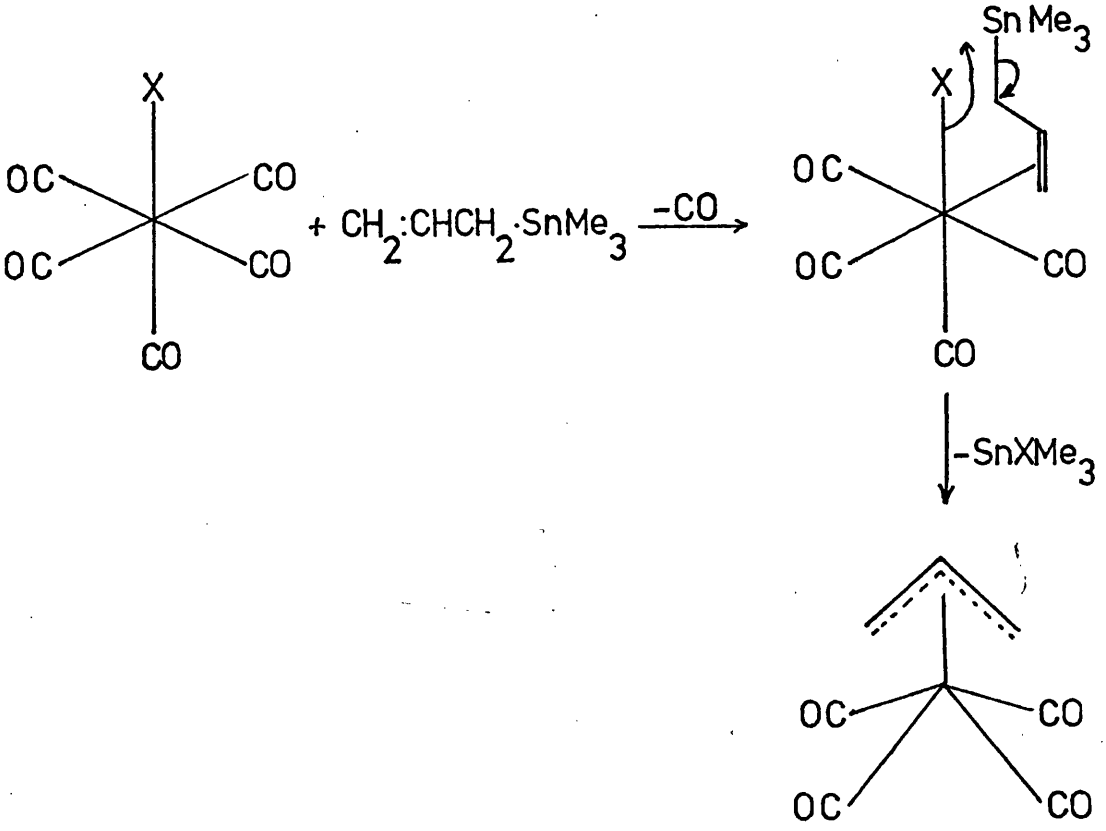

Scheme 1-3. Proposed mechanism for the reaction between allyl $SnMe_3$ and metal halide complexes.

(i,b) Oxidative additions.

Oxidative addition reactions are another general organometallic synthetic method and probably proceed by the formation of a η^1-allyl metal intermediate[134] (cf. Section 1.2.2.3.3.1 and Chapter 3). This is probably the most common procedure employed in the preparation of metal allyl complexes and a few

examples are given below.[113,157,158]

$[Mo(acac)(CO)_4]^- + allylCl = [MoCl(\eta^3\text{-allyl})(acac)(CO)_2]^- + 2CO$

$W(CO)_3pybipy + allylBr = WBr(\eta^3\text{-allyl})(CO)_2bipy + py + CO$

$[CpMo(CO)_3]^- + CH_2 : CHCH_2CH_2Br = CpMo(CO)_2(\eta^3\text{- crotyl}) + CO + Br^-$

It is normally observed that anionic carbonyl complexes are far more reactive towards these oxidative additions than the neutral compounds, which is in agreement with the mechanism proposed in Section 1.2.2.3.3.1 and Chapter 3.

(i,c) Addition of 1,3-dienes to metal hydrides and alkyls.

This method of synthesis was responsible for the isolation of the first recognised η^3-allyl complex, $Co(\eta^3\text{-crotyl})(CO)_3$, and is an example of an olefin insertion into a metal - hydrogen bond. The following reactions are examples of such synthesis[19,159]

$HCo(CO)_4 + CH_2 : CHCH : CH_2 = Co(\eta^3\text{-crotyl})(CO)_3 + CO$

$RMn(CO)_5 + CH_2 : CHCH : CH_2 =$ 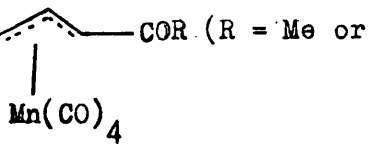 (R = Me or Ph).

The second reaction, that between $MeMn(CO)_5$ and butadiene, has also been examined using 1,1,4,4-tetradeuterobutadiene and it has been shown that a 1,4-hydrogen shift occurs in this reaction[159] giving rise to the η^3-complex of $CD_3\dot{C}H\ddot{C}H\ddot{C}DCOR$

(i,d) Conversion of η^1-allyl to η^3-allyl

As mentioned previously this probably occurs during the synthesis of many η^3-allyl species, but it may also be employed as a separate synthesis as shown below.[110,141,154,160]

$$CpMo(\eta^1\text{-allyl})(CO)_3 \xrightarrow{uv} CpMo(\eta^3\text{-allyl})(CO)_2 + CO$$

$$Mn(\eta^1\text{-allyl})(CO)_5 \xrightarrow[\text{or } t>80^\circ]{uv} Mn(\eta^3\text{-allyl})(CO)_4 + CO$$

$$Cp_2W(\eta^1\text{-allyl})_2 + HPF_6 \longrightarrow [Cp_2W(\eta^3\text{-allyl})]PF_6 + C_3H_6$$

(ii) Less general syntheses

In the literature there are many novel syntheses of specific allyl compounds and some of these are listed below[156,161-167]

$$[\eta^4\text{-}(CH_2)_3C]Fe(CO)_3 + HCl \longrightarrow (\eta^3\text{-2-methylallyl})FeCl(CO)_3$$

$$(\sigma\text{-cyclopropylacyl})Mn(CO)_5 + Ph_3P \longrightarrow (\eta^3\text{-allyl})Mn(CO)_3(PPh_3) + 3CO$$

$$[(\eta^3\text{-allyl})PdCl]_2 + Fe_2(CO)_9 \longrightarrow 2(\eta^3\text{-allyl})FeCl(CO)_3 + 2Pd + 3CO$$

$$2(\eta^7\text{-}C_7H_7)MoBr(CO)_3 \xrightarrow{NaOR} (\eta^3\text{-}C_7H_7)Mo(CO)_2(\mu\text{-OR})_3Mo(\eta^7\text{-}C_7H_7)$$

$$[(C_6H_6)Mo(\eta^3\text{-allyl})(\eta^4\text{-}CH_2CHCHCH_2)]^+ + H^- \longrightarrow (C_6H_6)Mo(\eta^3\text{-allyl})(\eta^3\text{-crotyl})$$

$$NiCl_2 + 2Ph_3P + C_4H_6 + [H] \xrightarrow[C_6H_6]{Zn/EtOH} [(Ph_3P)_2Ni(\eta^3\text{-crotyl})]^+$$

$$CpMo(CO)_3(\eta^1\text{-}CH_2C \vdots CR) + R'OH \longrightarrow \{CpMo(CO)_2[\eta^3\text{-}CH_2C(COOR')CHR]\}$$

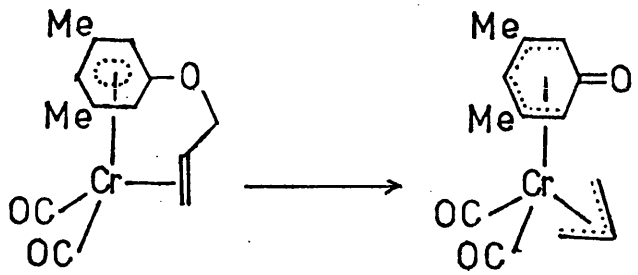

Table 1-9

Allyl complexes of the group VI transition metals

Species [a]	Metal [b]	Other ligands and substituents [b]	References
$M(\eta^1\text{-allyl})_2Cp_2$	Mo,W		160
$M(\eta^1\text{-allyl})Cp(CO)_3$	Cr,Mo,W		87,113,141
$*M_2(\eta^3\text{-allyl})_4$	Cr,Mo		168-170
$M(\eta^3\text{-allyl})_3$	Cr		113, 168
$M(\eta^3\text{-allyl})_4$	Mo,W		168
$MCl(\eta\text{-allyl})_2$	Cr		168
$[M(\eta^3\text{-allyl})Cp_2]^+$	Mo,W		113, 160
$[M(\eta^3\text{-allyl})(\eta^4\text{-}CH_2CHCHCH_2)(C_6H_6)]^+$	Mo		156
$[M(\eta^3\text{-allyl})(C_6H_6)L_2]^+$	Mo	L_2 = dppe,dmpe,dth	171
$M(\eta^3\text{-allyl})(\eta^3\text{-}CH_2CHCHCH_2R)(C_6H_6)$	Mo	R = H, CN, MeO, MeS	156
$M(\eta^3\text{-allyl})(C_6H_6R)L_2$	Mo	R = H, n-Bu; L_2 = dppe, dmpe, dth	171
$M(\eta^3\text{-allyl})(O_2CR)(C_6H_6)$	Mo	R = H, Me, Ph, CH_2CO_2Et	151
$MCl(\eta^3\text{-allyl})(C_6H_6)(Ph_3P)$	Mo		172
$[MCl(\eta^3\text{-allyl})(C_6H_6)]_2$	Mo		151
$M(\eta^3\text{-allyl})_2(C_6H_6)$	Mo		151
$MX(\eta^3\text{-allyl})Cp(NO)$	Mo	X = Cl, Br, I, NCS	26, 173-175

Table 1-9 (Contd)

Species [a]	Metal [b]	Other ligands and substituents [b]	References
$[M(\eta^3\text{-allyl})Cp(NO)(CO)]^+$	Mo		26, 173-175
$MCl(\eta^3\text{-allyl})(CO)_{4-n}(t\text{-BuNC})_n$	Mo	n = 2 to 4	176
$*MX(\eta^3\text{-allyl})(CO)_2L_2$	Mo, W	X = Cl,Br,I,NCS,CF_3CO_2; L_2 = bipy,phen,en, $C_6H_{11}N{:}CHCH{:}NC_6H_{11}$, dppm,dppa,dme,2py,2MeCN, $2Ph_3P$	113,119,177-181
$M(\eta^3\text{-allyl})Cp(CO)_2$	Cr,Mo,W		141,155,158,182
$M(\eta^3\text{-}C_5H_7)Cp(CO)_2$	Cr		141
$*M(\eta^3\text{-allyl})(RBpz_3)(CO)_2$	Mo	R = H, Me, Ph, pz	122,183,184
$*M(\eta^3\text{-allyl})(Et_2Bpz_2)(CO)_2(Hpz)$	Mo		120
$*M(\eta^3\text{-allyl})(R_2Bpz_2)(CO)_2$	Mo	R = H, Et, Ph	125-127
$M(\eta^3\text{-allyl})(R_2C_6H_3O)(CO)_2$	Cr	R = H, Me	167
$*[M(\eta^3\text{-allyl})(CO)_3L'L_2]^+$	Mo,W	L' = NH_3,MeCN,py,Ph_3P,Ph_3As,$(PhO)_3P$; L_2 = bipy,phen MeCN	113,180,185
$[MCl(\eta^3\text{-allyl})(CO)_2L_2]^-$	Mo,W	L_2 = acac, hfacac	157
$[M_2X_3(\eta^3\text{-allyl})_2(CO)_4]^-$	Mo,W	X = Cl, Br, I, MeO, EtO, PhS	113,186,187
$M(\eta^3\text{-}C_7H_7)(CO)_2(\mu\text{-OR})_3M(\eta^7\text{-}C_7H_7)$	Mo	R = Me,Ph	164
$[MCl(\eta^3\text{-allyl})(O_2CR)(CO)_3]^-$	Mo,W	R = Me, t-Bu	157

Table 1-9 (Contd)

Species [a]	Metal [b]	Other ligands and substituents [b]	References
$M_2Cl_3(\eta^3\text{-allyl})(CO)_6$	W		179
$MX(\eta^3\text{-allyl})(CO)_4$	W	X = Br, I	179

a) The term allyl represents the group C_3H_5 and its 2-substituted derivatives. Crystal and molecular structures have been determined for at least one example of each of the species marked with an asterisk.

b) Not all the combinations of the metals, ligands and substituents have necessarily been isolated.

As suggested by the various synthetic routes there are numerous examples of this type of metal - allyl complex and table 1-9 lists a wide range of such complexes for the group VI transition metals.

1.3.1.2.5. Reactions of the η^3-allyl ligand.

The allyl group coordinated to a group VIII metal has been shown to undergo a wide variety of reactions, many of them of great synthetic importance in organic chemistry[188]. Although much less investigated allyl complexes of the early transition metals have also been shown to be catalytically active, and table 1-10 lists metals whose allyl complexes catalyse the polymerisation of olefins.[23] Two such complexes are

Table 1-10

η^3-Allyl complexes active in polymerisation reactions

Olefin monomer	metal
mono-alkenes	Ti, Zr, Hf, Cr, Mo, W, Ni, Pd
vinyls	Ti, Zr, Hf, Cr, Mo, W, Ni, Pd
allenes	Ni, Pd
1,3-dienes	Ti, Zr, Hf, Cr, Mo, W, Co, Rh, Ir, Ni, Pd, Pt

$[M(CF_3CO_2)(\eta^3\text{-allyl})(CO)_2dme]$, where M = Mo or W, which have been found to be catalytically active for the polymerisation of 1,3-butadiene.[119] In addition during this work (cf. chapter 3), and independently of the above workers, it was observed that the complex $[MoCl(\eta^3\text{-allyl})(CO)_2(MeCN)_2]$ would cause the polymerisation of norbornadiene. Neither the polymer, a white brittle solid, nor the actual catalytic species were characterised; but the formation of the polymer appeared to be accelerated by the presence of a little air.

Other non-catalytic reactions of group VI allyl complexes involve reductive elimination of allyl halide or nucleophilic attack on the allyl ligand. This former type of reaction has been usefully employed in the synthesis of molybdenum(0) derivatives,[176,189-192]

(i) $MoBr(\eta^3\text{-allyl})(CO)_2(MeCN)_2 + 3Ph_3P \xrightarrow{C_6H_6}$

$Mo(CO)_2(MeCN)_2(Ph_3P)_2 + [Ph_3PC_3H_5]Br$

$\downarrow L_2$

$Mo(CO)_2(Ph_3P)_2L_2$

L_2 = Lewis bases, dienes or dinitriles

(ii) $MoCl(\eta^3\text{-allyl})(CO)_2(MeCN)_2 + 4RNC \longrightarrow Mo(CO)_2(RNC)_4 +$ allyl Cl $+ 2MeCN$

R = Me or Et

while nuoleophilic addition has resulted in the isolation of metallocyclobutane derivatives or olefin complexes.[160,182,193]

(iii) $[Cp_2W(\eta^3\text{-allyl})]^+ \xrightarrow{NaBD_4}$ 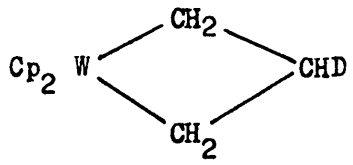

(iv) $[Cp_2W(\eta^3\text{-allyl})]^+ \xrightarrow{H^-} Cp_2W(\eta^2\text{-}CH_3CH{:}CH_2)$

(v) $CpMo(\eta^3\text{-crotyl})(CO)_2 \xrightarrow{Ph_3C^+} CpMo(CO)_2(\eta^4\text{-}CH_2{:}CHCH{:}CH_2)$

1.3.1.3. [$MX(\eta^3$-allyl$)(CO)_2L_2$] and related complexes.

Crystal structure determinations are limited to complexes of the type $M_2(\eta^3\text{-allyl})_4$ {M = Cr or Mo}, $[MX(\eta^3\text{-allyl})(CO)_2L_2]$ {M = Mo or W}, $[Mo(\eta^3\text{-allyl})(CO)_2L_3]$ and $[Mo(\eta^3\text{-allyl})(CO)_2L'L_2]^+X^-$. The first of these contains a multiple metal - metal bond and is related to the other chromium and molybdenum(II) metal-metal bonded species[16,194] $M_2(O_2CR)_4$ {M = Cr or Mo}, $Mo_2Cl_8^{4-}$ and $Mo_2(SO_4)_4^{4-}$, whereas the remaining complexes all contain the apparently stable $Mo^{II}(\eta^3\text{-allyl})(CO)_2$ entity. These latter complexes are formally seven-coordinate molybdenum(II) species, and the majority adopt the symmetric CTP structure shown in figure 1-18(A) and discussed in section 1.2.3, but several examples of the assymmetric CTP structure are also known Figure 1-18(B) .

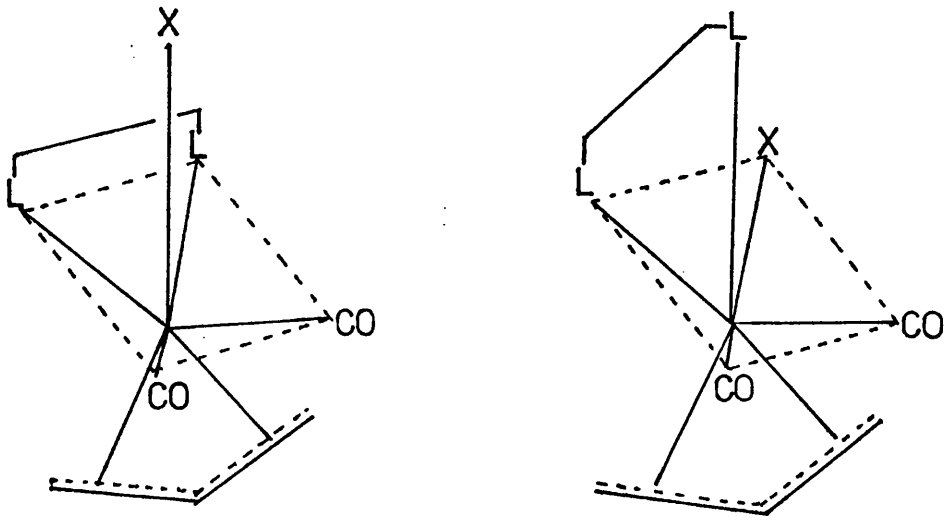

A.

L_2 = bipy; X = NCS, py

L_2 = phen; X = NCS

L_2 = $(C_6H_{11}NCH)_2$; X = Cl

L_2 = dme; X = O_2CCF_3

L_2 = Et_2Bpz_2; X = Hpz

B

L_2 = H_2Bpz_2; X = μ - H

L_2 = Ph_2Bpz_2; X = vacant

L_2 = dppe; X = Cl

Figure 1-18. Structures found for $[MX(\eta^3\text{-allyl})(CO)_2L_2]$ species

These seven-coordinate complexes were first reported by Murdoch[186] who prepared them by cleavage of the tri-halo-bridged anions (see below), Hull and Stiddard[113] subsequently reported

$$[Mo_2Cl_3(\eta^3\text{-allyl})_2(CO)_4]^- + 4py \longrightarrow 2[MoCl(\eta^3\text{-allyl})(CO)_2py_2] + Cl^-$$

two new preparative procedures for such species. These routes involved either the oxidative addition of allyl halides to the

complexes $Mo(CO)_4L_2$ and $M(CO)_3pyL_2$ (M = Mo or W and L_2 = bipy or phen) or anion exchange of the halogen in the resulting metal(II) complexes.

e.g. $Mo(CO)_4bipy + allylNCS \xrightarrow{THF} Mo(NCS)(\eta^3\text{-allyl})(CO)_2bipy + 2CO$

$C(CO)_3pybipy + allylBr \xrightarrow{THF} WBr(\eta^3\text{-allyl})(CO)_2bipy + CO + py$

$MoBr(\eta^3\text{-allyl})(CO)_2bipy + C_6F_5S^- \xrightarrow{Me_2CO} Mo(\eta^3\text{-allyl})(SC_6F_5)(CO)_2bipy + Br^-$

In this way these authors isolated and reported 29 complexes with the general formula $[MX(\eta^3\text{-allyl})(CO)_2L_2]$ and $[M(\eta^3\text{-allyl})(CO)_2pyL_2]^+$ (cf. Table 1-9), and showed that the carbonyl groups were <u>cis</u> to each other and that the allyl group was coordinated in a trihapto-manner. Other complexes of this stoichiometry have been prepared from the bis-methylcyanide adducts $[MX(\eta^3\text{-allyl})(CO)_2(MeCN)_2]$ by replacement of the relatively weakly bonded nitrile ligands.[175-177,180,195]

e.g.

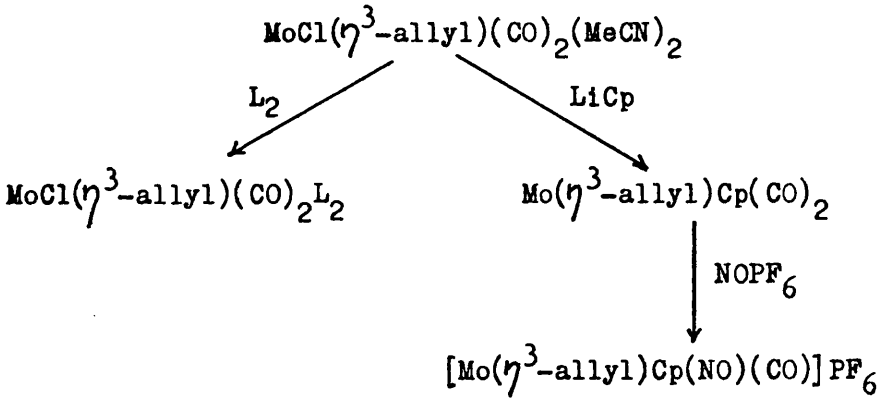

L_2 = α-diimines

L_2 = dppe, dppm

$L_2 = (RNC)_2$

Recently Doyle[157] reported the first anionic complexes of this stoichiometry {e.g. $[MoCl(\eta^3\text{-allyl})(\beta\text{-diketonato})(CO)_2]^-$}. These species were prepared by the mild oxidative addition of allyl chloride to anionic complexes (see below).

$$[Mo(acac)(CO)_4]^- + C_3H_5Cl \xrightarrow{THF} [MoCl(\eta^3\text{-allyl})(acac)(CO)_2]^-$$

$$[W(O_2CCH_3)(CO)_5]^- + C_3H_5Cl \longrightarrow [WCl(\eta^3\text{-allyl})(O_2CCH_3)(CO)_3]^-$$

Consequently the metal(II) - η^3 - allyl - dicarbonyl system is now known to occur in neutral, cationic and anionic complexes.

Chapter 2

Physical Methods, Starting Materials and Metal(0) Complexes

Chapter 2

Physical Methods, Starting Materials and Metal(0) Complexes

2.1 Physical Methods

This section describes the methods employed in the analysis and characterisation of the complexes discussed in this thesis.

2.1.1. Infra-red spectroscopy

Infra-red spectra in the range 4000 to 40cm^{-1} were recorded as detailed below. Not all samples were studied over the entire range.

2.1.1.1 4000 to 650 cm^{-1}

Spectra were obtained for Nujol or hexachlorobutadiene mulls held between NaCl plates, in addition some samples were examined as CH_2Cl_2 or MeCN solutions, using a Hilger and Watts Infragraph H1200 or Infrascan H900, or a Perkin-Elmer 237 spectrophotometer. A polystyrene film was used for wavenumber calibration.

2.1.1.2 650 to 200 cm^{-1}

A Nujol mull of the sample, sandwiched between CsI discs, was examined using the expanded scale facility of a Perkin-Elmer 621 spectrophotometer.

2.1.1.3 667 to 222 cm^{-1}

Spectra were obtained on vaseline mulls, held between polythene discs, using a Grubb-Parsons DM4 spectrophotometer.

2.1.1.4 450 to 40 cm^{-1}

The sample was dispersed in a pressed polythene disc and examined with a Beckmann RIIC FS720 interferometer. Fourier transforms of the interferograms were computed on an ICL 4-50 computer by means of a Fortran IV programme.

2.1.2 ^{1}H-n.m.r. spectra

N.m.r. spectra were obtained with a JEOL PS-100 spectrometer, together with the associated variable temperature controller, and using CD_2Cl_2, $CDCl_3$, $(CD_3)_2CO$ or CD_3CN solutions of the samples. TMS was used as an internal standard (δ_{TMS} = 0 ppm).

Results in the text are reported in the form: position in ppm (intensity, multiplicity, coupling constant in Hz) assignment.

2.1.3 Mass spectroscopy

Mass spectra were obtained with an AEI MS 12 spectrometer using a direct insertion probe and an ionizing energy of 70 eV. A source temperature of 220°C was normally used to volatilize the sample.

Only a few of the molybdenum complexes yielded mass spectra which showed metal containing fragments and these were readily recognised by the isotope pattern of molybdenum (Figure 2-1). Ion abundances in the text are expressed relative to the most abundant metal containing fragment which is set equal to 100% abundance.

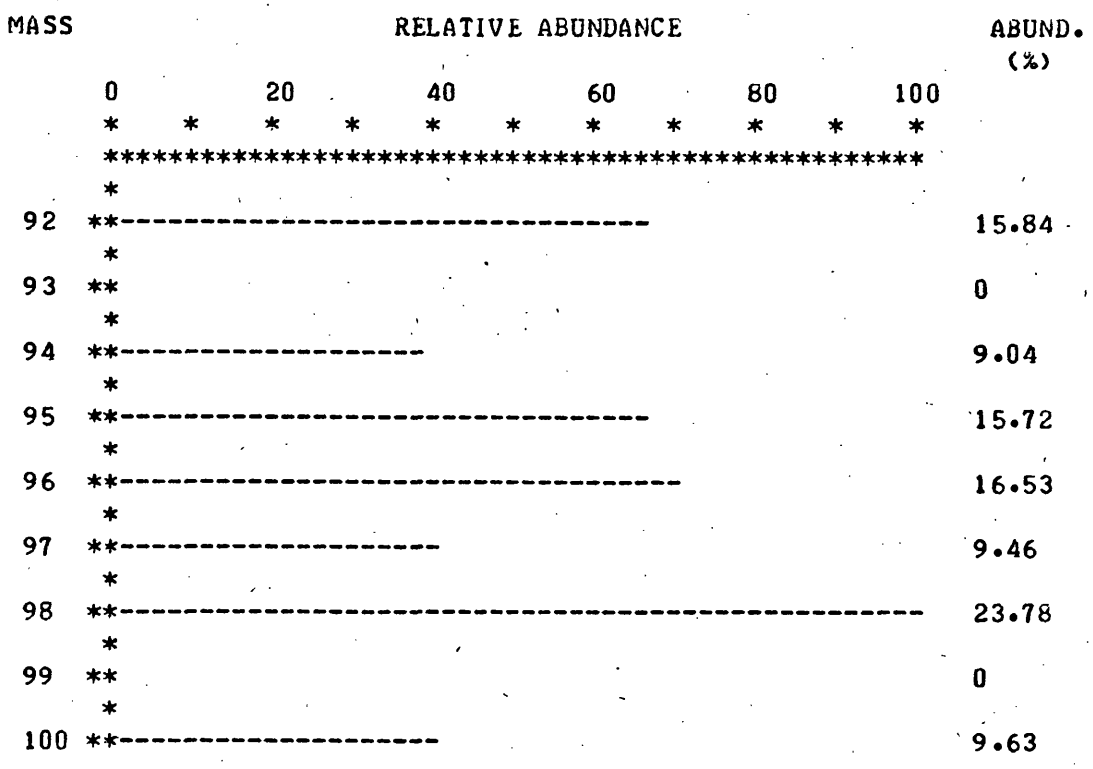

Figure 2-1. The isotope pattern of molybdenum

2.1.4. Esr spectroscopy

Spectra of powdered samples were recorded at 20°C using a Varian E-3 spectrometer.

2.1.5. GLC/mass spectroscopy

A GLC apparatus was connected to the gas sampling system of the mass spectrometer such that the eluate from the chromatograph could be selectively bled into the mass spectrometer, thus enabling the mass spectra of the various fractions of a mixture to be recorded.

2.1.6 Magnetic moments

Magnetic moments were obtained at room temperature by the Gouy method, with cobalt mercury thiocyanate $[CoHg(\mu\text{-}NCS)_4]$ as the calibrant. The observed susceptibilities were corrected for the diamagnetic components of the molecule to give the magnetic moment (μ) which is quoted in Bohr Magnetons (BM).

2.1.7. X-Ray powder photography

Samples were sealed in 0.5 mm Lindemann tubes and mounted in a Debye-Scherrer camera of 11.46 cm diameter. Exposure to the nickel filtered Cu-K radiation was for five hours or more and the resulting line intensities were estimated visually.

2.1.8 Elemental analysis

Samples were sent to Dr. Strauss, Oxford, to obtain C, H and N analyses of new complexes.

Molybdenum was determined gravimetrically either by ignition to the oxide or as molybdenyl oxinate.[196]

2.2. Synthetic chemistry

2.2.1 Reactants and solvents.

All reactants were of Laboratory Reagent grade and were used as supplied unless otherwise stated. Solvents, also of Laboratory Reagent grade unless otherwise noted, were dried by standard methods[197].

Prior to any reaction involving chromium, molybdenum or tungsten containing starting materials, the reaction system (including the reactants, the solvent and the reaction vessels) was thoroughly purged with dry nitrogen. An atmosphere of dry nitrogen was maintained throughout the reaction.

The new chromium(II) complexes (cf. Chapter 3) were particularly sensitive to oxidation and high vacuum techniques were sometimes employed in their syntheses.

2.2.2 Anions of potential three-electron-donor ligands

The sodium salts of acetylacetone (NaAcac) and salicylaldehyde (NaSalal) were prepared by similar procedures. The former was obtained as detailed in the literature[198] whilst the latter was prepared by an extension of this method as outlined below.

2.2.2.1 Preparation of NaSalal

To a stirred sample of salicylaldehyde (10 cm^3, 94mmol) was added an aqueous solution of sodium hydroxide (4.3 g, 108 mmol in 100 cm^3 H_2O). This mixture was stirred until the reaction was complete (ca. 30 min) when any insoluble material was removed by filtration. Solid sodium chloride (ca. 14 g) was added to the filtrate with stirring, until the product started to precipitate. The mixture was warmed to give a clear solution which was allowed to cool slowly. The product was collected at the filter, washed quickly with chilled water followed by acetone, and then dried in vacuo to give white platelets (6.8 g, 50% yield).

More product could be obtained from the filtrate by adding further quantities of sodium chloride as above.

On storage this product slowly darkens but can be readily purified by recrystallisation from aqueous sodium chloride as above.

2.2.3 Preparation of cis-$M(CO)_4L_2$

The complexes $M(CO)_4L_2$ (M = Cr, Mo, W; L_2 = bipy, dpa) were prepared by literature methods,[48,59] or extensions thereof as outlined below.

The parent metal hexacarbonyl [$M(CO)_6$; M = Cr, Mo or W] and an equimolar quantity of the bidentate ligand (L_2; bipy or dpa) were allowed to react in a refluxing hydrocarbon solvent (Table 2-1) until the white sublimate of hexacarbonyl ceased to form in the reflux condensor. After cooling to room temperature the crystalline product was collected at the filter, washed with toluene or xylene and dried *in vacuo*. Table 2-1 summarises the individual reaction conditions and products.

Table 2-1

Preparation of cis-$M(CO)_4L_2$

Reaction conditions			Products			
			L_2 = bipy		L_2 = dpa	
Metal	Medium	Time(hr)	Yield(%)	Colour	Yield(%)	Colour
Cr	toluene	7	98	Maroon	84	Khaki
Mo	toluene	2	99	Maroon	99	Yellow
W	xylene	7	99	Maroon	97	Yellow

2.2.4 Preparation of $M(CO)_3cht$

The complexes $M(CO)_3cht$ (M = Cr or Mo) were prepared by literature methods[199-202] in yields of approximately 60%.

2.2.5 Preparation of the anions $[MX(CO)_3L_2]^-$

Two routes were employed to obtain the complex anions $[MX(CO)_3L_2]^-$; M = Cr, Mo or W; X = halide or pseudohalide; L_2 = bipy or dpa. The first was that of Behrens[54] which involved the substitution of a bidentate and anionic ligand (e.g. bipy and Cl^-) for the cycloheptatriene in the complex $M(CO)_3cht$ (Equation 2-1).

$$M(CO)_3cht + X^- + L_2 \longrightarrow [MX(CO)_3L_2]^- + cht$$

Equation 2-1

$$M(CO)_4L_2 + X^- \longrightarrow [MX(CO)_3L_2]^- + CO$$

Equation 2-2

A new and more convenient route was developed during this work which avoids using the cycloheptatriene complex. The complex $M(CO)_4L_2$ was reacted directly with the required anion (equation 2-2) in a mixture of acetonitrile and toluene, under reflux, as summarised in table 2-2. After cooling to room temperature the product was collected at the filter, washed with a mixture of acetonitrile and toluene (in the same ratio as the solvent mixture) and then dried *in vacuo*. It was found necessary to store these anionic complexes under dry nitrogen and in the absence of light.

As many of these anions have been prepared previously (in combination with different cations to those employed here) only one representative analysis is given. Found: C, 56.1; H, 4.2; N, 5.50. Calculated for $(Ph_4As)[MoCl(CO)_3dpa]$ C, 56.5; H, 3.9; N, 5.65%.

Table 2-2

Preparation of $(Ph_4Z)[MX(CO)_3L_2]$; Z = As or P

$M(CO)_4L_2$	Anion source	MeCN: toluene	Reaction time (hr)	Yield (%)	Colour of product
$Cr(CO)_4bipy$	Ph_4AsCl	0:1	4	98	Dark green
$Cr(CO)_4dpa$*	Ph_4AsCl	0:1	4	75	Orange-red
$Mo(CO)_4dpa$	Ph_4AsCl*	1:4	2	90	Yellow
$W(CO)_4bipy$	Ph_4AsCl	1:4	2	75	Very dark
$W(CO)_4dpa$	Ph_4AsCl	1:4	3	94	Orange-yellow
$W(CO)_4bipy$	Ph_4PBr	1:2	4	60	Very dark
$W(CO)_4dpa$	Ph_4PBr	1:4	2	81	Orange

* This reactant was present in excess.

By reducing the toluene concentration in the solvent mixture the product remained in solution, thereby, enabling further reactions to be carried out on these anionic complexes without their prior isolation (cf. 3.2.3 and 3.2.5).

It was also found that the alkali metal cations Na^+ and K^+ could be employed in these syntheses (e.g. NaI and KSCN), especially where the anionic product was not isolated but merely reacted *in situ*.

2.2.6 Preparation of fac-[$Mo(CO)_3(MeCN)dpa$]

The complex $Mo(CO)_4dpa$ (0.48 g, 1.27 mmol) and an excess of acetonitrile (5 cm^3, 96 mmol) were allowed to react for 2 hr in refluxing toluene (20 cm^3). The product (0.36 g, 73% yield) was collected at the filter, washed with toluene and dried *in vacuo* to give a yellow solid [ν_{CO}(Nujol) 1905, 1795 and 1740 cm^{-1}. ^1H n.m.r: 2.12 (3, s)MeCN; 7.02 (4, m)aromCH; 7.72 (2, m)aromCH; 8.35 (1, br)N-H; 8.64(2, d, 5)aromCH].

2.2.7 Preparation of $MoCl(\eta^3\text{-allyl})(CO)_2(MeCN)_2$

This complex was prepared by the literature procedure[178] and was obtained as a yellow crystalline solid whose infra-red spectrum was in close agreement with that quoted by Dieck[178].

2.3 Spectral characterisation

The metal complexes were characterised by infra-red spectroscopy which gave results in close agreement with the literature values [48,54,59,178,199-202] for the known complexes. For the new compounds $[MX(CO)_3dpa]^-$; M = Cr, Mo, W; X = Cl and M = W; X = Br, and fac-[$Mo(CO)_3(MeCN)dpa$] the spectra were very similar to the known bipy analogues.

The disubstituted complexes $M(CO)_4L_2$ were air stable solids having the characteristic colours of maroon and yellow respectively for the bipy and dpa complexes, whereas the trisubstituted complexes $[MX(CO)_3L_2]^-$ and $M(CO)_3$cht were less air stable than the disubstituted complexes, with the dpa complexes more readily oxidised than the corresponding bipy complexes.

Table 2-3

CO stretching frequencies for metal carbonyl complexes[a]

Complex	L_2 = bipy			L_2 = dpa		
	Cr	Mo	W	Cr	Mo	W
$M(CO)_4L_2$	1998	2000	1998	2005	2010	2005
	1913	1922	1914	1910	1912	1900br
	1875	1876	1870	1870	1872	1867
	1818	1820	1817	1808	1790	1785
$Ph_4As[MCl(CO)_3L_2]$	1890	1912[b]	1877	1890	1897	1888
	1770	1780[b]	1764	1760	1770	1765
	1750	1720[b]	1746	1742	1748	1742
$Ph_4P[MBr(CO)_3L_2]$	-	-	1880	-	-	1880
			1770			1750[c]
			1750			

a) Measured as Nujol mulls. All bands very strong unless otherwise quoted.

b) Obtained for the Et_4N^+ salt

c) Possibly a doublet with maxima at ca. 1755 and ca. 1748 cm^{-1}

Generally it was observed that for the metal (0 and II) complexes[cf. Chapter 3 for the metal(II) complexes], bipy led to more crystalline products than dpa, which probably resulted from the low solubility of most of the dpa complexes.

Of the two methods used to prepare the anionic trisubstituted complexes $[MX(CO)_3L_2]^-$, the second procedure employing $M(CO)_4L_2$ is to be preferred as it uses readily available and stable starting materials and also leads to superior yields. These anionic complexes are very reactive and consequently readily decompose in aerated and strongly coordinating solvents, but the solids have stabilities of the order of 1 hour or more in air. Only the bromo- and chloro-complexes were isolated as solids with the other complexes (e.g. I^- and NCS^-) being formed in solution and reacted further to give complexes of the general formula $[MX(allyl)(CO)_2L_2]$ (cf. Chapter 3).

The bipy complexes $[MX(CO)_3bipy]^-$ have been assigned a <u>facial</u> configuration (Figure 2-2) on the basis of their infra-red spectra. This is also in accord with their ease of formation from $M(CO)_3cht$ at room temperature.

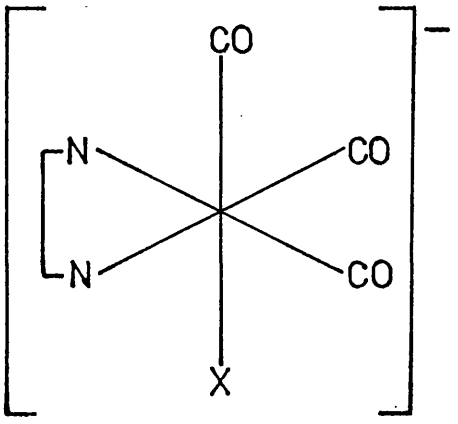

Figure 2-2 The probable configuration of the anionic complexes.

The analogous dpa complexes have similar infra-red spectra to these bipy complexes and are also likely to have this same configuration in the solid state.

Chapter 3

Preparation and Characterisation of Metal(II) Complexes.

Chapter 3

Preparation and Characterisation of Metal(II) Complexes

3.1 Introduction

A number of new complexes of chromium, molybdenum and tungsten, with the general formula $[MX(\eta^3\text{-allyl})(CO)_2L_2]$ ($M = Cr$; L_2 = bipy and $X = Cl$, Br, I or NCS: $M = Mo$; L_2 = bipy or dpa and $X = CH_3CO_2$, CF_3CO_2, $PhSO_2$ or p-$tolSO_2$: $M = Mo$ or W; L_2 = dpa and $X = Cl$, Br, I or NCS: $M = W$; L_2 = bipy and $X = CH_3CO_2$, $PhSO_2$ or p-$tolSO_2$: $M = W$; L_2 = dpa and $X = CH_3CO_2$ or CF_3CO_2), have been prepared by one or more of four synthetic routes. The spectroscopic properties of these compounds indicate that they are probably all structurally similar to other known molybdenum and tungsten(II) - η^3-allyl complexes. The formally seven-coordinate chromium(II) complexes are very unstable and readily disproportionate into chromium(0) and chromium(III) species.

3.2. Preparation of $[MX(\eta^3\text{-allyl})(CO)_2L_2]$

The precautions for excluding air and moisture, as outlined in Chapter 2, were employed during these reactions. One example of each of the four synthetic routes is described in detail with any significant variations from the prescribed methods for other complexes shown in table 3-1.

3.2.1. Route 1. From the metal hexacarbonyl

The complex $Mo(CO)_6$ (2.64 g, 10 mmol), dpa (1.71 g, 10 mmol) and an excess of allyl bromide (9 cm^3, 100 mmol) were allowed to react in refluxing THF (40 cm^3) for 3 hr. After cooling to room temperature the product [$MoBr(\eta^3$-allyl$)(CO)_2$dpa] was collected at the filter washed with THF and dried in vacuo.

3.2.2. Route 2. From $M(CO)_4L_2$

The complex $Mo(CO)_4$dpa (0.47 g, 1.24 mmol) and an excess of allyl isothiocyanate (2.5 cm^3, 30 mmol) were allowed to react in refluxing THF (20 cm^3) for 2 hr. Light petroleum (100 cm^3, b.pt. 40 - 60°C) was added to the cooled solution at room temperature, followed by refrigeration for 2 hr. at 0°C to precipitate the product [$Mo(NCS)(\eta^3$-allyl$)(CO)_2$dpa]. The complex was filtered off, washed with light petroleum (b.pt. 40 - 60°C) and dried in vacuo.

3.2.3. Route 3. The reaction between the complex anion $[MX(CO)_3L_2]^-$ and allyl halides or pseudohalides.

The salt Ph_4P[$WBr(CO)_3$bipy] (2.10 g, 2.5 mmol) was added to an excess of allyl bromide (2.5 cm^3, 30 mmol) in methanol (25 cm^3), and the mixture was stirred for 1 hr. at room temperature. The product [$WBr(\eta^3$-allyl$)(CO)_2$bipy] was collected at the filter, washed with methanol followed by water and dried in vacuo.

3.2.4. Route 4. Anion Exchange.

The complex [$MoCl(\eta^3$-allyl$)(CO)_2$bipy] (0.50 g, 1.3 mmol) and an excess of the salt CF_3CO_2Na (0.41 g, 3.0 mmol) were stirred together in acetone (20 cm^3) at room temperature for

3 days. The mixture was filtered, and water was slowly added to the filtrate to precipitate the product $[Mo(CF_3COO)(\eta^3\text{-allyl})(CO)_2bipy]$ which was collected at the filter , washed with water and dried *in vacuo*.

3.2.5. Preparation of the chromium complexes

Very precise reaction conditions were required for the successful isolation of the complexes $[CrX(\eta^3\text{-allyl})(CO)_2L_2]$, as they readily disproportionated and precipitated $Cr(CO)_4bipy$. Route 3 was the only suitable method for synthesising these complexes and the preparation of each compound is described below.

3.2.5.1. $[CrCl(\eta^3\text{-allyl})(CO)_2bipy]$

The complex $Ph_4As[CrCl(CO)_3bipy]$ (1.90 g, 2.7 mmol) was added slowly with stirring to a cooled (-40°C) solution of allyl chloride (1.5 cm^3, 18 mmol) in methanol (20 cm^3). After 10 minutes reaction the product $[CrCl(\eta^3\text{-allyl})(CO)_2bipy]$ was collected at the filter, quickly washed with cold methanol (-30 to -40°C) followed by water and dried *in vacuo*.

Care was taken when washing with water as the product forms an extremely fine suspension which passes through the sinter and slowly deposits $Cr(CO)_4bipy$.

The solid reactant $Ph_4As[CrCl(CO)_3bipy]$ may be replaced by a cooled (0°C), filtered solution of this salt formed *in situ* in acetonitrile.

3.2.5.2. [CrBr(η^3-allyl)(CO)$_2$bipy]

The complex Cr(CO)$_4$bipy (0.42 g, 1.3 mmol) and an excess of NaBr(0.77 g, 7.5 mmol) were allowed to react in refluxing acetonitrile (10 cm^3) for 3 hours. The resulting solution, which contains the complex Na[CrBr(CO)$_3$bipy], was cooled to 0°C and then added slowly with stirring to a cooled solution (-40°C) of allyl chloride (1 cm^3, 12 mmol) in methanol (10 cm^3). This mixture was stirred for 30 minutes at -40°C and then quickly filtered. The filtrate was evaporated to dryness, on a rotary evaporator without heating, to give the product [CrBr(η^3-allyl)(CO)$_2$bipy] which was washed with water and dried *in vacuo*.

3.2.5.3. [CrI(η^3-allyl)(CO)$_2$bipy]

The complex Cr(CO)$_4$bipy (0.39 g, 1.2 mmol) and NaI (0.76 g, 5.1 mmol) were allowed to react in refluxing acetonitrile (20 cm^3) for 3 hr. The solution was cooled to 0°C, filtered and the filtrate added dropwise to a cooled solution (-10°C) of allyl chloride (1 cm^3, 12 mmol) in methanol (15 cm^3), and this mixture was then stirred for 10 minutes. The product [CrI(η^3-allyl)(CO)$_2$bipy] was collected at the filter, washed with cold methanol (-10°C) followed by water and dried *in vacuo*.

3.2.5.4 [Cr(NCS)(η^3-allyl)(CO)$_2$bipy]

This complex was prepared in a similar manner to the iodo analogue but using KSCN in place of NaI.

3.2.6. Attempted preparation of $[MoCl(\eta^3\text{-allyl})(CO)_2nbn]$

The complex $[MoCl(\eta^3\text{-allyl})(CO)_2(MeCN)_2]$ (0.44 g, 1.42 mmol) and norbornadiene (5 cm^3, 50 mmol) were stirred together at room temperature for four days in acetone (20 cm^3). During this time a dark solution and an off-white precipitate formed. This mixture was filtered and the residue was washed with acetone and dried *in vacuo* to give an off-white rubbery solid (0.26 g). On standing a further quantity of this off-white material was deposited from the filtrate.

3-3 Results and discussion

3.3.1 Preparative methods

All of the procedures, where applicable (table 3.1), led to good yields (normally better than 75% and very frequently in excess of 90%), with route 2 generally resulting in slightly higher yields than route 1. Route 1 is to be preferred however, as it is a one stage synthesis and employs readily available starting materials. Because of the strong nucleophilic character of the anions $[MX(CO)_3L_2]^-$, route 3 provides an extremely facile method for carrying out allyl oxidations (reaction occurs at or below room temperature) and as such enables the isolation of thermally unstable compounds. Hence this route provides the only known synthesis of the chromium(II) complexes $[CrX(\eta^3\text{-allyl})(CO)_2bipy]$ (X = Cl, Br, I or NCS), and is the favoured procedure for the tungsten compounds which cannot normally be obtained by routes 1 or 2[113].

Table 3.1

Preparation of $[MX(\eta\text{-allyl})(CO)_2L_2]^*$

M	L_2	X	Route and Yield (%) 1	2	3	4	Colour
Cr	bipy	Cl	-	-	65	-	Red
		Br	-	-	74	-	Red
		I	-	-	80	-	Red
		NCS	-	-	39	-	Red
Mo	bipy	Cl	50(i)	97	61	-	Red
		Br	65	90	-	90	Red
		I	51	92	-	86(ii)	Red
		NCS	97(i)	96(iv)	90(viii)	95	Red
		OAc	86(i)	90(i)	44(vi,viii)	80(v)	Red
		CF_3CO_2	-	-	-	98	Red
		$PhSO_2$	-	-	-	94(v)	Red
		$tolSO_2$	-	-	-	93(v)	Red
Mo	dpa	Cl	50(i)	94	94	-	Yellow
		Br	91(i)	98	-	-	Yellow
		I	71	91	-	77	Yellow
		NCS	87(i)	88(iv)	-	92	Yellow
		OAc	-	-	-	54(ii,v)	Yellow
		CF_3CO_2	-	-	-	89	Yellow
		$PhSO_2$	-	-	-	67(v)	Yellow
		$tolSO_2$	-	-	-	68(v)	Yellow

Table 3.1 (Contd)

M	L_2	X	Route and Yield (%) 1	2	3	4	Colour
W	bipy	Cl	-	-	93	-	Maroon
		Br	-	-	78	-	Maroon
		I	-	-	-	80(iii)	Maroon
		NCS	-	-	-	91(iii)	Maroon
		OAc	-	-	-	82(ii,iii,v)	Maroon
		$PhSO_2$	-	-	-	80(ii,iii,v)	Maroon
		$tolSO_2$	-	-	-	90(ii,iii,v)	Maroon
W	dpa	Cl	-	-	98	-	Yellow
		Br	-	-	70	-	Yellow
		I	-	-	-	70(iii)	Yellow
		NCS	-	-	-	55(iii)	Yellow
		OAc	-	-	-	60(iii,v,vii)	Yellow
		CF_3CO_2	-	-	-	31(iii)	Yellow

* None of these complexes had reproducible melting points, all decomposing slowly above 190°C

(i) Toluene as the solvent.

(ii) Product precipitated during the reaction

(iii) Reaction carried out under reflux

(iv) Product precipitated by the addition of light petroleum (b.pt. 40 - 60°C).

(v) Methanol as solvent

(vi) Product precipitated on cooling in ice.

(vii) Product was contaminated with oxo-metal containing species.

(viii) The complex $[MX(CO)_3L_2]^-$ was reacted <u>in situ</u> (cf. p.83)

In many reactions, especially those producing the chromium complexes which quickly precipitated from solution at low temperatures, it was found that the acido ligand (X) present in the anionic complex $[MX(CO)_3L_2]^-$ was retained in the final product (Equation 3-1), but as the reaction temperature and time increased (e.g. With the tungsten complexes) then anion exchange (Equation 3-2) became a competing reaction leading to mixed products.

$$[MX(CO)_3L_2]^- + \text{allylY} \longrightarrow MX(\eta^3\text{-allyl})(CO)_2L_2 + Y^- \qquad \text{Equation 3-1}$$

$$MX(\eta^3\text{-allyl})(CO)_2L_2 + Y^- \longrightarrow MY(\eta^3\text{-allyl})(CO)_2L_2 + X^- \qquad \text{Equation 3-2}$$

On the basis of these observations (i.e. the great reactivity of the anionic complexes, and the retention of X in the product) the most likely mechanism for the allyl halide or pseudohalide oxidation of the intermediate involves the attack of an electrophilic allyl group on the metal atom of the anionic complex (Figure 3-1). There is strong evidence for this type of mechanism in some oxidative addition reactions of Group VIII complexes.[116,117,134]

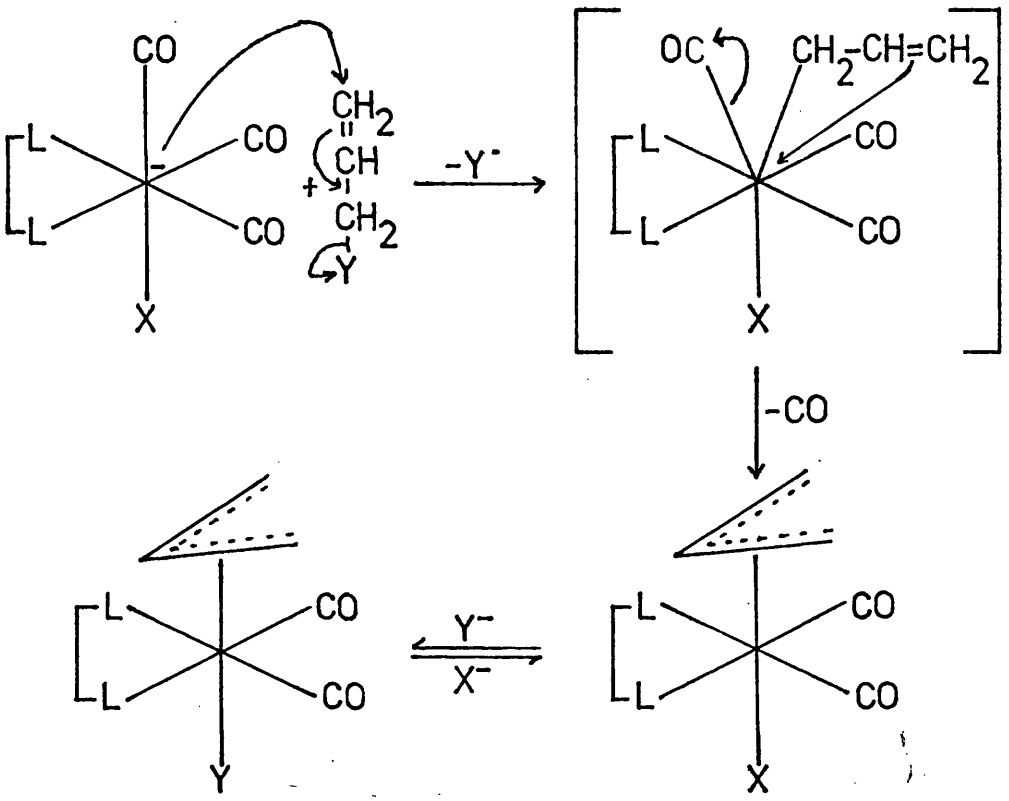

Figure 3-1 A proposed reaction scheme for synthetic route 3

It was also observed that the ease of oxidation of these anionic complexes was in the order Cr>> Mo > W which, for the proposed mechanism, is in agreement with the Pauling electronegativities[16] of the three metals.

Route 4, anion exchange provided a convenient synthesis for many otherwise unobtainable complexes (i.e. the required organic allyl derivative was not available or was not suitable for routes 1 and 2). The tungsten complexes $[WX(\eta^3\text{-allyl})(CO)_2L_2]$ underwent anion exchange only very slowly and required elevated temperatures which, in some instances led to the formation of

oxo-species. Hence the complexes $[WX(\eta^3\text{-allyl})(CO)_2L_2]$ ($X = CH_3CO_2$; L_2 = dpa and $X = CF_3CO_2$; L_2 = bipy, dpa) could only be obtained in a low state of purity whilst $[W(PhSO_2)(\eta^3\text{-allyl})(CO)_2dpa]$ and $[W(p\text{-tolSO}_2)(\eta^3\text{-allyl})(CO)_2dpa]$ could not be obtained at all.

3.3.2 Characterisation of the complexes

Table 3-2 contains selected analytical and infra-red data for the complexes $[MX(\eta^3\text{-allyl})(CO)_2L_2]$.

3.3.2.1 Mass spectroscopy

Generally the mass spectra of these metal(II) complexes failed to show any metal containing fragments, but simply showed the spectrum of the bidentate ligand (L_2; bipy or dpa). This presumably resulted from their low volatility leading to thermolysis prior to volatilisation. The only useful spectra were those of $[MoX(\eta^3\text{-allyl})(CO)_2bipy]$, where X was chloride or bromide, which showed trace amounts (less than 1% relative abundance) of metal containing fragments as summarised in table 3-3 and figure 3-2. In both of these spectra the most abundant metal containing species were $[MoX(allyl)bipy]^+$ and $[MoXbipy]^+$.

Table 3-2.

Selected infra-red and analytical data for $[MX(\eta^3\text{-allyl})(CO)_2L_2]$

M	X	Infra-red[a] ν_{CO}	ν_{MC}	ν_{MX}	Analysis[b] C	H	N
			L_2 = bipy				
Cr	Cl	1930	508	267	51.9	4.0	8.47
		1842	495		(52.8)	(3.8)	(8.21)
	Br	1928	506	218	45.5	3.5	6.97
		1850	492		(46.8)	(3.4)	(7.27)
	I	1918	493br		41.2	3.2	6.65
		1850			(41.6)	(3.1)	(6.48)
	NCS	1940	508		52.5	3.9	11.3
		1860	490		(52.9)	(3.6)	(11.6)
Mo	Cl	1930	508	271	-	-	-
		1842	467				
	Br	1928	509	212sh	-	-	-
		1845	469				
	I	1924	508		-	-	-
		1842	470				
	NCS	1943	510	263	-	-	-
		1855	468				
	OAc	1940	c		50.2	4.1	7.0
		1850			(50.0)	(3.9)	(6.9)
	CF_3CO_2	1953	c		44.5	3.3	6.1
		1860			(44.1)	(2.8)	(6.1)

Table 3-2 (Contd)

M	X	Infra-red[a] ν_{CO}	ν_{MC}	ν_{MX}	Analysis[b] C	H	N
			L_2 = bipy				
Mo	$PhSO_2$	1938	509		51.6	3.9	5.8
		1857	472		(51.4)	(3.7)	(5.7)
	$tolSO_2$	1932	o		51.6	4.1	5.4
		1835			(52.4)	(4.0)	(5.5)
W	Cl	1920	521	268	-	-	-
		1820	477				
	Br	1920	c	215sh	-	-	-
		1828					
	I	1920	522		-	-	-
		1835	478				
	NCS	1928	520	270	-	-	-
		1835	475				
	OAc	1927	521		41.1	3.5	5.6
		1833	473		(41.1)	(3.2)	(5.6)
	$PhSO_2$	1925	c		43.5	3.4	4.9
		1840			(43.6)	(3.1)	(4.8)
	$tolSO_2$	1923	c		43.0	3.8	4.7
		1823			(44.6)	(3.4)	(4.7)

Table 3-2 (Contd)

M	X	Infra-red[a] ν_{CO}	ν_{MC}	ν_{MX}	Analysis[b] C	H	N
				L_2 = dpa			
Mo	Cl	1928	514	255	45.0	3.7	10.5
		1842	464		(45.1)	(3.5)	(10.5)
	Br	1928	511	212sh	40.4	3.2	9.3
		1842	463		(40.5)	(3.2)	(9.5)
	I	1922	517		37.0	3.0	8.6
		1832	475		(36.7)	(2.9)	(8.6)
		1814[d]	497[d]				
	SCN	1927	510	242	45.6	3.5	13.2
		1839	463		(45.5)	(3.3)	(13.3)
	OAc	1947	511		47.8	4.2	9.8
		1850	463		(48.3)	(4.0)	(9.9)
	CF_3CO_2	1935	c		42.8	4.1	9.3
		1845			(42.8)	(2.9)	(8.8)
	$PhSO_2$	1935	511		49.5	4.1	8.1
		1855	463		(49.9)	(3.8)	(8.3)
	$tolSO_2$	1938			49.2	4.4	7.8
		1848			(50.9)	(4.0)	(8.1)
W	Cl	1915	522	258	36.7	3.2	8.5
		1825	473		(36.9)	(2.9)	(8.6)

Table 3-2 (Contd)

M	X	Infra-red[a] νCO	ν_{MC}	ν_{MX}	Analysis[b] C	H	N
				L_2 = dpa			
W	Br	1920	523	210sh	33.6	2.8	7.9
		1830	472		(33.8)	(2.6)	(7.9)
	I	1918	523		31.6	2.7	7.4
		1822	480		(31.1)	(2.4)	(7.3)
		1805[d]	501[d]				
	SCN	1920	520	238	38.7	3.4	10.9
		1830	470		(37.6)	(2.8)	(11.0)
	OAc	1933	c		e	e	e
		1840					
	CF_3CO_2	1925	525		e	e	e
		1830	476				

a) Measured as a Nujol mull. All bands are strong.

b) Quoted as % composition with the theoretical value in parentheses.

c) The spectrum was not recorded in this region.

d) Slightly less intense than the other two bands

e) These products were not analytically pure.

Table 3-3

Mass spectra of [MoX(η^3-allyl)$(CO)_2$bipy]

Fragment[a]	Lost	m/e[b]	
		X = Cl	X = Br
MoX(allyl)$(CO)_2$bipy	-	386	430
MoX(allyl)(CO)bipy	CO	358	402
MoX(allyl)bipy	2CO	330[c]	374[c]
MoXbipy	2CO + C_3H_5	289[d]	333[d]
Mo(allyl)bipy	2CO + X	295	e
Unknown		315	306
"		317	308
"		272	280
"		230	255

a) Only metalcontaining fragments are listed.

b) m/e Values are based on ^{35}Cl, ^{79}Br and ^{98}Mo.

c) Most abundant metal containing fragment.

d) Second most abundant metal containing fragment

e) This fragment was not observed.

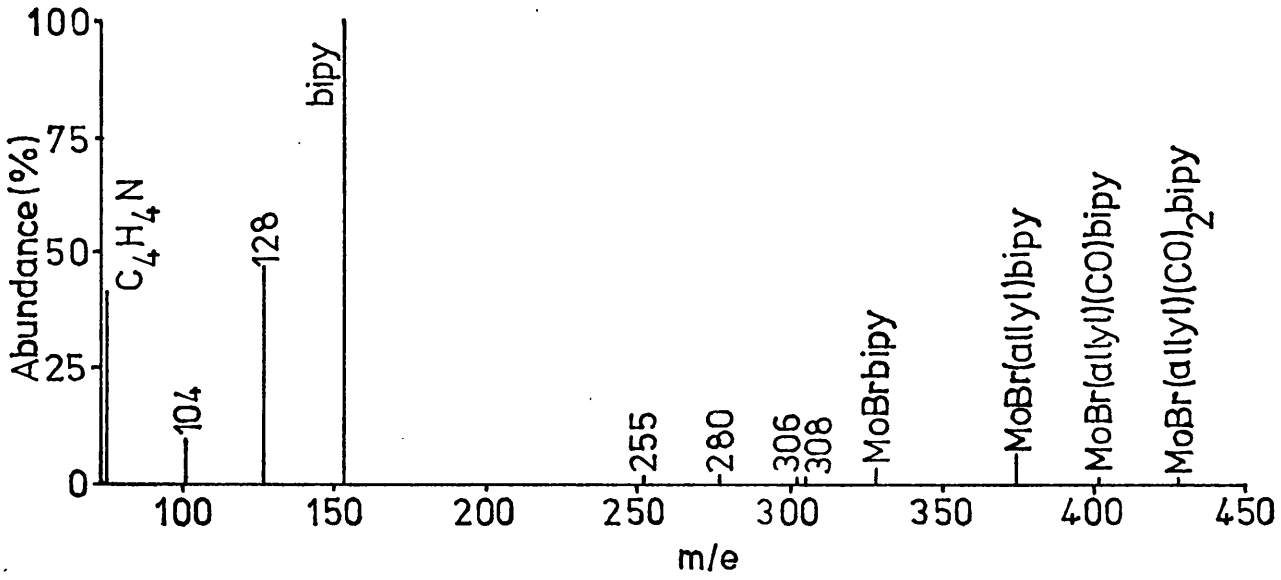

Figure 3-2 Mass spectrum of [MoBr(η^3-allyl)(CO)$_2$bipy]

3.3.2.2 ^{1}H-n.m.r. Spectroscopy

^{1}H-n.m.r. Spectroscopy is the best diagnostic tool for differentiating between the various bonding modes of the allyl group. Unfortunately the majority of these metal(II) complexes were insufficiently soluble in suitable solvents to obtain such spectra. The complexes [M(SCN)(η^3-allyl)(CO)$_2$dpa] (M = Mo or W) were just soluble enough in acetone to obtain reasonable results as summarised in table 3-4 and shown in figure 3-4.

Table 3-4

^{1}H-n.m.r. Spectrum of [M(SCN)(η^3-allyl)(CO)$_2$dpa]

Assignment[a]		δ[b] Molybdenum	δ[b] Tungsten
H_a	η^3-allyl	1.26(2,d,9.0)	1.44(2,d,8.5)
H_s	η^3-allyl	2.62(2,d,4.5)	2.78(2,d,6.0)
H_c	η^3-allyl	4.04(1,m)	3.24(1,tt[c])
$H_3 + H_5$	dpa[d]	7.28 (4,m)	7.26 (4,m)
H_4	dpa[d]	7.90(2,t,8.0)	7.96(2,t,8.0)
H_6	dpa[d]	8.47(2,d,5.5)	8.46(2,d,4.5)
N-H	dpa[d]	ca.9.8(1,br)	ca.9.8(1,br)

a) Suffixes refer to the positions given in figure 3-3.

b) Spectra were measured for d^6-acetone solutions with TMS as an internal standard.

c) Triplet of triplets.

d) Spectrum for free dpa: 6.84(2,t,6.8)H_5; 7.60(2,t,8.1)H_4; 7.78(2,d,8.1)H_3; 8.24(2,d,5.2)H_6; 9.07(1,br)N-H.

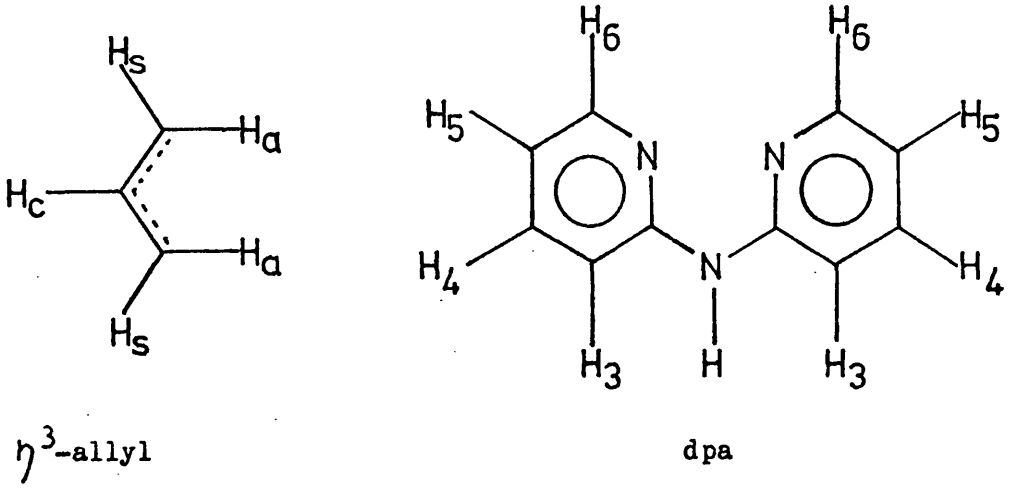

η^3-allyl dpa

Figure 3-3. Proton designation employed in table 3-4

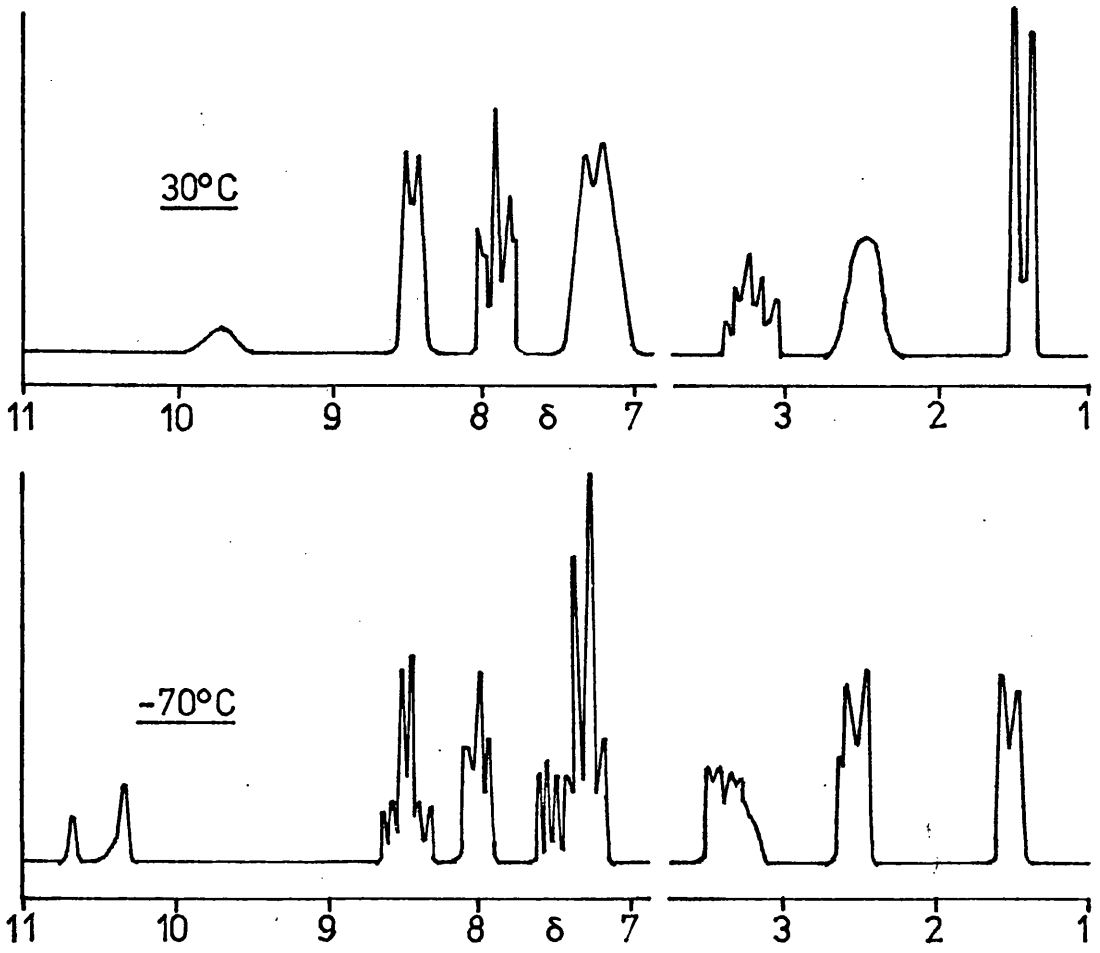

Figure 3-4. ^{1}H-n.m.r. spectrum of [W(SCN)(η^3-allyl)(CO)$_2$dpa]

The band positions, multiplicities and coupling constants obtained in the allyl region of these spectra are typical of a η^3-allyl group[113], thus showing these complexes to be dpa analogues of the well characterised bipy complexes [MX(η^3-allyl)(CO)$_2$bipy] [72,113].

Inspection of table 3-4 reveals that the ^{1}H-n.m.r. spectrum of dpa alters significantly on coordination to these complexes. The protons labelled 4,5 and 6 (Figure 3-3) shift to lower field on coordination, by 0.2 to 0.4 ppm, and the amine proton is

deshielded by 0.7 ppm, whereas the proton labelled 3 shifts to higher field by 0.5 ppm. The deshielding of the amine proton could be caused by hydrogen-bonding in these complexes as discussed later (Sections 3.3.3.1 and 3.3.3.2).

The spectrum of the tungsten thiocyanate complex was run at various temperatures between 50 and -70°C to check for temperature dependent phenomena. Although the allyl region did not alter significantly, additional low intensity bands were observed in the aromatic region at -70°C (Figure 3-4), indicating the presence of an isomeric species. At -20°C only one set of dpa resonances were clearly visible. These results can be interpretted in two ways. Either a new isomer appears only at low temperatures, or alternatively two isomeric forms are present but interconvert rapidly above -20°C and hence give rise to one set of signals at room temperature. Since the allyl region did not show corresponding sets of separate signals at low temperatures, the isomeric species must have very similar chemical environments for their allyl groups. Further discussion will be postponed until after consideration of the infra-red data (Sections 3.3.3.1 and 3.3.3.2).

3.3.2.3. Infra-red spectroscopy

The infra-red spectra (4000-650 cm^{-1}) were dominated by carbonyl and bidentate ligand bands which masked the weak bands expected for the η^3-allyl group (see Section 1.3.1.2.1)[151,178] However, there were no strong bands in the region 1500 to 1700 cm^{-1} which could be attributed to $\nu(CC)$ of a η^1-bonded allyl group, consequently both the infra-red and the limited n.m.r. data are in accord.

Table 3-2 summarises significant infra-red bands for the complexes. The spectra contain many similar features and are typical of cis-dicarbonyl complexes, with two C-O stretching bands of approximately equal intensity and separated by approximately 100 cm^{-1}. The observed values for the bipy complexes agree with the literature values, where available.[113] By careful comparison of the spectra of these metal(II) complexes with each other and with the corresponding $M(CO)_4L_2$ spectra it was possible to tentatively assign the M-C and M-halogen stretching vibrations. These vibrations occurred in the expected regions of the spectra [i.e. $\nu_{(MC)}$ 500 - 300 and $\nu_{(MX)}$ 350 - 200cm^{-1}] [27,28,203], with the M-C stretching vibrations occurring at approximately the same frequencies as in the cis-dicarbonyl complex $[Mo(CO)_2(Ph_3Sb)_4]$.[203]

Hence, spectroscopy indicates the presence of η^3-allyl and cis-dicarbonyl groups in each complex, and since these three ligands have always been found to adopt a fac-arrangement in known compounds of this stoichiometry, one of two reasonable

ligand arrangements seems likely for these new complexes (Figure 3-5). Structure A has been confirmed for

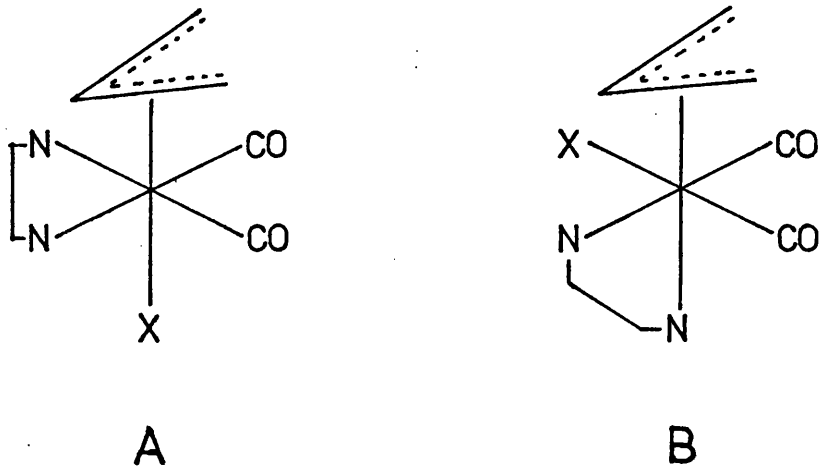

A B

Figure 3-5 Probable structures for $MX(\eta^3\text{-allyl})(CO)_2L_2$ species

$[Mo(NCS)(\eta^3\text{-allyl})(CO)_2bipy]$[17] whilst $[Mo(\eta^3\text{-allyl})(acac)(CO)_2py]$ has been shown to have structure B, with N-N replaced by acac and X replaced by py (see chapter 4 and figure 1-18). Thus without crystallographic or low temperature n.m.r. data it is not possible to determine which of these two structures is adopted by a particular compound.

The Cotton-Kraihanzel[204] C-O stretching force constants were calculated for a limited number of these complexes and are listed in table 3-5. The force constants (K) are lower (by approximately 1.5%) for the tungsten compounds than for the corresponding molybdenum complexes, and dpa leads to lower values than does bipy (by about 0.6%). These observations

are in agreement with the general trend in force constants obtained for the complexes $M(CO)_4L_2$ (M = Mo or W and L_2 = bipy or dpa) as discussed in chapter 7.

Table 3-5

C-O stretching force constants.

Complex	ν_{CO}[a]		Force constants[b]	
	A_1	B_1	k	K
$MoBr(\eta^3\text{-allyl})(CO)_2bipy$	1928	1845	0.63	14.38
$MoBr(\eta^3\text{-allyl})(CO)_2dpa$	1928	1842	0.65	14.36
$WBr(\eta^3\text{-allyl})(CO)_2bipy$	1920	1828	0.70	14.19
$WBr(\eta^3\text{-allyl})(CO)_2dpa$	1920	1830	0.68	14.21
$Mo(SCN)(\eta^3\text{-allyl})(CO)_2dpa$	1927	1839	0.67	14.33
	1946[c]	1861[c]	0.65	14.64
$W(NCS)(\eta^3\text{-allyl})(CO)_2bipy$	1928	1835	0.71	14.30
	1938[c]	1850[c]	0.67	14.49

a) Sample prepared as a Nujol mull, unless otherwise stated. Values quoted in cm^{-1}.

b) Force constants quoted in mdyne Å^{-1}

k is the CO - CO interaction force constant and

K is the C-O stretching force constant.

c) Sample dissolved in CH_2Cl_2.

3.3.3. Mode of coordination of the acido-ligands

3.3.3.1 The iodo-complexes

As shown in table 3-2 the compounds [MI(η^3-allyl)(CO)$_2$dpa] (M = Mo or W), give rise to additional infra-red absorptions in the C - O and M - C stretching regions of their spectra compared with the other complexes. These additional bands are strong and sharp but not quite as intense as the two accompanying bands.

In order to check whether these extra bands were due to solid state effects, solution spectra (Table 3-6 and figure 3-6) were obtained in the carbonyl stretching region.

Table 3-6

Solution infra-red spectra of [MI(η^3-allyl)(CO)$_2$dpa]

M	ν_{CO}* (cm^{-1})			
Mo	1950vs	1939vs	1865vs	1849vs
W	1942vs	1932sh	1853vs	1837s-vs

* Measured as saturated solutions in acetonitrile at room temperature.

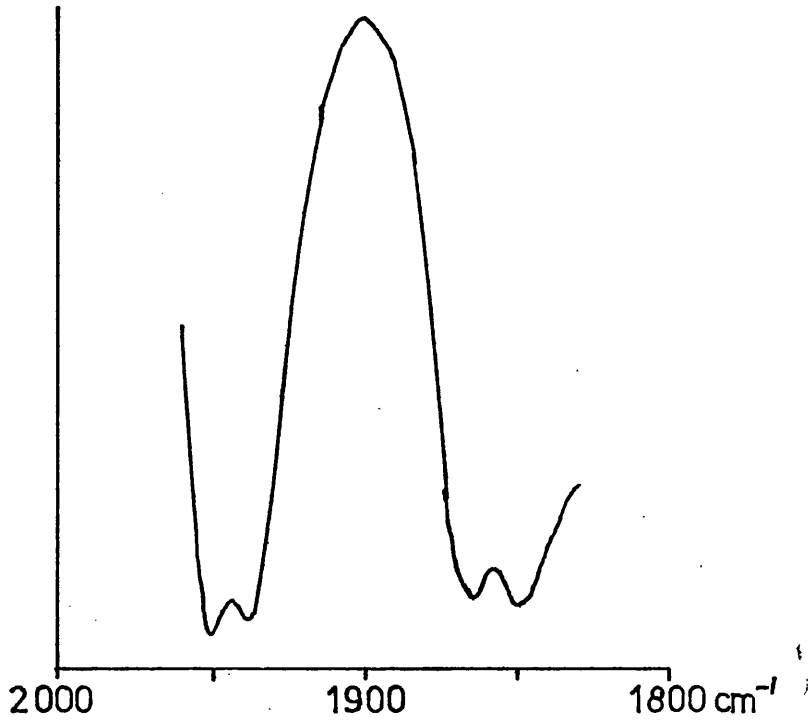

Figure 3-6. Solution infra-red spectrum of [MoI(η^3-allyl)$(CO)_2$dpa]

On dissolution of the samples the whole carbonyl spectrum shifted to higher energy (by 20 to 35 cm^{-1}) as expected[205]. Comparison of tables 3-2 and 3-6 reveals that the lower energy CO band still shows the same split as in the solid state and the previously non-split higher energy carbonyl band is now resolved into a doublet, thus giving a total of four bands for each complex. These spectra indicate that the observed split is a molecular property and not merely a lattice effect, thereby suggesting the possibility of isomeric species of some kind.

The infra-red spectra indicate that both species have a cis-dicarbonyl grouping and that no charged species are involved. Therefore geometrical isomerism (structures A and B, figures 3-5) or isomerism involving conformational changes in the allyl or dpa groups seems likely.

Conformational isomerism of the allyl group is well-known for both molybdenum and tungsten complexes [eg. $Cp_2Mo(\eta^3\text{-allyl})(CO)_2$][14] and in its simplest form, rotation about the metal-allyl bond could give rise to two isomers of $[MI(\eta^3\text{-allyl})(CO)_2dpa]$ (C and D, figure 3-7).

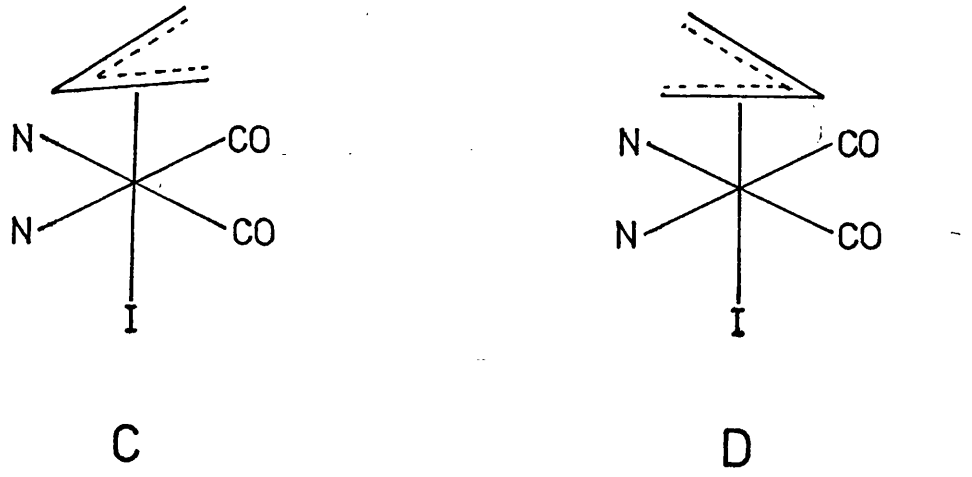

C D

Figure 3-7. Possible isomerism in $[MI(\eta^3\text{-allyl})(CO)_2dpa]$

Alternatively, isomerism could arise from conformational changes of the dpa ligand. Consideration of the acyclic nitrogen atom in dpa reveals the possibility of two extreme geometries about this atom; namely planar (sp^2) or tetrahedral (sp^3 including the lone pair of electrons) as shown in figure 3-8 .

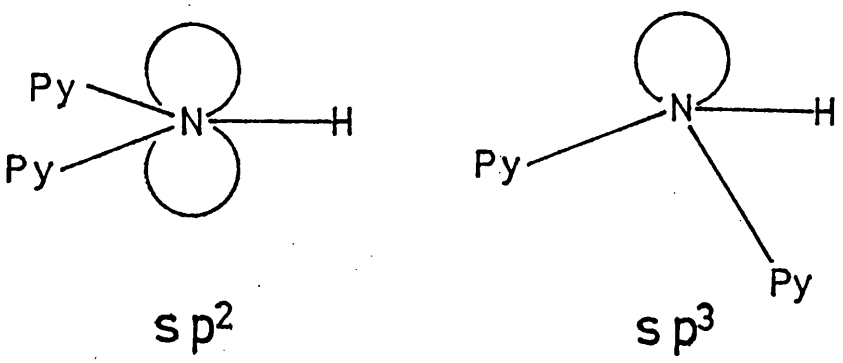

Figure 3-8. Possible conformational changes in dpa.

On electronic grounds the sp^2 arrangement is to be preferred as this allows the lone pair of electrons on this nitrogen atom to delocalise into the pyridine rings. Indeed, in the free ligand (the lower melting isomer, m.pt. 84°C) the acyclic nitrogen atom is co-planar with the pyridine rings[206]. A near planar geometry has also been found for this acyclic nitrogen atom in several copper complexes [66-68,207] [eg. $Cu(dpa)_2(ClO_4)_2$], but in order to relieve chelate ring strain a dihedral angle is introduced between the pyridine rings (i.e. the acyclic nitrogen atom has a planar environment but is not co-planar with the aromatic rings)[57].

A molecular model of $[MoX(\eta^3\text{-allyl})(CO)_2dpa]$ reveals that the amine hydrogen of a tetrahedral amine group would strongly interferewith either the allyl- or acido-group and that an approximately planar acyclic amine group leads to less chelate ring strain than a tetrahedral nitrogen atom.

In order to minimise this strain it is necessary to introduce a dihedral angle between the two pyridine rings, as observed experimentally for the copper complexes cited above.

The presence of this dihedral angle leads to a puckered chelate ring and can possibly give rise to two isomers with the acyclic amine group on either side of the CCMNN plane as shown in figure 3-9.

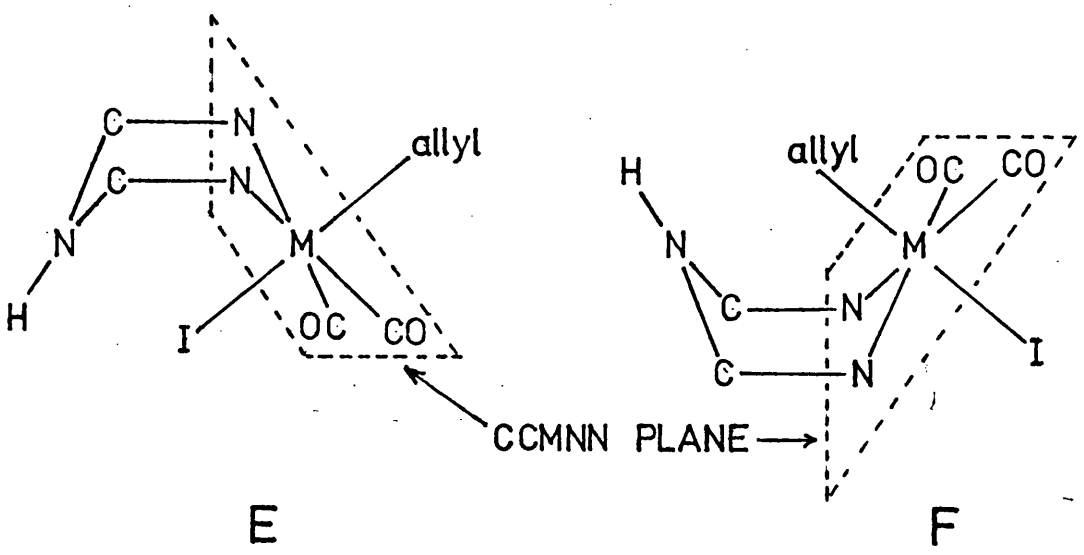

Figure 3-9. The puckered chelate ring and possible isomerism in metal-dpa complexes.

When the acido ligand (X) is very electronegative there is the possibility of a hydrogen-bond being formed between the amine-hydrogen atom and the acido-group. Hence when the ligand X is an oxygen- or nitrogen-donor ligand or one of the lighter halogen atoms (chlorine or bromine), the conformer with the acyclic amine group below the plane (E, figure 3-9) may well be stabilised relative to the other conformer. When the acido-group is bulky or not very electronegative (e.g. sulphur-donor ligands or an iodine atom) the isomers E and F may well be in equilibrium.

The various conformers should give rise to different n.m.r. spectra, but unfortunately attempts to obtain spectra for the complexes $[MI(\eta^3\text{-allyl})(CO)_2dpa]$ (M = Mo or W) were unsuccessful due to their very low solubilities.

Inspection of the NH stretching region of the infra-red spectrum of the halo-complexes (Table 3-7), shows the iodo-

Table 3-7

The NH stretching vibration in dpa complexes

Compound	ν_{NH}^{a} (cm^{-1})		
	Chromium	Molybdenum	Tungsten
$M(CO)_4dpa$	3390s	3360s	3340vs
$MCl(\eta^3\text{-allyl})(CO)_2dpa$	-	3280m,br	3282m,br
$MBr(\eta^3\text{-allyl})(CO)_2dpa$	-	3280m-s,br	3280m-s,br
$MI(\eta^3\text{-allyl})(CO)_2dpa$	-	3365s	3355s

a) Spectra obtained for Nujol mulls. ν_{NH} occurs at 3240 (m)cm^{-1} for free dpa.

complexes to have a sharp band above 3300cm^{-1} which is not present in the chloro- or bromo-complexes and is consistent with a loss of hydrogen-bonding in the iodo-compounds. The spectra of the iodo-complexes are similar to those of the $M(CO)_4dpa$ complexes in which there is no acido-group with which the dpa ligand can strongly hydrogen bond. In conclusion it would appear that the complexes $[MI(\eta^3\text{-allyl})(CO)_2dpa]$ (M = Mo or W) give

rise to isomers, both in the solid state and in acetonitrile solution, and that these isomers may arise because of the lack of hydrogen-bonding between the iodine atom and the acyclic amine hydrogen atom.

3.3.3.2 The thiocyanate complexes

Thiocyanate is an ambidentate ligand and, when monodentate, exhibits two modes of co-ordination, namely N-thiocyanato (isothiocyanate) or S-thiocyanato (thiocyanate). The mode of co-ordination is controlled by both electronic and steric factors. In general N-bonding occurs with "class a" metals and S-bonding to "class b" metals, although steric effects can alter this situation[208,209].

The N-bonded ligand gives rise to an approximately linear MNCS group whereas the S-bonded ligand forms a non-linear M - SCN unit (Figure 3-10) and is consequently more subject to steric interactions than the N-isomers.

Figure 3-10. The N- and S-thiocyanate ligand.

The "class a or b" (hard or soft respectively) nature of a metal[210] can be modified by its oxidation state and by the ligands to which it is coordinated. Increasing the oxidation state makes the metal "harder" whilst the presence of π-bonded ligands (CO, olefins, etc.) makes the metal "softer", consequently

it is possible to obtain borderline cases where N- and S-bonded isomers can both exist. For example the complex $[Mo(NCS)Cp(CO)_3]$ exhibits this form of isomerism[211], and other similar Group VI carbonyl species might be expected to behave in this way.

Table 3-8 summarises the C - N and M - X stretching vibrations for the thiocyanato-complexes $[M(NCS)(\eta^3\text{-allyl})(CO)_2L_2]$. The complex $[Mo(NCS)(\eta^3\text{-allyl})(CO)_2bipy]$ has been shown to contain an N-bonded thiocyanate group in the solid state[72], whilst the structures of the other thiocyanates, listed in table 3-8, have not been determined.

Table 3-8

Selected infra-red data for $[M(NCS)(\eta^3\text{-allyl})(CO)_2L_2]$

M[a]	L_2 = bipy		L_2 = dpa		
	ν_{CN}	ν_{MX}[b]	ν_{NH}	ν_{CN}	ν_{MX}[b]
Cr	2095vs	-	-	-	-
Mo	2095vs	263s	3285m,br	2105vs	242s
			(3350m)[c]	(2080s-vs)[c]	
W	2095vs	270s	3290m,br	2110vs	238s

a) Spectra obtained for Nujol mulls

b) X is the coordinated atom of the thiocyanate group

c) This band is not observed in every preparation of this complex.

It was observed that some specimens of the complex $[Mo(SCN)(\eta^3\text{-allyl})(CO)_2dpa]$ had additional bands at 3350, 2080 and 815 cm^{-1} in their infra-red spectra. The highest band is probably due to a non-hydrogen-bonded NH stretching vibration (p. 107), while the other bands may be assigned to a CN and a CS stretching vibration respectively. Other bands which may have occurred in the CS stretching region (700 - 800 cm^{-1}), and the NCS bending modes (ca. 480 cm^{-1} for M - NCS and ca. 420cm^{-1} for M - SCN[212]), were masked by the presence of strong ligand absorbances in these regions, hence it appears that the complex $[Mo(SCN)(\eta^3\text{-allyl})(CO)_2dpa]$ exhibits isomerism which involves either N- and S-bonded thiocyanate groups, or conformational changes of the dpa group as considered for the iodo-analogue (p. 104).

Based on the infra-red data ($\nu_{CN} > 2100cm^{-1}$; ν_{MS} ca. 240 cm^{-1} and the probable absence of ν_{CS} in the region 800 to 830 cm^{-1})[212-4] it would appear, though not conclusively, that the new complexes $[M(SCN)(\eta^3\text{-allyl})(CO)_2dpa]$ (M = Mo or W) are normally S-bonded thiocyanate compounds. This is in contrast to the N-bonded complex $[Mo(NCS)(\eta^3\text{-allyl})(CO)_2bipy]$, and presumably its chromium and tungsten analogues all of which have very similar infra-red spectra. In addition it seems likely that the irregularly formed isomer $[Mo(SCN)(\eta^3\text{-allyl})(CO)_2dpa]$ is probably N-bonded, having ν_{CN} below 2100 cm^{-1} and giving rise to a CS stretching vibration at 815 cm^{-1}. It was also observed that this isomer had a non-hydrogen-bonded NH group (ν_{NH}, 3350 cm^{-1}) whereas the normal isomer had a hydrogen-bonded

NH group. Due to the non-linearity of the metal-S-thiocyanate group the amine-hydrogen atom and the nitrogen atom of the thiocyanate group are very favourably positioned for the formation of a hydrogen bond (Figure 3-11). In these

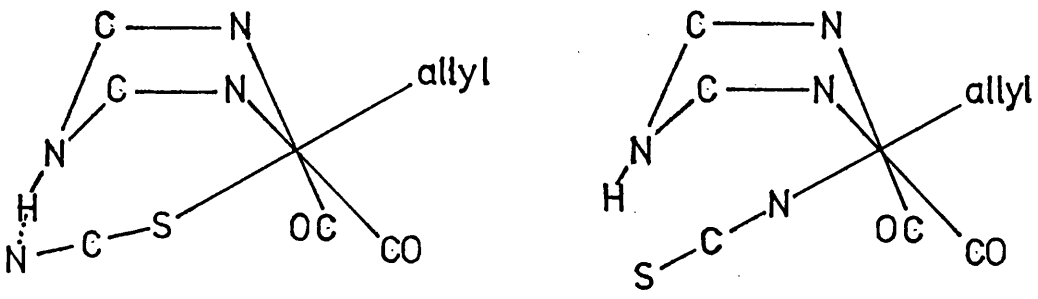

Figure 3-11. Possible hydrogen bonding in the complex $[Mo(NCS)(\eta^3\text{-allyl})(CO)_2dpa]$

circumstances the hydrogen bond may be sufficient to stabilise the S-isomer with respect to the N-isomer, which is found for the analogous bipy complexes.

In solution at room temperature no infra-red or ^{1}H-n.m.r. evidence could be found for the presence of more than one species for the complexes $[M(SCN)(\eta^3\text{-allyl})(CO)_2dpa]$. However, on reducing the temperature (below -20°C) additional bands were observed in the aromatic region of the ^{1}H-n.m.r. spectrum of the tungsten complex (p. 98).

As these spectral changes only occur in the dpa region of the spectrum it seems reasonable to expect the geometric changes to primarily involve this group. Thus it would appear that two dpa conformers, similar to those shown in figure 3-9 for the iodo-complexes, are in rapid equilibrium in solution. An alternative explanation involving N/S-isomerism of the thiocyanate group seems less likely as this would probably be a higher energy process and result in spectral changes occurring in the allyl as well as the dpa regions of the n.m.r. spectrum. Attempts to ascertain the best conditions for isolating these isomers failed which made it impossible to fully characterise them.

In conclusion it would appear that the bipy complexes of chromium, molybdenum and tungsten are all N-thiocyanate compounds, whereas the dpa complexes of molybdenum and tungsten appear to be S-bonded thiocyanates, with the possibility of an unstable N-bonded isomer for the molybdenum-dpa complex.

3.3.3.3 The acetate and trifluoroacetate complexes.

The carboxylate ligands (RCO_2^-) have three basic modes of co-ordination (Figure 3-12), namely monodentate, bidentate chelating and bidentate bridging. It is difficult to differentiate

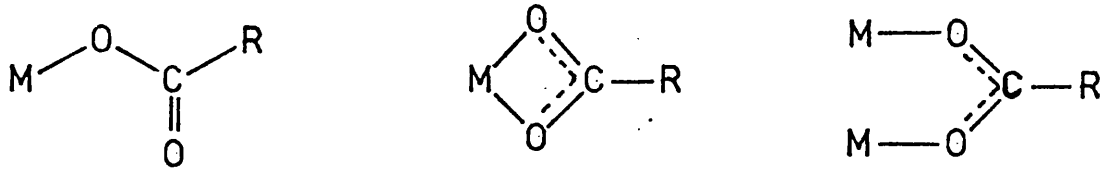

Monodentate | Bidentate chelating | Bidentate bridging

Figure 3-12. Bonding modes of carboxylate ligands.

between the two bidentate modes by infra-red spectroscopy, but it is generally possible to identify the monodentate species.

For the monodentate ligand there is a large separation (>150 and >250 cm^{-1} for the acetate and trifluoroacetate groups respectively) between the two CO stretching vibrations, which approximate to $\nu_{C=O}$ and ν_{C-O}.[215-6] Whereas for the bidentate carboxylate the separation between the two CO stretching vibrations [$\nu_{CO_2(assym)}$ and $\nu_{CO_2(sym)}$] will be similar to that found in the free ion ($\Delta\nu_{CO_2}$ = 143 and 230 cm^{-1} for $CH_3CO_2^-$ and $CF_3CO_2^-$ respectively)[215-6]. In addition the local symmetry of the carboxylate ligand will be lower for a monodentate species relative to a bidentate ligand. Hence monodentate complexes of $CF_3CO_2^-$ give rise to three CF stretching vibrations in their infra-red spectra[215], whilst the more symmetric bidentate complexes of this ligand may only show two CF stretching bands. However, this criterion must be used with caution, as the doubly degenerate ν_{FCF_2} band of the isolated bidentate $CF_3CO_2^-$ group (C_{2v} symmetry) may be split due to low overall molecular symmetry of the complex. Hence a bidentate group may be mistaken for a monodentate ligand.

The relevant infra-red data is summarised in Table 3-9, and reveals the presence of three CF stretching vibration for each of the CF_3CO_2 complexes, together with a large separation between the two CO stretching vibrations ($\Delta\nu_{CO}$ = 265 to 314

Table 3-9

Selected infra-red data for the carboxylate complexes $[M(RCO_2)(\eta^3\text{-allyl})(CO)_2L_2]$

M[a]	R	L_2 = bipy		L_2 = dpa	
		ν_{CO}	ν_{CH} or ν_{CF}	ν_{CO}	ν_{CH} or ν_{CF}
Mo	CH_3	1620s	2980m	1595s	2980m
		1315s		1330s	
	CF_3	1690vs	1195vs	1665s	1195vs
		1417s	1180sh	1420s	1160s
			1140vs		1130s
W	CH_3	1630s	2970m	1615s	2975m
		1316s		1325s	
	CF_3	-	-	1680s	1195vs
				1425sh	1160s
					1140s

a) Spectra obtained for Nujol and hexachlorobutadiene mulls.

and 245 to 273 cm^{-1} for the CH_3CO_2 and CF_3CO_2 complexes respectively) for each complex. Based on this data the new carboxylate complexes $[M(RCO_2)(\eta^3\text{-allyl})(CO)_2L_2]$ (M = Mo or W, R = CH_3 or CF_3 and L_2 = dpa; M = Mo, R = CF_3 and L_2 = bipy; M = Mo or W, R = CH_3 and L_2 = bipy) are formulated with monodentate carboxylate ligands, leading to the expected 18-electron configuration for the central metal atom. Indeed the spectra of the coordinated groups in these complexes were very similar to those reported for $[M(CF_3CO_2)(\eta^3\text{-allyl})(CO)_2dme]$, M = Mo or W, which have been shown by X-ray crystallographic studies to contain monodentate

CF_3CO_2 ligands.[119]

3.3.3.4 The sulphinate complexes

The sulphinate group (RSO_2^-) has several possible modes of coordination to a transition metal and figure 3-13 illustrates the four types of coordination which may occur in monomeric complexes.

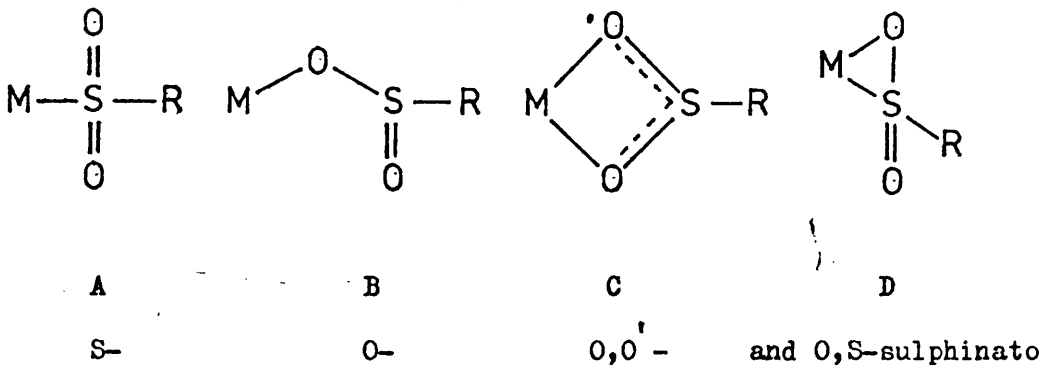

Figure 3-13. The coordination of the sulphinate group

Due to changes in the SO bond order of the sulphinate group it is usually possible to differentiate between the first three of these four bonding modes (i.e. S-, O- and O,O'-sulphinato) by infra-red spectroscopy.[217] The fourth mode S,O-sulphinato, is more difficult to confirm but fortunately this mode of bonding is rare, especially in mononuclear complexes. Consideration of figure 3-13 shows that, relative to the free anion, ν_{SO_2} (symmetric and assymmetric) should increase for the S-bonded species, while for the O-bonded ligand one might expect ν_{SO} (coordinated) to decrease and

ν_{SO} (uncoordinated) to increase. The remaining species 0,0'-sulphinato, should be similar to the free anion. This is supported by observed spectra[217] which are as follows:

(a) 0,0'-sulphinato; $\nu_{as}SO_2$ ca. 1000 and $\nu_{s}SO_2$ ca. 950 cm^{-1}. These modes are 10 to 80 cm^{-1} lower than the free anion.

(b) O-sulphinato; ν_{SO}(uncoordinated) 1100 - 1050 and ν_{SO} (coordinated) ca. 900 cm^{-1}. This latter value is 100 - 200 cm^{-1} lower than the free anion.

(c) S-sulphinato; ν_{as} SO_2 1250 - 1100 and $\nu_{s}SO_2$ 1100 - 100 cm^{-1}.

The band positions observed in this work (Table 3-10) and the absence of SO vibrations in the region 1100 to 1250 cm^{-1} are consistent with the ligand being present as a monodentate

Table 3-10

Selected infra-red data for $[M(\eta^3\text{-allyl})(RSO_2)(CO)_2L_2]$

M[a]	R	L_2 = bipy		L_2 = dpa	
		ν_{SO} (uncoord.)	ν_{SO}(coord.)	ν_{SO}(uncoord.)	ν_{SO}(coord.)
Mo	C_6H_5	1088	865	1050	920
	$CH_3C_6H_4$	1058	875	1040	905
W	C_6H_5	1090	855	-	-
	p-$CH_3C_6H_4$	1065	868	-	-

a) Spectra were measured for Nujol mulls. All bands are strong.

oxygen-donor group (i.e. B, figure 3-13). This is in contrast to the complex $[MoCp(MeSO_2)(CO)_3]$ which is known to be S-bonded (i.e. A, figure 3-13)[218]. The reason for this change in coordination may be at least partially due to steric factors as the S-isomer would require a larger coordination site than would the O-bonded isomer.

3.3.4. The chromium(II) analogues

The new chromium complexes $[CrX(\eta^3\text{-allyl})(CO)_2bipy]$ (X = Cl, Br, I or NCS) appear from their infra-red spectra to be very similar to the analogous molybdenum and tungsten complexes, thus they may be considered as formally seven-coordinate chromium(II) species. Chromium(II) allyl carbonyl complexes are not very common (cf. table 1-9), thus the fascile synthesis described earlier forms an important extension to chromium(II) chemistry. The complexes $[CrI(\eta^3\text{-allyl})(CO)_2bipy]$ was found to be essentially diamagnetic ($\chi_m$ca. 250 x $10^{-6}cm^3mol^{-1}$), with traces of chromium(III) impurities probably causing this slight paramagnetism.

Unlike the analogous molybdenum and tungsten complexes, these new complexes have very low stabilities towards solvents, which lead to decomposition and the precipitation of the complex $Cr(CO)_4bipy$. A disproportionation reaction occurs in neutral or basic solution to give the chromium(0) species and a chromium(III) species which was not isolated. This instability precluded any n.m.r. studies on these compounds.

All attempts to carry out reactions, such as anion exchange or reaction with three-electron donor ligands, with these complexes also failed, leading to $Cr(CO)_4$bipy if the complex dissolved, and to no reaction if the complex was insoluble.

3.3.4.1 Decomposition of $[CrCl(\eta^3\text{-allyl})(CO)_2bipy]$

The complex $[CrCl(\eta^3\text{-allyl})(CO)_2bipy]$ was decomposed both thermally and in aqueous media (2M HCl, 2M NaOH and water), with the gaseous and solid products being examined by infra-red spectroscopy. In each case the liberated gas contained propene and carbon monoxide, and in addition thermolysis produced $Cr(CO)_6$ in the gas phase.

3.3.4.1.1 In aqueous media

During the aqueous reactions two products were formed, one was shown to be $Cr(CO)_4$bipy and the second was an uncharacterised green soluble material which gave an esr spectrum typical of a chromium(III) species. It was found that the reaction was far quicker in acid media (2M HCl) than it was under neutral (H_2O) or basic (2M NaOH) conditions, and it is possible that the sodium hydroxide plays very little part in the decomposition. In addition it was observed that considerably less $Cr(CO)_4$bipy was formed when the medium was 2M HCl than when water or 2M NaOH was used.

The following schemes summarise the available data, but only $Cr(CO)_4$bipy, propene and carbon monoxide have been fully characterised as reaction products. Qualitative tests indicated that the green material from base hydrolysis contained Cr, Cl and bipy, but was probably not a single complex.

Scheme 1. 2M HCl:

$$CrCl(\eta^3\text{-allyl})(CO)_2\text{bipy} \xrightarrow{HCl} [\text{unknown Cr(III)}] + CH_3CH{:}CH_2 + CO$$

Scheme 2. 2M NaOH or H_2O:

$$CrCl(\eta^3\text{-allyl})(CO)_2\text{bipy} \xrightarrow{H_2O} [\text{unknown Cr(III)}] + CH_3CH{:}CH_2 + CO + Cr(CO)_4\text{bipy}$$

It is probable that both of these schemes will be in competition with their relative importance dependent on the pH.

3.3.4.1.2 Thermolysis

On gentle warming of a sample of the chloro-complex in vacuo the first gases liberated were propene and carbon monoxide; $Cr(CO)_6$ volatilised on further heating leaving a dark green solid residue. This residue contained free bipyridyl (ether extractable) as well as coordinated bipyridyl.

This reaction is more difficult to rationalise than the aqueous reactions as there is a deficit of hydrogen atoms, which should possibly lead to a gaseous mixture containing biallyl(hexa-1,5-diene), propene, allene or propyne (Schemes 3 to 5).

Scheme 3: $2(CH_2 : CHCH_2^{\bullet}) = CH_2 : CHCH_2CH_2CH : CH_2$

Scheme 4: $2(CH_2 : CHCH_2^{\bullet}) = CH_3CH : CH_2 + CH_2 : C : CH_2$

Scheme 5: $2(CH_2 : CHCH_2^{\bullet}) = CH_3CH : CH_2 + CH_3C : CH$

Careful examination of the infra-red spectrum of the gaseous products failed to produce any evidence for the presence of allyl chloride, biallyl, allene or propyne. The only other sources of hydrogen atoms are bipyridyl or traces of moisture in the reactants or reaction vessel. Again a disproportionation reaction is occurring yielding Cr(III) and Cr(0) species; but under these conditions $Cr(CO)_6$ is formed rather than $Cr(CO)_4$bipy. In view of the sensitivity of the starting material towards atmospheric oxygen and moisture, no further attempts were made to rationalise this reaction.

3.3.5. Attempted preparation of [$MoCl(\eta^3$-allyl$)(CO)_2$nbn]

Although this preparation failed to produce the desired product, the reaction between [$MoCl(\eta^3$-allyl$)(CO)_2(MeCN)_2$] and nbn proved to be interesting as it produced an off-white rubbery material which contained only traces of molybdenum. On drying in vacuo this product became fairly brittle and would not mull with Nujol or hexachlorobutadiene.

The initial filtrate still contained a cis-dicarbonyl species as shown by evaporating a little of the filtrate onto an infra-red plate and recording the spectrum (ν_{CO} = 1940s and 1850s cm^{-1}), but it did not prove possible to isolate this species. Thus neither of the products were fully characterised but it would appear that the system $[MoCl(\eta^3\text{-allyl})(CO)_2(MeCN)_2]$-acetone causes the polymerisation of norbornadiene. A little oxygen may be required to promote this reaction as the initial formation of the product was very slow but on the admission of air during the filtration, more of the product was rapidly formed.

3.4. Conclusion.

The new compounds $[MX(\eta^3\text{-allyl})(CO)_2L_2]$ all appear to be structurally similar to the well characterised complex $[Mo(NCS)(\eta^3\text{-allyl})(CO)_2bipy]$[72]. Thus they are pseudo-octahedral (or capped trigonal prismatic[219] if the allyl group is regarded as a bidentate ligand [Figure 1-18]) with the monodentate acido- and the allyl-ligands probably trans to each other, and with the remaining square plane occupied by the central metal atom, a bidentate nitrogen ligand and a pair of mutually cis-carbonyl groups (Figure 3-5, A). It is also possible that some of the complexes adopt a variation of this structure in which one end of the bidentate ligand has exchanged coordination sites with the acido-ligand (Figure 3-5, B).

The iodo-complexes $[MI(\eta^3\text{-allyl})(CO)_2dpa]$ (M = Mo or W) exhibit isomerism which is best explained in terms of conformational changes in the dpa group. The lack of hydrogen-bonding between the iodine atom and the acyclic amine group of dpa probably causes this form of isomerism, which is not observed for the corresponding chloro- and bromo-complexes.

The complexes $[M(SCN)(\eta^3\text{-allyl})(CO)_2dpa]$ (M = Mo or W) may contain S-bonded thiocyanate groups in contrast to $[Mo(NCS)(\eta^3\text{-allyl})(CO)_2bipy]$, which is known to be N-bonded[72]. It is possible that the S-bonded thiocyanate group is stabilised by a N - H - N hydrogen bond between the acyclic amine group of dpa and the nitrogen atom of the S-thiocyanate ligand. In addition the complex $[Mo(SCN)(\eta^3\text{-allyl})(CO)_2dpa]$ gave rise to an intermittently formed isomer which probably contains an N-bonded thiocyanate group; whilst the tungsten complex exists as a mixture of two isomers in solution at low temperatures. These two isomers probably result from conformational changes in the dpa ligand.

In all the complexes isolated the acido-group appears to act as a simple monodentate ligand analogous to the halide ligands, allowing the central metal atom to achieve an 18e configuration.

The new chromium complexes $[CrX(\eta^3\text{-allyl})(CO)_2bipy]$ (X = Cl, Br, I or NCS), which are the first known examples of this Cr(II) - allyl - carbonyl system, are much less stable than the analogous molybdenum and tungsten complexes and can

only be prepared at low temperatures. As yet it has not proven possible to study the reactions of these complexes due to their ready disproportionation in solution.

Chapter 4

Three-Electron Donor Ligand Complexes of Molybdenum(II)

Chapter 4.

Three-Electron Donor Ligand Complexes of Molybdenum(II)

4.1 Introduction

The three-electron donor ligands studied (LL_a = acac, dedc, dmdc, salal and sal:NPh) reacted with the complexes $[MX(\eta^3\text{-allyl})(CO)_2L_2]$ (X = Cl, Br; L_2 = bipy, dpa) in the presence of pyridine to give the new complexes $[Mo(\eta^3\text{-allyl})LL_a(CO)_2py]$, with just one exception. Reaction of the salt Nasalal with the bipy complex $[MoX(\eta^3\text{-allyl})(CO)_2bipy]$ resulted in anion exchange, rather than displacement of bipy, with the formation of the complex $[Mo(\eta^3\text{-allyl})(salal)(CO)_2bipy]$.

The analogous series of chromium and tungsten(II) complexes containing these ligands could not be prepared.

The new molybdenum complexes have been characterised by means of their analysis and spectroscopic properties (infra-red, n.m.r. and mass spectra), and have been shown to be stereochemically non-rigid molecules.

Possible mechanisms for the formation and isomerisation of these complexes are discussed in the light of a recently determined [220] crystal structure of the acetylacetonate complex.

4.2 Experimental

All the preparations except those involving the ligand sal:NPh, were carried out by the procedure outlined below, with the salt Na^+acac^- being replaced by an equivalent molar quantity of the relevant salt $NaLL_a$. The procedure adopted for the sal:NPh complex is described subsequently.

With the exception of the salal complexes, the same product was obtained regardless of which of the starting materials [MoX(η^3-allyl)(CO)$_2$bipy] or [MoX(η^3-allyl)(CO)$_2$dpa], with X = Cl or Br, was used.

4.2.1. [Mo(η^3-allyl)(acac)(CO)$_2$py]

The reactants, [MoCl(η^3-allyl)(CO)$_2$bipy] (0.35 g, 0.91 mmol), Naacac (0.44 g, 3.60 mmol) and pyridine (5 cm^3, 62 mmol), were stirred together in de-oxygenated acetone (20 cm^3) for 3 days at room temperature. The resulting mixture was filtered, and water (10 cm^3) was added to the filtrate which was then rotary evaporated, at room temperature, until the product [Mo(η^3-allyl)(acac)(CO)$_2$py] started to separate as an oil. On standing at 0°C the product crystallised and was collected at the filter, washed with water and dried in vacuo.

4.2.2. [Mo(η^3-allyl)(sal:NPh)(CO)$_2$py]

The reactants [MoCl(η^3-allyl)(CO)$_2$dpa] (0.42 g, 1.06 mmol), Nasalal (0.21 g, 1.49 mmol), aniline (1cm^3, 11 mmol) and pyridine (2 cm^3, 25 mmol) were stirred together in acetone (20 cm^3) at room temperature for three days. The resulting mixture was filtered, water (10 cm^3) was added to the filtrate which was then rotary evaporated at room temperature, until the product [Mo(η^3-allyl)(sal:NPh)(CO)$_2$py] started to crystallise. After standing at 0°C for one hour the product was collected at the filter, washed with water and dried in vacuo.

4.2.3 The products

All the products were susceptible to air oxidation, especially while in solution, thus all manipulations were carried out in the absence of air. The complex $[Mo(\eta^3\text{-allyl})(dedc)(CO)_2py]$ was particularly sensitive to air and was readily oxidised to the known deep purple compound $[Mo_2O_3(dedc)_4]$[221].

Table 4-1 lists the products together with their analyses.

Table 4-1

Analytical data for the products

$Mo(\eta^3\text{-allyl})(LL_a)(CO)_2L$		Yield	Colour	Analysis(%)[a]		
LL_a	L	(%)		C	H	N
acac	py	86	Yellow	49.2	5.1	3.9
				(48.5)	(4.6)	(3.8)
salal	py	52[b]	Red	52.2	4.2	3.8
				(51.9)	(3.8)	(3.6)
salal	bipy	68[c]	Maroon	56.5	4.4	6.0
				(56.2)	(3.8)	(6.0)
sal:NPh	py	87	Orange	58.9	4.5	5.8
				(59.0)	(4.3)	(6.0)
dmdc	py	92	Deep Yellow	39.8	4.4	7.3
				(40.0)	(4.1)	(7.1)
dedc	py	88	Deep Yellow	42.1	5.3	6.6
				(42.9)	(4.8)	(6.7)

a) Calculated value in parentheses

b) Obtained from the complex $[MoCl(\eta^3\text{-allyl})(CO)_2dpa]$

c) Obtained from the complex $[MoCl(\eta^3\text{-allyl})(CO)_2bipy]$

4.3 Results and discussion

4.3.1 Characterisation of the new complexes

The analytical (C, H and N) and spectroscopic data for the new complexes, with the single exception of [Mo(η^3-allyl)(salal)$(CO)_2$bipy], indicated that the halide ion and the neutral bidentate nitrogen ligand (formally 1- and 4-electron donors respectively) in the starting materials had been replaced by pyridine (2-electron donor) and an anionic 3-electron donor, so that overall neither the oxidation state nor the number of valence electrons of the central metal atom were altered.

Information on the stereo-chemistries of these products, and the ligand bonding modes in [Mo(η^3-allyl)(salal)$(CO)_2$bipy], was obtained by spectroscopic examination of the complexes as outlined below.

4.3.2 Infra-red Spectroscopy.

The number, positions and relative intensities of the metal carbonyl C-O stretching vibrations in the infra-red spectra (Table 4-2) confirm that the products still contain the cis-dicarbonyl grouping.

Table 4-2

Selected infra-red data for the complexes $Mo(\eta^3\text{-allyl})(LL_a)(CO)_2L$

LL_a	L	Infra-red[a] (cm^{-1}) ν_{CO}	Ligand (LL_a) bands
acac	py	1918, 1830	1585, 1525, 1275 ($\nu_{C=C}$ and/or ν_{C-C}
salal	py	1932, 1840	1620 (ν_{CO})
salal	bipy	1930, 1842	1670 (ν_{CO})
sal:NPh	py	1930, 1850	1605 (ν_{CN})
dedc	py	1918, 1822	1505(ν_{CN}), 1150(ν_{NC_2}), 997(ν_{CS})
dmdc	py	1923, 1838	1490(ν_{CN}), 1150(ν_{NC_2}), 980(ν_{CS})

a) Measured as Nujol and C_4Cl_6 Mulls with all bands very strong.

4.3.2.1 Bonding of the anionic ligands

a) Acac

The ligand acac normally exhibits two modes of coordination[222], namely O,O'-enolate or C-ketonate (Figure 4-1).

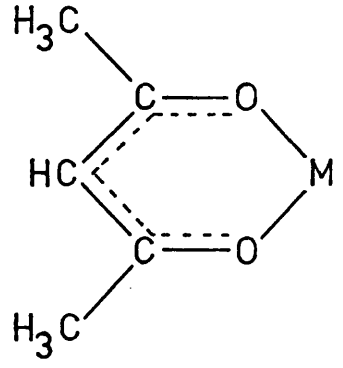

O,O'-enolate

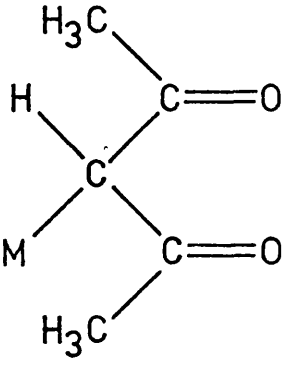

C-ketonate

Figure 4-1 The normal bonding modes of acac

Due to changes which occur in the local symmetry, and in the C-O and C-C bond orders, of the acac group it is usually possible to differentiate between these bonding modes by infra-red spectroscopy. As is to be expected (cf. figure 4-1) the CO stretching vibrations occur at lower energies for 0,0'-enolate complexes (<1600 cm^{-1}) than for C-ketonate complexes (>1600 cm^{-1}). The 0,0'-enolate complexes contain a planar pseudo-aromatic chelate ring and give rise to aromatic CH stretching (ca. 3080 cm^{-1}) and bending (in-plane ca. 1210 and out-of-plane ca. 820 cm^{-1}) vibrations.[223,224] In contrast the C-ketonate structures will be non-planar and will give rise to a CH stretching vibration at ca. 2940 cm^{-1} and will not show the CH bending vibrations mentioned above.[225] The out-of-plane CH bending vibration occurs as a strong sharp band in the infra-red spectra of enolate species, thus this band and the CO stretching vibration are of great diagnostic value.[222]

The infra-red data given in table 4-2 for the complex [Mo(η^3-allyl)(acac)$(CO)_2$py] is consistent with an 0,0'-enolate species (i.e. $\nu_{CO} < 1600$ cm^{-1}).

b) Salal

The ligand salal can co-ordinate as a simple phenate group or as a bidentate ligand, co-ordinating through the aldehydic and phenate oxygen atoms. The bidentate ligand should give rise to a lower energy carbonyl CO stretching vibration than the monodentate phenate species.

The value of $\nu_{C=O}$ found for the complex $[Mo(\eta^3\text{-allyl})(salal)(CO)_2py]$ (cf. table 4-2) is consistent with the presence of a bidentate salal group[226]. The complex $[Mo(\eta^3\text{-allyl})(salal)(CO)_2bipy]$ exhibits a $\nu_{C=O}$ band at 1670 cm^{-1} which is high for a bidentate group[226] and probably indicates that salal is present as a monodentate phenate ligand. In addition the infra-red bands observed for bipy in this complex are very similar to those found for the bipy complexes discussed in chapter 3, thus indicating normal bidentate behaviour for this ligand and an eighteen electron configuration for the central molybdenum atom.

c) Sal:NPh

This ligand is simply the N-phenyl imine of salicylaldehyde and will show similar modes of coordination (i.e. monodentate phenate or bidentate via O,N-coordination). The bidentate ligand should give rise to a CN stretching vibration in the region 1590-1630 cm^{-1}, whereas the phenate species should have a CN stretching vibration in the region 1640-1660 cm^{-1} [226,227]. Consequently the band observed at 1605 cm^{-1} for the complex $[Mo(\eta^3\text{-allyl})(sal:NPh)(CO)_2py]$ (cf. table 4-2) is consistent with bidentate sal:NPh as expected.

Due to extensive coupling of molecular vibrations it is difficult to fully interpret the infra-red spectra of metal-Schiff base complexes.[228] Even the fairly simple complexes $[Cu(sal:NR)_2]$ and $[Cu(PhCOCHC\{:NR\}CH_3)_2]$ are too complex to allow any theoretical analysis of the infra-red spectra.[228] Such complexes should not be considered by the normal group frequency approach as isotopic

studies ($^{15}N/^{14}N$)[228] have shown that the CN vibrations are strongly coupled to other ligand modes. For this reason, no further assignments have been attempted.

d) Dimethyl- and diethyldithiocarbamate

Dithiocarbamate ligands also have two modes of attachment in mononuclear complexes, namely monodentate and bidentate, through one or both of the sulphur atoms respectively. Infra-red spectroscopy provides a possible means of differentiating between these bonding modes. The CN stretching band (The "dithiouride" band[229]) occurs in the regions 1530 - 1490 cm^{-1} and 1490 - 1478 for the bidentate and monodentate ligand respectively[229,230]. In addition the bidentate species gives rise to a singlet near 995 cm^{-1} for the CS stretching vibration whereas the monodentate ligand exhibits a doublet in the same region.[229]

Inspection of table 4-2 reveals that the infra-red spectra of the complexes of both dmdc and dedc are consistent with a bidentate dithiocarbamate group.

The ^1H-n.m.r. spectrum of the complex [Mo(η^3-allyl)(dmdc)$(CO)_2$py] is also indicative of a bidentate dmdc ligand (δ_{Me} = 3.16 ppm)[230]. Unfortunately the n.m.r. spectrum of the corresponding dedc complex was complicated by decomposition products, and could not be used as confirmation of the bidentate nature of dedc.

4.3.3 ^{1}H-n.m.r. spectroscopy

All of the room temperature spectra (Table 4-3) confirm the presence of a η^3-allyl group as found in the reactant complexes (cf. chapter 3).

Comparison of the spectra of the complexes [Mo(η^3-allyl)(salal)$(CO)_2$bipy] and [Mo(η^3-allyl)(salal)$(CO)_2$py] reveal different resonant frequencies for the aldehydic protons (i.e. 9.03 and 8.90 ppm respectively). This observation may be used to support the conclusions drawn from the infra-red spectra that these complexes contain monodentate and bidentate salal groups respectively.

Further examination of the ^{1}H-n.m.r. spectrum of [Mo(η^3-allyl)(salal)$(CO)_2$bipy] reveals several bipy resonances which integrate to only one proton signal (cf. table 4-3). This may be interpreted as indicating either the presence of a monodentate bipy group or an unsymmetric molecular structure (Figure 4-3). The second interpretation is preferred as this is in agreement with the infra-red spectrum; but it must be borne in mind that the infra-red data was obtained for solid samples. Thus at this stage it is not possible to draw any firm conclusions as to the structure of this compound.

Table 4-3

^{1}H-nmr spectra for the complexes [Mo(η^3-allyl)(LLa)(CO)$_2$L]

LLa	L	solvent	δ	Assignment[a]	
acac	py	CD_2Cl_2	1.42(2,d,8)	H_a	η^3-allyl
			3.35(3,m)	H_s+H_c	"
			7.35(2,m)	H_m	pyridine
			7.78(1,m)	H_p	"
			8.35(2,d,5)	H_o	"
			1.87(6,s)	Me	acac
			5.12(1,s)	CH	"
Salal	py	$CDCl_3$	1.52(2,br)	H_a	η^3-allyl
			3.18(1,br)	H_c	"
			3.44(2,br)	H_s	"
			7.20(2+1,m)[b]	H_m	pyridine
			7.62(1,t,7)	H_p	"
			8.40(2,d,6)	H_o	"
			6.37(1,t,7)	H(aromatic)	salal
			6.72(1,d,8)	"	"
			6.98(1,d,10)	"	"
			7.20(1+2,m)[b]	"	"
			8.90(1,s)	HCO	"

Table 4-3 (Contd)

LLa	L	solvent	δ	Assignment[a]
salal	bipy	$CDCl_3$	1.30(2,d,8)	H_a η^3-allyl
			3.19(2,s)	H_s "
			3.52(1,m)	H_c "
			6.52(1,t,7)	$H_{(aromatic)}$ salal+bipy
			6.98(1,d,8)	" "
			7.42(5,m)	" "
			7.95(3,m)	" "
			8.36($\frac{1}{2}$,d,8)	" "
			8.60($\frac{1}{2}$,t,6)	" "
			8.85(1,d,5)	" "
			9.03(1,s)	HCO salal
sal=NPh	py	$CDCl_3$	1.43(1,d,8)	H_a η^3-allyl
			1.66(1,d,9)	H_a "
			2.99(1,m)	H_c "
			3.62(2,m)	H_s "
			7.66(1,t,8)	H_p pyridine
			8.30(2,m)	H_o "
			6.43(1,t,7)	$H_{(aromatic)}$ sal=NPh + pyridine(H_m)
			6.75 to 7.44(10)	"
			7.78(1,s)	HC=N sal=NPh
dmdc	py	CD_3CN	1.32(2,d,10)	H_a η^3-allyl
			ca. 3.08(2,d)[c]	H_s "
			4.14(1,m)	H_c "
			7.36(2,m)	H_m pyridine
			7.84(1,m)	H_p "
			8.72(2,d,6)	H_o "
			3.16(6,s)	Me dmdc

Table 4-3 (Contd)

LLa	L	solvent	δ	Assignment[a]	
dedc[d]	py	CD_3CN	2.0(6,t,8)	CH_3	dedc
			4.56(3,q,7)	CH_2	"
			8.30(2,t,6)	H_m	pyridine
			8.79(1,t,7)	H_p	"
			9.68(2,d,5)	H_o	"

a) The terms used in the assignment are specified in figure 4.2.

b) These bands are coincident with a relative intensity of 3 (ie. 2+1).

c) This band is partially obscured by the methyl resonance.

d) This spectrum is complicated by the partial decomposition of the complex.

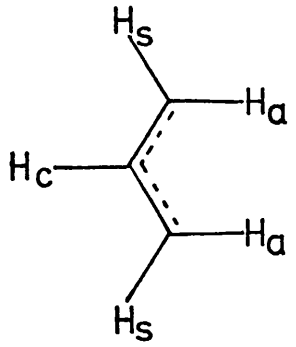

η^3-allyl

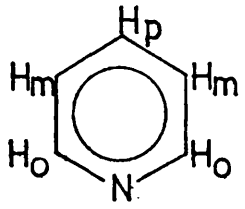

pyridine

Figure 4-2. Nomenclature used in table 4.3

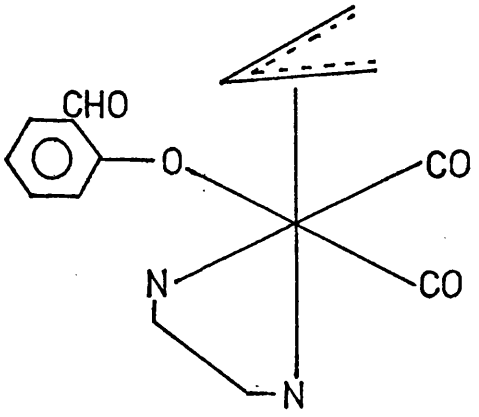

Figure 4-3. The possible unsymmetric structure of $[Mo(\eta^3\text{-allyl})(salal)(CO)_2bipy]$

All the pyridine complexes $[Mo(\eta^3\text{-allyl})(LL_a)(CO)_2py]$, except the sal:NPh compound, give rise to room temperature ^1H-n.m.r. spectra which are consistent with the more symmetric structure (A, figure 4-4) or with a structure of lower symmetry

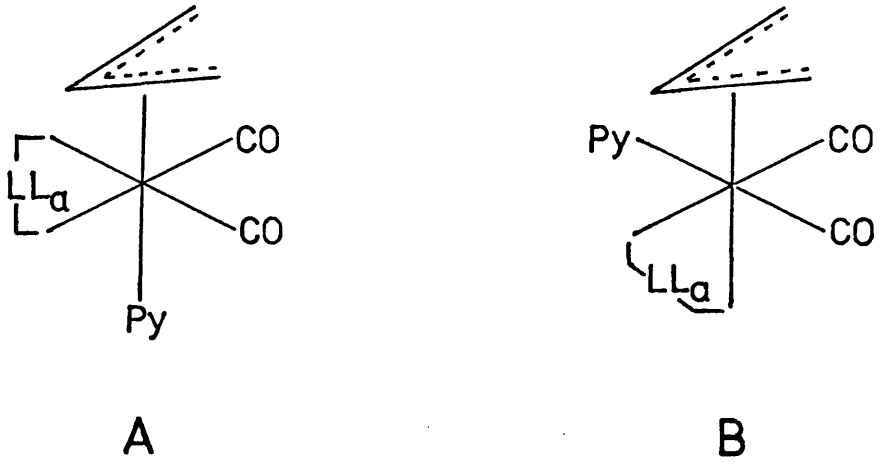

Figure 4-4. Isomeric structures for $[Mo(\eta^3\text{-allyl})(LL_a)(CO)_2py]$

exhibiting fluxional behaviour. The room temperature spectrum of the complex [Mo(η^3-allyl)(sal:NPh)$(CO)_2$py] is consistent with any of three structures based on (A) and (B) of figure 4-4 (of. figure 4-5).

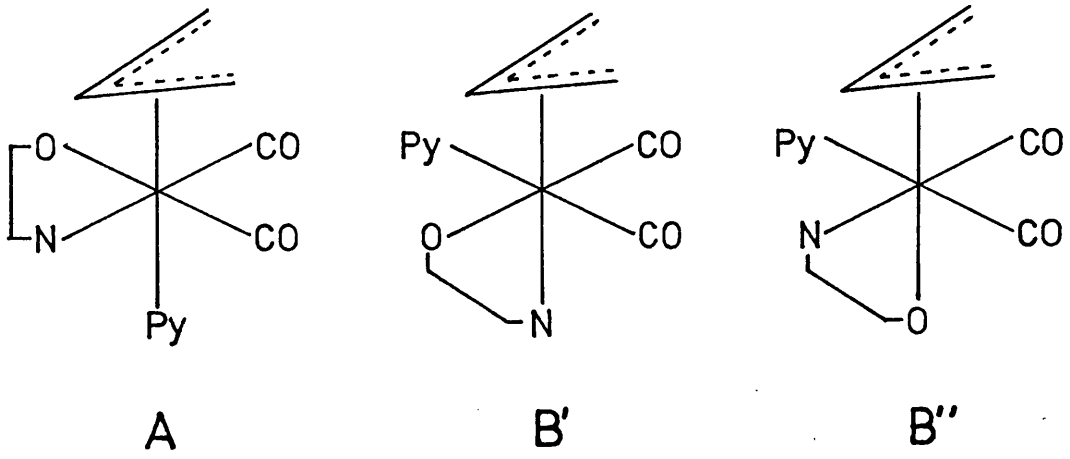

Figure 4-5. Possible isomers of [Mo(η^3-allyl)(sal:NPh)$(CO)_2$py]

In order to differentiate between the various isomers and obtain more information on the fluxional behaviour of these molecules, variable temperature studies of the acac and sal:NPh complexes were undertaken.

4.3.4 Variable temperature n.m.r. studies

The ^{1}H-n.m.r. spectrum of [Mo(η^3-allyl)(sal:NPh)$(CO)_2$py] simplified above room temperature (Figure 4-6) and the allyl protons H_a and H_s became equivalent in pairs. Because of the low symmetry of the O,N-bonded ligand (Figure 4-5) this must result from stereochemical non-rigidity at elevated temperatures in solution. The low symmetry of this complex makes it impossible to ascertain which isomer occurs in solution at

room temperature but, due to the number and integrated areas of the observed bands, it would appear that only one isomer is present in $CDCl_3$ solution at and below room temperature.

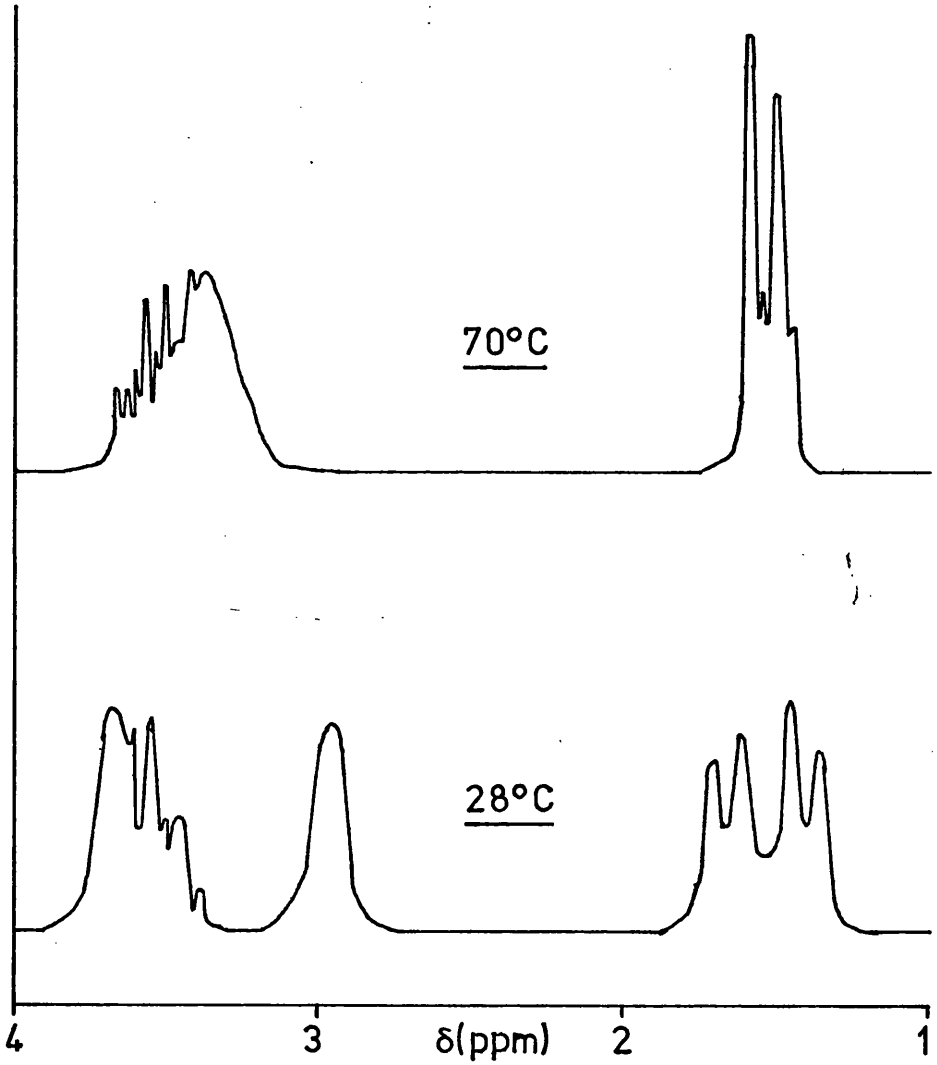

Figure 4-6. ^{1}H-n.m.r. spectrum of $[Mo(\eta^3\text{-allyl})(sal{:}NPh)(CO)_2py]$ at 28 and 70°C

The low temperature n.m.r. spectrum of the acac complex was expected to be easier to interpret as the symmetric isomer A (Figure 4-4) should produce a simple 1 : 2 : 2 resonance pattern for the allyl protons, whereas for the less symmetric isomer B all four syn and anti allyl protons should give separate signals. In d^6-acetone low temperature ^{1}H-n.m.r. spectroscopy (Figure 4-7) revealed the presence of almost 100% of the assymmetric isomer B, whereas in $CDCl_3$ the low temperature spectrum (Figure 4-7 and table 4-4) was more complex and indicated the presence of more than one isomer in solution. These spectra were finally interpreted (Table 4-5) with the aid of recently completed ^{13}C-n.m.r.[283] and X-ray crystallographic[220] studies, which showed that the solid state structure was basically that of isomer B (Figure 4-4) while in solution at low temperatures both isomers A and B coexist. Comparison of the various band intensities in the ^{1}H- and ^{13}C-n.m.r. spectra lead to the isomer ratio of 3 : 5 (A : B) for $[Mo(\eta^3\text{-allyl})(acac)(CO)_2py]$ in $CDCl_3$ solution at -60^oC.

For both complexes $[Mo(\eta^3\text{-allyl})(LL_a)(CO)_2py]$, LL_a is sal:NPh or acac, it was found that at elevated temperatures (50^oC and above in $CDCl_3$ solution) the co-ordinated pyridine readily exchanged with added free pyridine.

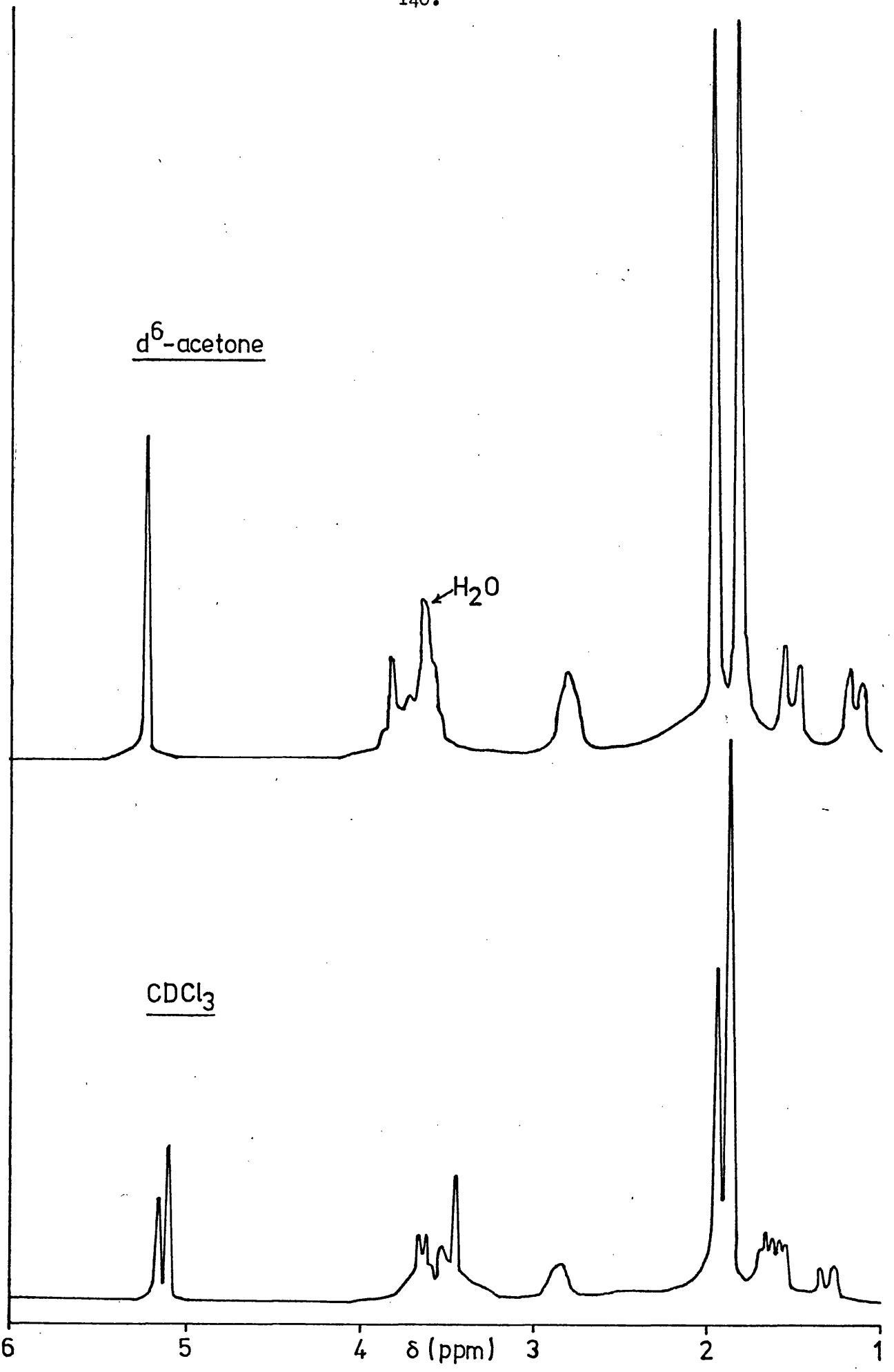

Figure 4-7. ^{1}H-n.m.r. spectrum of [Mo(η^3-allyl)(acac)(CO)$_2$py] in $CDCl_3$ and d^6-acetone at -70°C

Table 4-4

^{1}H-n.m.r. Spectrum of [Mo(η^3-allyl)(acac)(CO)$_2$py]

δ(ppm)		Assignment[a]
$CDCl_3$(-70°C)[b]	$(CD_3)_2CO$(-60°C)	
1.23 (d)	1.16 (d)	H_a
1.56 (dd)[c]	1.52 (d)	H_a
1.81 (s)	1.80 (s)	Me
1.89 (s)	1.94 (s)	Me
2.78 (m)	2.78 (m)	H_c
ca 3.4 (m)		H_c
3.44 (dd)[c]	3.63 (dd)[c]	H_s
5.00 (s)	5.19 (s)	H_β
5.04 (s)		H_β
7.19 (m)	7.51 (t)	py - H_m
7.35 (m)		py
7.66 (m)	7.98 (t)	py - H_p
ca 7.7 (m)		py
8.12 (d)	8.35 (d)	py - H_o
8.48 (d)		py

a) See figure 4-8 for terminology

b) This spectrum is the same at -60°C

c) Overlapping doublets, see figure 4-7

Table4-5

^{1}H- and ^{13}C-n.m.r. spectra of sym. and assym. $Mo(\eta^3\text{-allyl})(acac)(CO)_2py$

δ(ppm)[a] sym.	assym.	Assignment
	1.23 (d)	H_a2
1.56 (d)	1.56 (d)	H_a1
	1.81 (s)	Me_2
1.89 (s)	1.89 (s)	Me_1
ca 3.4 (m)	2.78 (m)	H_c
3.44 (d)	3.44 (dd)[b]	H_s1 and H_s2
5.04 (s)	5.00 (s)	H_β
7.35 (m)	7.19 (m)	py - H_m
ca 7.7 (m)	7.66 (m)	py - H_p
8.48 (d)	8.12 (d)	py - H_o
227.94	228.19[c]	C_1 and C_2
188.75	189.05	C_α
	185.96	C_γ
150.65	150.29	py - C_o
124.74	124.38	py - C_m
138.20	137.67	py - C_p
71.17	72.26	C_β
ca 100.2	100.11	C_A2
61.16	60.55	C_A1
	57.27	C_A3
28.21	28.21	Me_1
	27.61	Me_2

a) Measured for a $CDCl_3$ solution. See fig. 4-8 for terminology.

b) Overlapping doublets, see figure 4-7.

c) Resolved into two bands in $(CD_3)_2CO$

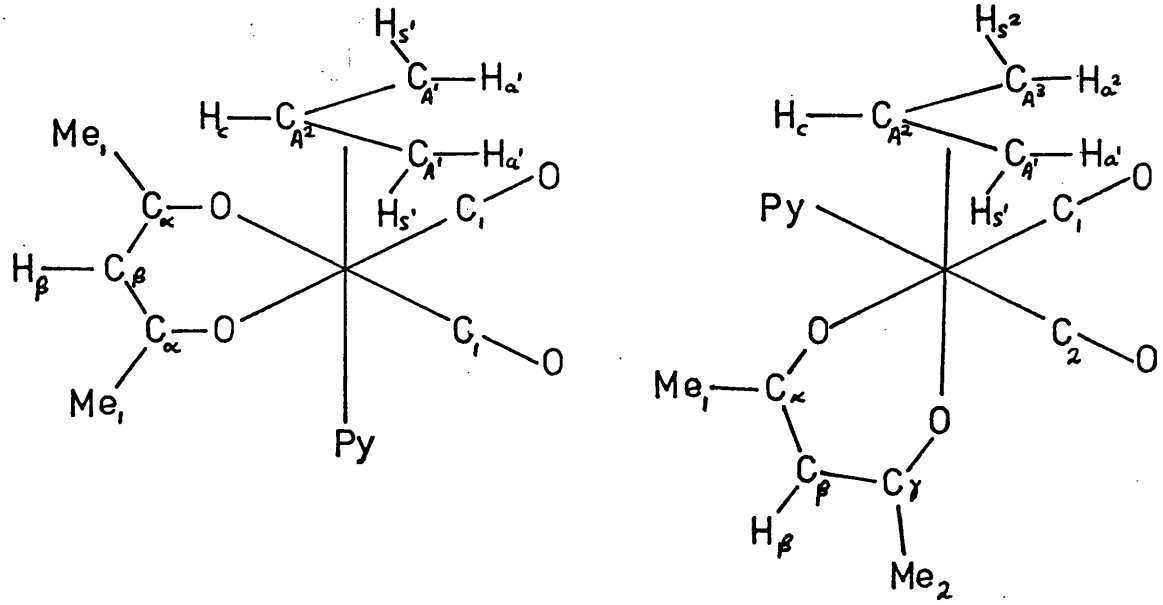

Figure 4-8 Sym- and assym- [Mo(η^3-allyl)(acac)$(CO)_2$py] and the terminology used with the n.m.r. spectra.

4.3.5. Mass spectroscopy

Metal containing fragments were obvious from the isotope pattern of molybdenum (Figure 2-1), but such fragments were only present in fairly low abundances. Table 4-6, which does not include non-molybdenum containing fragments summarises the mass spectra of the complexes [Mo(η^3-allyl)(LL_a)$(CO)_2$py], where LL_a is acac, salal, sal:NPh or dedc. The parent ion was only observed for the acac complex, and even then it was present in an extremely low abundance (i.e. $< 1\%$). The ion $[Mo(allyl)(LL_a)]^+$, formed by the loss of pyridine and two carbonyl groups, had a relatively high abundance for each complex examined. Thus this ion must be relatively stable under the conditions found in the mass spectrometer.

The salal and sal:NPh complexes gave rise to new ions in addition to those created by the simple loss of ligand groups (e.g. CO and py) as shown in figures 4-9 and 4-10.

Table 4-6

Mass spectrum of $[Mo(\eta^3\text{-allyl})(LL_a)(CO)_2py]$

I	Relative abundance of I^+ (%)			
	Acac	Salal	Sal:NPh	Dedc
$Mo(allyl)(LL_a)(CO)_2py$	Tr			
$Mo(allyl)(LL_a)(CO)_2$	36	18	Tr	29
$Mo(allyl)(LL_a)(CO)$	23	18	24	16
$Mo(allyl)(LL_a)$	100	55	100	71
$Mo(allyl)(C_6H_5O)$		100		
$Mo(allyl)(C_{12}H_{10}N)$			67	
$Mo(allyl)(EtNCS_2)$				100
$Mo(allyl)(LL_a)(CO)py$				9
$Mo(C_{14}H_{14}N)$			29	
$Mo(C_{13}H_{13}N)$			21	
$Mo(C_{12}H_{12}N)$			38	

One such ion for the salal complex was $[Mo(allyl)(C_6H_5O)]^+$ which appears to arise by the loss of CO from the salal ligand and may indicate decarbonylation of salal to give the simple phenate ligand PhO.

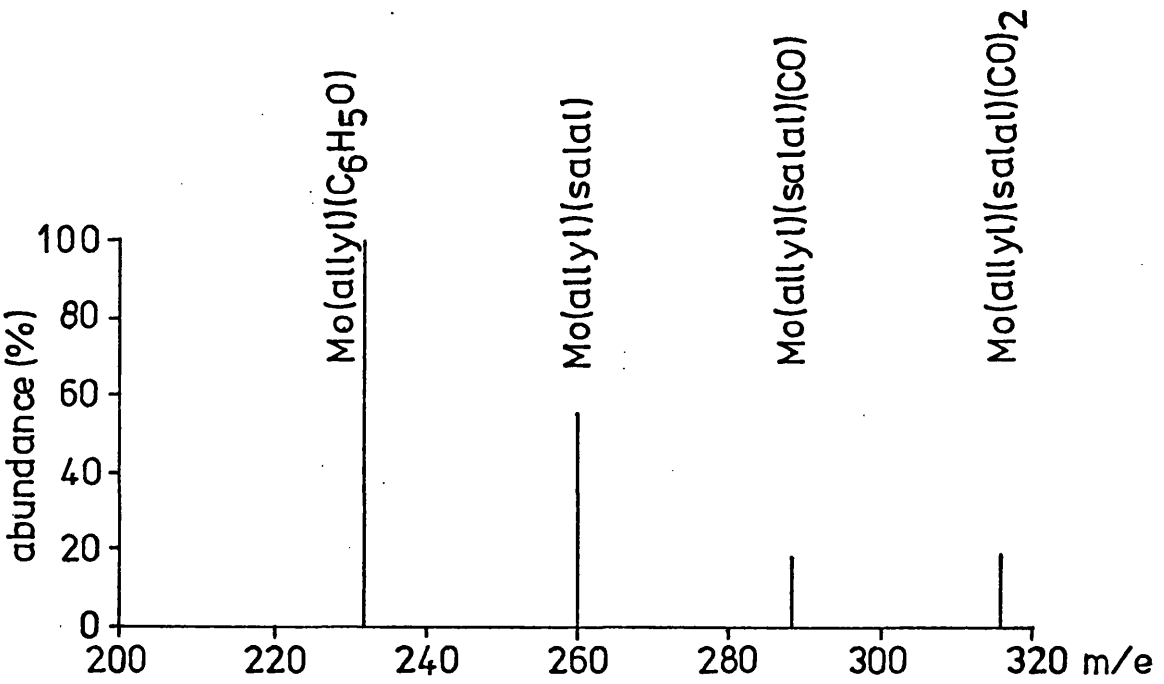

Figure 4-9 Mass spectrum of [Mo(η^3-allyl)(salal)$(CO)_2$py]

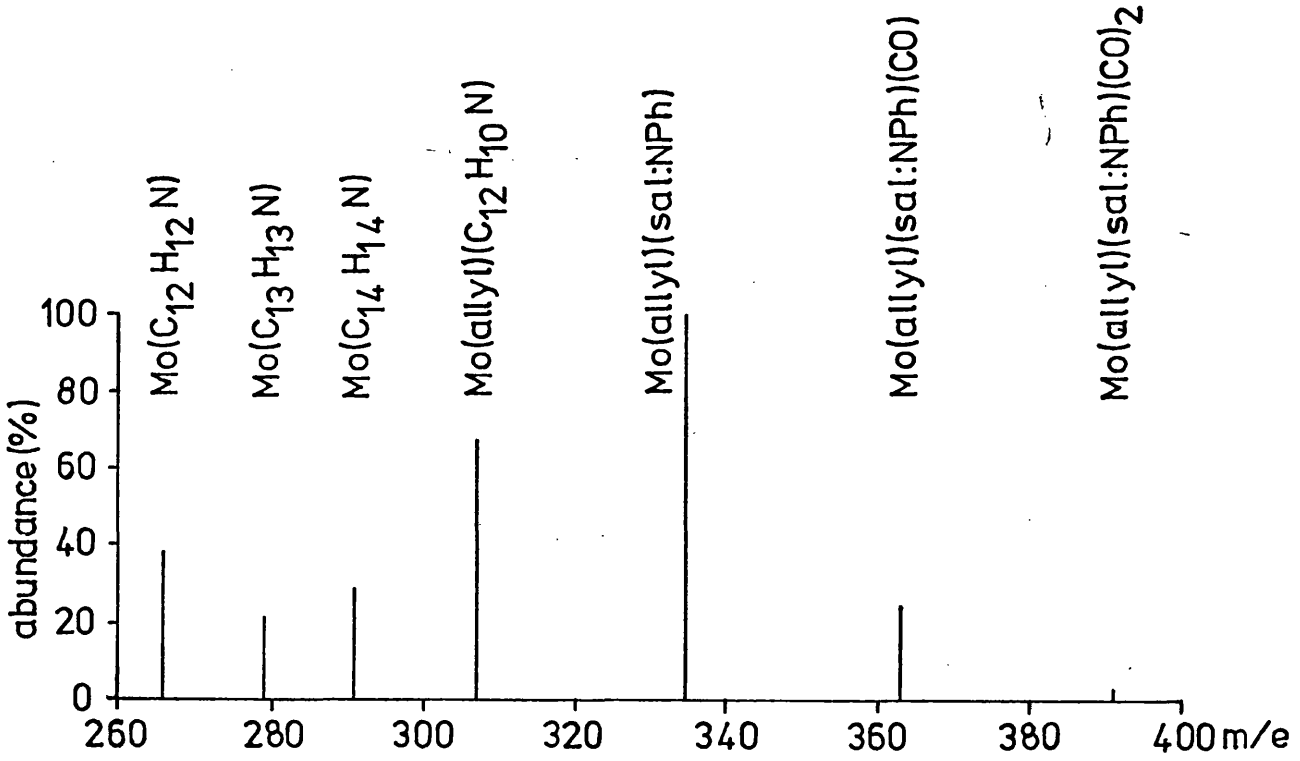

Figure 4-10 Mass spectrum of [Mo(η^3-allyl)(sal:NPh)$(CO)_2$py]

Alternatively, CO may be formed by the loss of the phenoxy oxygen together with the carbon atom to which it is bonded, resulting in the ligand C_5H_4CHO (cyclopentadienylcarboxaldehyde; cpca). It was also found that the sal:NPh complex similarly lost carbon monoxide (Figure 4-10), which in this case must be eliminated from the ring to give the ligand C_5H_4CHNPh (i.e. the N-phenyl imine of cpca). A species of this sort, cpca or its N-phenyl imine, would be stabilised by extensive delocalisation (Figure 4-11). Consideration of the phenate ion (P_1 to P_4 in figure 4-11) shows that delocalisation can only occur with loss of the aromatic stabilisation energy, whereas cpca (C_1 to C_6 in figure 4-11) retains its aromaticity except in canonical form C_6. Thus cpca and the related N-phenyl imine should be fairly stable entities both in the mass spectrometer and perhaps in normal coordination chemistry.

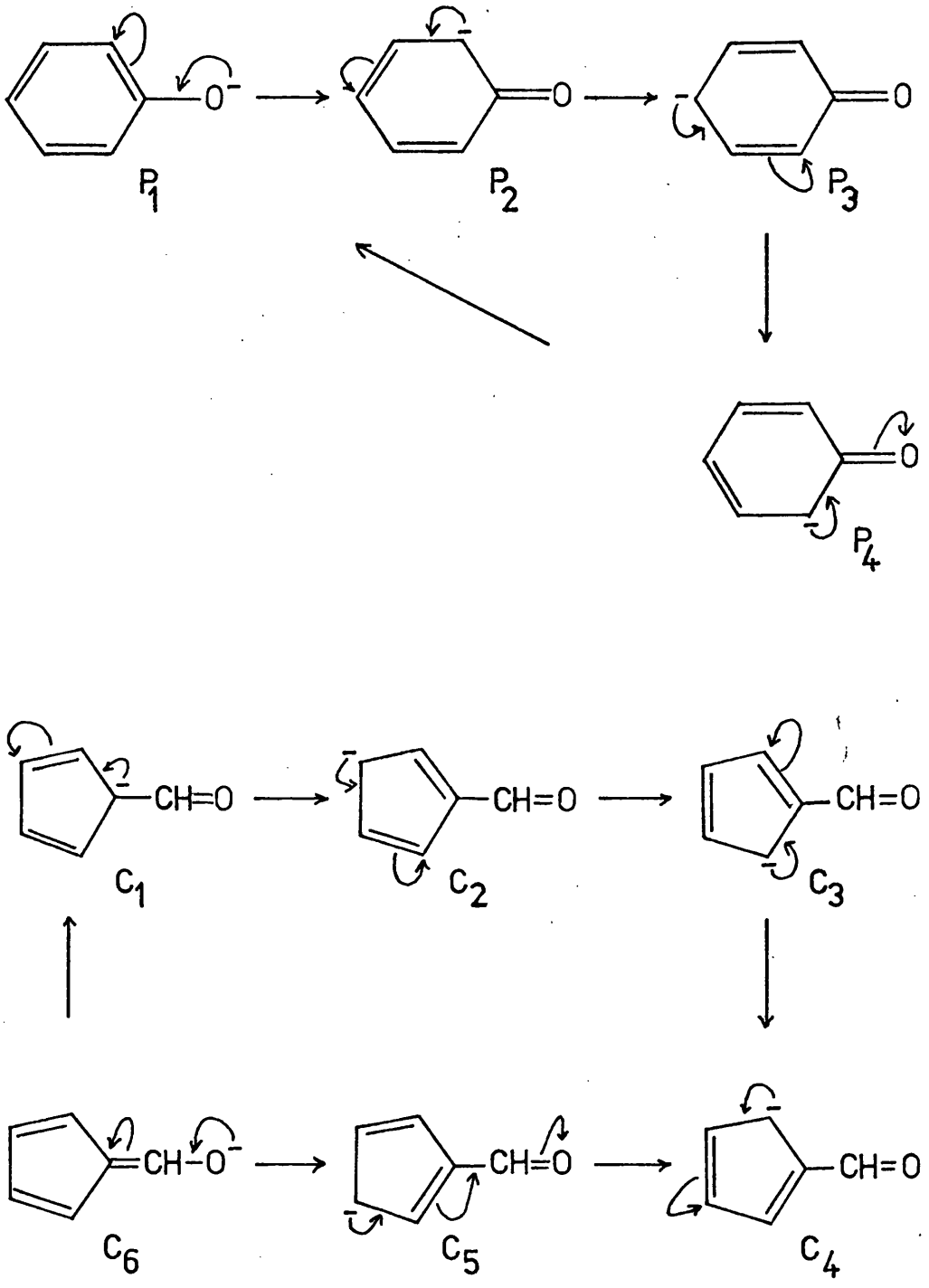

Figure 4-11 Electron delocalisation in the phenate and opca ions.

4.3.6 The molecular structure of $[Mo(\eta^3\text{-allyl})(acac)(CO)_2py]$[220]

The molecular structure of the complex $[Mo(\eta^3\text{-allyl})(acac)(CO)_2py]$ has recently been determined[220] and it can be described in terms of a distorted octahedron with the η^3-allyl group and one acac oxygen atom occupying opposing vertices, with the equatorial plane containing a cis pair of carbonyl groups, the pyridine nitrogen atom and the second acac oxygen atom (Figure 4-12, I). This is basically the ligand arrangement shown in structure B, figure 4-4.

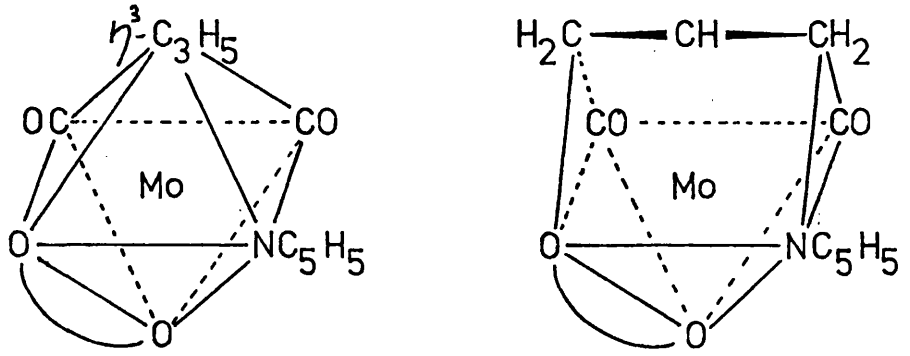

I II

Figure 4-12. The idealised molecular structure of $[Mo(\eta^3\text{-allyl})(acac)(CO)_2py]$

Alternatively this complex can be thought of as being seven-coordinate with a bidentate allyl group. Thus its molecular structure may be described in terms of a capped trigonal prism with the capping position occupied by one of the acac oxygen atoms, and the capped face containing a cis pair of carbonyl groups, the pyridine nitrogen atom and the second acac

oxygen atom. The allyl group then bridges the two remaining co-ordination sites (Figure 4-12, II). Figure 4-13 shows the observed molecular structure of $[Mo(\eta^3\text{-allyl})(acac)(CO)_2py]$.

This molecular structure differs from those determined by Fenn and Graham[72,73,118] and Cotton[120] which have a symmetric structure similar to that shown in figure 4-4, A (i.e. both of the co-ordinating atoms of the bidentate ligand occupy chemically equivalent sites, whereas the acac oxygen atoms are chemically inequivalent in the present complex). A recent preliminary communication[128] indicates that the complex $[MoCl(\eta^3\text{-allyl})(CO)_2dppe]$ also has an unsymmetric structure (i.e. similar to figure 4-4, B) although no interatomic distance or angles have yet been published.

It is not possible at this stage to indicate why this change in stereochemistry should occur for these two compounds, but the co-existence of both a symmetric and an unsymmetric isomer in $CDCl_3$ solution at low temperatures indicates that the energy difference between the two forms is only a few $kJmol^{-1}$.

It would be interesting to determine the molecular structures of other complexes with bidentate three electron donor ligands (e.g. salal, sal:NPh, dmdc and dedc) in order to ascertain whether the observed structure is peculiar to the acac complex or typical of the complexes of these three-electron donor ligands. The structure of the complex $[Mo(\eta^3\text{-allyl})(sal:NPh)(CO)_2py]$ is currently being investigated by M.G.B. Drew at the University of Reading.

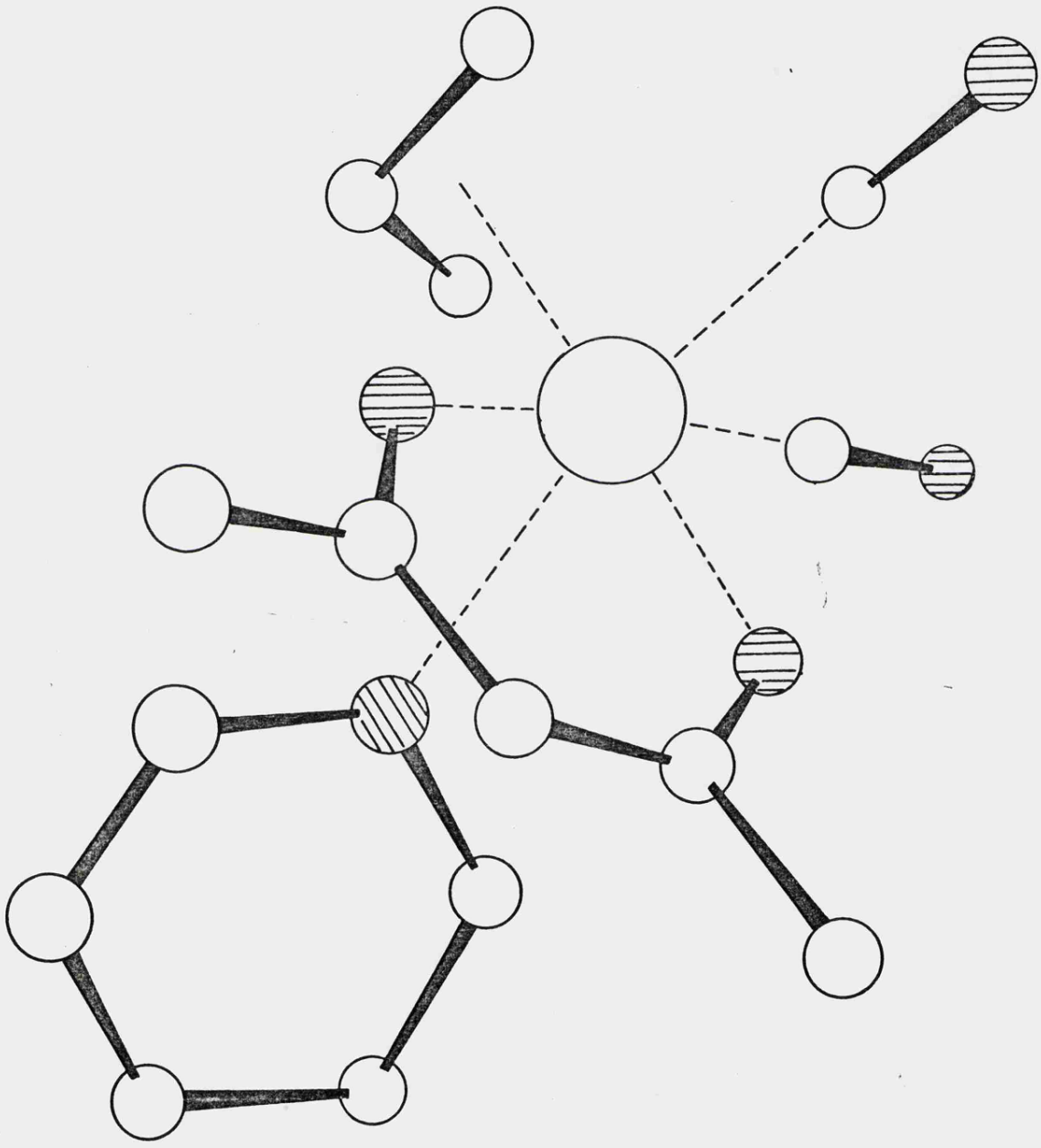

Figure 4-13. The molecular structure of [Mo(η^3-allyl)(acac)$(CO)_2$py]

4.3.7. A possible reaction scheme for the formation of LL_a complexes

It is known that the complexes $[MoX(\eta^3\text{-allyl})(CO)_2bipy]$, where X is a halogen, can react with replacement of X^- to give neutral or cationic complexes.[113] This consideration, taken in conjuction with the previously discussed n.m.r. (Sections 4.3.3 and 4.3.4) and structural data (Section 4.3.6) leads to the following reaction scheme (Scheme 4-1).

Whilst most information is available for the acac complex, the other three-electron donor ligands are expected to react similarly. In support of Scheme 4-1 an intermediate complex of type 3 has been isolated, namely $[Mo(\eta^3\text{-allyl})(salal)(CO)_2bipy]$, which was prepared from the reaction between Nasalal and $[MoCl(\eta^3\text{-allyl})(CO)_2bipy]$ (i.e. 1 to 3 in Scheme 4-1), as well as from the reaction between bipy and $[Mo(\eta^3\text{-allyl})(salal)(CO)_2py]$ (i.e. 5a or 5b to 3 in Scheme 4-1). Unfortunately it has not been possible to cause this particular intermediate to react further as predicted by the remainder of the scheme; although the analogous dpa complex, which was not isolated, readily undergoes further substitution. The point at which reaction terminates must be strongly influenced by the relative basicity of the L_2 (e.g. bipy) and LL_a (e.g. salal) groups.

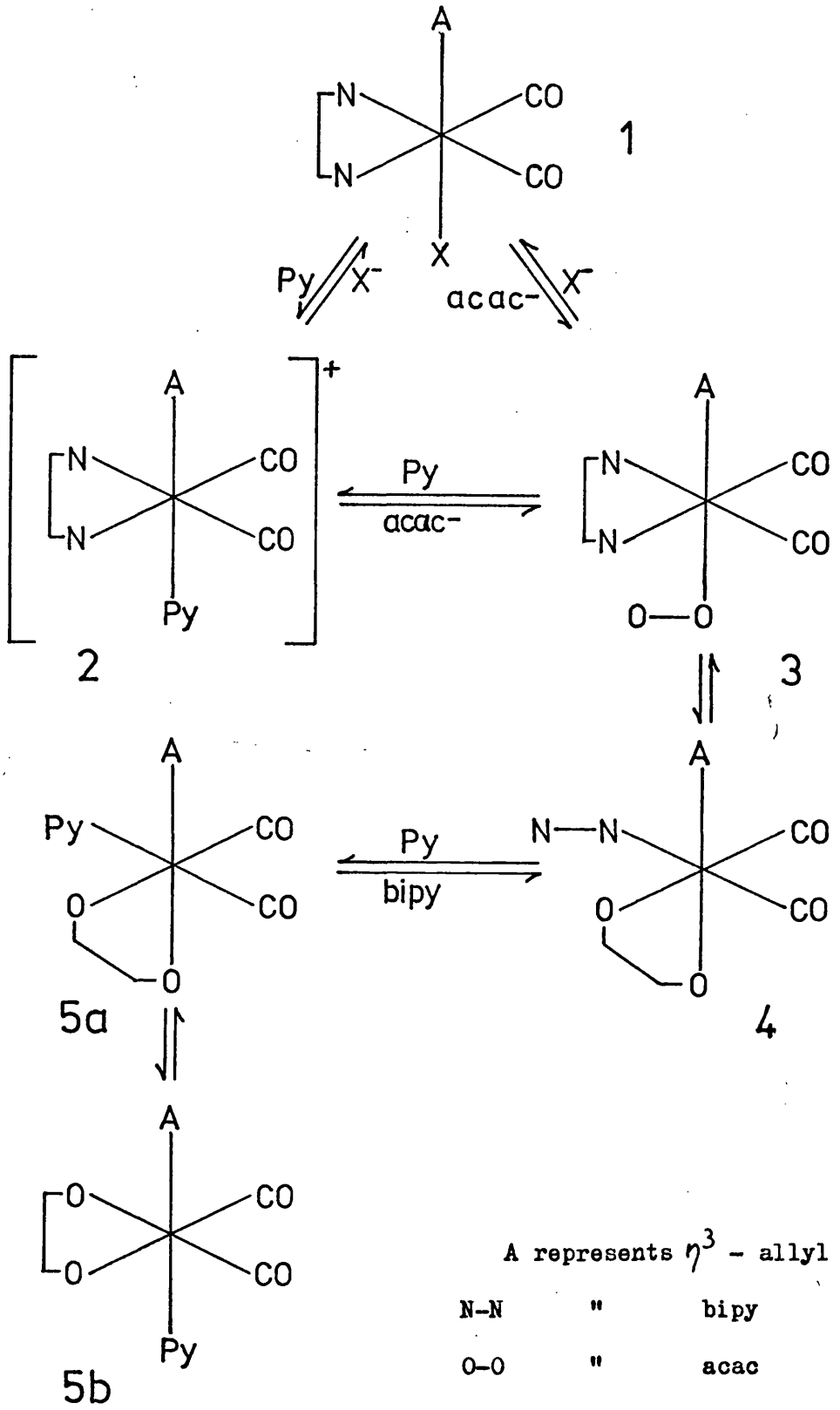

Scheme 4-1. A possible reaction scheme for the formation of $[Mo(\eta^3\text{-allyl})(LL_a)(CO)_2py]$

Hence it should be possible to obtain circumstances where both a reactive intermediate (e.g. 3 in Scheme 4-1) and a final fully substituted product (5a or 5b) can be isolated, which would help substantiate the proposed scheme.

4.3.8. Fluxional nature of $[Mo(\eta^3\text{-allyl})(LL_a)(CO)_2py]$

The variable temperature n.m.r. spectra of the complexes $[Mo(\eta^3\text{-allyl})(LL_a)(CO)_2py]$, where LL_a is acac or sal:NPh, demonstrated that these compounds can exhibit stereochemical non-rigidity in solution. Two acceptable schemes can be outlined to account for these observations; a) a dissociative route (Scheme 4-2) and b) a rotation of one half of the molecule relative to the other half (Scheme 4-3) as proposed[183,184] for certain molybdenum(II) pyrazolylborato complexes.

a) Scheme 4-2

For a dissociative mechanism either of two pathways (i.e. I - V - IV or I - II - III - IV) may be envisaged. The former proceeding via a square pyramidal intermediate (V) which may be attacked from above or below the square plane by pyridine with the formation of complex IV or I respectively. The second route would involve loss of pyridine followed by a rearrangement of the 5-co-ordinate intermediate and re-co-ordination of pyridine.

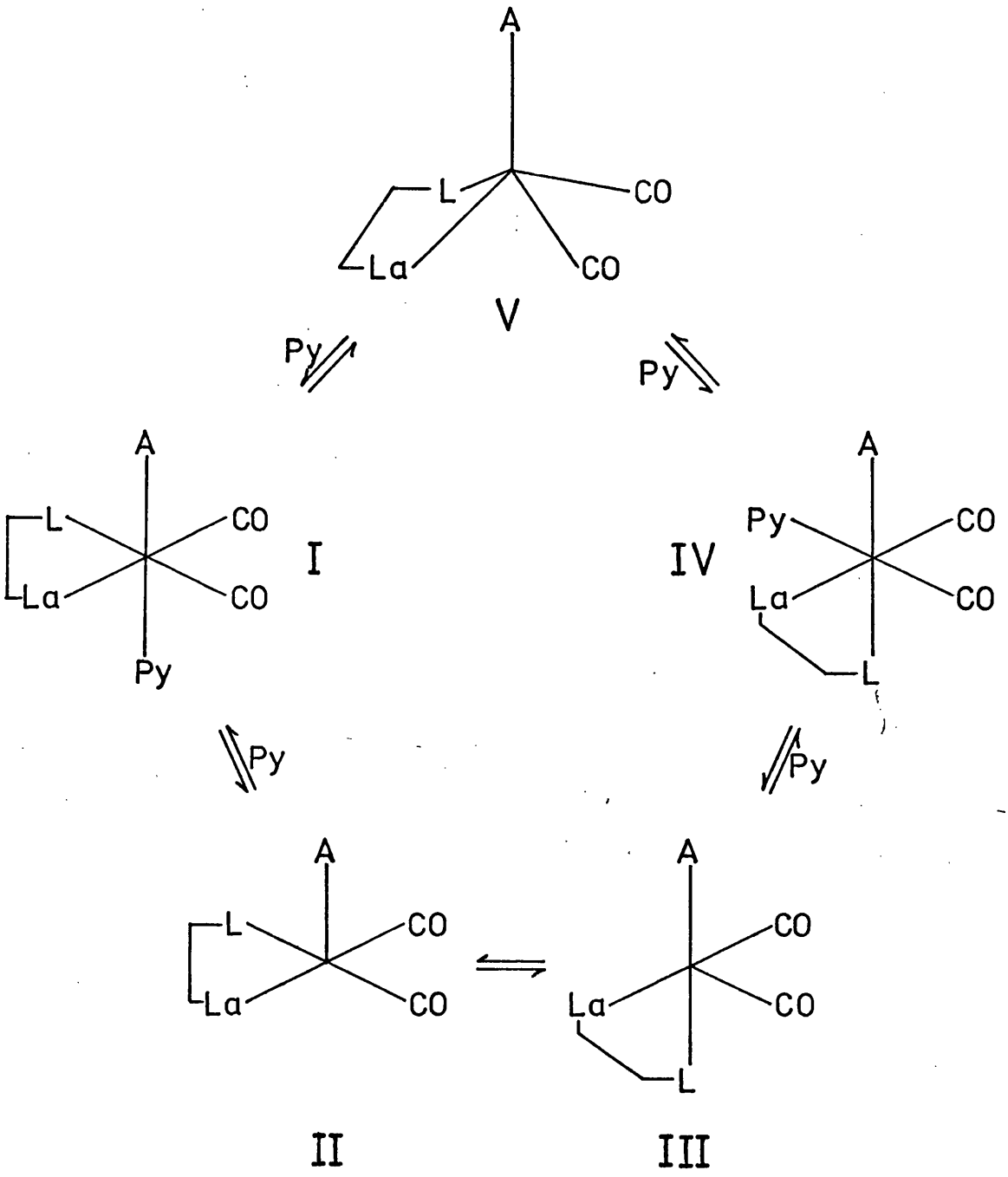

Scheme 4-2. Isomerisation via a dissociative mechanism

(A represents η^3-allyl)

If the observed fluxional nature of these complexes involves this scheme, then in the presence of excess pyridine fast exchange between free and co-ordinated pyridine should be observed. Such an exchange is observed but only at elevated temperatures, whereas isomerisation of the acac complex occurs at and below room temperature. Thus at best, this route can only be a high temperature alternative to the normal trigonal twist mechanism.

b) Scheme 4-3.

The mechanism outlined in this scheme involves a trigonal twist of the (LL_a)py unit relative to the (allyl)$(CO)_2$ moiety and passes through a high energy trigonal prismatic stereochemistry.

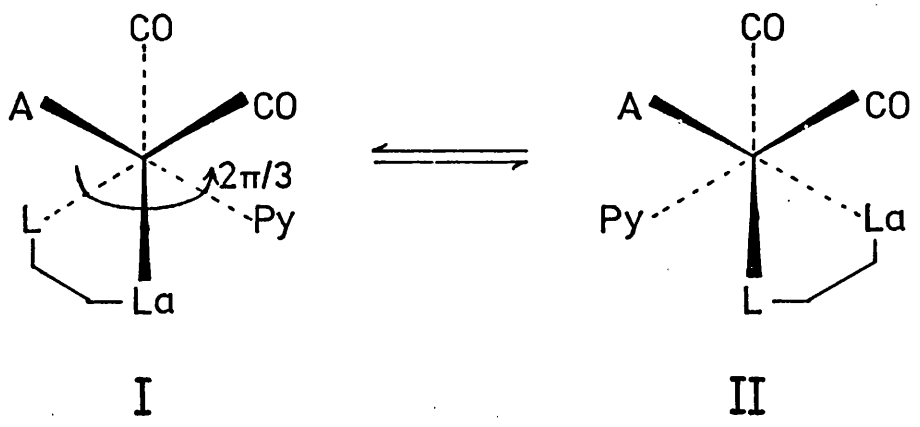

Scheme 4-3. Isomerisation by a molecular twist (A represents η^3-allyl).

Such a mechanism has already been proposed[183,184] for the fluxional molecule [Mo(η^3-2-methallyl)(pz_4B)$(CO)_2$] (Figure 4-14). At 60°C the ^1H-n.m.r. spectrum reveals

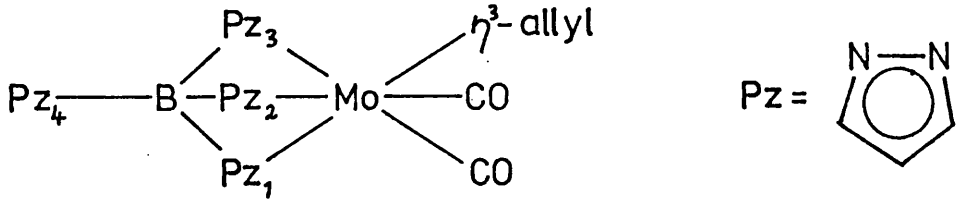

Figure 4-14. Simplified structure of [Mo(η^3-2-methallyl)(pz_4B)$(CO)_2$]

three equivalent (i.e. pz_1, pz_2 and pz_3) and one non-equivalent (i.e. pz_4) pyrazolylborato group. Whereas at -60°C there are two equivalent (i.e. pz_2 and pz_3) and two non-equivalent (i.e. pz_1 and pz_4) pyrazolylborato groups, which is consistent with the structure given in figure 4-14). On raising the temperature the n.m.r. spectrum of the non-co-ordinated pz group and the η^3-allyl group remain almost unchanged, whereas the spectrum of the three co-ordinated pz groups becomes time averaged on the n.m.r. time scale.

Hence conformational changes in the allyl group can be discounted, and if a dissociative mechanism is involved in scrambling the pz groups, then all four groups should be time averaged. Thus a mechanism whereby the three co-ordinated pz groups rotate about the Mo····B axis was proposed and satisfactorily explains the experimental observations.

It was also found that 3-substitution of the pz groups led to a slowing down of this isomerisation. This could possibly explain the observed differences between the rate of isomerisation of the acac and sal:NPh complexes $[Mo(\eta\text{-allyl})(LL_a)(CO)_2py]$, as the phenyl group may sterically hinder the rotation of the L_3Mo grouping. Such a steric interaction would increase the activation energy and, consequently, reduce the rate of isomerisation.

4.4 Conclusion

These complexes of bidentate three-electron donor ligands {i.e. $[Mo(\eta^3\text{-allyl})(LL_a)(CO)_2py]$ where LL_a is acac, salal, sal:NPh, dmdc or dedc} extend the number and type of known (η^3-allyl)dicarbonylmolybdenum(II) species, and reveal interesting sterochemical aspects of molybdenum(II) chemistry.

Solutions of acac complex in $CDCl_3$, exhibit a low energy transition between two isomeric forms as observed by

^{1}H- and ^{13}C-n.m.r. spectroscopy. Isomerism occurs to a much lesser extent in d^{6}-acetone solutions with the less symmetric isomer (Figure 4-4, B) being the major constituent. X-ray crystallography[220] confirms that it is this less symmetric isomer which crystallises out from an acetone solution.

For the corresponding sal:NPh complex it is not possible to identify which isomer is present in solution, due to the lack of symmetry of this ligand, but ^{1}H-n.m.r. spectroscopy indicates the presence of only one isomer in $CDCl_3$ solution at and below room temperature. Above room temperature fluxional behaviour was once again observed.

Chapter 5.

Further Oxidation Reactions of Molybdenum(0) and (II) Complexes.

Chapter 5

Further Oxidation Reactions of Molybdenum(0) and (II) Complexes

5.1 Introduction

This chapter contains various oxidation reactions of molybdenum(0) and (II) complexes which are not conveniently discussed in the other chapters. These reactions are considered under three headings:

a) Attempted allyl cyanide oxidations of molybdenum(0)

b) Oxidative additions of allyl analogues

c) Oxidations under forcing conditions.

5.2. Attempted allyl cyanide oxidations of molybdenum(0)

Attempts to prepare the complex $[Mo(CN)(\eta^3\text{-allyl})(CO)_2L_2]$ (L_2 = bipy or dpa) by the routes employed in chapter 3 [allyl pseudohalide oxidation of neutral and cationic molybdenum(0) complexes or anion exchange with halo-molybdenum(II) complexes] did not lead to high yields of the expected complexes, but resulted in a variety of products depending on the reaction conditions employed.

5.2.1 Experimental

5.2.1.1 The reaction between allyl cyanide and $Mo(CO)_4L_2$

The complex $Mo(CO)_4$dpa (0.35 g, 0.93 mmol), or an equimolar mixture of $Mo(CO)_6$ and dpa, was allowed to react with an excess of allyl cyanide (2 cm^3, 25 mmol) for 2 hours in refluxing toluene (25 cm^3). After cooling to room temperature the yellow product

[$Mo(CO)_3$(allylCN)dpa] (0.37 g, 97% yield) was collected at the filter, washed with toluene and dried in vacuo. (Found: C, 48.2; H, 3.52; N, 13.2. Calc. for $MoO_3C_{17}H_{14}N_4$: C, 48.8; H, 3.35; N, 13.4%).

5.2.1.2 The reaction between allyl chloride and K[$Mo(CN)(CO)_3$bipy]

The complex $Mo(CO)_4$bipy (0.41 g, 1.13 mmol) was reacted with an excess of KCN (0.2 g, 3 mmol) in refluxing acetonitrile (20 cm^3) for 3 hours. The resulting solution, which contains the complex K[$Mo(CN)(CO)_3$bipy] {ν_{CO}(MeCN solution): 1910s and 1890s cm^{-1}}[54], was cooled to room temperature and added dropwise with stirring, to a methanolic solution (11 cm3) of allyl chloride (1 cm^3, 12 mmol). After stirring for 30 minutes a dark purple solid (A, 0.03 g) was collected at the filter, washed with methanol and dried in vacuo.

Water was added to the filtrate with stirring to precipitate the second product as deep orange crystals (complex B, 0.10 g), which were washed with water and dried in vacuo.

5.2.1.3 The reaction between KCN and [$MoCl(\eta^3$-allyl$)(CO)_2$bipy]

The complex [$MoCl(\eta^3$-allyl$)(CO)_2$bipy] (0.34 g, 0.88 mmol) was allowed to react with an excess of KCN (0.3 g, 5 mmol) in refluxing absolute ethanol (25 cm^3) for 4 hours. After cooling to room temperature the mixture was filtered and the filtrate evaporated to approximately 5 cm^3 on a rotary evaporator to give a red solid in very low yields (complex C, 0.02 g). This product was collected at the filter washed with ethanol followed by water and finally dried in vacuo.

5.2.2 Results and discussions

5.2.2.1 The allyl cyanide reactions

The reaction between allyl cyanide and the complex $Mo(CO)_4$dpa gave rise to a yellow product which, from its analytical and infra-red data (ν_{CO} : 1915 vs, 1805 vs and 1765 vs cm^{-1}; ν_{NH}: 3320 m cm^{-1}; ν_{CN}: not observed), was identified as the complex [$Mo(CO)_3$(allyl cyanide)dpa]. In addition a weak infra-red band at 1650 cm^{-1} could be attributed to C = C stretching ($\nu_{C=C}$, allyl CN = 1645 cm^{-1}) and is consistent with N-bonded allyl cyanide.

Comparison of the infra-red spectrum of this product with spectra of known fac-trisubstituted molybdenum carbonyl complexes {[$Mo(CO)_3X_2Y$]; X = Y = MeCN or py[231]; X_2 = bipy[52] or dpa[58], Y = MeCN.} indicated that this product should also be formulated as the facial isomer.

Attempts to cleave the allyl - cyanide bond, by employing higher temperatures (refluxing xylene), more polar solvents (DMF, MeCN or MeOH) or ultraviolet irradiation of [$Mo(CO)_3$(N-allyl cyanide)dpa] gave no evidence for any products other than the trisubstituted carbonyl derivative.

When the allyl cyanide reaction was attempted with $Mo(CO)_4$bipy, under the conditions employed for the $Mo(CO)_4$dpa - C_3H_5CN reaction, very little reaction occurred and $Mo(CO)_4$bipy could be recovered almost quantitatively. On raising the reaction temperature, by using refluxing xylene as the solvent (ca. 140°C), a low yield of a very dark solid was

obtained. This solid had an infra-red spectrum containing four bands in the metal carbonyl region (ν_{CO} 1940 s, 1880 s-vs, 1850 s and 1770 vs cm^{-1} in Nujol). These band positions were in accord with a mixture containing a facial-tricarbonyl derivative (1880 and 1770 cm^{-1}) and a cis-dicarbonyl complex (1940 and 1850 cm^{-1}). Possibly the complexes $[Mo(CO)_3(N\text{-allyl cyanide})bipy]$ and $[Mo(CN)(\eta^3\text{-allyl})(CO)_2bipy]$ were formed under these conditions, however, it did not prove possible to separate the mixture or obtain a single pure product from this reaction so further characterisation was not attempted.

5.2.2.2 Allyl oxidation of $K[Mo(CN)(CO)_3bipy]$ and CN^- exchange reactions.

Both the reactions of $K[Mo(CN)(CO)_3bipy]$ with allyl chloride and $[MoCl(\eta^3\text{-allyl})(CO)_2bipy]$ with KCN, led to low yields (24% and 7% respectively)of reddish solids (complexes B and C respectively) whose infra-red spectra (Table 5-1) were

Table 5-1

Infra-red data for the cyano-complexes

Complex	ν_{CN} [a]	ν_{CO} [a]	Colour
A		1940m, 1895m	Purple
		1855m, 1775m	
B	2110m	1940vs, 1865vs	Deep orange
C	2110m	1940vs, 1848vs	Red

a) Spectra obtained in Nujol.

consistent with the expected product $[Mo(CN)(\eta^3\text{-allyl})(CO)_2bipy]$. Closer inspection of the spectra and the appearance of these products indicated that they may be isomeric or two different compounds, but due to the low yields these routes were not pursued further.

In addition to the dicarbonyl product the allyl chloride oxidation of the complex $K[Mo(CN)(CO)_3bipy]$ gave rise to a dark purple solid (complex A) whose infra-red spectrum (Table 5-1) is similar to that of the product obtained from the reaction between allyl cyanide and $Mo(CO)_4bipy$ in xylene (p. 161), and may be formulated in a similar way. Again the mixture could not be separated.

5.2.3 Conclusion

It would appear that the complex $[Mo(CN)(\eta^3\text{-allyl})(CO)_2bipy]$ probably does exist but that it is not readily prepared by any of the procedures outlined in Chapter 3 for the other allyl analogues.

This cyano-complex may be worthy of further investigation as the ligands CO and CN^- are isoelectronic and hence may exhibit isomerism as outlined in figure 5-1.

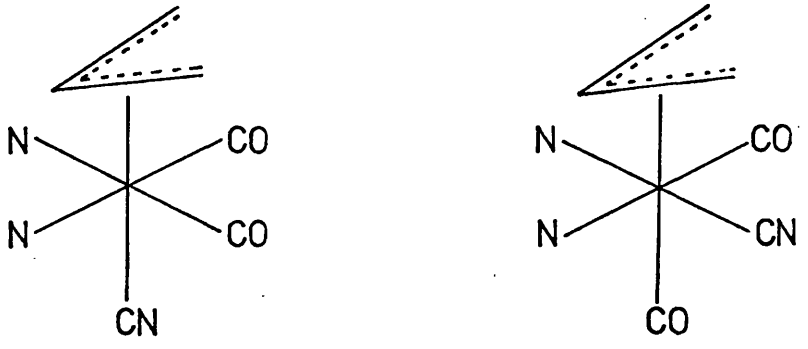

Figure 5-1 Possible isomerism for the complex $[Mo(CN)(\eta^3\text{-allyl})(CO)_2bipy]$

5.3 Oxidations involving allyl analogues

In order to demonstrate the general synthetic value of the anionic complexes $[MoX(CO)_3L_2]^-$ for synthesising allyl derivatives, one of the anions $\{[Mo(NCS)(CO)_3bipy]^-\}$ was reacted with the allyl analogues 3-bromocyclohexene and cinnamyl chloride (3-chloro-1-phenylprop-1-ene; $C_6H_5CH{:}CHCH_2Cl$) under mild conditions as indicated below.

5.3.1 Experimental

The complex $Mo(CO)_4bipy$ (1.43 g, 3.93 mmol) was allowed to react with an excess of KSCN (2.04 g, 21 mmol) for 3 hours in refluxing acetonitrile (50 cm^3) (cf. chapter 3) to give a deep red solution which contained the complex $K[Mo(NCS)(CO)_3bipy]$.

Aliquots (10 cm^3) of this solution were cooled to 0°C and an excess of the oxidant (1 cm^3) (i.e. cinnamyl chloride , 3-bromocyclohexene or allyl chloride) was added with stirring. After 2 minutes the mixture was filtered, and the filtrate was collected in iced water to precipitate the product, which was collected at the filter, washed with water and dried *in vacuo*.

5.3.2 Results and Discussion

The results of these oxidations are summarised in Table 5-2. In each case the spectroscopic properties of each product were consistent with the expected complex, $[Mo(NCS)(\eta^3\text{-}R)(CO)_2bipy]$ (R = allyl analogue). In the 3-bromocyclohexene reaction the product may consist of isomeric forms as indicated by the CN stretching region of the infra-red

Table 5-2

Reaction of allyl analogues with [Mo(NCS)(CO)$_3$bipy]

Allyl analogue	Infra-red data [a]		Colour and yield(%)
	ν_{CN}	ν_{CO}	
cinnamyl chloride	2070vs	1935vs	purple solid
		1860vs	60
3-bromocyclohexene	2090s	1915vs	purple solid
	2060s	1830vs	80
allyl chloride	2080vs	1950vs	red solid[b]
		1860vs	

a) Spectra measured in Nujol, ν_{CS} was not observed.

b) This product was contaminated with K[Mo(NCS)(CO)$_3$bipy]

spectrum which exhibited two CN bands. Re-precipitation from acetonitrile by the careful addition of water did not alter the spectrum. Since these reactions were only attempted to demonstrate the synthetic potential of these anionic complexes no efforts were made to confirm the presence of, or to isolate, these possible isomers.

When allyl chloride was used as the oxidant the product was contaminated with unreacted K[Mo(NCS)(CO)$_3$bipy], which indicates that cinnamyl chloride and 3-bromocyclohexene are more reactive towards these anionic molybdenum(0) complexes under the conditions employed than is the parent allyl halide. This increased reactivity may possibly be explained by steric and electronic factors. The formation of a carbonium ion, by

the loss of a bromide ion from 3-bromocyclohexene, leads to a lessening of the ring strain and hence the carbon-halogen bond will tend to be activated relative to the allyl halides. Whereas the carbonium ion obtained by the loss of a chloride ion from cinnamyl chloride, will be stabilised by delocalisation of the charge around the aromatic ring (Figure 5-2) which once again will lead to activation of the carbon-halogen bond.

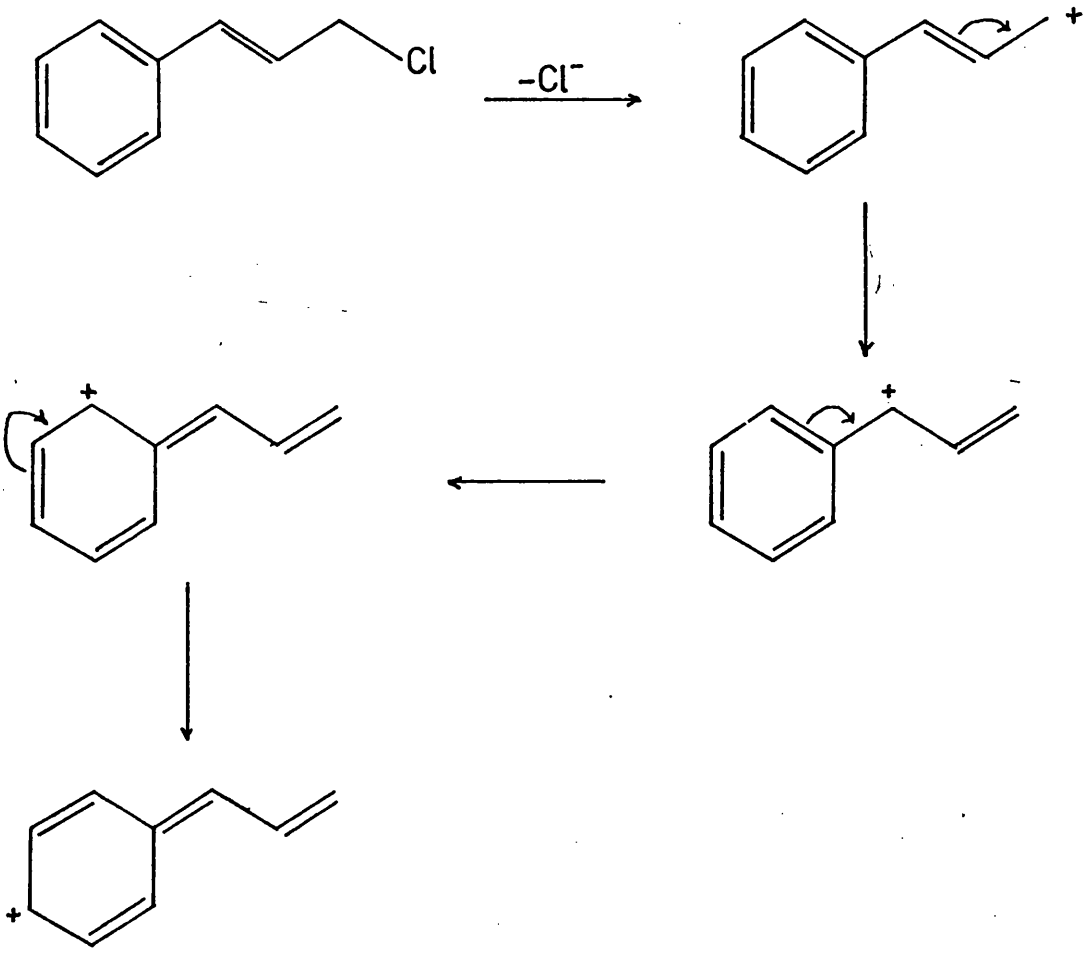

Figure 5-2. Charge delocalisation in the cinnamyl carbonium ion.

5.3.3 Conclusion

The anionic molybdenum(0) species $[Mo(NCS)(CO)_3bipy]^-$ was found to be reactive towards oxidative addition of the allyl halide analogues cinnamyl chloride and 3-bromocyclohexene and hence it would appear that these and related highly nucleophilic anions { e.g. $[M(CO)_5]^{2-}$, M = Cr or W[232] and $[V(CO)_5]^{3-}$ [233] } will be of general value for the synthesis of allyl derivatives.

5.4 Oxidation of molybdenum(0) and (II) under forcing conditions.

Since allyl halides are capable of oxidising Mo(0) to Mo(II) it was anticipated that reactions under more forcing conditions [or employing reactive halides which will not form stable molybdenum(II) species] might result in the formation of molybdenum complexes containing higher metal oxidation states. Such expectations were realised but the resultant molybdenum complexes were invariably contaminated with organic by-products.

5.4.1 Experimental

5.4.1.1 Allyl bromide and acetyl chloride oxidations

The complex $Mo(CO)_4L_2$ (L_2 = dpa for the allyl bromide reaction and L_2 = dpa or bipy for the acetyl chloride reaction) was allowed to react with an excess of acetyl chloride or allyl bromide in refluxing toluene. After 4 hours the mixture was cooled to room temperature and the brown product was collected at the filter, washed with toluene and dried in vacuo.

It was found that the complex [MoBr(η^3-allyl)$(CO)_2$dpa] could be used in place of $Mo(CO)_4$dpa in the allyl bromide reaction, whilst an equimolar mixture of $Mo(CO)_6$ and L_2 (bipy or dpa) yielded the same product as $Mo(CO)_4L_2$ in the acetyl chloride reaction.

5.4.1.2 Benzyl chloride oxidations

The reactants, $Mo(CO)_4L_2$ (L_2 = bipy or dpa) and an excess of benzyl chloride, were allowed to react in refluxing THF for 20 hours. After cooling to room temperature the product was collected at the filter, washed with THF and dried *in vacuo*.

5.4.1.3 The reaction between dpa and allyl bromide

The reactants, dpa (0.5 g, 1.8 mmol) and allyl bromide (5 cm^3, 55 mmol), were heated together for 3 hours in refluxing toluene (25 cm^3). After cooling to room temperature the viscous yellow-brown oil was isolated and washed with toluene by decantation. This oil was dissolved in chloroform and precipitated by the slow addition of ether. The resulting solid was re-precipitated as above to give a pale yellow solid (m.pt. 186°C; Found: C, 44.7; H, 4.4; N, 15.5. Calc. for dpa.HBr.H_2O: C, 44.4; H, 4.4; N, 15.6%). Thermolysis at 60°C for 16 hours resulted in a weight loss equivalent to one mole of water per mole of product.

5.4.2 Results and discussion

5.4.2.1 The allyl bromide reaction

It was found that when $Mo(CO)_4$dpa was replaced by an equimolar mixture of $Mo(CO)_6$ and dpa the reaction stopped at the intermediate molybdenum(II) complex [$MoBr(\eta^3$-allyl$)(CO)_2$dpa]. This appears to be a particle size effect, as when the [$MoBr(\eta^3$-allyl$)(CO)_2$dpa] so produced was finely ground the reaction proceeded to the brown product. The X-ray powder pattern of the yellow intermediate was identical to that of a normal sample of [$MoBr(\eta^3$-allyl$)(CO)_2$dpa].

The reaction was investigated by means of infra-red spectroscopy, magnetochemistry and GLC/mass spectrometry as outlined below.

5.4.2.1.1 Infra-red spectroscopy

Infra-red spectroscopy (4000 - 650cm^{-1}) showed the absence of carbonyl and oxo species and the presence of co-ordinated dpa in the final brown solid. The complex $MoBr_4$dpa was thought to be the most likely product, but careful examination of the infra-red spectrum (Table5-3) showed additional bands due to the presence of dpa.HBr.H_2O [as indicated by comparison with authentic samples of $MoBr_4$dpa[58] and dpa.HBr.H_2O (cf. section 5.4.1.3)]. Moreover the product was not found to be analytically pure (Found: C, 24.9; H, 2.2; N, 7.6. Calc. for $MoBr_4C_{10}H_9N_3$: C, 20.4;

Table 5-3

Infra-red data[a] for the allyl bromide oxidation product.

Product	$MoBr_4dpa$[b]	$dpa.HBr.H_2O$	Tentative assignment
		3350m	ν_{OH}
3300m	3300s		ν_{NH}
1660m-s		1665s	Aromatic ring breathing
1630s	1630s		"
1610m-s		1610s	"
1585s	1580s		"
1560m		1560m	"
770s-vs	770s-vs	770s	CH out of plane bend.

a) Measured in Nujol

b) See ref. 58

c) See section 5.4.1.3

H, 1.5; N, 7.2%). Based on the carbon analysis the $MoBr_4dpa$ contained approximately 19% $dpa.HBr.H_2O$ impurity. Washing with acetonitrile reduced the amount of contamination but also dissolved much of the molybdenum complex.

5.4.2.1.2 Magnetic moment

The brown solid had a magnetic moment of 2.53 BM at 23°C, based on a molecular weight of 587 (i.e. $MoBr_4dpa$). This value is in good agreement with a pure sample of $MoBr_4dpa$ (μ = 2.63 BM)[58] when allowance is made for the diamagnetic contaminant, and is typical of a d^2 heavy metal paramagnetic complex of this type[234].

5.4.2.1.3 GLC/mass spectroscopy

In order to elucidate the nature of the organic products formed, the allyl bromide oxidation was carried out at high concentrations [$Mo(CO)_4$dpa (1 g, 2.64 mmol), allyl bromide (8 g, 66 mmol) and toluene (10 cm^3)] and the resulting filtrate was examined by GLC which showed the presence of three species. The retention times and the GLC/mass spectra, compared with reference samples run under the same conditions, indicated the presence of allyl bromide, toluene and hexa-1,5-diene (bi-allyl). Hence, hexa-1,5-diene was formed as the only new volatile organic product. A reaction scheme consistent with the observed major products is given below (Scheme 5-1). However, one or more competitive reactions involving attack

$$Mo(CO)_4dpa + C_3H_5Br \longrightarrow MoBr(\eta^3\text{-allyl})(CO)_2dpa + 2CO$$

$$\downarrow 3C_3H_5Br$$

$$MoBr_4dpa + 2(C_3H_5\text{-}C_3H_5) + 2CO$$

Scheme 5-1 A possible scheme for the allyl bromide-dpa reaction.

of allyl bromide on dpa (cf. 5.4.1.3) must also occur to account for the formation of dpa.HBr.H_2O. (Scheme 5-2).

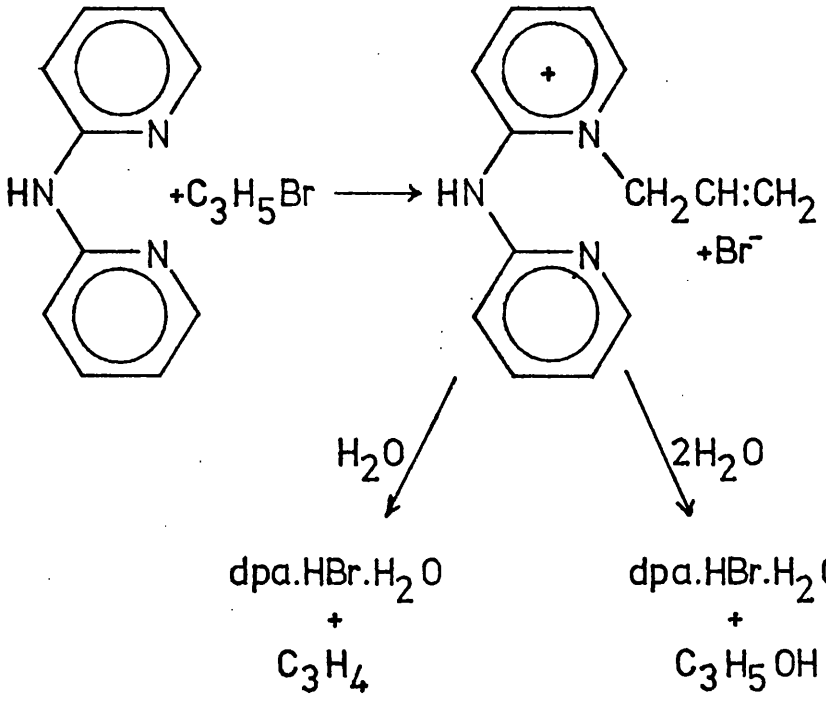

Scheme 5-2 A possible scheme for the formation of dpa.HBr.H_2O

The water is probably absorbed during the re-precipitation stages which were not carried out in the absence of air. It is known that sterically crowded alkyl pyridinium compounds can abstract a proton from the N-alkyl group with the formation of a pyridinium halide and an olefin[235]. Thus if an alkyl pyridinium intermediate was formed two routes for its decomposition can be envisaged, either proton abstraction (as discussed above) or hydrolysis, leading to allene or allyl alcohol respectively. No evidence was found for allene (or propyne to which it may have isomerised) or allyl alcohol but as this was only a minor reaction it is possible that even if present these species may not have been detected.

A similar reaction did not occur when bipy replaced dpa or allyl chloride replaced allyl bromide. This may be a consequence of the greater basicity of dpa (cf. Chapter 6) and perhaps also indicates that an important step in the

reaction is the cleavage of the carbon-halogen bond with the formation of an allylpyridinium intermediate.

5.4.2.2 The acetyl chloride reaction

This reaction proved to be more complex than the allyl bromide reaction and GLC/mass spectrometry showed the presence of at least six volatile organic products, only one of which was identified.

Infra-red spectroscopy (4000 to 650 cm^{-1}) of the brown molybdenum containing solid showed the absence of carbonyl and oxo species and the presence of the co-ordinated bidentate ligand (bipy or dpa). In addition the infra-red spectrum of the dpa products (Table 5-4) also showed the presence of acetylated dpa (adpa) which has been shown to co-ordinate through the two pyridine nitrogen atoms[58]. Co-ordinated adpa was only a minor product in reactions involving $Mo(CO)_4$dpa, whereas when -

Table 5-4

Infra-red data for the acetylchloride oxidation products.

Oxidation of:			Assignment
$Mo(CO)_4$dpa	$Mo(CO)_6$ + dpa	$Mo(CO)_4$bipy	
3300-3200m			ν_{NH}
		3070w	Aromatic CH stretch
1710m	1710ms		ν_{CO} (acyl CO)
1655s	1660s		Aromatic ring breathing
1630s			"
1605s-vs	1610s-vs	1605s	"
1580s			"
1560s	1565s		"
		765s-vs	Aromatic CH out of plane bend
		725m	"

the reactants were $Mo(CO)_6$ and dpa then co-ordinated adpa became the major product.

By analogy with the allyl halide reaction $MoCl_4L_2$ (L_2 = bipy, dpa or adpa) was expected to be the major metal containing product, but analytically pure samples could not be obtained (Found: C, 35.2; H, 2.6; N, 7.2. Calc. for $MoCl_4C_{10}H_8N_2$: C, 30.4; H, 2.0; N, 7.1%).

A gas-volumetric examination of the bipy system showed the loss of only four moles of carbon monoxide per mole of $Mo(CO)_4$bipy. Hence there can be no decarbonylation of the acetyl chloride during this reaction. The filtrate from this reaction was collected on sodium carbonate, to remove the excess acetyl chloride, and then examined by GLC/mass spectroscopy which showed the presence of six volatile fractions, excluding toluene. The mass spectra of the two major fractions (fraction one and six) are summarised in figure 5-3, with Scheme 5-3 showing a possible fragmentation route for the sixth fraction. The fragmentations marked with an asterisk in Scheme 5-3 (i.e. 148 to 113 and 106 to 71) are supported by the observation of metastable peaks at m/e values of 86 and 48. The additional metastable peaks at m/e = 85 and 46.5 (Figure 5-3) represent the loss of ^{37}Cl (i.e. 150 to 113 and 108 to 71) which, for the sake of clarity, have not been included in Scheme 5-3. This sixth fraction may

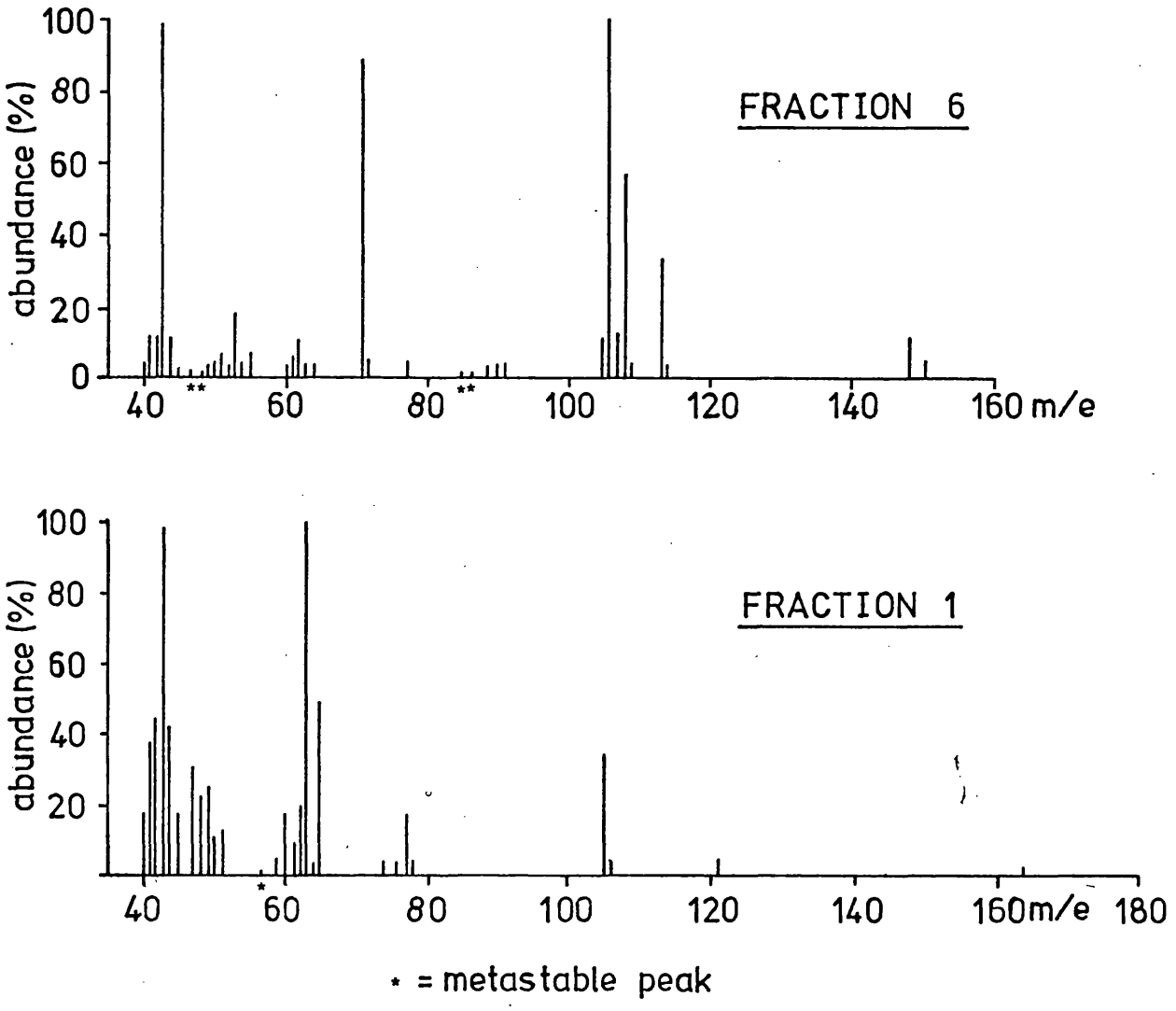

Figure 5-3 Mass spectra of fractions one and six.

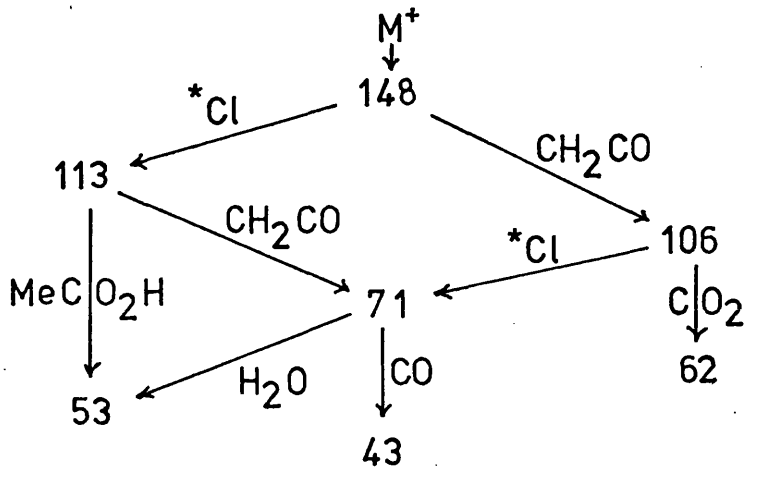

Scheme 5-3 A possible fragmentation scheme for fraction six

m/e	
?	Parent molecular ion
148	$HCO(CH_2CO)_2Cl$
113	$HCO(CH_2CO)_2$
106	$HCOCH_2COCl$
71	$HCOCH_2CO$
62	C_2H_3Cl
53	C_3HO
43	CH_3CO

well be a condensation polymer of acetyl chloride with the empirical formula $H(CH_2CO)_nCl$.

i.e. $nCH_3COCl \xrightarrow{Mo(CO)_4bipy} H(CH_2CO)_nCl + (n-1)HCl$

Such a species could well exist in several isomeric forms, for example if n is assumed to be 3, two structures may be envisaged [i.e. $CH_3COCH_2COCH_2COCl$ or $(CH_3CO)_2CHCOCl$]. Naturally as n increases the possible number of isomers will rapidly increase.

It did not prove possible to positively identify the fragments observed for the first fraction (Figure 5-3), but the metastable peak observed at m/e = 56.5 represents the loss of CO (or C_2H_4) from the fragment of m/e = 105 to give the fragment of m/e = 77 units.

Due to the complicated nature of this interesting reaction, and later the non-availability of the GLC/mass spectroscopy facility, further study was not possible.

5.4.2.3 The benzyl chloride reaction

The reaction between $Mo(CO)_4$dpa and benzyl chloride resulted in a diamagnetic sandy yellow solid which, from its infra-red and analytical data (Table 5-5) contained co-ordinated dpa and carbon monoxide and had C, H and N analysis in close agreement with the empirical formula $[Mo_2Cl_4(C_7H_7)(CO)_2(dpa)_2]$. The same product was formed by ultraviolet irradiation of the reactants.

Table 5-5

Analytical and infra-red data for $[Mo_2Cl_4(C_7H_7)(CO)_2(dpa)_2]$

C[a]	H	N	Infra-red	Assignment
41.7	3.47	10.1	3280m	ν_{NH} and ν_{CH} (aromatic)
(42.3)	(3.04)	(10.2)	3240m	"
			3190m-s	"
			3140m	"
			3080m	"
			3040m	"
			1903vs	ν_{CO}
			1850vs	ν_{CO}
			1638s	Aromatic ring breathing
			1610m-w	"
			1585s	"
			1530mbr	"
			1475vs	"
			775s-vs	CH out of plane bend

a) Values in parentheses are calculated for $Mo_2Cl_4C_{29}H_{25}N_6O_2$

The infra-red spectrum of this product showed no evidence for a $-CH_2-$ group (ν_{CH} 2960 to 2850 cm^{-1})[111] as would be expected for a σ-benzyl species, which may indicate the presence of a η^3-benzyl group, a tropenium group or a tropyllium cation. Due to the intense dpa bands in the infra-red spectrum no absorptions could be definitely assigned to the C_7H_7 moiety, and n.m.r. spectroscopy which would readily differentiate between these various bonding modes, was precluded by the insolubility of the product in suitable solvents.

The observed carbonyl stretching bands (ν_{CO}, 1903 and 1850cm^{-1}) are not typical of other cis-dicarbonyl molybdenum(II) complexes, and at this stage it is not possible to make any firm structural proposals.

When $Mo(CO)_4$bipy was reacted with benzyl chloride no carbonyl containing complex similar to that obtained from $Mo(CO)_4$dpa could be detected. The red-brown product so formed was identified as impure $MoCl_4$bipy.

5.4.3 Conclusion

The oxidation of molybdenum(0) and (II) under forcing conditions proved to be rather interesting, and generally led to impure molybdenum(IV) derivatives MoX_4L_2, but unfortunately it has not been possible to identify all the organic products.

Molybdenum(0) and (II) causes the reductive coupling of allyl bromide with the formation of hexa-1,5-diene (bi-allyl) and $MoBr_4$dpa, contaminated with dpa.HBr.H_2O.

The reaction between molybdenum(0) and acetyl chloride proved to be far more complex. No carbonyl containing intermediates were isolated and at least six organic products were formed. One of these (Fraction No. 6) appeared to be a condensation polymer of acetyl chloride, but none of the minor constituents could be identified from their mass spectra. In addition acetyl chloride had a slight tendency to acetylate the acyclic amine group of co-ordinated dpa [i.e. $Mo(CO)_4$dpa] and readily acetylated free dpa prior to its co-ordination to the metal [i.e. $Mo(CO)_6$ + dpa].

The reaction between benzyl chloride and the complexes $Mo(CO)_4L_2$, L_2 = bipy or dpa, revealed a difference between the reactions of the bipy and dpa complexes. The bipy complex readily reacted to give impure $MoCl_4$bipy whilst the dpa complex gave a sandy yellow solid of unknown structure with the empirical formula $[Mo_2Cl_4(C_7H_7)(CO)_2(dpa)_2]$.

Chapter 6

Comparative Reactions of 2,2'-Bipyridine and Di-(2-pyridyl)amine

Chapter 6

Comparative Reactions of 2,2'-Bipyridine and Di-(2-pyridyl)amine

6.1 Introduction

The ligands bipy and dpa generally form very similar complexes, but due to the greater flexibility and basicity of dpa (pK_a = 6.99)[69] relative to bipy (pK_a = 4.44)[57] their reactions are not necessarily identical. This chapter outlines a few observed differences in the molybdenum chemistry of these two ligands.

Initial investigations centred on the relative stability of some of their complexes, namely $Mo(CO)_4L_2$ and $[MoBr(\eta^3\text{-allyl})(CO)_2L_2]$ (L_2 = bipy or dpa). Thus exchange and competition reactions were studied in an attempt to compare the thermodynamic stabilities of these complexes. Subsequently the reaction between dpa and $Mo(CO)_3$cht was investigated and compared with the corresponding bipy reaction[56].

6.2 Experimental

6.2.1 The exchange of co-ordinated bipy and dpa

The reactants (Table 6-1) in stoichiometric proportions (Equations 6-1 to 6-4) were allowed to interact in refluxing solvent (toluene or THF). After cooling to room temperature the resulting complex was collected at the filter, washed with

$Mo(CO)_4L_2 + L_2' = Mo(CO)_4L_2' + L_2$ Equation 6-1

$Mo(CO)_6 + L_2 + L_2' = Mo(CO)_4L_2' + L_2 + 2CO$ Equation 6-2

$MoBr(\eta^3\text{-allyl})(CO)_2L_2 + L_2' = MoBr(\eta^3\text{-allyl})(CO)_2L_2' + L_2$ " 6-3

$Mo(CO)_6 + L_2 + L_2' + allylBr^* = MoBr(\eta^3\text{-allyl})(CO)_2L_2' + L_2 + 4CO$ " 6-4

* allyl Br in excess

a little solvent and dried in vacuo.

Table 6-1

Summary of the exchange reactions

Reactants	Reaction time and medium	Product
1. $Mo(CO)_4$bipy and dpa	1 hr in toluene	$Mo(CO)_4$bipy
2. $Mo(CO)_4$dpa and bipy	"	$Mo(CO)_4$bipy
3. $Mo(CO)_6$, bipy and dpa	"	$Mo(CO)_4$bipy
4. $MoBr(\eta^3$-allyl$)(CO)_2$bipy and dpa	2 hr in THF	$MoBr(\eta^3$-allyl$)(CO)_2$bipy
5. $MoBr(\eta^3$-allyl$)(CO)_2$dpa and bipy	"	$MoBr(\eta^3$-allyl$)(CO)_2$bipy
6. $Mo(CO)_6$, bipy, dpa and allyl bromide[a]	"	$MoBr(\eta^3$-allyl$)(CO)_2$bipy[b]

a) Allyl bromide in excess

b) Reaction did not go to completion and unreacted $Mo(CO)_6$ could be recovered.

The products were identified by means of their colour and their infra-red spectra.

6.2.2 The reaction between $Mo(CO)_3$cht and dpa

An equimolar mixture of $Mo(CO)_3$cht and dpa were allowed to react together for 3 days at room temperature in benzene to give an insoluble yellow solid. (Analysis: C, 48.9; H, 3.3; N, 14.2. Calc. for $Mo_2C_{36}H_{27}O_6N_9$: C, 49.5; H, 3.1; N, 14.4%).

6.2.3 The reaction between $[Mo(CO)_3(dpa)_{1.5}]$ and liquid SO_2

The yellow product from the above reaction was allowed to react with liquid sulphur dioxide at its boiling point ($-10^{\circ}C$), with the excess sulphur dioxide being removed in a stream of nitrogen gas to yield a brown solid.

6.3 Results and discussion

6.3.1 The replacement of co-ordinated dpa by bipy

It is possible to calculate the thermodynamics of exchange reactions from a consideration of the formation processes for each complex as in Scheme 6-1. The competition reactions, on the

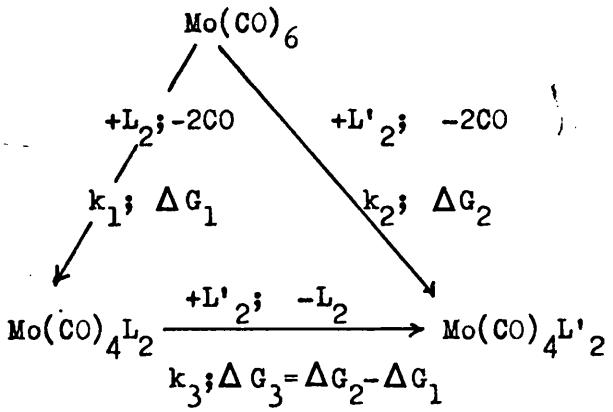

Scheme 6-1 Formation and exchange processes for $Mo(CO)_4L_2$

other hand, are more difficult to analyse as the complexes $Mo(CO)_4L_2$ and $Mo(CO)_4L'_2$ will be formed at rates proportional to the rate constant k_1 and k_2 respectively, but one of these complexes [i.e. $Mo(CO)_4L_2$] will be removed at a rate proportional to k_3. Thus the experimental observations will depend on the relative values of k_1, k_2 and k_3.

During the competition reaction it is possible, if the kinetics are favourable (i.e. $k_1 \gg k_2$, $k_1 \gg k_3$ and $\Delta G_2 > \Delta G_1$), to observe the formation of the thermodynamically less stable product $[Mo(CO)_4L_2]$ as an early and transient species. Frequently though, the kinetics will be such that the less stable complex $[Mo(CO)_4L_2]$ will be removed almost as rapidly as it is formed ($k_3 > k_1$) or the more stable complex $[Mo(CO)_4L'_2]$ will be formed at such a rate as to mask the presence of the other complex ($k_2 \gg k_1$). Hence in many cases these competition reactions merely lead to negative conclusions.

In all cases (exchange and competition) the final product will be the thermodynamically more stable complex $[Mo(CO)_4L'_2]$ or possibly a mixture of complexes $[Mo(CO)_4L_2$ and $Mo(CO)_4L'_2]$ especially if the free energies of formation (ΔG_1 and ΔG_2) are similar or the reaction is stopped before completion.

During reactions 2 and 3 (Table 6-1) a red coloration $[Mo(CO)_4bipy]$ formed as soon as the reflux temperature was reached, whilst in experiment 1 no reaction was observed. Thus suggesting that at the temperature employed (ca. 110°) the ligand dpa is readily replaced by bipy to form the thermodynamically more stable complex $Mo(CO)_4bipy$. It is not possible to make any positive conclusions about the kinetics of formation of the complexes $Mo(CO)_4L_2$ (L_2 = bipy or dpa) (Experiment 3) as the exchange reaction is far too rapid at 110°C to enable any $Mo(CO)_4dpa$ to be detected, even if it were formed.

These reactions were reported for the complexes $[MoBr(\eta^3\text{-allyl})(CO)_2L_2]$ (L_2 = bipy or dpa) (Experiments 4 to 6 in Table 6-1) and again it was found that bipy would replace dpa, but at the temperature used (ca. 65°C) the exchange was slower with the colour of the product in experiment 5 gradually changing from yellow to red during reflux. As a result of this reduction in the exchange rate experiment 6 should, if the rate of formation of $[MoBr(\eta^3\text{-allyl})(CO)_2dpa]$ is significantly greater than that of the corresponding bipy complex, give rise to a yellow colouration at the beginning of the reaction. Such a yellow colouration was not observed, suggesting that the rate of formation of the complex $[MoBr(\eta^3\text{-allyl})(CO)_2dpa]$ is not significantly, if at all, greater than that of the bipy analogue.

Hence it can be said that the complexes $Mo(CO)_4bipy$ and $[MoBr(\eta^3\text{-allyl})(CO)_2bipy]$ are both thermodynamically more stable than their dpa analogues, and that the kinetics of the formation reactions (Scheme 6-1) are not significantly, if at all, in favour of the formation of the complex $[MoBr(\eta^3\text{-allyl})(CO)_2dpa]$. These results will be considered in relation to the C - O stretching force constants in Chapter 7.

6.3.2 Reactions of $Mo(CO)_3cht$

The insoluble product from the reaction between $Mo(CO)_3cht$ and dpa is formulated from its analytical (cf. 6.2.2) and infra-red data (ν_{NH}, 3320m; ν_{CO}, 1915vs, 1810vs and 1735vs cm^{-1}),

as $[Mo(CO)_3(dpa)_{1.5}]$. Such a complex could exist as a dimer (Figure 6-1, A or B) or a polymer (Figure 6-1, C or D).

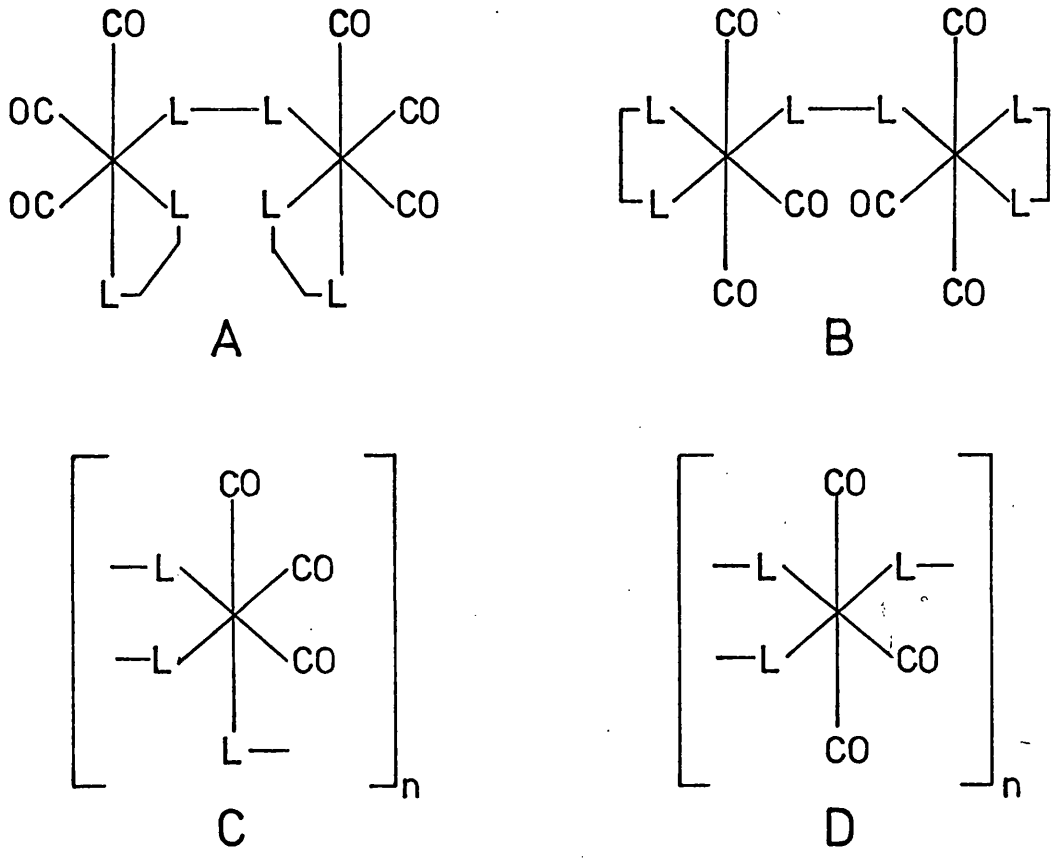

Figure 6-1. Possible structures of $Mo(CO)_3(dpa)_{1.5}$

These species are related to trisubstituted hexacarbonyl complexes [i.e. $M(CO)_3L_3$] and as such may adopt a facial (Figure 6-1, A or C) or a meridinal (B or D) geometry for the three carbonyl groups. If all three L groups are equivalent, the facial isomer will give rise to two strong CO stretching bands (A_1 and E) with the lower energy band (E) being a little more intense and normally slightly broader than the A_1 band. If the three L groups are not equivalent [i.e. fac-$M(CO)_3X_2Y$]

three strong CO stretching bands (2A' and A") of approximately equal intensity are to be expected. The degree of separation of the two lowest energy bands (A" and A') is a function of the difference in the bonding properties of X and Y, but typically is of the order of 20 to 50 cm^{-1}.[236]

The meridinal isomer should give rise to three infra-red active CO stretching vibrations ($2A_1$ and B_1, or if the three L groups are not equivalent, 2A' and A") but examples of this type are not as well documented as the facial case. Generally these meridinal complexes are characterised by one strong and two very much less intense carbonyl bands.[27,237] Hence the complex $[Mo(CO)_3(dpa)_{1.5}]$ poses a problem, having three strong carbonyl stretching bands in its infra-red spectrum but with a very large separation (75 cm^{-1}) between the two lowest energy bands. If the complex is assumed to have a facial tricarbonyl grouping then one would expect only a moderate separation of the A" and A' modes as bridging and chelating dpa cannot have greatly differing donor properties. Thus in $[Mo(CO)_3pybipy]$[236] and $[Mo(CO)_3pydpa]$[58] the A" - A' separations are 48 and 40 cm^{-1} respectively and even $[Mo(CO)_3phen(Ph_2Se)]$[236] has a separation of only 64 cm^{-1}. If the complex is assumed to contain a meridinal tricarbonyl grouping then the highest and lowest energy bands (1915 and 1735 cm^{-1}, $2A_1$ or 2A') seem to be unusually intense. Thus it is not possible to deduce from the infra-red data alone which isomeric form the complex $[Mo(CO)_3(dpa)_{1.5}]$ adopts but, as meridinal trisubstituted hexacarbonyl complexes are normally only formed with strongly

pi-bonding ligands such as phosphines, a facial isomer would seem more likely, possibly with a large degree of distortion due to the bridging dpa groups.

When Behrens[56] studied the reaction between $Mo(CO)_3cht$ and bipy he found that the product was a carbonyl bridged dimer for which he proposed the structure shown in figure 6-2. This difference in the reaction products{$[Mo(CO)_3bipy]_2$ and

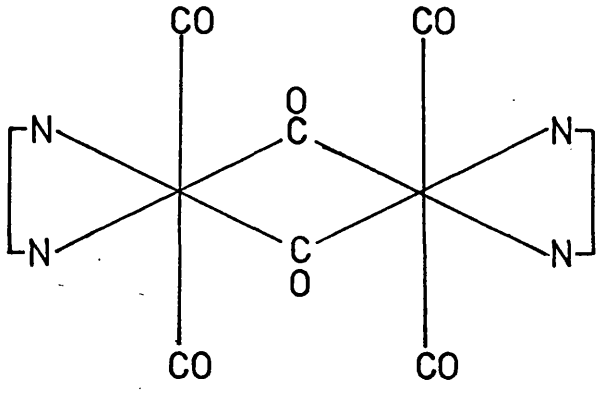

Figure 6-2. Proposed structure of $[Mo(CO)_3bipy]_2$

$[Mo(CO)_3(dpa)_{1.5}]$}probably reflects the greater flexibility of dpa, with respect to bipy, thus making bridge formation more feasible for the former.

6.3.3 The reaction between $[Mo(CO)_3(dpa)_{1.5}]$ and SO_2

The infra-red spectrum of this brown solid indicated the presence of co-ordinated SO_2 (ν_{SO}, 1125s and 930m cm^{-1}) and co-ordinated dpa. The carbonyl stretching bands (ν_{CO}, 1990vs,

1915vs and 1870vs cm^{-1}) were consistent with an $[M(CO)_3X_2Y]$ stereochemistry for the complex. The magnitude of the split between the two lowest energy bands (45 cm^{-1}) and the observance of three approximately equally intense carbonyl bands suggests a facial geometry for the tricarbonyl grouping. Hence the product appears to be fac-$[Mo(CO)_3(SO_2)dpa]$ and bears a close spectroscopic resemblance to $[Mo(CO)_3(SO_2)bipy]$ (ν_{CO}, 1984vs, 1908vs and 1869vs; ν_{SO}, 1124vs and 926vs cm^{-1}).[51] Thus dissolution in SO_2 results in a breakdown of the polymeric or bridging structure of $[Mo(CO)_3(dpa)_{1.5}]$ and the formation of an SO_2 adduct.

6.4 Conclusion

The reactions which involved exchange of, or competition between the ligands bipy and dpa indicated that the complexes $Mo(CO)_4bipy$ and $[MoBr(\eta^3\text{-allyl})(CO)_2bipy]$ were thermodynamically more stable than their dpa analogues. In addition the kinetics of formation of the complex $[MoBr(\eta^3\text{-allyl})(CO)_2dpa]$ are not significantly, if at all, greater than those for the formation of the related bipy complex.

The greater flexibility of dpa, compared with bipy, was demonstrated by the reaction between $Mo(CO)_3cht$ and dpa which resulted in the formation of a dpa bridged complex $[Mo(CO)_3(dpa)_{1.5}]$, whose stereochemistry could not be definitely assigned from the infra-red data. This product is not similar to the complex obtained by Behrens[56] from the analogous bipy reaction which was formulated as a carbonyl bridged dimer. The complex $[Mo(CO)_3(dpa)_{1.5}]$ reacts readily with liquid SO_2 to give $[Mo(CO)_3(SO)_2dpa]$ which probably exists as the facial isomer.

Chapter 7

Carbonyl Stretching Force Constants for *cis*-$L_2M(CO)_4$ Complexes

Chapter 7.

Carbonyl Stretching Force Constants for cis-$L_2M(CO)_4$ Complexes

7.1 Introduction

Since the discovery of metal carbonyls[6] there has been a great deal of interest in these complexes due primarily to their rather unusual bonding and unexpectedly high stability. As their bonding involves both σ-donation and π- acceptance of electron density by the carbonyl carbon atoms, it has long been postulated that the M - C and C - O bonds should be sensitive indicators of the M - L bond properties in substituted metal carbonyl complexes.

As the metal carbonyl CO stretching vibrations occur in a fairly clear part of the infra-red spectrum (2200 - 1700 cm^{-1}), and usually give rise to intense absorption bands, infra-red spectroscopy has been used extensively in the study of these complexes.[27,31,238] Spectra may be used in a qualitative manner, for example in the prediction of geometric isomers, and in the discussion of mean electronic variations between similar complexes, but many workers[27,31,238] regard it to be advantageous to put this information into a more quantitative form - i.e. force constants. This view is not unanimous, and Bower and Stiddard[239] consider it to be no more than transferring information from one form to another. This may be true for the highly symmetric $M(CO)_6$ $\{O_h\}$ and trans-$L_2M(CO)_4$ $\{D_{4h}\}$ species considered by them, but it is not true for species of lower symmetry which give rise to more complex spectra.

Any attempt to calculate rigorous force constants (where rigour means complete exactness) is complicated by a lack of data, as invariably there are more unknowns (force constants) than observed values (vibrational band positions). In many cases the available data can be sufficiently increased by using isotopically labelled complexes. Even then the observed band positions should not be used directly in calculations as they require correction for anharmonicity.

Many workers have attempted to overcome these difficulties by making the minimum number of approximations, based on chemical knowledge or intuition. Early attempts at making rational approximations for the octahedral complexes were based on the separation of the σ- and π-bonding frameworks (the symmetry factored model), and letting all the force constants be solely dependent on the π-bonding framework. The most detailed study was carried out by Jones[240]. The majority of his work has been on the non-substituted tetrahedral and octahedral metal carbonyl complexes of nickel and the group VIB metals, but his procedure is not readily applied to substituted complexes.

Probably the most popular, but less rigorous procedure, is that proposed by Cotton[204] and his co-workers. Whereas this method involves less valid approximations than Jones it is readily applied to substituted metal carbonyl complexes. Many workers, especially Jones,[241-3] have criticised Cotton's approach but as stated by Cotton his method is valid as long as allowance is made for the inherent limitations of the method.

Several workers[244-250] have modified the basic Cotton approach in attempts to give the calculated force constants more credibility. Any modification is bound to make the procedure more complex to apply, hence a balance has to be struck between the rigour required and the complexity of the method adopted.

As this section refers principally to cis-disubstituted hexacarbonyls the following discussion will be restricted to species of this geometry.

7.2 The Cotton-Kraihanzel procedure.

The Cotton-Kraihanzel[204] (C - K) procedure forms the basis of the methods used to calculate CO force constants in this work, thus it is necessary to state the approximations made in this approach and how such approximations limit the method. The six approximations made by Cotton[204] are as follows:

a) All interactions between the CO stretching modes and any other vibrational mode are insignificant (This is the high energy factored model).

b) The observed band positions are used without attempting to make any corrections for anharmonicity.

c) The coupling between the various vibrating carbonyl groups is entirely non-mechanical, due to the damping effect of the relatively heavy central metal atom.

d) The substituent groups are treated as being spherical point masses leading to an idealised geometry (C_{2v}).

With these assumptions Cotton obtained what he loosely termed "exact" secular equations, but there were still too many unknowns, thus using a π-interaction force field Cotton made the following additional assumptions:

e) All interactions between mutually cis-carbonyl groups are equivalent, and the interaction between mutually trans-carbonyl groups is exactly double that of the cis-carbonyl groups.

$$cisA = cisB = \tfrac{1}{2}trans \qquad \text{(cf. Figure 7-1)}$$

f) For substituents with less π-acceptor ability (π-acidity) than carbon monoxide the CO stretching force constants will be such that K_1 is less than K_2 (cf. Figure 7-1) and all the force constants will be real and positive.

This last assumption (i.e. $K_1 < K_2$) is made in order to limit the number of possible assignments for the observed spectrum.

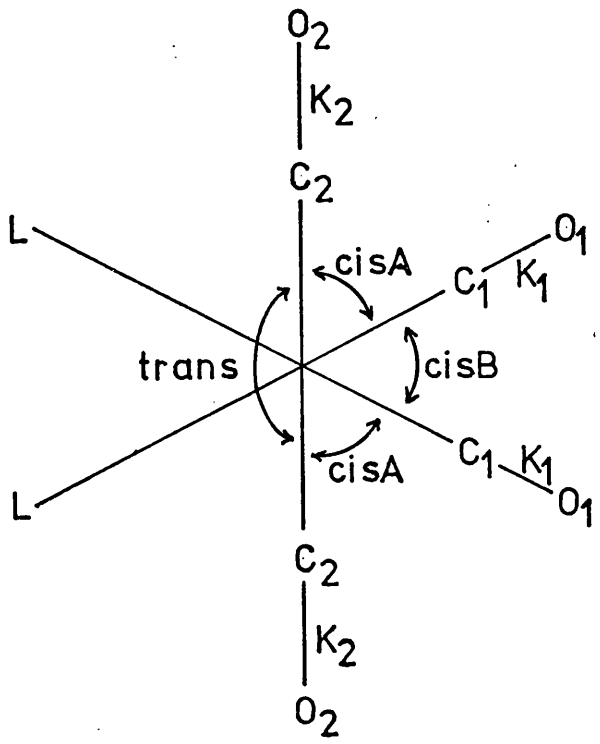

Terminology:

This work	Cotton[204]
cisA	k_c
cisB	k'_c
trans	k_t
K_1	K_1
K_2	K_2
X = cisB/cisA	-
Y = trans/cisA	-

Figure 7-1 Force constants and terminology for cis-$L_2M(CO)_4$ complexes.

7.2.1 Criticism of the C - K approach

The least valid approximation made in the C - K approach is the inter-relating of the interaction force constants (cisA = cisB = $\frac{1}{2}$trans). Whilst the reasoning for this relationship seems rational for the parent hexacarbonyls, it can be seen that as the symmetry is lowered from O_h, the d_π-orbitals (d_{xy}, d_{xz} and d_{yz}) will no longer be equivalent, and may have significantly different overlap properties with the carbonyl groups. Hence, the relationship between the interaction force constants could well change for complexes of lower symmetry.

For C_{2v} symmetry it is possible using either the Jones procedure[240], with allowance for the substituent groups (L) having different π-acceptor properties to those of carbon monoxide, or by using very simple molecular orbital theory and considering only the π-orbitals to arrive at an expression for Y (trans/cisA) equal to 2.0, but no simple relationship has been found for X (cisB/cisA).

Stone[244] and coworkers have used the Jones[240] procedure together with angular correction terms to obtain a value of 1.4 for Y and a value of X that was a function of the substituents π-acidity.

All the above values for X and Y were calculated on the assumption that for each vibrational mode the interaction force constants are primarily dependent on the π-electron density between the carbonyl groups involved in that vibration, and that the M - C σ-framework is completely unaffected by these vibrations. The former assumption seems reasonable, but as it has been accepted that these complexes owe their stability to the synergic effect, any change in the π-electron system is expected to have a significant effect on the σ-framework and vice-versa. This leads to a very complex bonding scheme and means that the ratios X and Y for the interaction force constants may well be more complex than those derived by the above workers.

Recently Jones[240] has carried out a detailed study of the complexes $M(^{x}C^{y}O)_6$ (M = Cr, Mo or W; x = 12; y = 16 or 18 and x = 13; y = 16) and by using these isotopically enriched species the number of observed vibrational bands were sufficiently increased to avoid using the C - K approximations. Contrary to the C - K approach Jones found that the interaction for mutually cis-carbonyl groups was greater than that for mutually trans-carbonyl groups (i.e. cisA ≡ cisB > trans. The equivalence of cisA and cisB arises from the high symmetry [O_h] of these species). This was taken to indicate that the simple π-interaction force field was not appropriate and that the interaction terms arise mainly from mutual polarisations caused by the large oscillating dipole moments. Whilst this work of Jones[240] probably invalidates Cotton's[204] assumption regarding the relationship between the interaction terms, it does not invalidate the rest of the C - K procedure which does not rely on π-orbital considerations.

7.2.2 Modifications to the C - K approach

Several groups of workers have tried to devise procedures which avoid using the C - K assumptions regarding the interaction force constants. Stone[244] used a calculated value of Y(trans/cisA) = 1.4 together with the three most certain band positions (A^1_1, B_1 and B_2) and allowed X(cisB/cisA) to vary within the limits 0.8 and 1.9 until the best fit was obtained for the unused A_1^2 band position. Delbeke[245-48,251] made a thorough examination of the results obtained by letting

Y = 1.4 (Stone's value) and 2.0 (Cotton's assumpton) while using all four observed band positions and an algebraic solution of the secular equations to obtain a value for X. As a result of this investigation Delbeke found that the value of 2.0 for Y was more frequently consistent with the criteria outlined by Cotton (i.e. $K_2 > K_1$; cisA, cisB and trans all real and positive).

Jernigan and Brown[249] carried out a brief review of force constants for cis-disubstituted hexacarbonyls and proposed an iterative procedure using the three most certain band positions (A_1^1, B_1 amd B_2) and allowing both X' (cisA/cisB) and Y' (trans/cisB) to vary within limits (X' = 0.4 to 1.4 and Y' = 0.7 to 3.0) until an exact fit was found for the unused A_1^2 band position. While the above modification removes the objection of assumed values for both X and Y, it does assume that the least certain band (A_1^2) is precisely located at the observed value.

Even if the relationship between the interaction force constants is resolved the problem of the neglected coupling between the CO stretching vibrations and other molecular vibrations, as well as the anharmonicity of the observed band positions, still remains. Most workers choose to ignore these problems and allow them to be absorbed into the apparent force constants. Jones[252,253] has calculated the anharmonic corrections for $M(CO)_6$ (M = Cr, Mo or W) and $MnBr(CO)_5$ and found these to be by no means negligable, with values as large $40cm^{-1}$ for some of the modes. The force field used by Jones included the

interaction terms ignored by Cotton[204], and showed appreciable coupling between the CO and MC stretching vibrations. This is not altogether surprising as whenever a CO bond is stretched both the carbon and oxygen atoms must move to some extent and, therefore, a CO stretch must cause the MC bond to contract somewhat.

Whilst it seems reasonable to ignore anharmonicity, and the interaction terms mentioned above, when calculating the force constants for a closely related series of complexes, it is most desirable that they be included in isotopic studies. Especially as Bor[254], using a model of an isolated carbonyl group attached by the carbon atom to an infinite mass, has shown that the MC/CO stretch/stretch interaction force constant is dependent on the reduced mass of the carbonyl group.

Recently Chen and Hsiang[250] have modified the C - K approached for cis-disubstituted hexacarbonyls by using the criterion of maximum interaction between the CO stretching vibrational modes, as applied to fac-trisubstituted hexacarbonyls by Stone[244]. Using this criterion together with all four observed band positions Chen[250] obtained an algebraic solution of the C - K secular equations[204], but Chen seems to have interchanged the C - K assignment for the B_1 and B_2 modes and consequently his calculated force constants K_1 and K_2 are contrary to the C - K criteria that K_2 should be greater than K_1. Other workers[244-248] who have interchanged the assignments for the B_1 and B_2 modes have also interchanged the relevant secular equations. This amounts to no more than using the second mirror plane, σ_v' which is at 90^o to the σ_v

plane used by Cotton, to define the symmetry of the B vibrational modes. One of these mirror planes (σ_v) bisects the L-M-L bond angle whilst the other plane (σ'_v) bisects both of L-M-CO(1) bond angles (Figure 7-2). The present work follows Cotton in using the $\sigma_{v(xz)}$ plane to define the B_1 and B_2 vibrational modes.

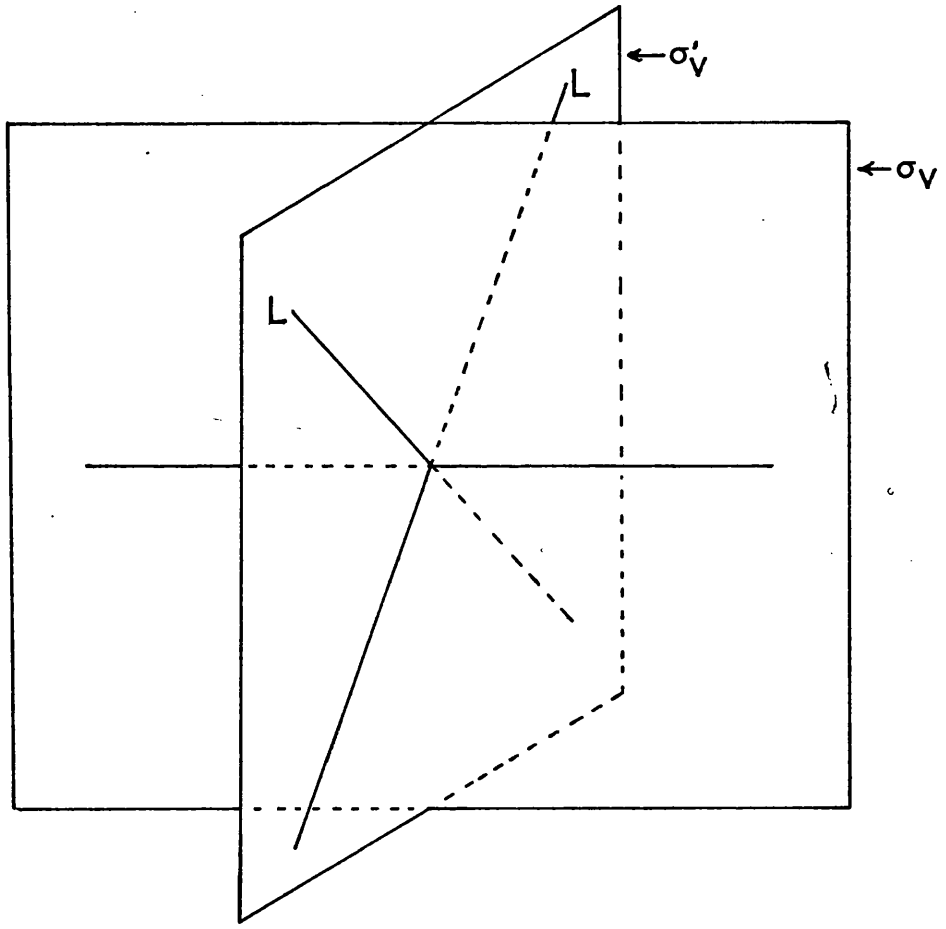

Figure 7-2 Mirror planes in cis-$L_2M(CO)_4$ species

7.3 The new procedure.

As a part of this investigation it was decided to try to determine CO stretching force constants by a modified C - K approach which would retain the best features of this basic method whilst making no numerical assumptions for the ratios of the interaction constants. It was thought that a combination of the criterion of maximum interaction[244,250] together with the Jernigan[249] approach might be a suitable starting point for this work. This approach requires only three of the four observed band positions (A_1^1, B_1 and B_2) and allows the interaction force constants to be completely independent of each other. It is also possible to predict the band position for the unused mode (A_1^2) as a check against serious errors. It seemed more natural to use cisA as the common factor for the ratios X and Y, as cisA is the interaction constant which defines the coupling between the two A_1 modes. This means that whereas Jernigan[249] let X' = cisA/cisB and Y' = trans/cisB, this work uses X = cisB/cisA and Y = trans/cisA (i.e. X = 1/X' and Y = Y'/X').

The new modification which is used throughout the rest of this work is an iterative procedure, in both X and Y, and is described in the five steps which follow:

a) X is given the initial value of 0.8

b) The value of Y is increased from 0.8 to 3.5 in steps of 0.1 until step (c) is satisfied.

c) The force constants and the unused band position A_1^2 are calculated at each value of Y until a maximum value is found for the predicted band position. This maximum value is refined by allowing Y to vary in steps of 0.001 near the maximum.

i.e. $\partial(\nu_c)/\partial Y = 0$; X constant

d) X is progressively increased by 0.1 and steps (b) and (c) repeated until step (e) is satisfied. If X reaches the arbitary value of 2.0 then the case is abandoned.

e) At each maximum value of the predicted band position cisA is compared with the previous iterations so that the maximum value of cisA can be obtained. This value of cisA is refined by allowing X to vary in steps of 0.001 near the maximum. At this point the expressions

$$\partial(\nu_c)/\partial Y = 0; \quad X \text{ constant}$$

and $\partial(\text{cisA})/\partial X = 0$

are simultaneously satisfied.

The values of X and Y defined by step (e) give rise to an individual set of force constants which are taken as being the new modified force constants, and the calculated band position for the unused A_1^2 mode is used in the discussion of their validity.

The above steps (a - e) are illustrated in figures 7-3 and 7-4 and the calculations were performed with double precision accuracy on an ICL system 4.50 computer. The programme was written in Fortran IV in such a way that as well as giving the

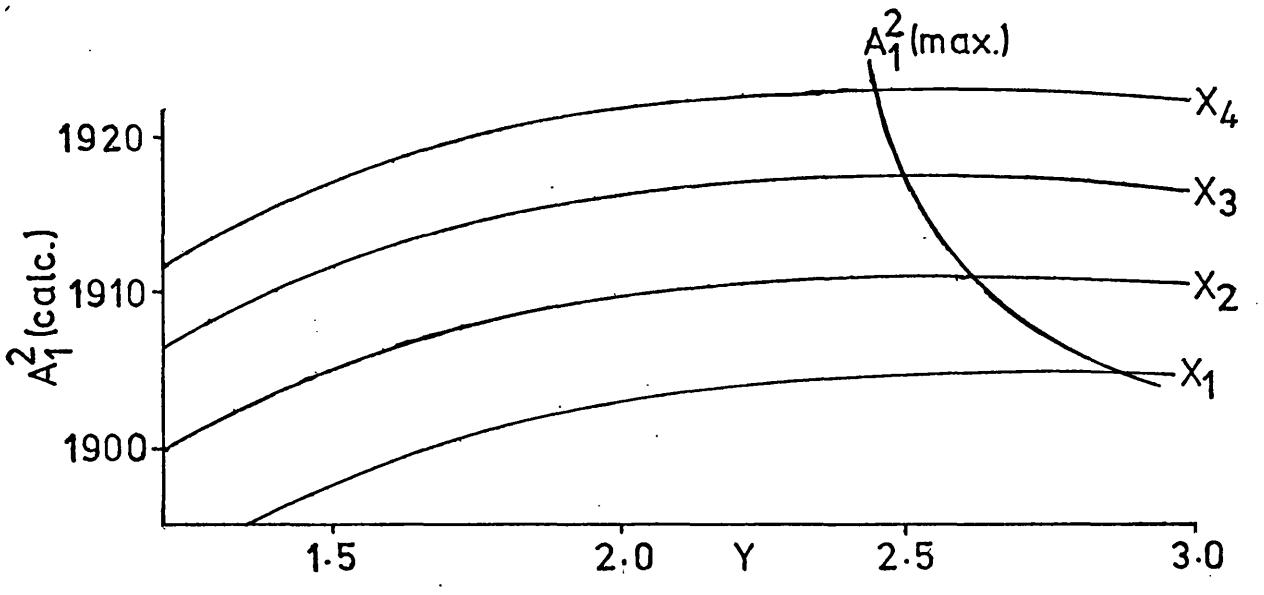

Figure 7-3 The variation of the predicted band position (A_1^2) against Y steps (b) and (c)

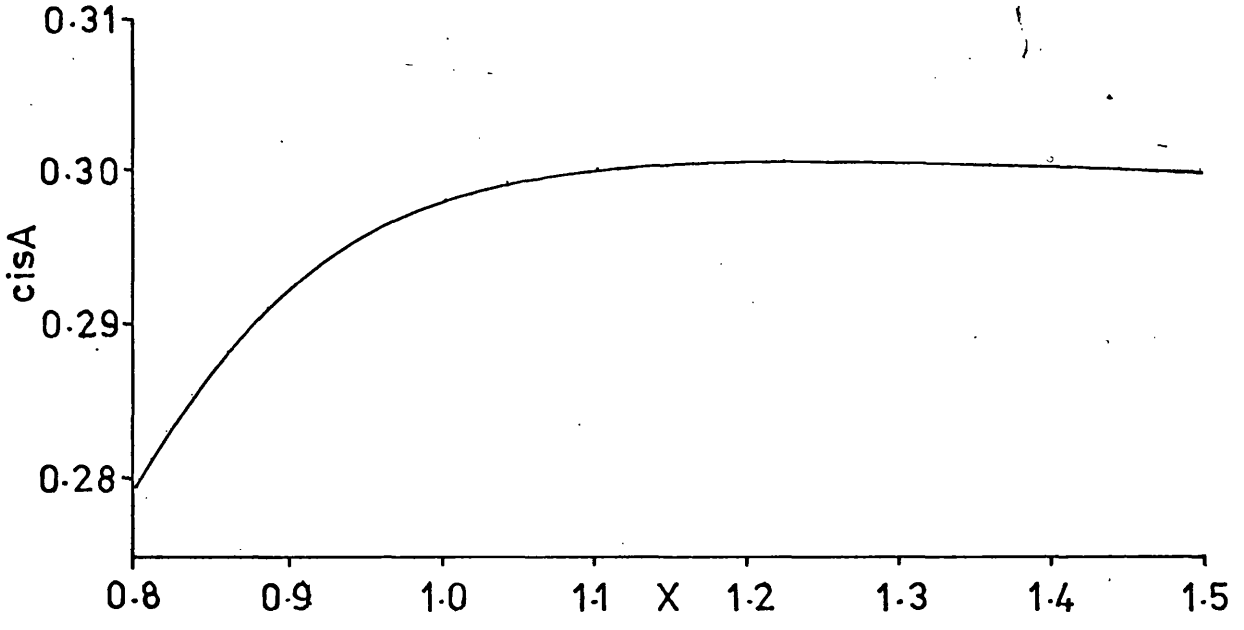

Figure 7-4. The variation of cisA against X with A_1^2(calc) being kept a maximum steps (d) and (e)

above results it also determined force constants according to the basic Cotton[204] approach and the Jernigan[249] modification.

In step (c) the maximum value of the predicted band position (A_1^2) was used as this leads to a single set of force constants, whereas at non-maximal values each of the force constants will have two acceptable values. The maximum value of cisA was taken as this was expected to correspond to the most stable vibrational system.

7.4 Calculated force constants

Tables 7-1 to 7-3 contain the force constants as calculated by the new procedure together with those obtained by the C - K[204] and Jernigan[249] procedures. These tables represent a variety of donor atoms and metals to ensure that the new procedure is generally applicable to cis-$L_2M(CO)_4$ complexes.

The complexes $M(CO)_4L_2$ where M = Cr, Mo or W and L_2 = dpa, adpa or bdpa have been included in order to compare small variations in force constants with the electronic changes in these complexes.

7.4.1 Discussion of the calculated force constants

If as is usually assumed for metal carbonyl complexes the M - C and C - O bond properties are complementary, it should be possible to make qualitative predictions concerning the CO stretching force constants from a consideration of the bonding properties of the ligands and the metals in a related series of complexes.

Table 7-1: Force constants[a] for cis-$M(CO)_4L_2$ complexes (L = Group V donor ligands).

Complex[b]	ν_{CO} (cm^{-1})				Ref.	Solvent	Force constants (m dyne/Å)					A_1^2 calc(cm^{-1})	ΔA_1^2(cm^{-1})
	A_1^1	A_1^2	B_1	B_2			cisA	cisB	trans	K_1	K_2		
$Cr(CO)_4(MeCN)_2$	2019	1882	1908	1843	255	Nujol	0.37			14.09	15.44	1874	-8
							0.41	0.48	0.69	14.20	15.39		
							0.41	0.52	0.68	14.24	15.38	1886	4
$Mo(CO)_4(MeCN)_2$	2023	1881	1912	1833	255	Nujol	0.38			13.95	15.52	1886	-15
							0.44	0.58	0.66	14.15	15.43		
							0.44	0.56	0.67	14.13	15.43	1879	-2
$W(CO)_4(MeCN)_2$	2023	1880	1900	1840	255	Nujol	0.41			14.08	15.39	1873	-7
							0.43	0.50	0.78	14.17	15.36		
							0.43	0.55	0.77	14.22	15.34	1884	4
$Cr(CO)_4en$	2004	1855	1873	1810	70	CH_3NO_2	0.43			13.66	15.02	1845	-10
							0.45	0.55	0.81	13.77	14.98		
							0.45	0.57	0.81	13.80	14.97	1858	3
$Mo(CO)_4en$	2015	1864	1890	1818	70	CH_3NO_2	0.42			13.76	15.26	1853	-11
							0.46	0.56	0.77	13.91	15.19		
							0.46	0.58	0.76	13.93	15.19	1867	3
$W(CO)_4en$	2006	1852	1867	1809	70	CH_3NO_2	0.45			13.66	14.97	1844	-8
							0.45	0.53	0.88	13.74	14.96		
							0.46	0.58	0.87	13.80	14.94	1858	6

Table 7-1 (Contd)

Complex[b]	ν_{CO} (cm^{-1})				Ref.	Solvent	Force constants (m dyne/Å)					A_1^2 calc(cm^{-1})	ΔA_1^2 (cm^{-1})
	A_1^1	A_2^2	B_1	B_2			cisA	cisB	trans	K_1	K_2		
$Cr(CO)_4$tmen	2005	1879	1868	1839	249	CS_2	0.43			14.09	14.95	1868	-11
							0.39	0.49	0.88	14.14	14.98		
							0.39	0.49	0.88	14.15	14.98	1879	0
$Mo(CO)_4$tmen(1)	2012	1880	1880	1843	249	CS_2	0.42			14.14	15.11	1873	-7
							0.39	0.46	0.86	14.18	15.13		
							0.40	0.50	0.85	14.22	15.12	1884	4
$Mo(CO)_4$tmen(2)	2014	1888	1881	1856	27	hexadecane	0.42			14.33	15.12	1883	-5
							0.37	0.40	0.88	14.32	15.17		
							0.37	0.47	0.87	14.38	15.15	1894	6
$W(CO)_4$tmen(1)	2005	1872	1864	1838	249	CS_2	0.44			14.08	14.91	1867	-5
							0.39	0.43	0.93	14.07	14.96		
							0.39	0.50	0.91	14.14	14.94	1879	7
$W(CO)_4$tmen(2)	2007.8[c]	1880.0	1861.3	1821.1	256	$CHCl_3$	0.46			13.86	14.92	1854.0	-26.0
							0.43	0.67	0.91	14.07	14.90		
							0.43	0.55	0.93	13.99	14.92	1866.9	-13.1
$Cr(CO)_4(py)_2$	2020	1878	1899	1837	70	CH_3CN	0.40			14.03	15.36	1870	-8
							0.43	0.51	0.76	14.13	15.32		
							0.43	0.54	0.75	14.17	15.31	1882	4

Table 7-1 (Contd)

Complex[b]	$\nu_{CO}(cm^{-1})$				Ref.	Solvent	Force constants (m dyne/Å)					A_1^2calc(cm^{-1})	ΔA_1^2(cm^{-1})
	A_1^1	A_2^2	B_1	B_2			cisA	cisB	trans	K_1	K_2		
$Mo(CO)_4(py)_2$	2025	1881	1907	1839	70	CH_3CN	0.39			14.05	15.48	1872	-9
							0.44	0.52	0.73	14.18	15.42		
							0.44	0.55	0.73	14.21	15.41	1885	4
$W(CO)_4(py)_2$	2012	1869	1888	1828	70	$CHCl_3$	0.41			13.90	15.21	1861	-8
							0.43	0.50	0.78	14.00	15.17		
							0.43	0.55	0.77	14.04	15.16	1873	4
$Cr(CO)_4bipy$	2012	1880	1905	1828	70	$CHCl_3$	0.36			13.86	15.38	1860	-20
							0.43	0.61	0.62	14.11	15.28		
							0.43	0.54	0.64	14.04	15.29	1873	-7
$Mo(CO)_4bipy$	2017	1878	1909	1829	70	$CHCl_3$	0.37			13.88	15.45	1862	-16
							0.44	0.59	0.64	14.10	15.35		
							0.44	0.56	0.64	14.07	15.36	1875	-3
$W(CO)_4bipy(1)$	2010	1873	1899	1826	70	$CHCl_3$	0.37			13.84	15.31	1858	-15
							0.43	0.56	0.66	14.03	15.23		
							0.43	0.55	0.67	14.01	15.23	1871	-2
$W(CO)_4bipy(2)$	2007.6[c]	1871.5	1896.7	1826.2	256	$CHCl_3$	0.37			13.84	15.27	1858.2	-13.3
							0.42	0.55	0.67	14.01	15.20		
							0.42	0.53	0.67	14.00	15.20	1870.4	-1.1

Table 7-1 (Contd)

Complex[b]	ν_{CO} (cm^{-1})				Ref.	Solvent	Force constants (m dyne/Å)					A_1^2 calc (cm^{-1})	ΔA_1^2 (cm^{-1})
	A_1^1	A_1^2	B_1	B_2			cisA	cisB	trans	K_1	K_2		
$Cr(CO)_4dpa$	1999	1873	1895	1822	58	CH_2Cl_2	0.35			13.76	15.20	1853	-20
							0.41	0.60	0.60	14.00	15.11		
							0.41	0.52	0.62	13.93	15.12	1865	-8
$Mo(CO)_4dpa$	2001	1872	1900	1823	58	CH_2Cl_2	0.34			13.76	15.26	1854	-18
							0.41	0.58	0.58	14.00	15.16		
							0.42	0.52	0.60	13.94	15.17	1866	-6
$W(CO)_4dpa$	1996	1866	1886	1817	58	CH_2Cl_2	0.37			13.70	15.10	1849	-17
							0.41	0.58	0.65	13.91	15.01		
							0.41	0.53	0.66	13.86	15.03	1861	-5
$Cr(CO)_4adpa$	1998	1885	1895	1838	58	CH_2Cl_2	0.34			13.98	15.18	1866	-19
							0.37	0.55	0.61	14.19	15.12		
							0.37	0.47	0.63	14.11	15.13	1877	-9
$Mo(CO)_4adpa$	2000	1882	1901	1838	58	CH_2Cl_2	0.34			13.99	15.25	1867	-17
							0.38	0.52	0.59	14.17	15.18		
							0.38	0.48	0.60	14.12	15.19	1878	-4
$W(CO)_4adpa$	1998	1875	1887	1833	58	CH_2Cl_2	0.36			13.93	15.11	1862	-13
							0.38	0.50	0.68	14.07	15.06		
							0.38	0.49	0.69	14.05	15.06	1873	-2

Table 7-1 (Contd)

Complex[b]	$\nu_{CO}(cm^{-1})$ A_1^1	A_1^2	B_1	B_2	Ref.	Solvent	Force constants (m. dyne/Å) cisA	cisB	trans	K_1	K_2	A_1^2 calc(cm^{-1})	$\Delta A_1^2(cm^{-1})$
$Cr(CO)_4$bdpa	1998	1874	1887	1834	58	CH_2Cl_2	0.36			13.95	15.11	1863	-11
							0.38	0.48	0.69	14.07	15.07		
							0.38	0.48	0.69	14.07	15.07	1874	0
$Mo(CO)_4$bdpa	1999	1879	1899	1835	58	CH_2Cl_2	0.33			13.93	15.23	1864	-15
							0.38	0.52	0.59	14.12	15.16		
							0.38	0.49	0.60	14.09	15.16	1875	-4
$W(CO)_4$bdpa	1997	1884	1892	1838	58	CH_2Cl_2	0.35			13.99	15.15	1866	-18
							0.37	0.54	0.63	14.18	15.09		
							0.37	0.47	0.65	14.11	15.10	1877	-7
$Cr(CO)_4(PH_3)_2$	2030	1942	1942	1923	257	hexane	0.28			15.22	15.80	1941	-1
							0.25	0.25	0.60	15.19	15.83		
							0.26	0.33	0.58	15.26	15.81	1949	7
$Mo(CO)_4(PH_3)_2$(1)	2040	1947	1934	1925	257	hexane	0.33			15.30	15.77	1944	-3
							0.27	0.29	0.73	15.25	15.84		
							0.28	0.35	0.72	15.32	15.82	1953	6
$Mo(CO)_4(PH_3)_2$(2)	2036	1946	1932	1923	258	cyclo hexane	0.33			15.26	15.72	1941	-5
							0.27	0.30	0.71	15.23	15.79		
							0.27	0.35	0.70	15.28	15.77	1950	4

Table 7-1. (Contd)

Complex[b]	$\nu_{CO}(cm^{-1})$ A_1^1	A_1^2	B_1	B_2	Ref	Solvent	Force constants (m dyne/Å) cisA	cisB	trans	K_1	K_2	A_1^2 calc(cm^{-1})	ΔA_1^2(cm^{-1})
$W(CO)_4(PH_3)_2$	2037	1941	1941	1923	257	hexane	0.31			15.24	15.83	1942	1
							0.26	0.24	0.67	15.18	15.88		
							0.27	0.35	0.64	15.28	15.85	1951	10
$Cr(CO)_4$dmpe	2009	1921	1900	1894	40	hexane	0.33			14.82	15.25	1912	-9
							0.27	0.34	0.73	14.83	15.31		
							0.27	0.35	0.73	14.83	15.31	1922	1
$Mo(CO)_4$dmpe	2020	1929	1909	1903	40	hexane	0.34			14.97	15.40	1922	-7
							0.28	0.33	0.75	14.96	15.47		
							0.28	0.36	0.75	14.98	15.46	1931	2
$W(CO)_4$dmpe	2017	1922	1902	1897	40	hexane	0.35			14.88	15.31	1916	-6
							0.28	0.32	0.78	14.85	15.39		
							0.29	0.36	0.77	14.90	15.38	1926	4
$Cr(CO)_4$dppe	2009	1918	1903	1887	249	CS_2	0.33			14.71	15.29	1907	-11
							0.29	0.35	0.70	14.73	15.33		
							0.29	0.37	0.70	14.75	15.32	1917	-1
$Mo(CO)_4$dppe	2020	1925	1912	1894	249	CS_2	0.34			14.83	15.44	1915	-10
							0.30	0.39	0.71	14.87	15.47		
							0.30	0.38	0.71	14.87	15.48	1925	0

Table 7-1 (Contd)

Complex[b]	ν_{CO} (cm^{-1}) A_1^1	A_1^2	B_1	B_2	Ref.	Solvent	Force constants (m dyne/Å) cisA	cisB	trans	K_1	K_2	A_1^2 calc (cm^{-1})	ΔA_1^2 (cm^{-1})
$W(CO)_4$dppe(1)	2017	1918	1903	1888	249	CS_2	0.36			14.75	15.34	1909	-9
							0.31	0.38	0.76	14.77	15.38		
							0.31	0.39	0.75	14.78	15.38	1919	1
$W(CO)_4$dppe(2)	2016	1912	1901	1876	204	$CHCl_3$	0.36			14.58	15.32	1900	-12
							0.33	0.44	0.74	14.65	15.33		
							0.33	0.42	0.75	14.63	15.34	1910	-2
$W(CO)_4$dppe(3)	2017.6[c]	1918.5	1899.3	1873.6	256	$CHCl_3$	0.37			14.55	15.32	1898.4	-20.1
							0.33	0.53	0.75	14.70	15.32		
							0.34	0.43	0.77	14.61	15.34	1908.4	-10.1
$[Ta(CO)_4dppe]^-$	1908	1800	1779	1752	259	THF	0.38			12.78	13.55	1779	-21
							0.34	0.53	0.77	12.93	13.56		
							0.35	0.44	0.79	12.83	13.57	1791	-9
$[Re(CO)_4dppe]^+$	2110	2027	2017	1997	260	$CHCl_3$	0.31			16.42	17.05	2016	-11
							0.28	0.39	0.63	16.49	17.06		
							0.28	0.36	0.64	16.46	17.07	2024	-3
$Cr(CO)_4$diars	2005	1914	1894	1885	249	CS_2	0.34			14.69	15.17	1904	-10
							0.28	0.36	0.74	14.71	15.22		
							0.28	0.36	0.74	14.71	15.22	1914	0

Table 7-1 (Contd)

Complex[b]	$\nu_{CO}(cm^{-1})$ A_1^1	A_1^2	B_1	B_2	Ref.	Solvent	Force constants (m dyne/Å) cisA	cisB	trans	K_1	K_2	A_1^2 calc(cm^{-1})	ΔA_1^2(cm^{-1})
$Mo(CO)_4$diars	2018	1922	1907	1894	249	CS_2	0.36			14.83	15.38	1914	-8
							0.29	0.35	0.74	14.84	15.43		
							0.29	0.38	0.74	14.86	15.42	1924	2
$W(CO)_4$diars	2013	1914	1896	1887	249	CS_2	0.36			14.74	15.24	1907	-7
							0.30	0.34	0.79	14.72	15.31		
							0.30	0.38	0.78	14.76	15.30	1918	4
$Cr(CO)_4$dpsp	2007	1924	1897	1891	261	CCl_4	0.34			14.78	15.20	1909	-15
							0.27	0.40	0.72	14.84	15.26		
							0.27	0.35	0.73	14.79	15.27	1919	-5
$Mo(CO)_4$dpsp	2024	1934	1913	1893	261	CCl_4	0.35			14.82	15.48	1915	-19
							0.31	0.49	0.71	14.96	15.49		
							0.31	0.43	0.72	14.91	15.50	1929	-5
$W(CO)_4$dpsp	2018	1925	1906	1892	261	CCl_4	0.36			14.82	15.35	1912	-13
							0.30	0.41	0.74	14.86	15.41		
							0.30	0.38	0.74	14.84	15.41	1923	-2

a, Data for Tables 7.1-3 are presented in the order C-K Jernigan and finally the new procedure for each complex.

b, The number in parenthesis differentiates between data from different sources for a particular complex.

c, Band positions are corrected for overlap, see Ref. 256.

Table 7-2. Force constants* for cis-$M(CO)_4L_2$ complexes (L = Group VI donor ligand)

Complex[b]	νCO (cm^{-1}) A_1^1	A_1^2	B_1	B_2	Ref.	Solvent	Force constants (m. dyne/Å) cisA	cisB	trans	K_1	K_2	A_1^2 calc(cm^{-1})	ΔA_1^2 (cm^{-1})
$[Cr(CO)_4acac]^-$	2005	1848	1877	1795	262	CH_2Cl_2	0.43			13.44	15.08	1832	-16
							0.48	0.63	0.77	13.64	14.99		
							0.48	0.61	0.77	13.63	15.00	1847	-1
$[Mo(CO)_4acac]^-$	2000	1839	1865	1779	262	CH_2Cl_2	0.45			13.23	14.94	1818	-21
							0.51	0.70	0.80	13.48	14.84		
							0.51	0.65	0.81	13.43	14.85	1834	-5
$[W(CO)_4acac]^-$	2001	1818	1869	1754	262	CH_2Cl_2	0.45			12.87	15.00	1797	-21
							0.56	0.74	0.75	13.16	14.86		
							0.56	0.72	0.76	13.14	14.86	1816	-2
$Cr(CO)_4dth(1)$	2015	1911	1894	1874	249	CS_2	0.39			14.56	15.24	1898	-13
							0.33	0.45	0.79	14.63	15.27		
							0.33	0.43	0.79	14.61	15.28	1908	-3
$Cr(CO)_4dth(2)$	2020	1914	1898	1869	263	$CHCl_3$	0.39			14.49	15.32	1895	-19
							0.35	0.53	0.78	14.64	15.32		
							0.36	0.46	0.79	14.56	15.34	1906	-8
$Mo(CO)_4dth(1)$	2023	1911	1903	1878	249	CS_2	0.38			14.62	15.39	1903	-8
							0.34	0.41	0.79	14.66	15.41		
							0.34	0.44	0.78	14.68	15.41	1913	2

Table 7-2 (Contd)

Complex[b]	ν_{CO} (cm^{-1}) A_1^1	A_1^2	B_1	B_2	Ref.	Solvent	Force constants (m.dyne/Å) cisA	cisB	trans	K_1	K_2	A_1^2 calc(cm^{-1})	ΔA_1^2(cm^{-1})
$Mo(CO)_4$dth(2)	2030	1919	1905	1868	263	$CHCl_3$	0.40			14.50	15.46	1897	-22
							0.37	0.60	0.79	14.69	15.44		
							0.38	0.49	0.81	14.58	15.46	1908	-11
$W(CO)_4$dth(1)	2016	1906	1891	1874	249	CS_2	0.38			14.57	15.22	1898	-8
							0.33	0.40	0.83	14.58	15.27		
							0.34	0.43	0.82	14.61	15.26	1908	2
$W(CO)_4$dth(2)	2023	1910	1896	1867	263	$CHCl_3$	0.40			14.48	15.32	1894	-16
							0.37	0.52	0.82	14.59	15.33		
							0.37	0.47	0.83	14.54	15.34	1905	-5
$Cr(CO)_4$mtb	2025	1921	1906	1889	264	C_6H_{12}	0.37			14.78	15.42	1912	-9
							0.32	0.40	0.79	14.81	15.46		
							0.32	0.41	0.79	14.82	15.46	1922	1
$Mo(CO)_4$mtb	2031	1925	1913	1895	264	C_6H_{12}	0.37			14.87	15.52	1918	-7
							0.32	0.38	0.79	14.88	15.57		
							0.32	0.41	0.78	14.92	15.56	1928	3
$W(CO)_4$mtb	2027	1917	1904	1892	264	C_6H_{12}	0.38			14.84	15.40	1914	-3
							0.32	0.33	0.84	14.78	15.48		
							0.32	0.41	0.82	14.87	15.46	1924	7

Table 7-2 (Contd.)

Complex[b]	$\nu_{CO}(cm^{-1})$ A_1^1	A_1^2	B_1	B_2	Ref.	Solvent	Force constants (m.dyne/Å) cisA	cisB	trans	K_1	K_2	A_1^2 calc(cm^{-1})	ΔA_1^2(cm^{-1})
$Cr(CO)_4$mtn	2023	1920	1905	1881	264	C_6H_{12}	0.35			14.64	15.43	1906	-14
							0.36	0.47	0.76	14.76	15.42		
							0.36	0.43	0.77	14.72	15.43	1916	-4
$Mo(CO)_4$mtn	2030	1923	1913	1885	264	C_6H_{12}	0.38			14.72	15.53	1910	-13
							0.34	0.47	0.76	14.81	15.54		
							0.34	0.49	0.75	14.83	15.53	1925	2
$W(CO)_4$mtn	2025	1915	1905	1882	264	C_6H_{12}	0.38			14.72	15.41	1910	-5
							0.34	0.41	0.79	14.72	15.45		
							0.34	0.43	0.79	14.74	15.44	1917	2
$Cr(CO)_4$pse	2015	1900	1900	1860	265	$CHCl_3$	0.37			14.34	15.32	1887	-13
							0.36	0.49	0.73	14.46	15.31		
							0.36	0.47	0.72	14.44	15.31	1898	-2
$Mo(CO)_4$pse	2012	1900	1900	1864	265	$CHCl_3$	0.36			14.39	15.30	1890	-10
							0.35	0.44	0.72	14.47	15.29		
							0.35	0.44	0.72	14.47	15.29	1900	0
$W(CO)_4$pse	2017	1900	1900	1870	265	$CHCl_3$	0.37			14.50	15.33	1896	-4
							0.34	0.38	0.77	14.50	15.35		
							0.35	0.44	0.76	14.56	15.34	1906	6

* see footnotes to Table 1.

Table 7-3. Force constants* cis-$M(CO)_4L_2$ complexes (L = Group VII donor ligand).

Complex[b]	$\nu_{CO}(cm^{-1})$ A_1^1	A_1^2	B_1	B_2	Ref.	Solvent	Force constants (m.dyne/Å) cisA	cisB	trans	K_1	K_2	A_1^2 calc(cm^{-1})	ΔA_1^2(cm^{-1})
$[Mn(CO)_4Br_2]^-$	2089	1987	2013	1942	266	$CHCl_3$	0.27			15.50	16.91	1966	-2
							0.35	0.55	0.44	15.78	16.80		
							0.36	0.46	0.46	15.69	16.82	1978	-9
$[Mn(CO)_4I_2]^-$	2078	1983	2004	1941	266	$CHCl_3$	0.26			15.48	16.75	1964	-19
							0.33	0.51	0.43	15.73	16.65		
							0.33	0.43	0.45	15.64	16.66	1974	-9
$[Re(CO)_4I_2]^-$	2108	1980	2000	1925	267	$CHCl_3$	0.38			15.35	16.92	1957	-23
							0.44	0.67	0.66	15.64	16.81		
							0.45	0.57	0.68	15.53	16.83	1971	-9
$Fe(CO)_4Cl_2$	2164	2108	2124	2084	268	$CHCl_3$	0.15			17.69	18.52	2097	-11
							0.20	0.31	0.24	17.85	18.45		
							0.21	0.26	0.25	17.80	18.46	2103	-5
$Fe(CO)_4Br_2$	2148.5	2097.2	2106.7	2073.8	268	Hexane	0.15			17.52	18.23	2086.3	-10.9
							0.19	0.30	0.26	17.67	18.18		
							0.19	0.24	0.27	17.61	18.19	2091.7	-5.5

Table 7-3. (Contd)

Complex[b]	$\nu_{CO}(cm^{-1})$ A_1^1	A_1^2	B_1	B_2	Ref.	Solvent	Force constants (m.dyne/Å) cisA	CisB	trans	K_1	K_2	A_1^2 calc(cm^{-1})	ΔA_1^2(cm^{-1})
$Fe(CO)_4I_2$ (1)	2128.8	2083.5	2083.5	2060.3	268	Hexane	0.16			17.30	17.85	2072.2	-11.3
							0.17	0.29	0.29	17.43	17.82		
							0.17	0.22	0.30	17.36	17.83	2076.7	-6.8
$Fe(CO)_4I_2$ (2)	2131	2085	2087	2062	269	Hexane	0.16			17.33	17.91	2074	-11
							0.17	0.29	0.28	17.46	17.87		
							0.18	0.22	0.29	17.39	17.88	2079	-6
$Ru(CO)_4I_2$	2160	2095	2106	2067	269	Hexane	0.20			17.45	18.31	2083	-12
							0.24	0.36	0.34	17.62	18.25		
							0.24	0.30	0.35	17.56	18.26	2089	-6
$Os(CO)_4Br_2$	2178	2090	2113	2051	270	C_6H_{12}	0.25			17.23	18.52	2072	-18
							0.32	0.50	0.39	17.49	18.42		
							0.33	0.41	0.41	17.40	18.44	2082	-8
$Os(CO)_4I_2$	2163	2085	2100	2050	269	Hexane	0.23			17.20	18.28	2069	-16
							0.28	0.45	0.39	17.42	18.20		
							0.29	0.36	0.40	17.34	18.21	2077	-8

* see footnote to table 1.

Ligands may be divided into two broad classes; those with only σ-bonding capabilities and those with both σ- and π-bonding properties. The extent of σ-donation by a particular set of monodentate ligands, such as amines, to any particular metal should, to a first approximation, be related to the ligands basicity (pK_a). As the ligands pK_a value is strictly a measure of the interaction between the ligand and a proton there may well be cases where steric considerations cause apparent anomalies in the M - L bond strength. When a polydentate ligand is involved there are two additional complications. Whereas the ligand basicities are normally quoted as monobasic species, an n-dentate ligand should be considered as an n-basic base and, secondly, any strain (angular distortion) in the chelate ring will cause a weakening of the M - L bond. This makes it difficult to compare systems involving polydentate ligands unless their chelate rings are of the same size and rigidity.

It is to be expected that as the σ-donation from the ligand to the metal increases there will be an increase of electron density on the metal, which must at least partially be communicated to the carbonyl carbon atoms. Hall and Fenske[271] have shown that this increase in electron density at the carbonyl carbon atom will cause a decrease in the CO stretching force constant, irrespective of whether the transfer of electron density is <u>via</u> the M - C σ- or π-molecular orbitals. Hence, as the basicity of the ligand increases the CO stretching force constants (K_1 and K_2) should decrease.

When the ligand enters into M - L π-back bonding there will normally be a lessening of the electron density on the metal which should result in a relative increase in the CO stretching force constants. It has been stated[249,272] that this back-bonding for ligands with the following donor atoms decreases in the order $P \geqslant As > S > N$. Inspection of Tables 7-1 and 7-2 reveal that K_1 and K_2 give rise to the order $P \sim As \geqslant S > N$ for complexes with the relevant donor atoms, which is in agreement with the expected π-acidity of the ligands. Phosphorus, arsenic and sulphur donor ligands gave rise to fairly similar CO stretching force constants but nitrogen donor ligands clearly gave rise to smaller force constants as expected due to the lack of suitable π-acceptor orbitals on nitrogen.

The carbonyl force constants should also be influenced by the central metal atom. For the parent hexacarbonyls the M - C bond properties vary as follows:

M - C σ- bond strength[252] W > Mo > Cr

M - C π- bond strength[273-75] W > Mo > Cr

Inspection of Tables 7-1 and 7-2 suggested that for non-π-bonded ligands the CO stretching force constants decrease in the order Mo > Cr > W, thus suggesting the electron density on the carbonyl carbon atoms[271] to decrease in the order W > Cr > Mo. All three methods of calculation lead to this overall order, although the new procedure is the most consistent in terms of both K_1 and K_2.

If it is assumed that the metals in these substituted carbonyl complexes retain the same relative bonding properties as in the parent hexacarbonyls, then it is difficult to explain the calculated force constants in terms of σ- and π-bonding changes. However, it is encouraging that the CO stretching force constants calculated for these cis-$L_2M(CO)_4$ species lie in the same order as that found for the parent hexacarbonyls[273-276].

Consideration of the M - C σ-bonding in the parent hexacarbonyls would lead to the electron density on the carbonyl carbon atom decreasing in the order Cr>Mo>W. Whereas consideration of the M - C π-back-bonding would have the opposite effect on the electron density, i.e. the electron density on the carbonyl carbon atom would decrease in the order W>Mo>Cr. Based on the calculated force constants the electron density for the carbonyl carbon atoms in the complexes $M(CO)_6$ and cis-$L_2M(CO)_4$ appear to lie in the order W>Cr>Mo. If as is usually assumed these CO stretching force constants reflect the extent of M - C π-back bonding and that the σ-bonding is essentially constant, then the force constants, and the electron densities, for the metals chromium and molybdenum appear to be interchanged. One possible way to account for this interchange is to assume that there is a much weaker σ-bond in the chromium complexes than in the molybdenum complexes (i.e. the M - C σ-bond strength decreases in the order W>Mo≫Cr). This would lead to there being proportionally more electron density on the carbonyl carbon atoms of the chromium species, and possible lead to the orders given above for the CO stretching force constants (i.e. Mo>Cr>W) and the electron density on the carbonyl carbon atom (i.e. W>Cr>Mo).

Probably the most important point to be shown by these comparisons is that the relationship between the CO stretching force constants and the M - C bond properties is rather complicated.

7.5 The predicted band shift and graph theory

Simple graph theory shows that when two bands overlap (Figure 7-5) the two maxima tend to move towards each other (i.e. the observed separation is less than the actual separation for the band maxima). Hence consideration of a typical cis-$L_2M(CO)_4$

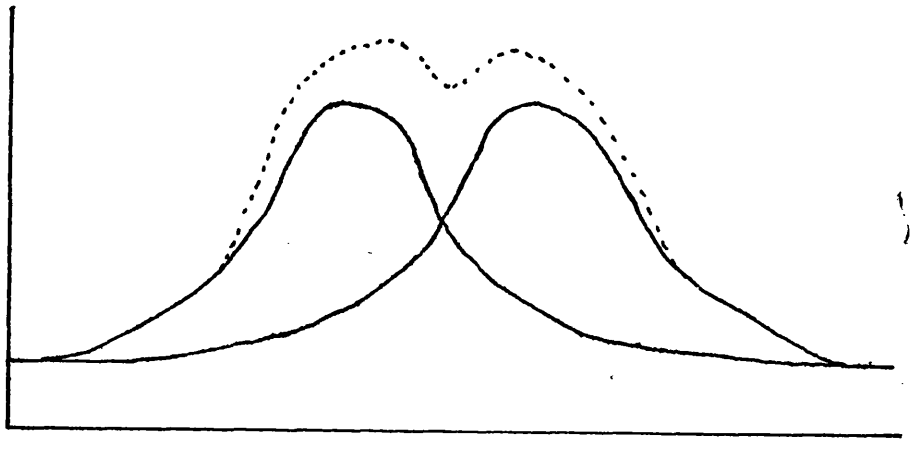

Figure 7-5. The addition of overlapping bands.

spectrum (Figure 7-6) shows that the A_1^2 and B_1 bands should move apart on deconvolution. As the A_1^2 band is the weaker of this pair, its position should move more than the B_1 band, and therefore it is usually assumed that the B_1 band position is as observed whilst the A_1^2 band position is taken to be uncertain. The A_1^2 and B_1 band positions may of course be interchanged (as in phosphine complexes) or even accidently degenerate [e.g. $FeI_2(CO)_4$],

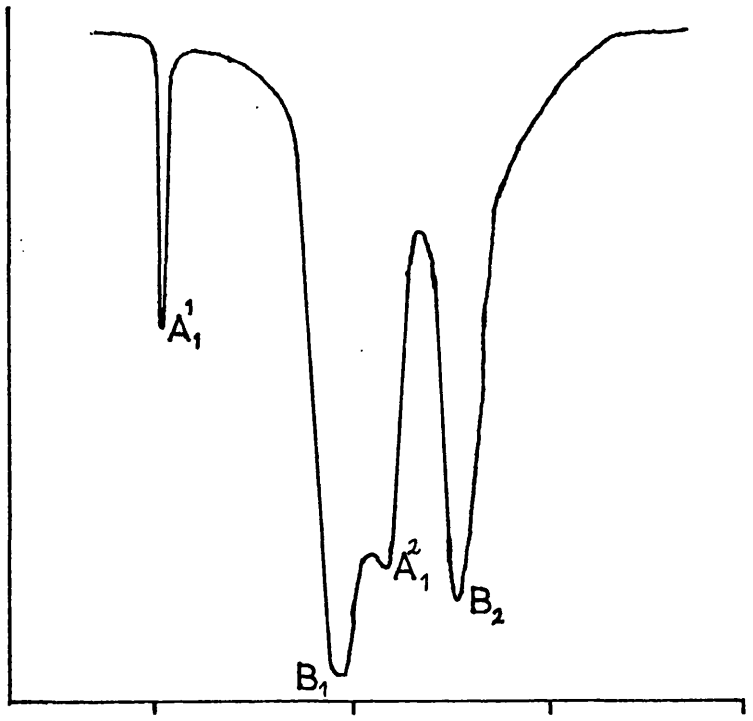

Figure 7-6. Infra-red spectrum of a typical cis-$L_2M(CO)_4$ complex.

but in each case the intensities[277] should still be B_1 greater than $A_1{}^2$. The $A_1{}^1$ and B_2 band positions will also be subject to small uncertainties but very much less than the $A_1{}^2$ band, hence the $A_1{}^1$ and B_2 band positions are usually taken to be as observed.

Inspection of tables 7-1 to 7-3 shows that in the majority of cases (i.e. 52 out of 72 examples) the band shift predicted by the new procedure is in agreement with graph theory. The other methods (i.e. Cotton's[204] and Jernigan's[249]) do not consistently predict this greater separation of the $A_1{}^2$ and B_1 bands.

7.6. Contrary band shifts

Inspection of Tables 7-1 to 7-3 reveals that the following ligands lead to abnormal band shifts in at least some of their complexes: MeCN(Cr and W), en(Cr, Mo and W),py(Cr, Mo and W), dppe(Cr,W[2], Ta and Re), dpsp(Cr, Mo and W), dth(Cr[1 and 2], Mo[2] and W [2]) and mtn(Cr). Some of these ligands lead to a lowering of the C_{2v} symmetry of the $M(CO)_4$ grouping, and consequently Cotton's secular equations[204] are not strictly applicable in these cases.

In the following sections these anomolous shifts will be discussed in terms of the symmetry of the complexes, which in many cases will involve buckled chelate rings. Many of these chelate rings will give rise to fluxional behaviour in solution and on the n.m.r. time scale may appear to have a time averaged C_{2v} symmetry. However, the absorption of infra-red radiation is a far more rapid process and the absolute molecular symmetry rather than the time averaged symmetry, will be observed.[278]

7.6.1 The pyridine complexes

Consideration of the ligand pyridine reveals three possible geometries for the complexes, cis-$py_2M(CO)_4$ (Figure 7-7).

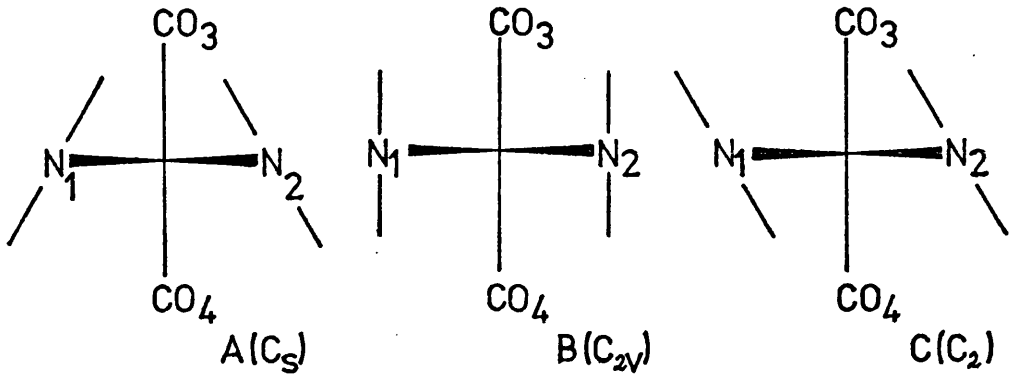

Figure 7-7. Possible inclinations of the pyridine rings in $M(CO)_4py_2$

Cotton[70] suggested that co-ordinated pyridine molecules do not align their aromatic rings with the x, y or z planes of a carbonyl complex, hence structures A or C seem the most likely for $M(CO)_4py_2$ complexes.

Assuming C_s symmetry (Figure 7-7, A) the molecule would give rise to three A' and one A" mode (cf. the appendix) for the CO stretching vibrations (Figure 7-8, I). The three A' modes

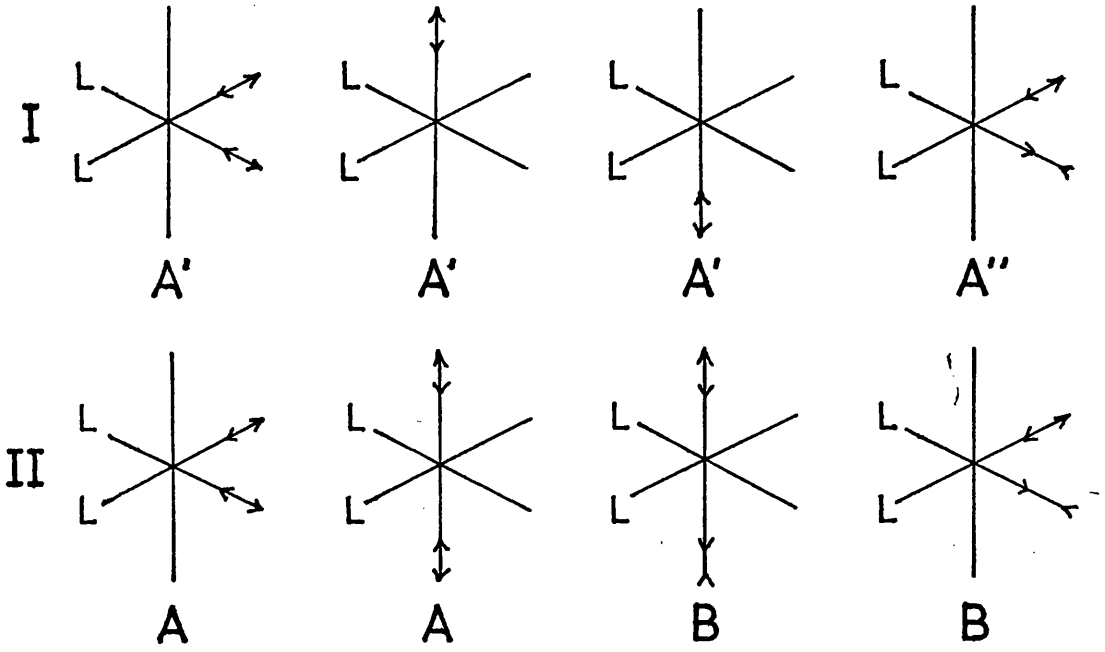

Figure 7-8. Vibrational modes for $M(CO)_4L_2$ species, I under C_s and II under C_2 symmetry.

may couple and the C_s system can be represented by the following secular equations.

(The terminology is given in Figure 7-9, I):

$$3A' \quad \begin{vmatrix} \mu(K_1 + \text{cisB}) - \lambda & \sqrt{2}\,\mu\,\text{cisA}_1 & \sqrt{2}\,\mu\,\text{cisA}_2 \\ \sqrt{2}\,\mu\,\text{cisA}_1 & \mu K_2 - \lambda & \mu\,\text{trans} \\ \sqrt{2}\,\mu\,\text{cisA}_2 & \mu\,\text{trans} & \mu K_3 - \lambda \end{vmatrix} = 0$$

$$A'' \quad \lambda = \mu(K_1 - \text{cisB})$$

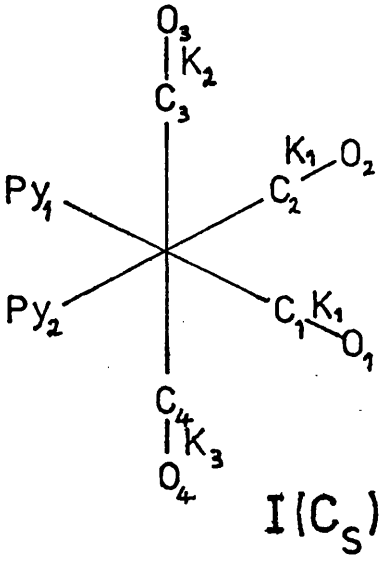

I (C_s)

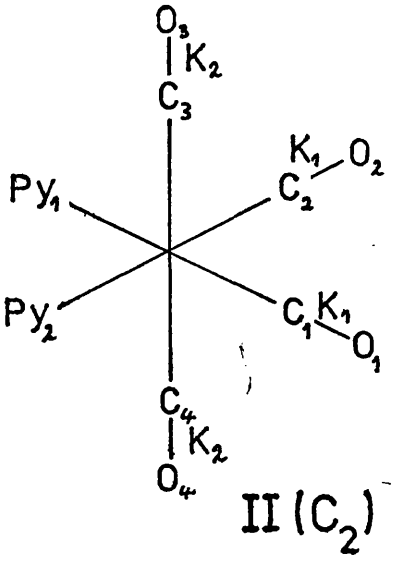

II (C_2)

Interaction force constants:

CO_1	with CO_2	cisB	cisB
CO_1	with CO_3	cisA_1	cisA_1
CO_1	with CO_4	cisA_2	cisA_2
CO_2	with CO_3	cisA_1	cisA_2
CO_2	with CO_4	cisA_2	cisA_1
CO_3	with CO_4	trans	trans

Figure 7-9 Force constants and terminology used for $M(CO)_4py_2$

Inspection of these secular equations show there to be seven unknowns and only four observable values, thus the problem is insoluble without making at least three approximations. Two obvious approximations are to let $cisA_1$ equal $cisA_2$ and K_2 equal K_3, this then reduces to the same problem as the other C_{2v} complexes but with even less rigour.

If the complex adopts a C_2 symmetry (Figure 7-7, C) it will give rise to two A and two B modes for the CO stretching vibrations (Figure 7-8, II). As before modes of the same symmetry may couple which leads to the following secular equations (see figure 7-9, II for terminology):

$$2A \quad \begin{vmatrix} \mu(K_1 + cisB) - \lambda & \mu(cisA_1 + cisA_2) \\ \mu(cisA_1 + cisA_2) & \mu(K_2 + trans) - \lambda \end{vmatrix} = 0$$

$$2B \quad \begin{vmatrix} \mu(K_1 - cisB) - \lambda & \mu(cisA_1 - cisA_2) \\ \mu(cisA_1 - cisA_2) & \mu(K_2 - trans) - \lambda \end{vmatrix} = 0$$

Inspection of these secular equations show there to be six unknowns and only four observable values, hence two approximations are required in order to solve this problem. By making the approximation $cisA_1$ equals $cisA_2$ this problem reduces to the C_{2v} case but again with less rigour.

It would appear that all cis - $L_2M(CO)_4$ complexes may be analysed by the Cotton secular equations,[204] but with decreasing rigour as the symmetry is lowered from C_{2v}. Strictly the Cotton secular equations should only be applied to the halo-complexes (Table 7-3) as all the other complexes will depart, to some extent, from C_{2v} symmetry, but fortunately the majority of complexes studied seem to approximate fairly well to the higher symmetry case.

7.6.2 Five membered chelate rings

A saturated five membered chelate ring will tend to buckle (Figure 6-10) in order to relieve the angle distortion at the sp^3 carbon atoms. Thus buckling reduces the symmetry of the

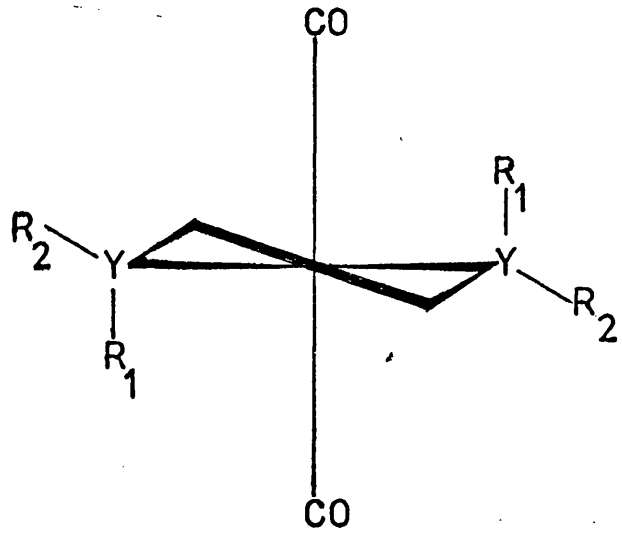

Figure 7-10. Buckling of five membered chelate rings.

$M(CO)_4L_2$ species to C_2 and the secular equations given for the C_2 isomer of $M(CO)_4py_2$ would also apply here.

The ligands en and dppe, which fail to give the normal band shifts, fall into this category and consequently the calculated force constants have even less rigour than usual. It is perhaps surprising that the ligands tmen, dmpe and pse do not lead to anomalous band shifts as these ligands also give rise to saturated five membered chelate rings.

When the donor atom is a group 6A element (e.g. sulphur in dth) the situation is further complicated as R_1 and R_2 (Figure 7-10) are no longer equivalent (e.g. R_1 = Me and R_2 is a lone pair of electrons for dth). Hence there is the possibility of cis-(axial, equatorial-) or trans- (axial, axial- or equatorial, equatorial-) isomerism in these complexes, where the terms cis- and trans- are relative to the SMS plane (i.e. the YMY plane in figure 7-10). The two trans-isomers will both have C_2 symmetry (cf. the secular equations for C_2 - $M(CO)_4py_2$), whilst the cis-isomer will have C_1 symmetry and, therefore, give rise to four A modes for the CO stretching vibrations (Figure 7-11). These four vibrational modes may

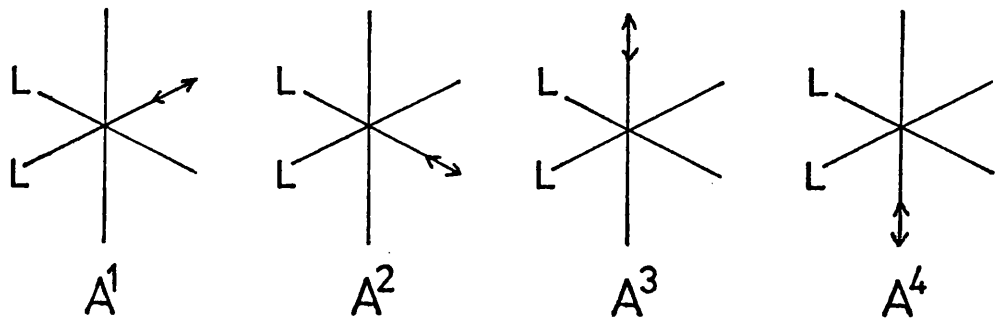

Figure 7-11 Vibrational modes for C_1-$M(CO)_4L_2$ complexes

couple with each other and can be represented by the following secular equations (see Figure 7-12 for terminology):

$$\hat{4}A \quad \begin{vmatrix} \mu K_1 - \lambda & \mu cisB & \mu cisA_1 & \mu cisA_2 \\ \mu cisB & \mu K_2 - \lambda & \mu cisA_3 & \mu cisA_4 \\ \mu cisA_1 & \mu cisA_3 & \mu K_3 - \lambda & \mu trans \\ \mu cisA_2 & \mu cisA_4 & \mu trans & \mu K_4 - \lambda \end{vmatrix} = 0$$

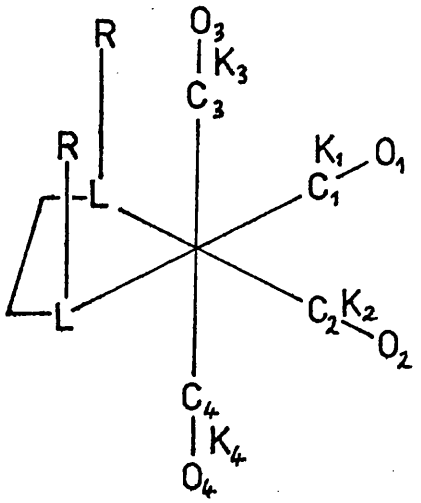

Interaction force constants:

CO_1 with CO_2 = cisB

CO_1 " CO_3 = $cisA_1$

CO_1 " CO_4 = $cisA_2$

CO_2 " CO_3 = $cisA_3$

CO_2 " CO_4 = $cisA_4$

CO_3 " CO_4 = trans

Figure 7-12. Terminology used for C_1 - $M(CO)_4L_2$ complexes

As can be seen from these secular equations there are ten unknown variables and consequently at least six approximations are required to solve this problem.

Inspection of Table 7-2 shows that the dth complexes of molybdenum and tungsten give rise to normal and abnormal band shifts depending on which set of data is processed. This shows above all, and as stated by Orgel[277], the importance of using accurate band positions in the calculation of force constants.

7.6.3 Six-membered chelate rings

A saturated six-membered chelate ring can be thought of in much the same way as a cyclohexane molecule. Hence the chelate ring will tend to buckle so as to give a chair or a boat conformation, with the chair form generally being stereochemically more likely. Thus $M(CO)_4L_2$ complexes which contain six-membered chelate rings should possess C_s symmetry, with the mirror plane bisecting this ring and containing the pair of mutually trans-carbonyl groups. This C_s symmetry may of course be lowered by the groups attached to the donor atoms.

The ligand dpsp, which gives rise to anomalous band shifts, belongs to this category and consequently should be analysed by the secular equations given for the C_s isomer of $M(CO)_4py_2$.

7.6.4 Unsaturated chelate rings

Where the ligand forming the chelate ring is extensively conjugated (e.g. $acac^-$ or bipy) the chelate ring will tend to be planar, and so the complex $M(CO)_4L_2$ may retain its C_{2v} symmetry. Even where the conjugation does not extend to the co-ordinating atom (e.g. the ortho-phenylene type ligands such as diars) the chelate ring may still tend to be planar.

For the o-phenylene type ligands with a group 6A donor atom (e.g. sulphur in mtb) the situation is again complicated by the possibility of cis-, trans-isomerism leading to C_s or C_2 symmetry respectively. Thus the secular equations given for the pyridine complexes should be used in these cases.

The solid state molecular structure of $Cr(CO)_4$mtb has been determined[264] and the two methyl groups lie on the same side of the SCrS plane (i.e. the cis-isomer) giving rise to C_s symmetry for the molecule.

Inspection of Table 7-2 reveals that for the complex $Cr(CO)_4$mtn the predicted band shift is contrary to graph theory and this may possibly be accounted for by the lowering of the symmetry as discussed above, although the complex $Cr(CO)_4$mtb seems to give the normal band shift even though it is known to have only C_s symmetry in the solid state.[264]

Hence, for all except two of the complexes in Tables 7-1 to 7-3 [i.e. $M(CO)_4(MeCN)_2$; M = Cr or W], it would appear that predicted band shifts which are contrary to graph theory may be accounted for on symmetry grounds. However, the lack of C_{2v} symmetry does not always lead to anomalous band shifts. The two exceptions, $Cr(CO)_4(MeCN)_2$ and $W(CO)_4(MeCN)_2$, would be expected to be fairly close to C_{2v} symmetry, and except for possible uncertainties in the observed band positions, no explanation can be offered for the anomalous band shifts for these complexes.

7.7 Deconvoluted spectra

Hyde and Darensbourg[256] have recently used a Cauchy-Gauss procedure to deconvolute the observed infra-red spectra of cis-$L_2M(CO)_4$ complexes. Whilst the observed CO stretching vibrational band positions were not given for every complex

studied, making it impossible in many cases to discuss the calculated band shifts, the calculated band positions can still be used in the various procedures for calculating force constants.

In the three cases where Hyde and Darensbourg[256] quoted both the observed and the calculated band positions, the band shifts are in agreement with graph theory with the exception of the B_2 band which moves to slightly higher wavenumbers in each case.

Consideration of the complex $W(CO)_4$bipy (Labelled [2] in Table 7-1) shows very good agreement between Hyde and Darensbourg's calculated value for the A_1^2 band position[256] and the band position predicted by the new procedure, the difference being 1.1 cm^{-1}. Unfortunately such good agreement was not obtained for the complexes $W(CO)_4$tmen and $W(CO)_4$dppe (labelled [2] and [3] respectively in Table 7-1).

As these authors[256] have quoted both the calculated and the observed spectral data for the complex $W(CO)_4$tmen it is possible to discuss this example further. From Table 7-4 and using the intensity criteria stated earlier (i.e. $B_1 > A_1^2$)[277] there is a discrepancy between the assignments arrived at for the observed and calculated spectra. The calculated intensities lead to the assignment stated by Hyde and Darensbourg (i.e. The band positions lie in the order $A_1^1 > A_1^2 > B_1 > B_2$) whereas the observed band intensities would lead to an interchange of the assignments for the A_1^2 and B_1 modes. On applying the C - K

Table 7-4

Comparison of the observed and calculated infra-red spectra of $W(CO)_4$tmen

ν_{CO}[a] (cm^{-1})				Force constants[b] (mdyne/Å)					A_1^2(calc)	ΔA_1^2
A_1^1	A_1^2	B_1	B_2	cisA	cisB	trans	K_1	K_2	(cm^{-1})	(cm^{-1})
2007.8[c]	1876.0	1859.0	1820.5	0.47			13.85	14.89	1853.4	-22.6
	(0.322)	(0.303)	(0.219)	0.43	0.64	0.93	14.03	14.89		
				0.43	0.55	0.95	13.94	14.91	1866.6	- 9.4
2007.8[c]	1859.0	1876.0	1820.5	0.43			13.81	15.07	1854.0	- 5.0
				0.43	0.48	0.84	13.86	15.05		
				0.43	0.55	0.82	13.94	15.04	1866.2	7.2
2007.8[d]	1880.0	1861.3	1821.1	0.46			13.86	14.92	1854.0	-26.0
	(0.189)	(0.239)	(0.160)	0.43	0.67	0.91	14.07	14.90		
				0.43	0.55	0.93	13.99	14.92	1866.9	-13.1
2007.8[d]	1861.3	1880.0	1821.1	0.42			13.81	15.11	1854.5	- 6.8
				0.43	0.50	0.81	13.89	15.08		
				0.43	0.55	0.79	13.94	15.07	1866.5	5.2

a) Values in parenthesis are the absorbances at the band maximum

b) Force constants are presented in the order Cotton, Jernigan and the new procedure.

c) Observed band positions (ref. 256)

d) Calculated band positions (ref. 256).

procedure[204] to the analysed spectrum of $W(CO)_4$tmen it was found that both assignments were acceptable (i.e. $K_2 > K_1$ with a real and positive interaction constant) but the assignment used by Hyde and Darensbourg (i.e. A_1^2 = 1880.0 and B_1 = 1861.3cm^{-1}) gave a slightly less acceptable value for the C - K predicted band position. The new procedure would also favour the assignment predicted by the C - K approach (A_1^2 = 1861.3 and B_1 = 1880.0 cm^{-1}), although the agreement for the A_1^2 band position is not very good for either assignment. It is interesting to note that both the C - K and the new procedures agree with the $M(CO)_4$tmen assignments given elsewhere (M = Mo[27] and M = Cr, Mo, W[249]) even though these still have band positions in the order $A_1^2 \geqslant B_1$. It is possible, therefore, that the above calculated values for $W(CO)_4$tmen are in error, but it must also be borne in mind that each worker[27,249,256] used a different solvent and that there may be some unexpected solvent interactions. These various $M(CO)_4$tmen spectra are summarised in table 7-1 and possibly warrant further careful study.

7.8 The ratios cisB/cisA and trans/cisA

During the calculation of force constants by the new procedure (Tables 7-1 to 7-3) it was found that the value of X(cisB/cisA) was surprisingly constant, with the limits of 1.26 and 1.28. The ratio Y (trans/cisA) was far more variable lying in the range 1.38 to 2.84. However, it has already been argued (Section 7.2.1) that the ratio Y need not necessarily be constant, but at the same time there is no obvious reason why X should be constant.

Partial differentiation of the secular equations failed to show any mathematical reason for this near constant value of X, and simple molecular orbital theory or the Jones[240] procedure, both applied only to the π-bonding framework, suggest that X should be a variable (Section 7.2.1).

Unfortunately the variation in X is as large for the same complex, using data from different sources, as it is between various complexes. Hence at this stage, and without a detailed statistical analysis of a large number of samples, it is not possible to say whether the ratio X is connected with any particular molecular property.

7.9 Comparison of the ligands dpa, adpa and bdpa

Consideration of Tables 7-1 to 7-3 reveal that the most favourable complexes for comparison should be those containing the ligands dpa, adpa and bdpa as these species are most likely to have the same size and similar rigidity for their chelate rings. The electron releasing properties of the N - R group (where R is hydrogen, acetyl or benzoyl) in these ligands should lead the basicity of the heterocyclic nitrogen atoms to decrease in the order dpa > bdpa > adpa. Thus it should follow that the CO stretching force constants decrease in the reverse order, i.e. adpa > bdpa > dpa. Inspection of Table 7-5, which summarises the relevant data, reveals that there is no single order for the force constants; but the two most frequently observed orders are adpa > bdpa > dpa (K_1 for Cr and Mo by each of the three procedures), which is as predicted above, and bdpa > adpa > dpa (K_1 and K_2 for W by each of the three procedures).

Table 7-5

CO stretching force constants for the complexes dpa-, adpa- and bdpa $M(CO)_4$

Complex	Force constants mdyne/Å					
	K_1^a	K_2^a	K_1^b	K_2^b	K_1^c	K_2^c
$Cr(CO)_4$dpa	13.76	15.20	14.00	15.11	13.93	15.12
$Cr(CO)_4$adpa	13.98	15.18	14.19	15.12	14.11	15.13
$Cr(CO)_4$bdpa	13.95	15.11	14.07	15.07	14.07	15.07
$Mo(CO)_4$dpa	13.76	15.26	14.00	15.16	13.94	15.17
$Mo(CO)_4$adpa	13.99	15.25	14.17	15.18	14.12	15.19
$Mo(CO)_4$bdpa	13.93	15.23	14.12	15.16	14.09	15.16
$W(CO)_4$dpa	13.70	15.10	13.91	15.01	13.86	15.03
$W(CO)_4$adpa	13.93	15.11	14.07	15.06	14.05	15.06
$W(CO)_4$bdpa	13.99	15.15	14.18	15.09	14.11	15.10

a) Calculated by the C - K approach

b) Calculated by the Jernigan approach

c) Calculated by the new procedure.

Whilst this lack of consistency in the ordering of the force constants is disappointing it has already been suggested (Section 7.2.1) that the MCO bonding is rather complex and it may be that the predictions were based on too simple a model, or that tungsten differs significantly from the other two metals in these complexes. It is known that the geometry of the acyclic nitrogen atom in these ligands can vary from pyramidal to planar[65-67] depending on the electronic and steric requirements of the whole complex. Any change in this geometry would also create differences in the M - L bond strengths and consequently modify the CO stretching force constants.

7.10 Comparison of the ligands bipy and dpa

During the chemical comparison of the ligands bipy and dpa it was observed that for the species $Mo(CO)_4L_2$ (L_2 = dpa or bipy) a carbonyl group was far more readily replaced when L_2 was dpa rather than bipy to yield a facial-tricarbonyl complex, (Chapter 5). It was hoped that the CO stretching force constants would predict this behaviour. The relevant force constants, calculated by all three procedures, are given in Table 7-6.

It was also observed that bipy would displace dpa from its complexes (Chapter 6) which indicated that bipy must form thermodynamically more stable complexes than dpa. This is also substantiated by the reaction of the dicarbonyl complexes $[MoCl(\eta^3\text{-allyl})(CO)_2L_2]$ with Nasalal which displaces dpa but not bipy (Chapter 4).

Table 7-6

CO stretching force constants for bipy- and dpaM$(CO)_4$

Complex	Force constants mdyne Å^{-1}					
	K_1^a	K_2^a	K_1^b	K_2^b	K_1^c	K_2^c
$Cr(CO)_4$dpa	13.76	15.20	14.00	15.11	13.93	15.12
$Cr(CO)_4$bipy	13.86	15.38	14.11	15.28	14.04	15.29
$Mo(CO)_4$dpa	13.72	15.26	14.00	15.16	13.94	15.17
$Mo(CO)_4$bipy	13.88	15.45	14.10	15.35	14.07	15.36
$W(CO)_4$dpa	13.70	15.10	13.81	15.01	13.86	15.03
$W(CO)_4$bipy	13.84	15.31	14.03	15.23	14.01	15.23

a) Calculated by the C - K procedure

b) Calculated by the Jernigan procedure

c) Calculated by the new procedure

Comparison of the force constants K_1 and K_2 (Table 7-6) indicates a greater electron density on the carbonyl carbon atoms of the dpa complexes relative to the bipy complexes. This was shown by all three procedures and indicates that dpa is probably the stronger base towards the metals chromium molybdenum and tungsten, which is supported by the literature pK_a values (dpa, $pK_a = 6.99$[57] and bipy, $pK_a = 4.44$[69]). It is difficult to predict which set of complexes will have the stronger M - C bond due to the synergic nature of this bond but the π-interaction model which is a gross over simplification, would suggest that the stronger the base the stronger will be the

M - C bond. Hence, dpa might give rise to stronger M - C bonds than bipy.

Dobson and Memering[279] have carried out a kinetic study of the reaction:

$M(CO)_4bipy + L \longrightarrow M(CO)_3Lbipy + CO$ (M = Mo or W: L = Lewis base)

and their results suggest that the reaction proceeds by three separate routes as outlined below (N - N represents bipy). If it is assumed that

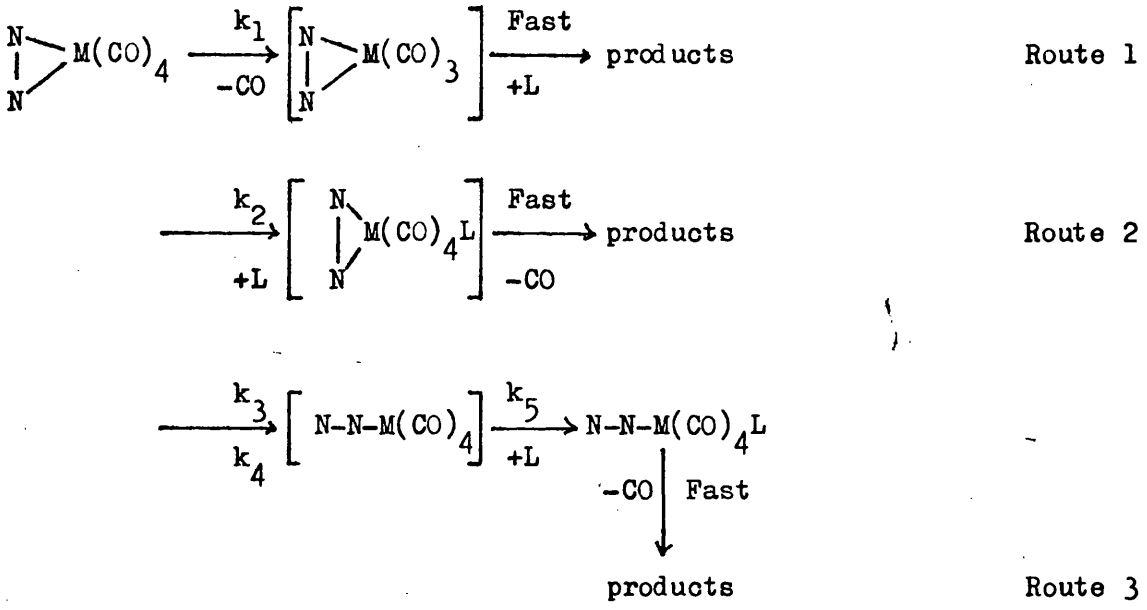

the reaction scheme for $M(CO)_4dpa + L$ is similar to that for the bipy reaction, then routes 1 to 3 may be used to rationalise the chemical observations mentioned earlier.

Route 1 will be favoured if the M - C bond is weakened by L_2, whilst routes 2 and 3 will be promoted by a decrease in the electron density on the metal. Route 3 will also be favoured by a weak M - L bond and a flexible N - N system.

As dpa creates more electron density on the metal than does bipy, routes 1, 2 and 3 all become less favourable for dpa complexes on purely electronic grounds. But due to the presence of the exo-cyclic NH group, the ligand dpa is more flexible than bipy, consequently routes 2 and 3 may be enhanced by dpa on steric grounds.

In summary it would appear that the electronic and steric factors work in opposition and, from the observed chemistry of these ligands, it would seem that the steric considerations are of greater importance in determining the reactivity of these particular complexes.

7.11 Comparison of force constants within an isoelectronic series

Inspection of the complexes $[M(CO)_4dppe]^n$ (M = W, Re or Ta and n = 0, 1 or -1 respectively) in table 7-1 reveals that as the negative charge on the complex increases, the CO stretching force constants decrease (Figure 7-13). All three methods of calculation prove satisfactory in showing this trend; and hence for comparisons involving large differences in force constants, the C - K method (which is the simplest to apply) is perfectly adequate.

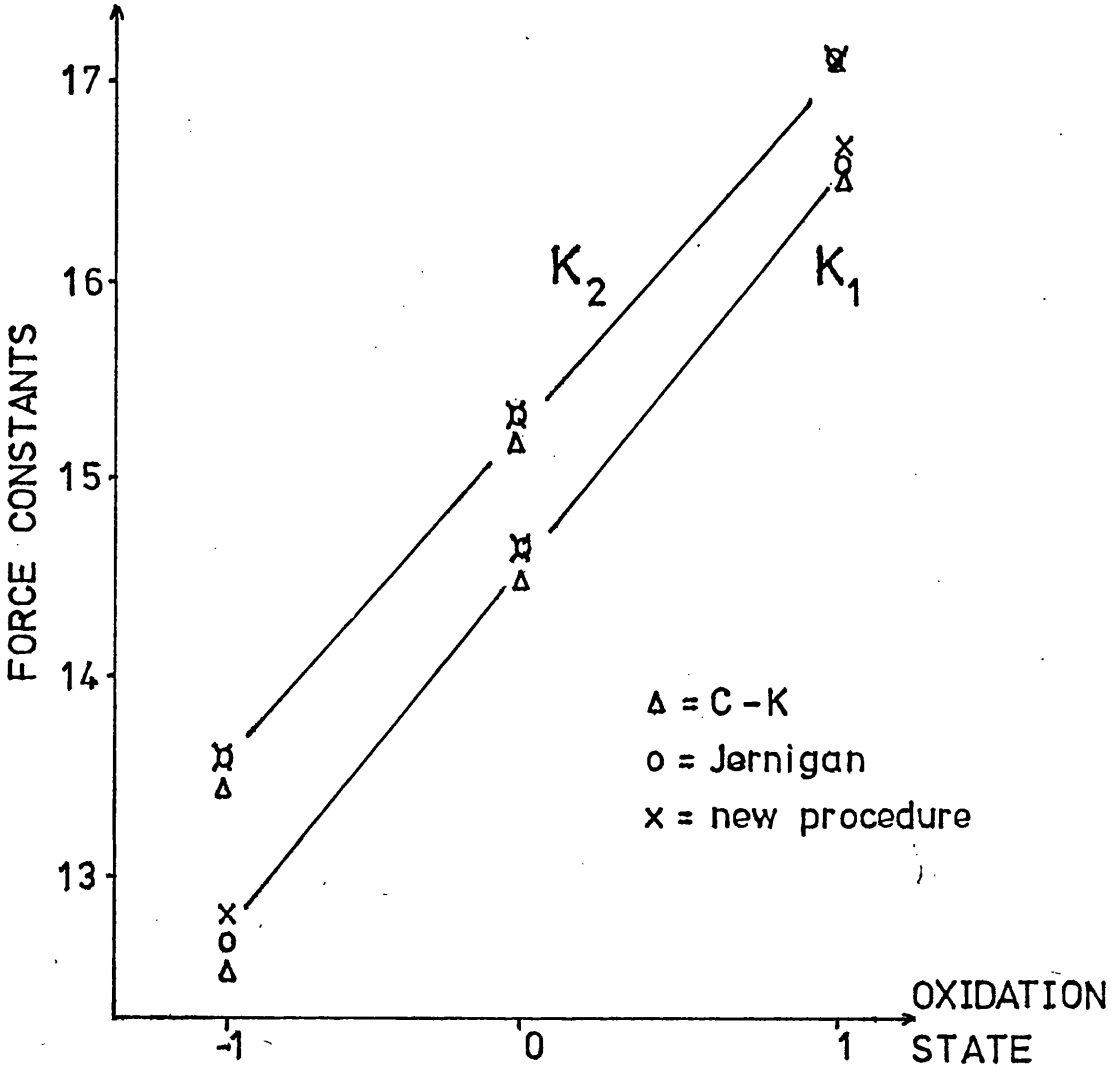

Figure 7-13. CO stretching force constants versus oxidation state for the isoelectronic complexes $[M(CO)_4dppe]^n$ (M = W, Re or Ta and n = 0, 1 or -1 respectively)

7.12 The new procedure and isotopically substituted $FeI_2(CO)_4$

In order to test the new procedure as rigorously as possible it was decided to apply it to the isotopically substituted $FeI_2(CO)_4$ complexes.[268,280] Before proceeding the relevant secular equations had to be derived for the species of various symmetries created by these substitutions. By comparison with

other carbonyl complexes[204] it was found that these secular equations could be obtained by inspection, but as confirmation these equations were also derived by the procedures given in Wilson, Decius and Cross[281]. These derivations, both by inspection and formally, are given in the Appendix. As the calculated reduced mass of $C^{18}O$ ($1/\mu^*$) led to discrepancies between the observed and calculated band positions for the $FeI_2(C^{18}O)_4$ species, it was necessary to use an apparent reduced mass (1/M) as given below[268].

$M = \mu(\nu^*/\nu)^2$ where $1/\mu$ = reduced mass $^{12}C^{16}O$

ν^* = an observed band position for $FeI_2(C^{18}O)_4$

ν = the corresponding band position for $FeI_2(C^{16}O)_4$

This discrepancy is probably due to the neglect of anharmonicity and various vibrational interaction terms (e.g. MC stretch - CO stretch interaction), both of these being dependent on the reduced mass of the carbonyl group[254].

Table 7-7 contains the observed and calculated band positions for the isotopically substituted $FeI_2(CO)_4$ species, and whilst the values obtained by the new procedure are not as close as Johnson's[268], which is to be expected as Johnson used a best-fit approach, they are still moderately good.

Table 7.7

Calculated and observed band positions for the complexes $FeI_2(C^{16}O)_x(C^{18}O)_y$

Complex[a]	Symmetry	Band	Band positions			
			Observed[b]	Robinson[b]	Jernigan	This work
$FeI_2(CO)_4$	C_{2v}	A_1	2128.8	2128.8	2128.8	2128.8
		A_1	2083.5	2083.5	2083.5	2076.8
		B_1	2083.5	2083.5	2083.5	2083.5
		B_2	2060.3	2060.3	2060.3	2060.3
$1\text{-}(C^{18}O)FeI_2(CO)_3$	C_s	A'	2126	2125.8	2125.4	2126.1
		A'	2023.5	2023.5	2023.3	2021.1
		A'	2075.5	2075.8	2076.1	2070.7
		A"	2083.5	2083.5	2083.5	2083.5
$2\text{-}(C^{18}O)FeI_2(CO)_3$	C_s	A'	2118.9	2118.5	2118.9	2117.9
		A'	2045.1	2045.8	2045.0	2044.7
		A'	2083.5	2083.5	2083.6	2078.0
		A"	2060.3	2060.3	2060.3	2060.3
$1,1'\text{-}(C^{18}O)_2FeI_2(CO)_2$	C_{2v}	A_1	2126	2123.2	2122.4	2123.7
		A_1	2041	2041.2	2041.5	2033.7
		B_1	2083.5	2083.5	2083.5	2083.5
		B_2	2013.2	2013.2	2012.7	2012.7
$1,2\text{-}(C^{18}O)_2FeI_2(CO)_2$	C_1	A	2023.5	2022.9	(2025)[c]	(2022)[c]
		A	2045.1	2046.5	(2042)	(2043)
		A	2115	2114.4	(2117)	(2116)
		A	2075.5	2076.8	(2073)	(2070)
$2,2'\text{-}(C^{18}O)_2FeI_2(CO)_2$	C_{2v}	A_1	2104	2103.9	2105.2	2100.3
		A_1	2060.3	2060.0	2058.3	2056.4
		B_1	2035.4	2035.9	2035.4	2035.4
		B_2	2060.3	2060.3	2060.3	2060.3
$1\text{-}(CO)FeI_2(C^{18}O)_3$	C_s	A'	2094	2094.0	2094.8	2091.7
		A'	2023.5	2022.6	2022.3	2020.0
		A'	2060.3	2060.0	2058.7	2057.4
		A"	2035.4	2035.9	2035.4	2035.4

Table 7.7 (Contd)

Complex[a]	Symmetry	Band	Band positions			This
			Observed[b]	Robinson[b]	Jernigan	work
2-(CO)$FeI_2(C^{18}O)_3$	C_s	A'	d	2111.0	2110.4	2111.3
		A'	2035.4	2035.9	2035.4	2029.6
		A'	2052	2053.0	2053.2	2051.5
		A"	2013.2	2013.2	2012.7	2012.7
$FeI_2(C^{18}O)_4$	C_{2v}	A_1	2079	2080.1	2079.6	2079.6
		A_1	2035.4	2035.9	2035.4	2028.8
		B_1	2035.4	2035.9	2035.4	2035.4
		B_2	2013.2	2013.2	2012.7	2012.7

a) Substituent numbering is according to Cotton[204] (i.e. 1 and 2 are trans and cis respectively to iodine.

b) Values quoted in Robinson paper.[268]

c) Computation of this symmetry lost precision.

d) Band not observed.

The values obtained in this work for the complex 1,2-$(C^{18}O)_2Fe(CO)_2$ (C_1, the substituent numbering follows that of Cotton[204]) are only approximate as the computation of the 4 x 4 determinant was loosing accuracy (see the appendix). This loss of accuracy was probably due to the large differences between the diagonal and off-diagonal elements of the determinant, and to the involved nature of the trigonometric solution of the resulting quartic equation[282].

Inspection of table 7-7 reveals that the band positions calculated by the new procedure are always equal to or less than the observed values. The maximum observed error being 7 cm^{-1} whilst the mean and standard deviations are 1.9 and 3.0 cm^{-1} respectively. Although the values obtained by the new procedure do not agree as closely as Johnson's[268] or Jernigan's[249] they are still acceptible considering the approximations inherent in the method, namely the neglect of anharmonicity and the assumption of "pure" CO stretching modes.

It must be pointed out that the values Johnson[268] quotes as being obtained by the C - K procedure[204] are in fact wrong. These results were obtained by substituting $k_c = k_c^1 = \frac{1}{2}k_T$ into his equations. This substitution leads to:

$k_c = (\lambda_1 + \lambda_2 - \lambda_3 - \lambda_4)/6\mu$ [equivalent to cisA]

$k_1 = (\lambda_1 + \lambda_2 - \lambda_3 + 5\lambda_4)/6\mu$ [equivalent to K_1]

$k_2 = (\lambda_1 + \lambda_2 + 2\lambda_3 - \lambda_4)/3\mu$ [equivalent to K_2]

Therefore, these values are not C - K values as they assume the lower energy A_1 band position (i.e. A_1^2) to be accurate and actually use this value in the calculation of the force constants.

There is also a typographical error in Johnson's last secular equation which should read:

$$k_c = \frac{1}{\mu}\sqrt{\left(\frac{\lambda_1 - \lambda_2}{4}\right)^2 - \left(\mu k_2 - \frac{\lambda_1 + \lambda_2 + 2\lambda_3}{4}\right)^2}$$

7-13 Conclusion

One aspect of the force constants that has not been studied in this work is the separation of the σ- and π-bonding properties of the various ligands. Graham[42] has proposed a relationship between the CO stretching force constants and the bonding properties of the ligands as follows:

$$\Delta K_1 = \Delta\sigma + 2\Delta\pi$$

$$\Delta K_2 = \Delta\sigma + \Delta\pi$$

These equations were derived for $LM(CO)_5$ species, and were used relative to an arbitrary standard [eg. $(C_6H_{11}NH_2)Mo(CO)_5$] , by assuming that any change in the electron density on the metal caused by the L - M σ-donation will be equally shared by all the carbonyl groups. Whereas any change in the electron density on the metal resulting from the M - L π- bond will be felt twice as much by the carbonyl group trans to L as by those cis to L.

The attempted formulation of such relationships seems a little premature until the arguments concerning the effect of σ- and π-bonding on the force constants are settled.

Hall and Fenske[271] have derived expressions relating the force constants to the electron density on the carbonyl carbon atoms for $M(CO)_5X$ species and have shown that both the M - C π- and σ-bonding orbitals are antibonding relative to the C - O bond order. Hence an increase in the electron density on the carbonyl carbon atom, irrespective of whether it is via the M - C π- or σ-bonds, will cause a decrease in the C - O bond order and, therefore, a decrease in the CO stretching force constant. It was also shown that the magnitude of this effect was similar for electron density communicated by either of the M - C bonding orbitals (π:σ :: 1.0 ::0.8). This means that in any analysis of the force constants both the σ- and π-bonding effects must be fully considered. It must also be borne in mind that Hall and Fenske[271] employed the C - K procedure[204] to obtain the force constants used in their derivation, hence should a new and completely acceptible approach for determining force constants be found, then it may be necessary to modify the Hall-Fenske relationship. This does not seem likely in the near future.

The force constants for the cis-$L_2M(CO)_4$ system have been determined by the methods proposed by Cotton[204] and Jernigan[249] and also by a new procedure outlined herein. Whereas Cotton used fixed values for the ratios X (cisB/cisA) and Y(trans/cisA)

and Stone[244] and Delbeke[245-248] allowed X to vary whilst keeping Y constant, it was observed that the new procedure, which allows both X and Y to vary, resulted in an almost constant value for X whilst Y varied. However, force constants calculated by this new procedure correlate well with the other two methods of calculation studied, and they are also consistent with experimental observations.

In the cases where the calculated value for the uncertain A_1^2 band position are contrary to simple graph theory, it is often possible to suggest simple physical reasons to account for these deviations.

In order to further test the new procedure it was used to predict the spectra for the various ^{18}O labelled $FeI_2(CO)_4$ species. The predicted and observed spectra are in reasonable agreement. All the predicted band positions are within -7 cm^{-1} of the observed values and have a standard deviation of 3 cm^{-1}, but the values are not in as close agreement as those of Johnson[268] who adopted a best-fit approach to refine his Cotton values.

It would be interesting to compare the various procedures by analysing complexes of C_{2v} symmetry and using data that have been corrected for anharmonicity together with secular equations which include actual, or physically reasonable, values for the MC - CO stretch - stretch interaction terms and MC stretching force constants.

Appendix

The Derivation of Secular Equations

Appendix

The Derivation of Secular Equations

This appendix is designed to derive the secular equations required for the isotopically substituted octahedral species cis-$L_2M(CO)_4$ only, and hence includes just sufficient detail for this purpose. A more comprehensive account may be found in the book of Wilson, Decius and Cross.[264]

As mentioned in Chapter 7 two methods of derivation have been used for these equations, the formal method of Wilson, Decius and Cross[264] and an empirical method of inspection. These procedures will be described by working through a typical example, namely 1-($C^{18}O$)$FeI_2(CO)_3$, which will be considered firstly by the formal procedure and secondly by inspection.

A.1 The formal derivation of secular equations[264].

A.1.1 Draw the molecule under consideration and assign it to a point group.

The assigning of molecules to point groups is dealt with by many books on symmetry[29,30]. In the case under consideration, 1-($C^{18}O$)$FeI_2(CO)_3$, the point group is C_s (Figure A-1).

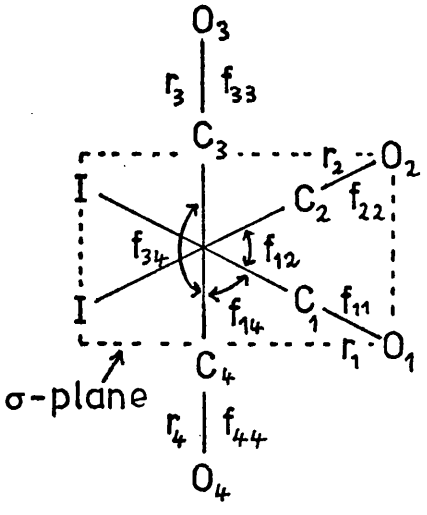

Nomenclature used in this work:

f_{11} and f_{22} become K_1

f_{33} and f_{44} become K_2

f_{12} becomes cisB

f_{13}, f_{14}, f_{23} and f_{24} become cisA

f_{34} becomes trans

Figure A-1 Symmetry elements, internal co-ordinates and valence force constants for 1-($C^{18}O$)$FeI_2(CO)_3$

A.1.2 Assign the internal co-ordinates for the required valence force constants.

In this work the "high energy factored model" has been employed. This means that only the CO stretching vibrations are considered and leads to the internal co-ordinates (r_i) being coincident with the C - O bonds (Figure A-1).

A.1.3 Determine the symmetry co-ordinates

The symmetry co-ordinates are obtained from the relationship given in equation A-1 (Ref. 264, p. 119 and 128). One internal co-ordinate (r_i) has to be taken from each of the

$$S^{\gamma} = \pi \Sigma_R \quad \chi^{\gamma}_R (Rr_i) \qquad \text{Equation A-1}$$

Where γ refers to the symmetry mode (eg. A')

R refers to a symmetry operation (eg. σ_h)

(Rr_i) is the internal co-ordinate created when the internal co-ordinate r_i is subjected to the operation R

χ^{γ}_R is the character of the operation R and the symmetry mode γ and is obtained from character tables[264,29,30]

π is a normalising factor.

symmetrically (or chemically) different groups of co-ordinates. Figure A-1 reveals that there are three distinct sets of internal co-ordinates, namely r_1, r_2 and $r_3 = r_4$. For greater clarity the character table has been included for C_s symmetry and is as follows:

C_s	E	σ_h
A'	1	1
A"	1	-1

where E and σ_h are symmetry operators (R)

A' and A" are symmetry modes (γ)

The digits are the characters (χ)

Consider r_1 (Figure A-1):

$$S_1^{A'} = \pi(r_1 + r_1)$$

$$= r_1$$

$$S_1^{A''} = 0$$

Subscripts have been added to S for clarity, and serve no other purpose.

Consider r_2 :

$$S_2^{A'} = r_2$$

$$S_2^{A''} = 0$$

Consider r_3:

$$S_3^{A'} = \pi(r_3 + r_4)$$

$$= 2^{-\frac{1}{2}}(r_3 + r_4)$$

$$S_3^{A''} = \pi(r_3 - r_4)$$

$$= 2^{-\frac{1}{2}}(r_3 - r_4)$$

As this is the only non-zero A" symmetry co-ordinate the subscript will be redundant in this case. Also in the interest of simplification the superscripts A' and A" will be replaced by ' and " respectively for this and all future cases (i.e. $S_3^{A'}$ becomes S_3' and $S_3^{A''}$ becomes S'').

It is now evident that the species under consideration [i.e. 1-($C^{18}O$)$FeI_2(CO)_3$] will give rise to four fundamental CO stretching vibrational modes, namely three A' and one A", and the symmetry co-ordinates S_i^γ relate these vibrations to the internal co-ordinates (Figure A-1). Hence the A" mode will consist of the out-of-phase stretching of the carbonyl groups labelled 3 and 4 in figure A-1. This vibration together with the other fundamentals is represented in figure A-2.

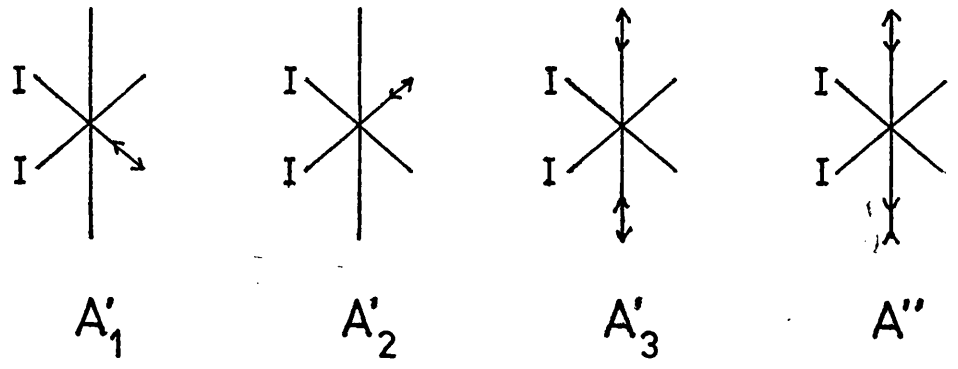

Figure A-2. Carbonyl stretching vibrational modes for 1-($C^{18}O$)$FeI_2(CO)_3$

A.1.4 Express the internal co-ordinates in terms of the symmetry co-ordinates.

The expressions for the symmetry co-ordinates (S^γ) may be manipulated in order to give the internal co-ordinates by normal algebraic means, but this may become very involved for some systems. Alternatively a simple transformation is given by Wilson, Decius and Cross (Ref. 264, p.128) as follows:

The coefficients of the internal co-ordinate r_1 in terms of the various symmetry co-ordinates S^γ are obtained by reading down the first column of the coefficients (i.e. those for r_1) in the expressions for the symmetry co-ordinates (i.e. S^γ in A.1.3). This is repeated for each of the internal co-ordinates r_i, and it is important to include the normalising factor in these coefficients.

Inspection of A.1.3 leads to the following expressions for the example under consideration.

$$r_1 = S_1'$$

$$r_2 = S_2'$$

$$r_3 = 2^{-\frac{1}{2}}(S_3' + S'')$$

$$r_4 = 2^{-\frac{1}{2}}(S_3' - S'')$$

A.1.5 Define the valence force constants

For each set of internal co-ordinates (A.1.3) a table is constructed with the rows and the columns labelled by the internal co-ordinates (r_i) in that set. The diagonal members of these tables are the valence stretch force constants (f_{ii}) and the off-diagonal members are the valence interaction force constants (f_{ij})

In the present case this leads to the following tables:

r_1

	r_1
r_1	f_{11}

r_2

	r_2
r_2	f_{22}

r_3 and r_4

	r_3	r_4
r_3	f_{33}	f_{34}
r_4	f_{43}	f_{44}

It is assumed that $f_{34} = f_{43}$ as the carbonyl groups must interact equally one with the other, and similarly $f_{33} = f_{44}$ as the carbonyl groups labelled 3 and 4 (Figure A-1) are indistinguishable. It is also assumed that the isotopic substitutions do not alter the value of the carbonyl stretching force constants from those of the parent $I_2Fe(CO)_4$ complex, thus $f_{11} = f_{22}$.

For convenience and to follow the nomenclature used in the literature[204] the force constants are named as follows (Figure A-1).

$f_{11} = f_{22}$ becomes K_1

$f_{33} = f_{44}$ " K_2

$f_{34} = f_{43}$ " trans

Substituting these names into the tables above leads to:

r_1 :

	r_1
r_1	K_1

r_2:

	r_2
r_2	K_1

r_3 and r_4:

	r_3	r_4
r_3	K_2	trans
r_4	trans	K_2

A.1.6 Define the symmetry force constants

The procedure (Ref. 264, p. 129 to 130) required to obtain these symmetry force constants (F_{ii}^{γ}) is given below and is performed for each fundamental vibrational mode.

The force constant in the first row of a valence force constant table (A.1.5) and in the column labelled by a given internal co-ordinate (r_i) is multiplied by the coefficient with which the internal co-ordinate (r_i) appears in the symmetry co-ordinate (S^{γ} , A.1.3) and divided by the coefficient of the co-ordinate which labels the first row of the force constants Table (A.1.5). This is repeated for each column and the results added together, which for the present case leads to the following relationships:

$$F_{11}' = K_1$$

$$F_{22}' = K_1$$

$$F_{33}' = K_2 + \text{trans}$$

$$F'' = K_2 - \text{trans}$$

A.1.7. Define the valence coupling constants

Only fundamentals of the same symmetry may couple, thus the three A' modes may couple with each other but not with the A" mode. The required procedure is similar to A.1.5 except the columns are labelled with one set of internal co-ordinates which participate in a vibration of the required symmetry (i.e. A'), whilst the rows are labelled with a different set of internal co-ordinates which also participate in a vibration of the required symmetry. This is repeated for all possible pairings of the appropriate fundamentals, and for the present example leads to the following tables.

A_1' coupling with A_2'

	r_2
r_1	f_{12}

A_1' coupling with A_3'

	r_3	r_4
r_1	f_{13}	f_{14}

A_2' coupling with A_3'

	r_3	r_4
r_2	f_{23}	f_{24}

Inspection of figure A-1 and applying similar reasoning to before (A.1.5), leads to the following equivalences. For convenience these force constants are renamed as indicated.

$f_{13} = f_{14} = f_{23} = f_{24}$ and becomes cisA

f_{12} becomes cisB.

Thus this terminology leads to the following tables:

A_1', A_2'	r_2
r_1	cisB

A_1', A_3'	r_3	r_4
r_1	cisA	cisA

A_2', A_3'	r_3	r_4
r_2	cisA	cisA

A.1.8 Define the symmetry coupling constants

This operation is similar to A.1.6 and the required procedure (Ref. 264, p. 131) is given below.

The valence coupling constant (f_{ij}) in the first row of the coupling constants Table (A.1.7) and in that column labelled by a given internal co-ordinate (r_i) is multiplied by the coefficient with which that internal co-ordinate appears in the symmetry co-ordinate (A.1.3), and divided by the coefficient of the internal co-ordinate which labels the first row of the coupling constants Table (A.1.7). This is repeated for each column and the results added together, which for the present example leads to the following relationships.

A_1' coupling with A_2' $\quad F_{12}' = \text{cisB}$

A_1' coupling with A_3' $\quad F_{13}' = 2^{-\frac{1}{2}}\text{cisA} + 2^{-\frac{1}{2}}\text{cisA}$

$\qquad\qquad\qquad\qquad\qquad\quad = \sqrt{2}\,\text{cisA}$

A_2' coupling with A_3' $\quad F_{23}' = \sqrt{2}\,\text{cisA}$

A.1.9 Write the F matrix in terms of the symmetry functions

The F matrix is simply a table labelled on both sides by the symmetry co-ordinates (A.1.3), with the diagonal elements being the symmetry force constants (A.1.6), and the off-diagonal elements being the symmetry coupling constants (A.1.8). Once again it is assumed that $F_{ab}^{\gamma} = F_{ba}^{\gamma}$ which for 1-($C^{18}O$)$FeI_2(CO)_3$ leads to the following matrix.

	S_1'	S_2'	S_3'	S''
S_1'	F_{11}'	F_{12}'	F_{13}'	0
S_2'	F_{12}'	F_{22}'	F_{23}'	0
S_3'	F_{13}'	F_{23}'	F_{33}'	0
S''	0	0	0	F''

A.1.10 Find the F matrix in terms of the valence force constants

Substitution of the expressions found in A.1.6 and A.1.8 for the symmetry force constants F_{ab}^{γ} leads to the required matrix as given below

F	S_1'	S_2'	S_3'	S''
S_1'	K_1	cisB	$\sqrt{2}$cisA	0
S_2'	cisB	K_1	$\sqrt{2}$cisA	0
S_3'	$\sqrt{2}$cisA	$\sqrt{2}$cisA	K_2+trans	0
S''	0	0	0	K_2-trans

A.1.11 Write the G matrix

For the high energy factored model this is simply a diagonal matrix in which the diagonal elements are equal to the reciprocal of the reduced mass of the relevant carbonyl groups. Consideration of figure A-2 together with the relationships μ = 1/reduced mass of $C^{16}O$ and μ^* = 1/reduced mass of $C^{18}O$ leads to the following matrix for the present case

G	S_1'	S_2'	S_3'	S"
S_1'	μ^*	0	0	0
S_2'	0	μ	0	0
S_3'	0	0	μ	0
S"	0	0	0	μ

A.1.12 Derive the secular determinant

In matrix terminology the secular determinant is given by $|GF-E\lambda| = 0$, where E is the unit matrix, λ is an Eigen value ($\lambda = 4\pi^2c^2\nu^2/N = 5.889\nu^2$) and G and F are the matrices found in A.1.11 and A.1.10 respectively. For the case under consideration the determinant is readily found to be as follows:

$$|GF-E\lambda| = \left|\begin{array}{ccc:c} \mu^*K_1-\lambda & \mu^*\text{cisB} & \sqrt{2}\mu^*\text{cisA} & 0 \\ \mu\text{cisB} & \mu K_1-\lambda & \sqrt{2}\mu\text{cisA} & 0 \\ \sqrt{2}\mu\text{cisA} & \sqrt{2}\mu\text{cisA} & \mu(K_2+\text{trans})-\lambda & 0 \\ \hdashline 0 & 0 & 0 & (K_2-\text{trans})-\lambda \end{array}\right| = 0$$

This determinant clearly factorises as indicated by the broken lines, with the resulting 3 x 3 determinant giving the three coupled A' roots and the A" root being given by the remaining expression.

A.2 The derivation of secular equations by inspection

In order to employ this procedure it is necessary to know the fundamental vibrational modes of the molecule under consideration. If these modes are in doubt they may be obtained from steps A.1.1 to A.1.3 of the formal procedure Once again the molecule 1-($C^{18}O$)$FeI_2(CO)_3$ will be used as the worked example.

A.2.1 Draw and label the fundamental vibrational modes

The fundamental vibrational modes are drawn such that modes of the same symmetry are grouped together (Figure A-2), and the required internal and valence force constants are labelled (Figure A-1).

A.2.2 Deduce the symmetry force constants

Each of the fundamentals has to be considered in turn, and if the mode involves a single carbonyl group then the symmetry force constant (F_{ii}^{γ}) will equal the valence stretching force constant (f_{ii}, figure A-1) of that carbonyl group. Where the fundamental involves two carbonyl groups then the symmetry force constant will be a linear combination of the relevant valence stretching force constant and the valence interaction force constant (Figure A-1). This linear combination being the sum for an in-phase vibration and the difference for an out-of-phase vibration (Figure A-2).

Consideration of 1-($C^{18}O$)$FeI_2(CO)_3$ leads to the following symmetry force constants.

$$F_{11}' = K_1$$
$$F_{22}' = K_1$$
$$F_{33}' = K_2 + \text{trans}$$
$$F'' = K_2 - \text{trans}$$

A.2.3 Obtain the coupling constants

As stated earlier only modes of the same symmetry may couple. Select two fundamental modes which may couple (Figure A-2) and deduce the valence interaction force constant (Figure A-1) which allows these modes to couple (e.g. The interaction force constant cisA permits the coupling of the A_1' and A_3' vibrational modes). The coefficient of this valence interaction force constant in the expression for the coupling constant (F_{ij}^{γ}) is the square root of the product of the effective number of carbonyl groups involved in each of the selected pair of vibrational modes. Where the effective number of carbonyl groups involved in a vibrational mode is the number of carbonyl groups being stretched less the number of carbonyl groups being compressed in that vibration. Hence, a vibrational mode which involves two carbonyl groups will have an effective number of two for an in-phase vibration and an effective number of zero for an out-of-phase vibration.

Consideration of $[1\text{-}(C^{18}O)FeI_2(CO)_3]$ and reference to figures A-1 and A-2 leads to the following relationship.

$$F_{12}' = \text{cisB}$$
$$F_{13}' = \sqrt{2}\,\text{cisA}$$
$$F_{23}' = \sqrt{2}\,\text{cisA}$$

A.2.4 Write the F matrix

The F matrix is a table labelled on both sides by the vibrational modes (Figure A-2), with the diagonal elements consisting of the symmetry force constants (A.2.2) involved in the relevant vibrations and the off-diagonal elements being the relevant coupling constants (A.2.3).

For the example under consideration the F matrix has the following form and is identical to the F matrix derived by the formal procedure.

F	A_1'	A_2'	A_3'	A"
A_1'	K_1	cisB	$\sqrt{2}$cisA	0
A_2'	cisB	K_1	$\sqrt{2}$cisA	0
A_3'	$\sqrt{2}$cisA	$\sqrt{2}$cisA	K_2+trans	0
A"	0	0	0	K_2-trans

A.2.5 Deduce the secular determinant

The secular determinant has the form $|GF-E\lambda| = 0$ and is obtained by multiplying each element of the F matrix as follows. The diagonal elements, considered individually, are multiplied by μ^* if the relevant fundamental (Figure A-2) involves $C^{18}O$, or otherwise by μ, and λ is subtracted from each of these products. The off-diagonal elements are multiplied by μ if both of the relevant modes involve only $C^{16}O$, or μ^* if they both involve only $C^{18}O$. Where one mode involves $C^{16}O$ and the other $C^{18}O$ the element is multiplied by $\sqrt{\mu\mu^*}$. Consideration of the present case together with figure A-2 leads to the

following determinant which clearly factorises as shown by the broken lines.

$$|GF-E\lambda| = \left|\begin{array}{ccc:c} \mu^*K_1-\lambda & \sqrt{\mu\mu^*}\,cisB & \sqrt{2\,\mu\mu^*}\,cisA & 0 \\ \sqrt{\mu\mu^*}\,cisB & \mu K_1-\lambda & \sqrt{2}\,\mu\,cisA & 0 \\ \sqrt{2\,\mu\mu^*}\,cisA & \sqrt{2}\mu cisA & \mu(K_2+trans)-\lambda & 0 \\ \hdashline 0 & 0 & 0 & \mu(K_2-trans)-\lambda \end{array}\right| = 0$$

At first sight this determinant appears to differ from that obtained by the formal approach, but the formal determinant is readily transformed[27] into the present form

A.3 Secular determinants for isotopically labelled cis-$I_2Fe(CO)_4$

Table A-1 contains the secular determinants required in Chapter 7 for the infra-red study of the isotopically labelled cis-$I_2Fe(CO)_4$ species. These determinants were tested by both an algebraic and a computed check. The algebraic check consisted of replacing every μ^* by μ and showing that the resulting determinants factorised to the non-substituted $FeI_2(CO)_4$ determinant. This was found to be so in every case.

In order to check both the computation and the secular determinants, the above substitutions were repeated and the resulting determinants, without factoring, were solved for λ, which in turn gave the vibrational band positions (ν ; $\lambda = 5.889\ \nu^2$). The calculated band positions should all agree with the values obtained from the determinant for the parent complex $FeI_2(CO)_4$.

Table A-1[a]

Secular determinants for ^{18}O labelled cis-$I_2Fe(CO)_4$ complexes

Vibrational mode	Formal derivation	Inspection
	i. $FeI_2(CO)_4$ (C_{2v} symmetry)	
$2A_1$	$\begin{vmatrix} \mu(K_1 + cisB)-\lambda & 2\mu cisA \\ 2\mu cisA & \mu(K_2 + trans)-\lambda \end{vmatrix} = 0$	$\begin{vmatrix} \mu(K_1 + cisB)-\lambda & 2\mu cisA \\ 2\mu cisA & \mu(K_2 + trans)-\lambda \end{vmatrix} = 0$
B_1	$\lambda = \mu(K_2 - trans)$	$\lambda = \mu(K_2 - trans)$
B_2	$\lambda = \mu(K_1 - cisB)$	$\lambda = \mu(K_1 - cisB)$
	ii $1\text{-}(C^{18}O)FeI_2(CO)_3$ (C_s symmetry)	
$3A'$	$\begin{vmatrix} \mu^* K_1 -\lambda & \mu^* cisB & \sqrt{2}\,\mu^* cisA \\ \mu cisB & \mu K_1-\lambda & \sqrt{2}\,\mu cisA \\ \sqrt{2}\mu cisA & \sqrt{2}\mu cisA & \mu(K_2 + trans)-\lambda \end{vmatrix} = 0$	$\begin{vmatrix} \mu^* K_1 -\lambda & \sqrt{\mu\mu}^* cisB & \sqrt{2\,\mu\mu}^* cisA \\ \sqrt{\mu\mu}^* cisB & \mu K_1-\lambda & \sqrt{2}\mu cisA \\ \sqrt{2\mu\mu}^* cisA & \sqrt{2}\mu cisA & \mu(K_2 + trans)-\lambda \end{vmatrix} = 0$
A''	$\lambda = \mu(K_2 - trans)$	$\lambda = \mu(K_2 - trans)$

Table A-1[a] (contd)

Vibrational Mode	Formal derivation	Inspection
	iii $2\text{-}(C^{18}O)FeI_2(CO)_3$ (C_s symmetry)	
3A'	$\begin{vmatrix} \mu(K_1 + \text{cisB})-\lambda & \sqrt{2}\mu\text{cisA} & \sqrt{2}\mu\text{cisA} \\ \sqrt{2}\mu\text{cisA} & \mu K_2-\lambda & \mu\text{trans} \\ \sqrt{2}\mu^*\text{cisA} & \mu^*\text{trans} & \mu^* K_2-\lambda \end{vmatrix} = 0$	$\begin{vmatrix} \mu(K_1 + \text{cisB})-\lambda & \sqrt{2}\mu\text{cisA} & \sqrt{2\mu\mu^*}\,\text{cisA} \\ \sqrt{2}\mu\text{cisA} & \mu K_2-\lambda & \sqrt{\mu\mu^*}\,\text{trans} \\ \sqrt{2\mu\mu^*}\,\text{cisA} & \sqrt{\mu\mu^*}\,\text{trans} & \mu^* K_2-\lambda \end{vmatrix} = 0$
A"	$\lambda = \mu(K_1 - \text{cisB})$	$\lambda = \mu(K_1 - \text{cisB})$
	iv. $1,1\text{-}(C^{18}O)_2FeI_2(CO)_2$ (C_{2v} symmetry)	
$2A_1$	$\begin{vmatrix} \mu^*(K_1 + \text{cisB})-\lambda & 2\mu^*\text{cisA} \\ 2\mu\,\text{cisA} & \mu(K_2 + \text{trans})-\lambda \end{vmatrix} = 0$	$\begin{vmatrix} \mu^*(K_1 + \text{cisB})-\lambda & 2\sqrt{\mu\mu^*}\,\text{cisA} \\ 2\sqrt{\mu\mu^*}\,\text{cisA} & \mu(K_2 + \text{trans})-\lambda \end{vmatrix} = 0$
B_1	$\lambda = \mu(K_2 - \text{trans})$	$\lambda = \mu(K_2 - \text{trans})$
B_2	$\lambda = \mu^*(K_1 - \text{cisB})$	$\lambda = \mu(K_1 - \text{cisB})$

Table A-1[a] (contd)

Vibrational mode	Formal derivation	Inspection
	v. $1,2\text{-}(C^{18}O)_2FeI_2(CO)_2$ (C_1 symmetry)	
4A	$\begin{vmatrix} \mu K_1-\lambda & \mu \text{ois}B & \mu \text{cis}A & \mu \text{cis}A \\ \mu^* \text{cis}B & \mu^* K_1-\lambda & \mu^* \text{cis}A & \mu^* \text{cis}A \\ \mu^* \text{cis}A & \mu^* \text{cis}A & \mu^* K_2-\lambda & \mu^* \text{trans} \\ \mu \text{cis}A & \mu \text{cis}A & \mu \text{trans} & \mu K_2-\lambda \end{vmatrix} = 0$	$\begin{vmatrix} \mu K_1-\lambda & \sqrt{\mu\mu^*}\,\text{cis}B & \sqrt{\mu\mu^*}\,\text{cis}A & \mu \text{cis}A \\ \sqrt{\mu\mu^*}\,\text{cis}B & \mu^* K_1-\lambda & \mu^* \text{cis}A & \sqrt{\mu\mu^*}\,\text{cis}A \\ \sqrt{\mu\mu^*}\,\text{cis}A & \mu^* \text{cis}A & \mu^* K_2-\lambda & \sqrt{\mu\mu^*}\,\text{trans} \\ \mu \text{cis}A & \sqrt{\mu\mu^*}\,\text{cis}A & \sqrt{\mu\mu^*}\,\text{trans} & K_2-\lambda \end{vmatrix} = 0$
vi	$2,2\text{-}(C^{18}O)_2FeI_2(CO)_2$ interchange μ and μ^* in iv	
vii	$1\text{-}(CO)FeI_2(C^{18}O)_3$ interchange μ and μ^* in ii	
viii	$2\text{-}(CO)FeI_2(C^{18}O)_3$ interchange μ and μ^* in iii	
ix	$FeI_2(C^{18}O)_4$ replace μ by μ^* in i	

a. The numbering of the substituent groups follows that of Cotton [204]

$\lambda = (5.889 \times 10^{-2})\nu^2$ where ν is in cm^{-1}.

This computational check was repeated by letting μ and μ^* equal M (M is the reciprocal of the "apparent" reduced mass of $C^{18}O^{268}$, Section 1.12) which should lead to the same values as the calculated values for $FeI_2(C^{18}O)_4$. The maximum observed errors by either substitution were as follows:

C_{2v} -	Determinants i, iv, vi and ix (Determinants i and ix were taken as the reference values)	0 cm^{-1}
C_s -	Determinants ii, iii, vii and viii	$\pm$ 0.025 cm^{-1}
C_1 -	Determinant v	$\pm$ 11.6 cm^{-1}

For the C_1 case the same error was found for the corresponding roots by either substitution, these being -11.6, +11.3, -11.2 and +11.3 for roots 1 to 4 respectively. As the 4 x 4 determinant (v) for this symmetry (C_1) factorises when tested albegraically, as above, and all attempts to find a mathematical error in the solution of the resulting quartic equation failed, it seems likely that the computation was loosing precision.

There are two reasonable ways in which this loss of precision could occur. Firstly expansion of this determinant, more so than the other determinants, produces greatly differing numbers (i.e. 81 x 10^{-8} to 40) which have to be added to or subtracted from each other. This could lead to significant errors even though double precision (i.e. 13 significant figures) was used throughout. The second possibility is that significant

errors were introduced during the rather involved solution of the quartic equation[265]. It is probable that both of these suggestions contribute, in varying degrees, to the loss of precision.

The figures quoted in the text, Chapter 7, are as computed for the various species with the exception of 1,2-$(C^{18}O)_2FeI_2(CO)_2$ (C_1 symmetry, determinant v), which has 11 cm^{-1} added to roots 1 and 3 and 11 cm^{-1} subtracted from roots 2 and 4 to give the approximate band positions as quoted.

References

References

1. W.P. Griffith, Q. Rev., Chem. Soc., 1962, 16, 188.

2. Stahl, "Experimentia, Observationes, Animadversions CCC numero chymicae et physicae", Berlin, 1731, p. 281.

3. Anon., "Miscellanae Berolinensia ad Incrementum scientiarum", Berlin, 1710, p. 277.

4. F. Basolo and R. Johnson, "Coordination Chemistry", W.A. Benjamin, Inc., New York, 1964.

5. G.B. Kauffman, Coord. Chem. Rev., 1975, 15, 1.

6. L. Mond, C. Langer and F. Quincke, J. Chem. Soc., 1890, 57, 749.

7. A. Job and A. Cassal, C.R. Hebd. Seances, Acad. Sci. Ser. B, 1926, 183, 392.

8. B.B. Owen, J. English, H.G. Cassidy and C.V. Dundon, J. Am. Chem. Soc., 1947, 69, 1723.

9. D.T. Hurd, Inorg. Synth., 1957, 5, 135.

10. B.B. Owen, J. English, H.G. Cassidy and C.V. Dundon, Inorg. Synth., 1950, 3, 156.

11. E.W. Abel and F.G.A. Stone, Q. Rev., Chem. Soc., 1970, 24, 498.

12. R.D. Riecke, K. Ofele and E.O. Fischer, J. Organomet. Chem., 1974, 76, C.19.

13. F.R. Hartley, "The Chemistry of Platinum and Palladium", Applied Science Publishers Ltd., London, 1973.

14. E. Frankland, Justus Liebigs Ann. Chem., 1849, 71, 171.

15. P.T. Moseley and H.M.M. Shearer, J. Chem. Soc., Chem. Commun., 1966, 876.

16. F.A. Cotton and G. Wilkinson, "Advanced Inorganic Chemistry", 3rd. Edn., Wiley-Interscience, New York, 1972.

17. G.E. Coates, M.L.H. Green, P. Powell and K. Wade, "Principles of Organometallic Chemistry", Methuen and Co. Ltd., London, 1971.

18. G. Wilkinson, M. Rosenblum, M.C. Whiting and R.B. Woodward., J. Amer. Chem. Soc., 1952, 74, 2125.

19. H.B. Jonassen, R.I. Stearns and J. Kenttamaa., J. Amer. Chem. Soc., 1958, 80, 2586.

20. R.F. Heck and D.S. Breslow, J. Am. Chem. Soc., 1960, 82, 750.

21. U. Belluco, "Organometallic and Coordination Chemistry of Platinum", Academic Press, London, 1974.

22. A. Agapiou and E. McNelis, J. Organomet. Chem., 1975, 99 C.47.

23. G.N. Schrauzer (Ed.), "Transition Metals in Homogeneous Catalysis", Marcell Dekker, Inc., New York, 1971.

24. H.J.M. Bowen, "Trace Elements in Biochemistry", Academic Press, London, 1966.

25. D.G. Brown, Prog. Inorg. Chem., 1973, 18, 177.

26. Climax 2nd Intl. Conf. Chem. and Uses of Molybdenum, Oxford, August, 1976.

27. P.S. Braterman, "Metal Carbonyl Spectra", Academic Press, London, 1975.

28. D.M. Adams, "Metal-Ligand and Related Vibrations", Edward Arnold Ltd., London, 1967.

29. D.S. Urch, "Orbitals and Symmetry", Penguin Books, Middlesex, England, 1970.

30. F.A. Cotton, "Chemical Applications of Group Theory", Interscience, London, 1963.

31. S.F.A. Kettle and I. Paul, Adv. Organomet. Chem., 1972, 10, 199.

32. J. Dalton, Inorg. Chem., 1971, 10, 1822.

33. H. Werner, Angew. Chem. Int. Ed. Engl. 1968, 7, 930.

34. H.W. Thompson and A.P. Garrett, J. Chem. Soc., 1934, 524.

35. A.P. Garrett and H.W. Thompson, J. Chem. Soc., 1934, 1817.

36. M.A. Graham, M. Poliakoff and J.J. Turner, J. Chem. Soc. A, 1971, 2939.

37. R.N. Perutz and J.J. Turner, J. Am. Chem. Soc., 1975, 97, 4791.

38. J.A. Pardue, M.N. Memering and G.R. Dobson, J. Organomet. Chem., 1974, 71, 407.

39. J.A. Connor, E.M. Jones and G.K. McEwen, J. Organomet. Chem., 1972, 43, 357.

40. J.A. Connor, J.P. Day, E.M. Jones and G.K. McEwen, J. Chem. Soc., Dalton Trans., 1973, 347.

41. J.A. Connor and P.I. Riley, J. Organomet. Chem. 1975, 94, 55.

42. W.A.G. Graham, Inorg. Chem., 1968, 7, 315.

43. E.W. Abel and F.G.A. Stone, Q. Rev., Chem. Soc., 1970, 24, 498.

44. W.R. McWhinnie and J.D. Miller, Adv. Inorg. Chem. Radiochem., 1969, 12, 135.

45. W.M. Carmichael, D.A. Edwards and R.A. Walton, J. Chem. Soc., A, 1966, 97.

46. C.G. Hull and M.H.B. Stiddard, J. Chem. Soc. A, 1966, 1633.

47. E. Konig and E. Lindner, Spectrochim. Acta Part A, 1972, 28, 1393.

48. M.H.B. Stiddard, J. Chem. Soc., 1962, 4712

49. L.W. Houk and G.R. Dobson, J. Chem. Soc. A, 1966, 317.

50. H. Behrens and N. Harder, Chem. Ber., 1964, 97, 433.

51. C.G. Hull and M.H.B. Stiddard, J. Chem. Soc. A, 1968, 710.

52. M.H.B. Stiddard, J. Chem. Soc., 1963, 756.

53. S.C. Tripathi and S.C. Srivastava, J. Organomet. Chem., 1970, 25, 193.

54. H. Behrens, E. Lindner and G. Lehnert, J. Organomet. Chem., 1970, 22, 665.

55. H. Behrens and N. Harder, Chem. Ber., 1964, 97, 426.

56. H. Behrens, E. Lindner and G. Lehnert, J. Organomet. Chem., 1970, 22, 439.

57. W.R. McWhinnie, Coord. Chem. Rev., 1970, 5, 293.

58. P.J. Harris, "Metal Carbonyl Derivatives of N-substituted 2,2'-Dipyridylamine", School of Chemistry, University of Bath, 1974.

59. G.C. Kulasingham and W.R. McWhinnie, J. Less-Common Met., 1966, 10, 72.

60. T.J. Hurley and M.A. Robinson, Inorg. Chem., 1968, 7, 33.

61. C.D. Burbridge and D.M.L. Goodgame, J. Chem. Soc. A, 1967, 694.

62. C.D. Burbridge and D.M.L. Goodgame, J. Chem. Soc. A, 1968, 237.

63. M. Goodgame, J. Chem. Soc. A, 1966, 63.

64. P.F.B. Barnard, J.C. Lancaster, M.E. Fernandopulle and W.R. McWhinnie, J. Chem. Soc., Dalton Trans., 1973, 2172.

65. W.R. McWhinnie, R.C. Poller and M. Thevarasa, J. Chem. Soc., A, 1967, 1671.

66. J.C. Lancaster, W.R. McWhinnie and P.L. Welham, J. Chem. Soc. A, 1971, 1742.

67. J.E. Johnson and R.A. Jacobson, J. Chem. Soc., Dalton Trans., 1973, 580.

68. J.E. Johnson, T.A. Beineke and R.A. Jacobson, J. Chem. Soc. A, 1971, 1371.

69. D.D. Perrin, "Dissociation Constants of Organic Bases in Aqueous Solutions", Butterworths, 1965.

70. C.S. Kraihanzel and F.A. Cotton, Inorg. Chem., 1963, 2, 533.

71. C.F. Bell, "Principles and Applications of Metal Chelation", Clarendon Press, Oxford, 1977.

72. A.J. Graham and R.H. Fenn, J. Organomet. Chem., 1969, 17, 405.

73. R.H. Fenn and A.G. Graham, J. Organomet. Chem., 1972, 37, 137.

74. E.O. Fischer and A. Maasbol, Angew. Chem., Int. Ed. Engl., 1964, 3, 580.

75. D.St.C Black and R.C. Srivastava, Aust. J. Chem., 1971, 24, 287.

76. J.P. Collman, Transition Met. Chem., 1966, 2, 1.

77. C.J. Pickett and D. Pletcher, J. Chem. Soc., Dalton Trans., 1975, 879.

78. R.E. Dessy and L. Wieczorek, J. Am. Chem. Soc., 1969, 91, 4963.

79. F.L. Wimmer, M.R. Snow and A.M. Bond, Inorg. Chem., 1974, 13, 1617.

80. A.M. Bond, J.A. Bowden and R. Colton, Inorg. Chem., 1974, 13, 602.

81. M.K. Lloyd, J.A. McCleverty and D.G. Orchard., J. Chem. Soc., Dalton Trans., 1973, 1743.

82. C.J. Pickett and D. Pletcher, J. Chem. Soc., Dalton Trans., 1976, 749.

83. J.F. White and M.F. Farona, J. Organomet. Chem., 1972, 37, 119.

84. J.E. Ellis, S.G. Hentges, D.G. Kalina and G.P. Hagen, J. Organomet. Chem., 1975, 97, 79.

85. R.G. Hayter, J. Am. Chem. Soc., 1966, 88, 4376.

86. M.R. Churchill, S.W.-Y. Chang, M.L. Berch and A. Davison, J. Chem. Soc., Chem. Commun., 1973, 691.

87. J.E. Ellis, J. Organomet. Chem., 1975, 86, 1.

88. L.B. Handy, J.K. Ruff and L.F. Dahl, J. Am. Chem. Soc., 1970, 92, 7312.

89. W. Douglas and J.K. Ruff, J. Organomet. Chem., 1974, 65, 65.

90. M.R. Churchill and S.W.-Y. Chang, Inorg. Chem., 1974, 13, 2413.

91. R.D. Wilson, S.A. Graham and R. Bau, J. Organomet. Chem., 1975, 91, C.49.

92. E.A. Allen, K. Feenan and G.W.A. Fowles, J. Chem. Soc., 1965, 1636.

93. M.G.B. Drew, Prog. Inorg. Chem., 1977, 23, 67.

94. M.G.B. Drew and A.P. Wolters, J. Chem. Soc., Chem. Commun., 1972, 457.

95. M.G.B. Drew and J.D. Wilkins, J. Organomet. Chem., 1974, 69, 271.

96. M.G.B. Drew, J. Chem. Soc., Dalton Trans., 1972, 1329.

97. M.G.B. Drew, A.J. Johans and A.P. Wolters, J. Chem. Soc., Chem. Commun., 1971, 819.

98. M.G.B. Drew and C.J. Rix, J. Organomet. Chem., 1975, 102, 467.

99. A. Mawby and G.E. Pringle, J. Inorg. Nucl. Chem., 1972, 34, 517.

100. M.G.B. Drew, J. Chem. Soc., Dalton Trans., 1972, 626.

101. M.L.H. Green and W.E. Lindsell, J. Chem. Soc. A, 1967, 686.

102. R. Kummer and W.A.G. Graham, Inorg. Chem., 1968, 7, 310.

103. E.M. Cradwick and D. Hall, J. Organomet. Chem., 1970, 25, 91.

104. M. Elder and D. Hall, Inorg. Chem., 1969, 8, 1268.

105. M. Elder and D. Hall, Inorg. Chem., 1969, 8, 1273.

106. W.R. Cullen and R.K. Pomeroy, Inorg. Chem., 1975, 14, 939.

107. F.W.B. Einstein and J.S. Field, J. Chem. Soc., Dalton Trans., 1975, 1628.

108. P.D. Brotherton, et al., Aust. J. Chem., 1974, 27, 2667.

109. T.S. Piper and G. Wilkinson, J. Inorg. Nucl. Chem., 1956, 3, 104.

110. M. Cousins and M.L.H. Green, J. Chem. Soc., 1963, 889.

111. R.B. King and A. Fronzaglia, J. Am. Chem. Soc., 1966, 88, 709.

112. F.A. Cotton and M.D. LaPrade, J. Am. Chem. Soc., 1968, 90, 5418.

113. C.G. Hull and M.H.B. Stiddard, J. Organomet. Chem., 1967, 9, 519.

114. R.G. Hayter, J. Organomet. Chem., 1968, 13, P.1.

115. J.W. McDonald and F. Basolo, Inorg. Chem., 1971, 10, 492.

116. P.K. Wong, K.S.Y. Lau and J.K. Stille, J. Am. Chem. Soc., 1974, 96, 5956.

117. J.P. Collman and M.R. MacLaury, J. Am. Chem. Soc., 1974, 96, 3019.

118. A.J. Graham and R.H. Fenn, J. Organomet. Chem., 1970, 25, 173.

119. F.Dawans, J. Dewailly, J. Meunier-Piret and P. Piret, J. Organomet. Chem., 1974, 76, 53.

120. F.A. Cotton, B.A. Frenz and A.G. Stanislowski, Inorg. Chim. Acta, 1973, 7, 503.

121. F.A. Cotton, C.A. Murillo and B.R. Stults, Inorg. Chim. Acta, 1977, 22, 75.

122. E.M. Holt, S.L. Holt and K.J. Watson, J. Chem. Soc., Dalton Trans. 1973, 2444.

123. A.J. Graham, D. Akrigg and B. Sheldrick, Cryst. Struct. Commun., 1976, 5, 891.

124. F.A. Cotton, M. Jeremic and A. Shaver, Inorg. Chim. Acta., 1972, 6, 543.

125. C.A. Kosky, P. Ganis and G. Avitabile, Acta Crystallogr. Sect. B, 1971, 27, 1859.

126. F.A. Cotton, B.A. Frenz and C.A. Murillo, J. Am. Chem. Soc., 1975, 97, 2118.

127. F.A. Cotton, T. LaCour and A.G. Stanislowski, J. Am. Chem. Soc., 1974, 96, 754.

128. J.W. Faller, D.A. Haitko, R.D. Adams and D.F. Chodosh., J. Am. Chem. Soc., 1977, 99, 1654.

129. P.S. Braterman and R.J. Cross, J. Chem. Soc., Dalton Trans., 1972, 657.

130. R.D.W. Kemmitt and M.A.R. Smith, Inorg. React. Mech., 1974, 3, 372.

131. J.C. Bailar, et al. (Eds.), "Comprehensive Inorganic Chemistry", Pergamon Press, New York, 1973, Vol. 4.

132. G. Raper and W.S. McDonald, J. Chem. Soc., Dalton Trans., 1972, 265.

133. L.M. Jackman and F.A. Cotton (Eds.), "Dynamic Nuclear Magnetic Resonance Spectroscopy", Academic Press, New York, 1975.

134. J.A. Kaduk, A.T. Poulos and J.A. Ibers, J. Organomet. Chem., 1977, 127, 245.

135. J.A. Kaduk and J.A. Ibers, J. Organomet. Chem., 1977, 139, 199.

136. A. Scrivanti, G. Carturan, U. Belluco, N.B. Pahor, M. Calligaris and L. Randaccio., Inorg. Chim. Acta, 1976, 20, L3.

137. H.L. Clarke and N.J. Fitzpatrick, J. Organomet. Chem., 1972, 40, 379.

138. G. Davidson, Organomet. Chem. Rev., Sect. A, 1972, 8, 303.

139. W.R. McClellen, H.H. Hoehn, H.N. Cripps, E.L. Muetterties and B.W. Houk, J. Am. Chem. Soc., 1961, 83, 1601.

140. H.-J.Neese and H. Burger, J. Organomet. Chem., 1971, 32, 213.

141. M.L.H. Green and P.L.I. Nagy, Adv. Organomet. Chem., 1964, 2, 325.

142. K. Vrieze and P.W.N.M. Van Leeuwen, Prog. Inorg. Chem., 1971, 14, 1.

143. S.F. A. Kettle and R.A. Mason, J. Organomet. Chem., 1966, 5, 573.

144. H.L. Clarke, J. Organomet. Chem., 1974, 80, 369.

145. D.C. Andrews and G. Davidson, J. Organomet. Chem., 1973, 55, 383.

146. G. Paliani, A. Poletti, G. Cardaci, S.M. Murgia and R. Catoliotti. J. Organomet. Chem., 1973, 60, 157.

147. K. Shobatake and K. Nakamoto, J. Am. Chem. Soc., 1970, 92, 3339.

148. D.C. Andrews and G. Davidson, J. Chem. Soc., Dalton Trans., 1972, 1381.

149. G. Davidson and D.C. Andrews, J. Chem. Soc., Dalton Trans., 1972, 126.

150. D.M. Adams and A. Squire, J. Chem. Soc. A, 1970, 1808.

151. M.L.H. Green, L.C. Mitchard and W.E. Silverthorn, J. Chem. Soc., Dalton Trans., 1973, 1403.

152. B.E. Mann, R. Pietropaolo and B.L. Shaw, J. Chem. Soc., Dalton Trans., 1973, 2390.

153. F.A. Cotton, J.W. Faller and A. Musco, Inorg. Chem., 1967, 6, 179.

154. E.W. Abel and S. Moorhouse, Angew. Chem. Int. Ed. Engl., 1971, 10, 339.

155. E.W. Abel and S. Moorhouse, J. Chem. Soc., Dalton Trans., 1973, 1706.

156. M.L.H. Green, L.C. Mitchard and W.E. Silverthorn, J. Chem. Soc., Dalton Trans., 1973, 1952.

157. G. Doyle, J. Organomet. Chem., 1977, 132, 243.

158. J.Y. Merour, C. Charrier, J. Benaim, J.L. Roustan and D. Commereuc, J. Organomet. Chem., 1972, 39, 321.

159. M. Green and R.I. Hancock, J. Chem. Soc. A, 1968, 109.

160. M. Ephritikhine, B.R. Francis, M.L.H. Green, R.E. Mackenzie M.J. Smith., J. Chem. Soc., Dalton Trans., 1977, 1131.

161. K. Ehrlich and G.F. Emerson, J. Am. Chem. Soc., 1972, 94, 2464.

162. M.I. Bruce, M.Z. Iqbal and F.G.A. Stone, J. Organomet. Chem., 1969, 20, 161.

163. A. Efraty, J. Organomet. Chem., 1973, 57, 1.

164. B. Kanellakopulos, D. Nothe, K. Weidenhammer, H. Wienand and M.L. Ziegler, Angew. Chem. Int. Ed. Engl., 1977, 16, 261.

165. G. Vitulli, P. Pertici, C. Agami and L. Porri, J. Organomet. Chem., 1975, 84, 399.

166. J.L. Roustan, J. Organomet. Chem., 1972, 38, C.37.

167. W.S. Trahanowsky and R.A. Hall, J. Am. Chem. Soc., 1977, 99, 4850

168. G. Wilke, et al., Angew. Chem., Int. Ed. Engl. 1966, 5, 151.

169. F.A. Cotton and J.R. Pipal, J. Am. Chem. Soc., 1971, 93, 5441.

170. T. Aoki, A. Furusaki, Y. Tomie, K. Ono and K. Tanaka., Bull. Chem. Soc. Jpn., 1969, 42, 545.

171. M.L.H. Green, L.C. Mitchard and W.E. Silverthorn, J. Chem. Soc., Dalton Trans., 1973, 2177.

172. M.L.H. Green and W.E. Silverthorn, J. Chem. Soc., Dalton Trans., 1973, 301.

173. J.A. McCleverty and A.J. Murray, J. Less-Common Met. 1977, 54, 174.

174. N.A. Bailey, W.G. Kita, J.A. McCleverty A.J. Murray, B.E. Mann and N.W.J. Walker, J. Chem. Soc., Chem. Commun., 1974, 592.

175. J.W. Faller and A.M. Rosan, J. Am. Chem. Soc., 1976, 98, 3388.

176. R.B. King and M.S. Saran, Inorg. Chem., 1974, 13, 2453.

177. A.T.T. Hsieh and B.O. West, J. Organomet. Chem. 1976, 112, 285.

178. H.T. Dieck and H. Friedel, J. Organomet. Chem., 1968, 14, 375.

179. C.E. Holloway, J.D. Kelly and M.H.B. Stiddard, J. Chem. Soc. A, 1969, 931.

180. B.J. Brisdon, J. Organomet. Chem., 1977, 125, 225.

181. J.W. Faller, D.A. Haitko, R.D. Adams and D.F. Chodosh., J. Am. Chem. Soc., 1977, 99, 1654.

182. J.W. Faller and A.M. Rosan, J. Am. Chem. Soc., 1977, 99, 4858.

183. P. Meakin, S. Trofimenko and J.P. Jesson, J. Am. Chem. Soc., 1972, 94, 5677.

184. S. Trofimenko, J. Am. Chem. Soc., 1969, 91, 3183.

185. P. Powell, J. Organomet. Chem., 1977, 129, 175.

186. H.D. Murdoch, J. Organomet. Chem., 1965, 4, 119.

187. H.D. Murdoch and R. Henzi, J. Organomet. Chem., 1966, 5, 552.

188. R. Baker, Chem. Rev., 1973, 73, 487.

189. H. Friedel, I.W. Renk and H.T. Dieck, J. Organomet. Chem., 1971, 26, 247.

190. H.T. Dieck and H. Friedel, J. Chem. Soc., Chem. Commun., 1969, 411

191. F. Hohmann, H. tom Dieck, T. Mack and D. Leibfritz., J. Organomet. Chem., 1977, 132, 255.

192. F. Hohmann and H.T. Dieck, J. Organomet. Chem., 1975, 85, 47.

193. F.W.S. Benfield, B.R. Francis and M.L.H. Green, J. Organomet. Chem., 1972, 44, C.13.

194. F.A. Cotton, C.E. Rice and G.W. Rice, J. Am. Chem. Soc., 1977, 99, 4704.

195. J.W. Faller, C.-C.Chen, M.J. Mattina and A. Jakubowski, J. Organomet. Chem., 1973, 52, 361.

196. A.I. Vogel, "Quantitative Inorganic Analysis", 3rd Edn., Longmans, England, 1961.

197. D.D. Perrin, W.L.F. Armarego and D.R. Perrin, "Purification of Laboratory Chemicals", Pergamon Press, Oxford, 1966.

198. R.G. Charles, Org. Synth., Coll. Vol., 4, 1963, 869.

199. E.W. Abel, M.A. Bennett, R. Burton and G. Wilkinson., J. Chem. Soc., 1958, 4559.

200. M.A. Bennett, L. Pratt and G. Wilkinson, J. Chem. Soc., 1961, 2037.

201. R.B. King and A. Fronzaglia, J. Chem. Soc., Chem. Commun., 1965, 547.

202. F.A. Cotton, J.A. McCleverty and J.E. White, Inorg. Synth., 1967, 9, 121.

203. C. Barbeau and J. Turcotte, Can. J. Chem., 1970, 48, 3583.

204. F.A. Cotton and C.S. Kraihanzel, J. Am. Chem. Soc., 1962, 84, 4432.

205. M. Davies (Ed.), "Infra-red Spectroscopy and Molecular Structure", Elsevier Publishing Co. London, 1963.

206. J.E. Johnson and R.A. Jacobson, Acta Crystallogr. Sect. B, 1973, 29, 1669.

207. W.R. McWhinnie, J. Chem. Soc., 1964, 5165.

208. G.J. Palenik, M. Mathew, W.L. Steffen and G. Beran, J. Am. Chem. Soc., 1975, 97, 1059.

209. G.J. Palenik, W.L. Steffen, M. Mathew, M. Li and D.W. Meek, Inorg. Nucl. Chem. Lett., 1974, 10, 125.

210. R.G. Pearson, J. Am. Chem. Soc., 1963, 85, 3533.

211. T.E. Sloan and A. Wojcicki, Inorg. Chem., 1968, 7, 1268.

212. A.H. Norbury, Adv. Inorg. Chem. Radiochem., 1975, 17, 231.

213. R.A. Bailey, T.W. Michelsen and W.N. Mills, J. Inorg. Nucl. Chem., 1971, 33, 3206.

214. D. Forster and D.M.L. Goodgame, Inorg. Chem., 1965, 4, 715.

215. K.O. Christe and P. Naumann, Spectrochim. Acta Part A, 1973, 29, 2017.

216. N.F. Curtis, J. Chem. Soc. A, 1968, 1579.

217. G. Vitzthum and E. Lindner, Angew. Chem., Int. Ed. Engl. 1971, 10, 315.

218. F.A. Hartman and A. Wojcicki, Inorg. Chem., 1968, 7, 1504.

219. J.C. Dewan, K. Henrick, D.L. Kepert, K.R. Trigwell, A.H. White and S.B. Wild, J. Chem. Soc., Dalton Trans., 1975, 546.

220. A.A. Woolf, unpublished results.

221. R. Colton and G.R. Scollary, Aust. J. Chem., 1968, 21, 1427.

222. D. Gibson, Coord. Chem. Rev., 1969, 4, 225.

223. J. Lewis, R.F. Long and C. Oldham, J. Chem. Soc., 1965, 6740.

224. G.T. Behnke and K. Nakamoto, Inorg. Chem., 1967, 6, 433.

225. G.T. Behnke and K. Nakamoto, Inorg. Chem., 1967, 6, 440.

226. R.H. Balundgi and A. Chakravorty, Inorg. Chem., 1973, 12, 981.

227. H. Brunner and W.A. Herrmann, Chem. Ber., 1972, 105, 770.

228. E.P. Dudek and G. Dudek, Inorg. Nucl. Chem. Lett., 1967, 3, 241.

229. D.C. Bradley and M.H. Gitlitz, J. Chem. Soc. A, 1969, 1152.

230. C. O'Connor, J.D. Gilbert and G. Wilkinson, J. Chem. Soc. A, 1969, 84.

231. B.L. Ross, J.G.Grasselli, W.M. Ritchey and H.D. Kaesz., Inorg. Chem., 1963, 2, 1023.

232. J.E. Ellis and G.P. Hagen, Inorg. Chem., 1977, 16, 1357.

233. J.E. Ellis and M.C. Palazzotto, J. Am. Chem. Soc., 1976, 98, 8264.

234. E.A. Allen, B.J. Brisdon and G.W.A. Fowles, J. Chem. Soc., 1964, 4531.

235. H.C. Beyerman and J.S. Bontekoe, Recl. Trav. Chim. Pays-Bas, 1955, 74, 1395.

236. L.W. Houk and G.R. Dobson, Inorg. Chem., 1966, 5, 2119.

237. R.H. Reinmann and E. Singleton, J. Chem. Soc., Dalton Trans., 1973, 841.

238. L.M. Haines and M.H.B. Stiddard, Adv. Inorg. Chem. Radiochem., 1969, 12, 53.

239. L.M. Bower and M.H.B. Stiddard, Inorg. Chim. Acta, 1967, 1, 231.

240. S. Kirschner (Ed.), " Advances in the Chemistry of Coordination Compounds", MacMillan, New York, 1961.

241. L.H. Jones, Inorg. Chem., 1968, 7, 1681.

242. F.A. Cotton, Inorg. Chem., 1968, 7, 1683.

243. L.H. Jones, Inorg. Chem., 1967, 6, 1269.

244. J. Dalton, et. al., J. Chem. Soc. A, 1968, 1195 to 1217.

245. F.T. Delbeke, E. Claeys, G.P. Van der Kelen and R.M. de Caluwe, J. Organomet. Chem., 1970, 23, 497.

246. F.T. Delbeke, E.G. Claeys, R.M. de Caluwe and G.P. Van der Kelen, J. Organomet. Chem., 1970, 23, 505.

247. F.T. Delbeke, E.G. Claeys, G.P. Van der Kelen and Z. Eeckhaut., J. Organomet. Chem., 1970, 25, 213.

248. F.T. Delbeke, E.G. Claeys and G.P. Van der Kelen, J. Organomet. Chem., 1970, 25, 219.

249. R.T. Jernigan, R.A. Brown and G.R. Dobson, J. Coord. Chem., 1972, 2, 47.

250. C. Chen and C.-C. Hsiang, J. Chin. Chem. Soc. (Taipei), 1973, 20, 13.

251. F.T. Delbeke, G.P. Van der Kelen and Z. Eeckhaut, J. Organomet. Chem., 1969, 16, 512.

252. L.H. Jones, R.S. McDowell and M. Goldblatt, Inorg. Chem., 1969, 8, 2349.

253. D.K. Ottesen, H.B. Gray, L.H. Jones and M. Goldblatt, Inorg. Chem., 1973, 12, 1051.

254. G. Bor, B.F.G. Johnson, J. Lewis and P.W. Robinson, J. Chem. Soc. A, 1971, 696.

255. F.A. Cotton, Inorg. Chem., 1964, 3, 702.

256. C.L. Hyde, and D.J. Darensbourg, Inorg. Chem., 1973, 12, 1075.

257. E.O. Fischer, E. Louis and W. Bathelt, J. Organomet. Chem., 1969, 20, 147.

258. C.G. Barlow and G.C. Holywell, J. Organomet. Chem., 1969, 16, 439

259. A. Davison and J.E. Ellis, J. Organomet. Chem., 1971, 31, 239.

260. E.W. Abel and S.P. Tyfield, Can. J. Chem., 1969, 47, 4627.

261. T. Fukumoto, Y. Matsumura and R. Okawara, Inorg. Nucl. Chem. Lett., 1973, 9, 711.

262. G. Doyle, J. Organomet. Chem., 1973, 61, 235.

263. H.C.E. Mannerskantz and G. Wilkinson, J. Chem. Soc., 1962, 4454.

264. R. Ros, M. Vidali and R. Graziani, Gazz. Chim. Ital., 1970, 100, 407.

265. R. Donaldson, G. Hunter and R.C. Massey, J. Chem. Soc., Dalton Trans., 1974, 288.

266. E.W. Abel and I.S. Butler, Trans. Faraday Soc., 1967, 63, 45.

267. E.W. Abel, I.S. Butler, M.C. Ganorkar, C.R. Jenkins and M.H.B. Stiddard, Inorg. Chem., 1966, 5, 25.

268. B.F.G. Johnson, J. Lewis, P.W. Robinson and J.R. Miller, J. Chem. Soc. A, 1968, 1043.

269. M. Pankowski and M. Bigorgne, J. Organomet. Chem., 1969, 19, 393.

270. L.A.W. Hales and R.J. Irving, J. Chem. Soc. A, 1967, 1389.

271. M.B. Hall and R.F. Fenske, Inorg. Chem., 1972, 11, 1619.

272. D.J. Darensbourg and M.Y. Darensbourg, J. Organomet. Chem., 1974, 83, 309.

273. P.J. Hendra and M.M. Qurashi, J. Chem. Soc. A, 1968, 2963.

274. S.Kh. Samvelyan, V.T. Aleksanyan and B.V. Iokshin, J. Mol. Spectrosc., 1973, 48, 47.

275. R. Paetzold and S. Abd-El-Mottaleb, J. Mo. Struct, 1975, 24, 357.

276. L.H. Jones, Spectrochim. Acta, 1963, 19, 329.

277. L.E. Orgel, Inorg. Chem., 1962, 1, 25.

278. A.G. Robiette, private communication.

279. M.N. Memering and G.R. Dobson, Inorg. Chem., 1973, 12, 2490.

280. I.S. Butler and H.K. Spendjian, J. Organomet. Chem. 1969, 18, 145

281. E.B. Wilson, Jr., J.C. Decius and P.C. Cross, "Molecular Vibrations", McGraw-Hill Book Co. Inc., New York, 1955.

282. G.A. Korn and T.M. Korn, "Mathematical Handbook for Scientists and Engineers", 2nd Edn., McGraw-Hill Book Co., New York, 1968.

283. B.J. Brisdon and A.A. Woolf, unpublished results.